ECOPHYSIOLOGICAL RESPONSES AND ADAPTATIONS TO RESOURCE SEASONALITY, NUTRITIONAL SYMBIOSIS IN THE THYASIRIDAE (MOLLUSCA: BIVALVIA) AS A CASE STUDY

by

© JOANY VALENTINA MARIÑO CORONADO

A thesis submitted to the School of Graduate Studies
in partial fulfillment of the requirements for the degree of
Doctor of Philosophy

Department of Biology
Faculty of Science
Memorial University of Newfoundland

September 2021
St. John's, Newfoundland and Labrador, Canada

A José Joaquín,
el mejor papá (y capitán) del mundo.

Ce sera comme si je t'avais donné, au lieu d'étoiles,
des tas de petits grelots qui savent rire...
—Antoine de Saint-Exupéry, Le Petit Prince.

ABSTRACT

Animals show a vast diversity of life-history traits and foraging strategies. Some of these traits arise as a plastic response to environmental conditions, while some strategies result from an adaptive evolutionary process. Regardless of their origin, constraints on energy acquisition play a crucial role in the emergence of both traits and strategies because they define the individual energy budget. For example, in many species, resource abundance determines individual energy input. Yet, other species have symbiotic partnerships through which they can increase their energy acquisition. However, the precise mechanisms whereby seasonal energy constraints can affect an individual's energy budget and translate to higher ecological levels remain unknown. In this thesis, I show the fundamental role of resource availability in driving trait flexibility and how nutritional symbiosis may be an adaptive foraging strategy in response to a seasonal resource abundance. Using a mechanistic description of individual metabolism, I demonstrate that resource availability is sufficient to explain interspecific trait variability. Moreover, peaks of seasonal food can increase individuals' biomass and reproductive output, hence explaining known ecogeographical rules. Focusing on thyasirid bivalves, I reveal how nutritional symbiosis can alter the host's energy budget and, consequently, define population dynamics. My results are the first step leading towards understanding the role of symbiosis in population and community dynamics. Broadly, this dissertation contributes to building the theoretical foundation necessary for a mechanistic understanding of how individual metabolism, together with environmental factors, determines species traits and population dynamics. Furthermore, my findings motivate experimental investigations to confirm the theoretical results and test the proposed hypotheses. Due to the current alterations to ecosystems, disentangling the mechanisms underlying life-history traits and foraging strategies is fundamental to understand and predict biodiversity dynamics under climate change.

GENERAL SUMMARY

Animal diversity is vast. From herbivorous elephants to omnivorous mice, diversity is reflected not only in species number but also includes variability in size, fecundity and feeding strategies. These aspects of animal diversity are shaped by limits on food intake, which define the individuals' energy budget. For example, in many animals, the available food determines the energy input, which can then be allocated towards growth and reproduction. Yet, other animals form long-term partnerships with organisms of different species —termed nutritional symbiosis— by which they can increase their food intake and thus energy input. However, how food seasonality can affect an organism's energy budget and translate beyond the individual to the population level remains unknown. In this thesis, I show the fundamental role of food availability in driving animal variability and how nutritional symbiosis can be a feeding strategy in response to seasonal food. Using a description of individual-level metabolism, I demonstrate how food availability can explain diversity in animal size and fecundity. Focusing on symbiotic marine clams, I reveal how nutritional symbiosis can alter the clams' energy budget, increase their population size and mitigate the effect of seasonal food. My results are the first step towards understanding how nutritional symbiosis can influence animals' populations and communities. Broadly, this dissertation contributes to building the foundation necessary for understanding how an individual's metabolism, together with environmental factors, determines species diversity and population dynamics. Due to the current alterations to ecosystems, disentangling the factors that promote species diversity is fundamental to understand, predict and prevent biodiversity loss under climate change.

ACKNOWLEDGMENTS

This thesis would not have been possible without the support of Amy Hurford and Suzanne Dufour, who gave me the opportunity to be part of their research groups. I am deeply grateful for the inspiration, encouragement, advice and independence that you gave me along the way. Thank you, Suzanne. Thank you, Amy.

I am grateful to have collaborated with Starrlight Augustine and Charlotte Récapet, whose conversations and scientific insights were tremendously valuable for this research. Special thanks to Bas Kooijman and the organizers and participants of the DEB 2017 and PSPM summer schools, which significantly impacted this thesis.

My sincere gratitude to Pat Gagnon and David Innes for being a part of my committee and providing valuable feedback on my research. Thanks to the lab instructors and staff in the Biology department, with whom it was a pleasure to teach. Thanks in particular to Bob Hooper, Fiona Cuthbert, Hope Bennett, Elizabeth Diegor, Ed Whelan, Bill Gin, and Jennifer Slade. Thanks to the staff at the Bonne Bay Marine Station, especially to Laurie Haycock and Dennis Rumbolt. Thanks to the staff at the QEII Library, the Internationalization Office and the IT Services. Also, thanks to Len Zedel, Oliver Stuecker, and all the participants of the Computing Workshops for many useful discussions.

I am grateful to my labmates and colleagues at the Theoretical Biology and the Marine Chemosymbiosis labs and the quasi-labmates at the Ecosystem Ecology and Botany labs. Thanks to Nico Peñafiel, Sander Boisen, Yanitza Trosel, Joe Moran, Fábio Frazão, Sovit Chalise, Joey Smokey, Joseph Baafi, Rachelle Dove and Daigo Kamada. Huge thanks to Elena Salogni, Damiano De Filippi, Abdou Fofana, Boni Nieto-Blazquez, Natalia de la Torre, and Fritz Pichardo because we did this journey together.

Thanks to Ted and Margarita Miller as well as to Amanda Crompton and Marc Bolli for giving me two families in St. John's. Many thanks to Sharon Hewitt and Alfredo Dyck for all the stimulating conversations, literature and music.

I also recognize the influence of my former mentors, who inspired my path into theoretical and quantitative biology and from whom I learned so much. Gracias a Carlos Mantilla, Maria-Josefina Hernandez, Diego Griffon, Jesús Alberto León, Mario Palacios y Wilmer Rojas.

Thanks to my friends across countries and continents: Marcial Quiroga, Geraldine & Kike Campos, Cristina Malpica, Arianna Thomas, Wence Herrera, Daniela Mendoza, Disleydis Petit, Fabio Padoan, Aarón Machado, Guillermo Flórez, Carlos Quevedo, MaFer López, Ángel Castillo, Mariauxy Pedrero and Alberto Díaz. Thanks also to Rita Samuseva.

Gracias a mi familia: Leonor, Orbe y José Joaquín, Nano y Liany, porque todo empezó en casa —esto también es de ustedes; mi camino no es más que la continuación del suyo—. También gracias a la familia en el Norte: Oleny, Ricardo, Hana, Begoña, Erwing y Otto, por traerme de nuevo al hogar en cada viaje.

Zu guter Letzt bedanke ich mich bei meiner neuen Familie, den Brechts, die mir —während einer Pandemie (!)— ein neues Zuhause in Hamburg gegeben haben. Ein ganz besonderer Dank geht an Rüdiger porque *la tierra giró para acercarnos*.

Thanks to everyone who contributed to finishing this thesis. I am indebted to the communities behind the multiple open-source software packages on which this research relies and to those who provide access to the knowledge behind paywalls and contribute to open science.

I received funding to support this dissertation from the School of Graduate Studies Baseline Fellowship. For Chapter 2, I received funding from a Mitacs Globalink Research Award. I also acknowledge the IOM for supporting my travel to Canada.

CO-AUTHORSHIP STATEMENT

Throughout this dissertation, I led the joint research with collaborators whose contributions are detailed below. These collaborators are also listed as co-authors in each thesis chapter.

CHAPTER 2: RESOURCE AND SEASONALITY DRIVE INTERSPECIFIC VARIABILITY IN A DYNAMIC ENERGY BUDGET MODEL
Charlotte Récapet worked with me to formulate and design this research; she also provided guidance for the simulations, analyses and manuscript preparation. Suzanne C. Dufour and Amy Hurford provided feedback throughout the research and contributed to the manuscript revision.

CHAPTER 3: DYNAMIC ENERGY BUDGET THEORY PREDICTS SMALLER ENERGY RESERVES IN THYASIRID BIVALVES THAT HARBOUR SYMBIONTS
Suzanne C. Dufour and Amy Hurford worked with me in the conception and design of this research. Suzanne C. Dufour contributed to field sampling and data collection. Starrlight Augustine provided guidance for the model parameterization. All co-authors contributed to the revision of the manuscript.

CHAPTER 4: SYMBIOSIS INCREASES POPULATION SIZE AND BUFFERS ENVIRONMENTAL FLUCTUATIONS IN A PHYSIOLOGICALLY-STRUCTURED MODEL PARAMETERIZED FOR THYASIRID BIVALVES
Suzanne C. Dufour and Amy Hurford worked with me to formulate and design this research. Amy Hurford provided guidance for the model derivation and numerical implementation. All co-authors contributed to the revision of the manuscript.

In all chapters, I am the main author of the research presented. I identified the research topic, conceived and planned the research, conducted the mathematical and statistical analyses, interpreted the results, wrote and prepared the manuscripts for peer review.

CONTENTS

GLOSSARY

Chemosynthesis

pathway through which bacteria —called chemoautotrophs— synthesize organic molecules from dissolved inorganic carbon molecules (e.g., carbon dioxide or methane) using the energy released by the oxidation of reduced inorganic compounds (e.g., hydrogen sulphide) or methane (Dubilier, Bergin, & Lott, 2008).

Environment

conditions and resources relevant for an organism's survival; the particular variables are species-specific (Futuyma & Kirkpatrick, 2005; Levins, 1968). In this thesis, I focus on the resource as the main environmental component.

Foraging strategy

how animals obtain food or nutrition. Of particular importance in this thesis are mixotrophy and nutritional symbiosis, which are considered generalist foraging or feeding strategies.

Host

an organism in a symbiotic relationship that provides a habitat for its symbionts and can exert some control over the association. In Chapters 3 and 4 of this thesis, the thyasirid bivalves are the hosts of the chemoautotrophic bacterial symbionts.

Life history

the major features of an organism affecting its population biology, particularly concerning survival and reproduction.

Life history strategy

life history traits together with their timing (e.g., age- or state- or stage-dependent traits) (Stearns, 1992).

Life history trait

a phenotypic feature of an organism directly related to reproduction and survival, thus directly affecting fitness (Stearns, 1992). For example, body size, biomass, clutch size.

Mixotrophy

feeding strategy in which animals combine nutritional input from symbionts with heterotrophic or autotrophic feeding.

Nutritional or trophic symbiosis

symbiotic association where at least one of the partners obtains a nutritional benefit from the association, which increases its metabolic capabilities. In Chapters 3 and 4 of this thesis, I consider a symbiosis where the host gains the nutritional benefit.

Passive phenotypic flexibility

phenotypic plasticity that stems from direct environmental influences on the organism's chemical, physiological, and developmental processes. It is considered a consequence of the environment but not an anticipatory response.

Phenotype

properties of an organism (e.g., morphological, physiological, behavioural, biochemical) manifested throughout its life (Futuyma & Kirkpatrick, 2005). The phenotype of a host is determined by the genotype, the environment, and the interaction between the environment and the genotypes of the host and its symbionts.

Phenotypic plasticity

environment-dependent phenotypic expression (Via & Lande, 1985), meaning that a single genotype can exhibit a range of different phenotypes in response to variation in the environment.

Reaction norm (or norm of reaction)

description of the phenotypic expression of a genotype across an environmental gradient.

Resource

sources of energy or environmental components required by organisms for growth, maintenance and reproduction. In this thesis, I examine food or nutrient supply as the main resource, which may be subject to seasonal variation. I consider chemosymbiotic bacteria as forming part of the nutrient supply for symbiotic hosts. For simplicity, I assume that the resource is not depleted as organisms consume it; hence, there is no resource density dependence.

Seasonality

contingent and predictable environmental variation within an astronomic (solar or calendar) year, which occurs at a rate relevant to the organism's lifespan.

Symbiont

any organism that spends at least one life history stage living in or on a single host individual (Halliday, Umbanhowar, & Mitchell, 2017). In Chapters 3 and 4 of this thesis, chemoautotrophic bacteria are the symbionts of the thyasirid bivalves.

Symbiosis

prolonged physical association between individuals of different species (de Bary, 1879). These associations form a continuum that can be categorized, according to the consequences of the interaction in the partners' fitness, as consumer-resource, commensalism, and mutualism. However, the outcomes are context-dependent (Parmentier & Michel, 2013;

Stachowicz, 2001). In Chapters 3 and 4 of this thesis, the symbiosis between thyasirid bivalves and chemoautotrophic bacteria is considered a consumer-resource interaction because the bacteria may not receive a fitness advantage from the association.

Trade-off

the antagonistic effect that occurs when a beneficial change in one trait is connected to a detrimental change in another trait (Stearns, 1989b). For example, investment in growth versus reproduction.

Transmission

the mode of acquisition of the symbionts by the hosts. In *vertical transmission*, the symbionts are passed directly from the parent to the offspring; in *horizontal transmission*, the symbionts are acquired from contemporary organisms that share the same habitat; and in *environmental transmission*, the symbionts are taken up from free-living populations of symbionts.

PRELUDE

It is a dynamic world,
where symbiosis and phenotypic plasticity are the rules,
not the exceptions.
—Gilbert, Bosch, and Ledón-Rettig, 2015.

In this thesis, I explore two closely interconnected topics in evolutionary ecology whose common thread is the interaction between the individual and the environmental conditions. I emphasize that the relationship of the individual to the environment is the basis for emergent properties at higher levels. Among the environmental components, I argue that resource availability acts as a major force driving the individual physiological responses because it can be the main constraint determining energy input. Thus, the core of this thesis is the study of responses and adaptations to resource variability.

I begin by providing the necessary background. For this, in Chapter 1, I define the concepts used throughout the thesis and give an overview of the previous research that serves to place this thesis in context. Then, I introduce the Dynamic Energy Budget theory, which provides a mechanistic description of the individual physiology in relation to the environment and thus serves as the main unifying framework of the thesis.

In Chapter 2, I focus on broad questions concerning individual responses to the environment and whether genetically fixed or environmental sources of variation contribute more to the phenotype. Here, I isolate the effect of the energy constraints by concentrating on resource availability as the main component of the environment that can influence phenotypic traits. Fixing the environmental context in this way allows considering the level of a given trait as a property of the organism (or, more specifically, the genotype). However, because the environment modulates the traits, the trait level can vary according to the environment. As a consequence, individual traits are considered as a property-in-an-environment. This means that to clarify the effect of the environment, we need to compare the responses of different organisms within different common environments, measuring every trait as a property in each environment. For this reason, in Chapter 2, I perform an extensive simulation study to systematically compare the energy budget and traits of different species across several environmental scenarios. Through my findings, I show that differential resource availability constrains energy acquisition and is sufficient to generate trait flexibility within individuals of the same species or among related species. My analysis explains mechanistically some empirical correlations between trait variation and environmental gradients (termed ecogeographical rules) that remain controversial. The results of this chapter serve as a starting point to understand physiological responses and adaptations to resource availability —*ceteris paribus*— in the rest of this thesis.

After establishing a baseline of passive responses to resource availability, in Chapters 3 and 4, I turn to look at adaptive foraging strategies that have likely evolved due to similar environmental constraints. More specifically, I focus on symbiotic partnerships that can enhance nutrient acquisition and, hence, release the limitations imposed by resource availability. As a case study, I consider two related bivalve species that inhabit a highly seasonal environment, one symbiotic and one asymbiotic. In Chapter 3, I characterize their interaction with the environment and show their differences in terms of their energy budgets. The dissimilarities between the species lead me to hypothesize that they exhibit contrasting adaptations to a seasonal resource: the asymbiotic species invests in energy storage to survive in periods of low resource availability, while the symbiotic species outsources nutrient acquisition from symbionts that can serve as an energy reserve. This novel hypothesis on a plausible role of the symbionts in these bivalves is likely to be relevant across trophic symbioses. Further, it has the potential to change our current understanding of the individual processes that form the base of ecosystem functioning.

The results of Chapter 3 made it clear that the effect of nutritional symbiosis on the individual energy budget can alter the demographic rates that determine population processes. Thus, the natural next step is to examine the implications of symbiosis at the population level. In Chapter 4, I develop a physiologically structured population model based on the individual energy budget that reveals the differences between the populations of symbiotic and asymbiotic bivalves. My findings show how trophic symbiosis can increase the bivalve host's population growth rate and mitigate the effect of a seasonal environment. Moreover, the results of Chapter 4 highlight the relevance of linking individual energetics and life history strategies to population dynamics and are the first step towards a general understanding of the role of symbiosis in populations' resilience.

Although Chapters 3 and 4 focus on bivalves as a case study, I argue that the mechanisms they reveal are general, being transferable and relevant in various trophic symbioses. Hence, in Chapter 5, I integrate the hypotheses that stem from the previous chapters to propose new predictions that explicitly address the responses of symbiotic hosts to resource availability. The analyses of these predictions further support that nutritional symbiosis can be an adaptive strategy that increases fitness by enhancing reproductive output, and that resource availability can be the driving force giving rise to trait flexibility. Finally, I place the main results of each chapter in the wider biological context, discussing some of their ramifications and possible future research.

1 INTRODUCTION

The diversity in life-history traits and strategies in animal species across temporal and spatial scales is vast (Healy, Ezard, Jones, Salguero-Gómez, & Buckley, 2019). Constraints on energy availability, such as seasonal resource abundance, play a crucial role in the emergence of plastic traits and adaptive strategies because they define the individual energy budget. However, the precise mechanisms whereby seasonal energy constraints can affect an individual's energy budget and translate to traits and strategies, or reflect at higher ecological levels of organization, remain largely unknown. Disentangling these bottom-up mechanisms is crucial for the maintenance of biodiversity and understanding the conditions that lead to the persistence of populations, communities and ecosystems (Miller & Rudgers, 2014; Mueller, Wisnoski, Peralta, & Lennon, 2020).

To elucidate how seasonal energy constraints can promote ecophysiological responses and adaptations, in the present thesis, I focus on investigating the individual energy flow, from energy availability and acquisition to allocation for metabolic processes. This approach requires first developing a baseline knowledge of how energy constraints determine individual trait variation (Chapter 2). Among the energy constraints, I emphasize the relevance of the resource because, at the most elementary level, it can define energy input. Then, I examine nutritional symbiosis as one adaptive strategy that can increase energy acquisition and alter the allocation patterns (Chapters 3 and 4). More specifically, I explore three hypotheses:

- Chapter 2: resource availability drives the energy allocation trade-offs that determine life history traits (particularly body size and reproductive output).

- Chapter 3: nutritional symbiosis provides the host with additional resource availability, altering its energy allocation pattern and life history traits.
- Chapter 4: the population dynamics of the hosts reflect the altered energy budget and life history traits of the individuals.

In this chapter, I synthesize the necessary background to set the scene for the rest of the thesis.

1.1 RESOURCE SEASONALITY AS THE MAIN ENVIRONMENTAL FACTOR DRIVING ECOPHYSIOLOGICAL RESPONSES AND ADAPTATIONS

A central component of the environment is variation across space and time, ranging from widespread and long-lasting to extremely local and transitory events (Lewontin & Levins, 2007a). Most environmental phenomena show seasonal oscillations, for example in temperature and precipitation, but even less pronounced fluctuations can vary in biologically important ways (Tonkin, Bogan, Bonada, Rios-Touma, & Lytle, 2017). Among these periodical oscillations, within-year seasonality is arguably one of the most well-known and strongest forms of ecosystem variation (Tonkin et al., 2017).

Organisms' life histories are intimately coupled to seasonality. For example, vital rates such as growth, reproduction and mortality can vary in response to environmental conditions that change seasonally (McNamara & Houston, 2008). Moreover, seasonality can explain general phenomena such as life history adaptations (McNamara & Houston, 2008), latitudinal diversity gradients (Dalby, McGill, Fox, & Svenning, 2014; Hurlbert & Haskell, 2003), and community structure (Chase, 2011; Chesson, 2000). Seasonality can thus be viewed as a selective pressure that drives the life histories of organisms into specific traits and strategies (Tonkin et al., 2017).

Seasonal environmental variability related to constraints on energy acquisition is considered a determinant factor in promoting phenotypic responses, such as trait flexibility (Kivelä, Välimäki, & Gotthard, 2013; Varpe, 2017). For instance, food abundance, availability, and quality influence the metabolic processes (e.g., growth, maturation, and reproduction) directly associated with individual traits (Bjorndal et al., 2013; Piovano et al., 2011). In this way, the environment plays an essential role in driving phenotypic expression as there are no phenotypic responses without an environmental cue preceding the development of the phenotype (Shapiro, 1976).

Seasonality is also thought to be a key factor in the evolution of foraging strategies (Kassen, 2002; Lynch & Gabriel, 1987). Evolutionary theory suggests that selection favours generalist strategies in populations experiencing environmental heterogeneity (Futuyma & Moreno, 1988; Levins, 1968; Lynch & Gabriel, 1987). Experimental results have confirmed such findings (Bell & Reboud, 1997; Kassen & Bell, 1998; Reboud & Bell, 1997). For example, selection experiments in *Chlamydomonas* in constant environments have led to the evolution of specialists, either autotrophic or heterotrophic. Conversely, in temporally varying environments, selection favours generalists capable of both autotrophic and heterotrophic nutrition. However, in spatially variable environments, both specialists can be retained in the population (Bell & Reboud, 1997; Kassen & Bell, 1998; Reboud & Bell, 1997). Broadly, these results suggest that ecological specialists tend to be selected in environments that are homogeneous in space or time, whereas generalists tend to be favoured in temporally varying environments (Ackermann & Doebeli, 2004; Futuyma & Moreno, 1988; Kassen, 2002; Levins, 1968; Lynch & Gabriel, 1987).

1.2 PHENOTYPIC FLEXIBILITY AS A RESPONSE TO RESOURCE SEASONALITY

Every organism is plastic in at least some traits —often in many traits—, underscoring that plasticity is pervasive and exists in many different forms (Windig, De Kovel, & De Jong, 2004). In general, plasticity involves sensitivity and variable response to environmental differences, such that the phenotype is induced by the environment, or equivalently, that the environment acts as a cue to form the genotype (Sarkar, 2004; Windig et al., 2004). In this way, a single genotype can produce different phenotypes, depending on the external conditions experienced (Lafuente & Beldade, 2019). Despite considerable research describing the patterns of phenotypic variation, a clear understanding of the underlying mechanisms and processes remains elusive (Gaston, Chown, & Evans, 2008).

Understanding the mechanisms that drive phenotypic plasticity and its consequences is crucial to unraveling the evolution and maintenance of biodiversity (Agrawal, 2001; Snell-Rood, 2013; Violle et al., 2012). Moreover, because phenotypic variation may influence population dynamics and community structure, leading to variation in ecosystem function, disentangling and quantifying trait variation is necessary to explain and predict biodiversity dynamics and resilience under environmental change (Cabral, Valente, & Hartig, 2017; Cardilini, Buchanan, Sherman, Cassey, & Symonds, 2016). Given that these rapid climatic changes can alter the interactions between organisms and their environments (Gilbert et al., 2015), it is fundamental to understand the underlying mechanisms giving rise to animal phenotypic variation.

The relationship between the phenotypic expression of a genotype to an environmental gradient is understood as a reaction norm, resulting from passive or active developmental processes (Doughty & Reznick, 2004). Passive processes, known as phenotypic modulation, reflect the flexibility of the phenotypic responses to physical and chemical features of the habitat (e.g., food and temperature Doughty & Reznick, 2004; Windig et al., 2004). For example, in the fruit fly *Drosophila mercatorum*, food level influences age and size at maturity (Gebhardt & Stearns, 1988). In contrast, active processes are characterized by largely anticipatory phenotypic changes in response to an environmental cue, reflecting the alteration of developmental pathways and regulatory genes (Forsman, 2015). In this sense, active phenotypic plasticity can be considered the result of an adaptive process, whereas passive phenotypic flexibility is not generally understood as adaptive (Doughty & Reznick, 2004). Phenotypic flexibility may reflect an adaptation only if selection in that environment has changed the form of the ancestral reaction norm (Doughty & Reznick, 2004; Stearns, 1989a). Regardless of their origin, phenotypic variation provides organisms with the ability to cope with environmental change, which is critical to their survival.

Phenotypic plasticity is widespread in seasonal habitats, allowing organisms to track the predictable environmental cycles and maximize their fitness (Piersma & Van Gils, 2011). For example, seasonal energy constraints commonly induce starvation periods in most organisms, and many of them can withstand temporal food scarcity through phenotypic plasticity (Pijpe, Brakefield, & Zwaan, 2007). One common strategy is to store the energy excess gained in periods of food abundance and use it in periods of food depletion (Pijpe et al., 2007). Energy constraints can also directly influence the amount of energy available for reproduction, affecting the reproductive output. For instance, female reptiles can modify their reproductive frequency, clutch and offspring size as a response to resource seasonality (James & Whitford, 1994; Madsen & Shine, 1999; Shine, Madsen, Elphick, & Harlow, 1997). In this sense, phenotypic flexibility can be considered a response to resource seasonality by which organisms can tolerate a variable energy input.

1.3 NUTRITIONAL SYMBIOSIS AS AN ADAPTATION TO RESOURCE SEASONALITY

Symbiotic interactions are ubiquitous. All multicellular organisms are formed by the association of a macroscopic host with bacteria, archaea and eukaryotic species (Gilbert et al., 2015). These associations are referred to as holobionts (Rosenberg, Koren, Reshef, Efrony, & Zilber-Rosenberg, 2007) or metaorganisms (Bosch & McFall-Ngai, 2011), and they may constitute a unit of evolutionary selection because the fitness of an animal depends on multiple organisms of several species (Gilbert et al., 2015). The increasing awareness that animals exist only within a partnership with symbionts has led to recognizing that we cannot study species in isolation if we want to grasp their physiology, development, ecology and evolution (Gilbert et al., 2015; Moran & Yun, 2015; Oliver, Degnan, Hunter, & Moran, 2009). In this context, the phenotype results from the interaction between the genome, the symbionts (and their genomes), and the abiotic environment (Gilbert et al., 2015). Thus, it is necessary to investigate not only the interaction between the organism and the environment, but also its symbiotic partnerships.

Trophic or nutritional symbiosis is a prevalent interaction whereby organisms outsource or gain access to crucial nutrition, consequently increasing the metabolic capabilities of the host (Moran, 2006). Hence, symbiosis can affect host life-history traits, such as fecundity and survival, which, in turn, determine population dynamics. However, how symbiosis can influence host physiology and ecology and how this would be translated into population and community dynamics is not well established (Yule, Miller, & Rudgers, 2013). Disentangling the bottom-up effect of trophic symbiosis on ecological timescales, in both constant and heterogeneous environments, is crucial to understanding the conditions that lead to the persistence of populations and communities (Miller & Rudgers, 2014).

Nutritional symbioses in which the host has a mixotrophic nutrition (i.e. the host can combine the nutritional input from the symbionts with heterotrophic or autotrophic feeding;

Rossi, Coppari, & Viladrich, 2017) can be considered to be generalist feeding strategies. For instance, mixotrophic symbioses are frequent in marine suspension feeders, which live in environments where light and plankton concentration are variable and often limiting (Grottoli, Rodrigues, & Palardy, 2006; Muller, Nisbet, Kooijman, Elser, & McCauley, 2001). In octocorals, such trophic flexibility has been proposed to maximize nutrient uptake, allowing for increased energy acquisition relative to asymbiotic species (Gori et al., 2012; Grottoli et al., 2006). Moreover, the loss of symbionts may not significantly affect the host's energetic input, making the host less affected by environmental variability (Fabricius, Genin, & Benayahu, 1995; Ferrier-Pagès et al., 2015; Rossi et al., 2017; Sorokin, 1991; Viladrich et al., 2017). Thus, in seasonal environments, symbionts can provide energy to a mixotrophic host and stabilize the discontinuous energy inputs in resource availability (Gori et al., 2012; Rossi et al., 2017; Viladrich et al., 2017). Nevertheless, there is still a major gap in our understanding of the precise mechanisms whereby trophic symbiosis can contribute to the host's energy budget.

1.4 NUTRITIONAL SYMBIOSIS IN THYASIRID BIVALVES

Among trophic symbioses, the association between chemosynthetic bacteria and invertebrate animals is a prominent example because of its prevalence in diverse habitats and within multiple phyla of hosts. Chemoautotrophic bacteria can establish symbiotic interactions with members of at least seven phyla of invertebrates and protists (Dubilier et al., 2008), while the association itself is termed chemoautotrophic symbiosis, chemosynthetic symbiosis or chemosymbiosis (Cavanaugh, Mckiness, Newton, & Stewart, 2006; Dubilier et al., 2008). Chemosymbiotic bacteria can be epibionts —attached to or covering the host surface— or endobionts —living within the host, either extracellularly or intracellularly— (Dubilier et al., 2008; Moran, 2006). As a nutritional strategy, chemosymbiosis allows hosts to gain previously inaccessible resources by outsourcing energy acquisition to the symbionts. Thus, symbionts can increase the ecological opportunity of mixotrophic hosts, allowing an expansion of their realized niche (Dubilier et al., 2008; Moran, 2006).

Chemosymbiotic interactions are widespread within the Bivalvia, phylogenetically and geographically (Roeselers & Newton, 2012). The prevalence of chemosymbiosis in bivalves, as well as the diversity and antiquity of these relationships, are likely to indicate that the establishment of symbiosis exerted an important influence in the emergence and diversification of higher bivalve taxa (Distel, 1998). Usually, bivalves harbour the bacterial symbionts in enlarged, simplified gills, and they have a rudimentary or absent digestive system (Cavanaugh et al., 2006; Roeselers & Newton, 2012; Taylor & Glover, 2010). Chemosymbiotic associations have been reported in six families of bivalves, namely: Solemidae, Nucinellidae, Mytilidae, Thyasiridae, Lucinidae and Vesicomydae (Taylor & Glover, 2010). It is obligate for all the species in Solemidae, Lucinidae and Vesicomyidae, whereas in Mytilidae, chemosymbiosis is limited to the subfamily Bathymodiolinae. The less understood groups are the Nucinellidae, where symbiosis has only been inferred from internal morphology, and the Thyasiridae, which contains both symbiotic and asymbiotic species (Taylor, Williams, & Glover, 2007).

The Thyasiridae is likely a monophyletic family with a recent origin, the first members being recognized from the Early Cretaceous (from 145 to 100 Ma) (Taylor & Glover, 2010; Taylor et al., 2007). Symbiotic thyasirids acquire their bacterial partners via environmental transmission from free-living populations of symbiotic bacteria (Batstone & Dufour, 2016; Dufour et al., 2014). Hosts maintain the bacterial symbionts extracellularly within the subfilamentar tissue of their gills, as opposed to all other known bivalves that harbour them intracellularly within specialized gill cells (Dando & Southward, 1986; Dufour, 2005). Furthermore, thyasirid hosts appear to vary widely in their nutritional reliance on symbionts (Dando & Spiro, 1993; Dufour & Felbeck, 2006). These features suggest a symbiotic interaction that is not fully integrated, indicating that the relationship between symbiotic thyasirids and chemosynthetic bacteria is at an early evolutionary stage (Batstone & Dufour, 2016; Roeselers & Newton, 2012). As such, the Thyasiridae stand out as an exceptional group to investigate chemosymbiosis (Taylor & Glover, 2010).

Thyasirids exhibit a variety of feeding strategies. Some asymbiotic species mainly rely on suspension feeding, obtaining nutrients through an inhalant tube constructed with their foot (Allen, 1958). Other asymbiotic thyasirids are deposit feeders, using the surface of the foot first to collect particulate organic matter, transfer it into the mantle cavity and then deposit it in the mouth (Reid, McMahon, Foighil, & Finnigan, 1992). Symbiotic thyasirids are flexible mixotrophs: they have nutritional input from suspension feeding but mainly rely on combining deposit feeding on free-living bacteria with predation on their bacterial symbionts, which are periodically endocytosed and digested (Dufour et al., 2014). Symbiotic thyasirids appear to consume their symbionts depending on environmental conditions, particularly the presence of sulphide and particulate food in the sediment (Dando & Spiro, 1993; Dufour & Felbeck, 2006). This mixotrophic nutrition is considered a strategy that allows symbiotic thyasirids to thrive in fluctuating environments (Dufour & Felbeck, 2006; Duperron et al., 2013). Both symbiotic and asymbiotic thyasirids construct ramifying burrows (Dufour & Felbeck, 2003; Zanzerl & Dufour, 2017). These tunnels, termed pedal tracts, consist of one or more channels, each made by insertions of their muscular foot in the sediment (Fig. 1.1), which in some species can extend up to 30 times the length of the shell (Dufour & Felbeck, 2003; Zanzerl & Dufour, 2017). In some asymbiotic thyasirids, the burrowing behaviour indicates microbial farming and pedal (deposit) feeding, in which the bivalves farm sulphur-oxidizing bacteria in the tunnel linings and collect them using their foot (Zanzerl, Salvo, Jones, & Dufour, 2019). Conversely, in chemosymbiotic thyasirids, empirical evidence suggests that the burrows are structures to mine sulphide from the interstitial water, which is required by the symbionts (Dufour & Felbeck, 2003).

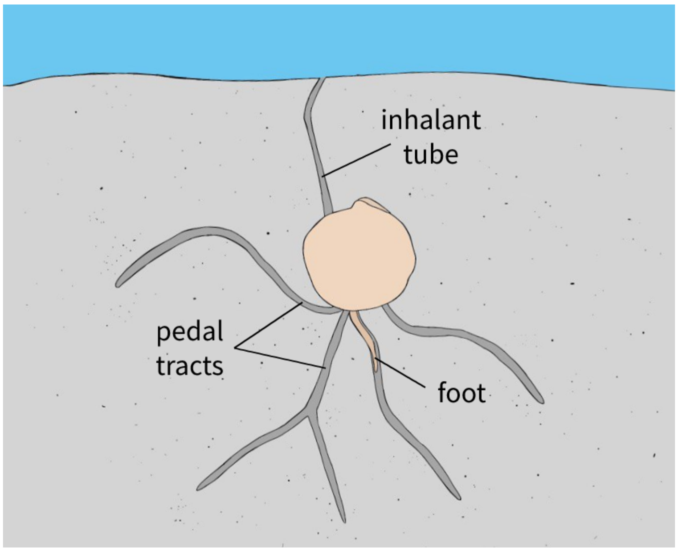

Figure 1.1. Thyasirid habit, showing the inhalant tube and branching pedal tracts (burrows) constructed with the foot. Some thyasirids can gain nutrition by suspension feeding, circulating oxygenated water and particulate organic matter through the inhalant tube (Allen, 1958). Some asymbiotic thyasirids are deposit feeders, using their foot to collect organic material from the pedal tracts (i.e., pedal feeding) (Zanzerl, Salvo, Jones, & Dufour, 2019). Moreover, thyasirids may use the pedal tracts for microbial farming along the tunnel lining (Zanzerl, Salvo, Jones, & Dufour, 2019). Symbiotic thyasirids can use the pedal tracts to acquire the sulphide required by their chemosymbiotic bacteria from the sediment (Dufour & Felbeck, 2003). Illustration not to scale.

Thyasirids have a cosmopolitan distribution in marine waters, living infaunally in the deep sea (i.e. cold seeps, whale falls and hydrothermal vents) or in soft, oxygen-poor and sulphide-rich sediments (e.g., shallow-water sea-grass sediments; Dubilier et al., 2008). As other burrowing bivalves, they are most abundant in sediments that have a sparse infauna, which has been attributed to the bioturbation that other burrowers produce, that disrupts the tunnel system and decreases the ability of the thyasirids to obtain sulphide (Dando, Southward, & Southward, 2004; Dufour & Felbeck, 2003). Two species of thyasirids are sympatric within the fjord of Bonne Bay (Newfoundland, Canada, Fig. 1.2), an environment that experiences strong seasonal cycles (Laurich, Batstone, & Dufour, 2015). The first species resembles *Thyasira gouldi* (in shell characteristics and internal anatomy) and therefore is referred to as *Thyasira* cf. *gouldi*. The second species, *Parathyasira* sp., is asymbiotic (Fig. 1.3; Batstone, Laurich, Salvo, & Dufour, 2014). The sympatry of these related species in Bonne Bay represents an outstanding opportunity to compare how different nutritional strategies can produce physiological differences, particularly in a habitat with seasonal forcing.

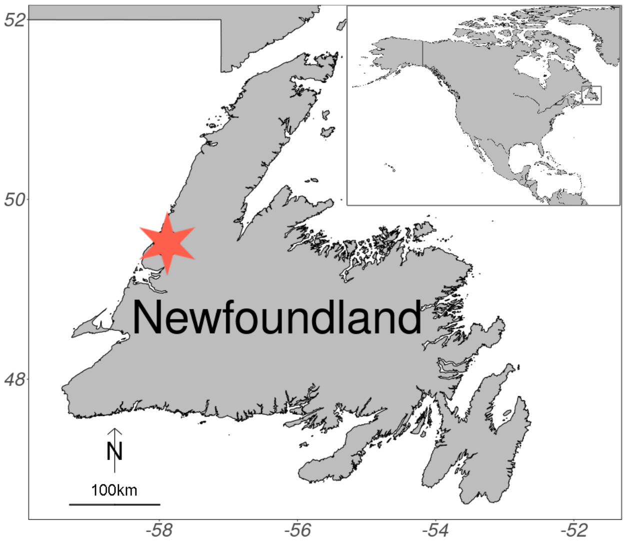

Figure 1.2. Map of the location of the fjord of Bonne Bay (Newfoundland, Canada), where the symbiotic *Thyasira* cf. *gouldi* and the asymbiotic *Parathyasira* sp. are sympatric. Individuals collected from this location are used as a case study in Chapters 3 and 4.

Figure 1.3. The asymbiotic *Parathyasira* sp. (left) and the symbiotic *Thyasira* cf. *gouldi* (right) collected from Bonne Bay (Newfoundland, Canada. Fig. 1.2), which are used as a case study in Chapters 3 and 4. Symbiotic *T.* cf. *gouldi* are mixotrophs, combining nutrition obtained from chemosymbiotic bacteria with organic matter and free-living bacteria from the sediment. In contrast, *Parathyasira* appears to rely more on the free-living bacteria, likely through microbial gardening along the pedal tracts (Zanzerl, Salvo, Jones, & Dufour, 2019). The scale bar is 2 mm, approximately.

Thyasira cf. *gouldi* forms a complex of cryptic species. This species complex has been provisionally described as three Operational Taxonomic Units (OTUs) according to consistent differences in shell shape and gill filament morphology, as well as variability in nuclear and mitochondrial gene sequences (Batstone et al., 2014). The complex of *T.* cf. *gouldi* displays a unique condition among bivalves that appear to belong to the same species: two of the OTUs are symbiotic and closely related with each other, while the third one is asymbiotic (Batstone et al., 2014). Symbiotic *T.* cf. *gouldi* (OTUs 1 and 2) associate with up to three 16S rRNA bacterial phylotypes (McCuaig, Liboiron, & Dufour, 2017), and epithelial gill cells have been shown to endocytose the bacteria, similar to other bivalves where this process is a pathway for nutrient transfer (Dufour & Felbeck, 2006). Symbiotic *Thyasira* cf. *gouldi* OTUs can only be distinguished based on their differences in nuclear and mitochondrial gene sequences, while the asymbiotic OTU can be identified according to shell outline and gill anatomy (Batstone et al., 2014). For this reason, in Chapters 3 and 4 of this thesis, I consider both symbiotic *Thyasira* cf. *gouldi* without discerning between OTUs 1 and 2.

1.5 SCALES OF VARIATION IN ECOPHYSIOLOGICAL RESPONSES AND ADAPTATIONS

The patterns emerging from the interaction between the organisms and the environment can be typically analyzed at different scales, namely: intraspecific, interspecific and assemblage-based (Gaston et al., 2008; Yom-Tov & Geffen, 2011). Intraspecific studies focus on explaining patterns in individual species' traits (e.g., fecundity according to the food supply in *Daphnia pulex*; McCauley, Murdoch, & Nisbet, 1990). Interspecific (or cross-species) research addresses the differences in the pattern of variation in the trait of interest among species, usually within the same clade or taxon (e.g., global variation in avian clutch size; Jetz, Sekercioglu, & Böhning-Gaese, 2008). Finally, the assemblage or community approach describes trait patterns in communities across different places (e.g., the latitudinal variation of body size in *Plethodon* salamanders' assemblages in North

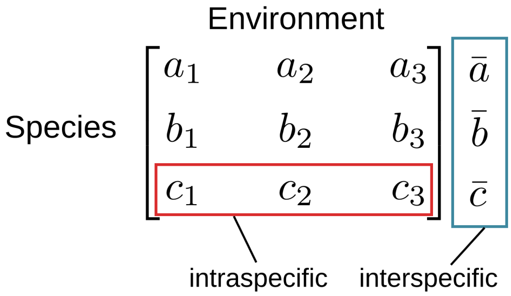

Figure 1.4. In this thesis, I address both intraspecific (Chapter 2) and interspecific differences (Chapters 2, 3 and 4). I consider resource abundance as the main environmental variable promoting intraspecific and interspecific variability. First, I focus on passive intraspecific and interspecific responses to resource abundance, particularly seasonal changes (Chapter 2). Then, I examine interspecific adaptations to resource seasonality, specifically nutritional symbiosis between two species of thyasirid bivalves (Chapters 3 and 4).

America; Olalla-Tárraga, Bini, Diniz-Filho, & Rodríguez, 2010). Gaps and biases in the knowledge of trait data among species make studies considering the interspecific approach scarcer than those regarding intraspecific or assemblage variation (Gaston et al., 2008). Additionally, even in the most well-studied species (e.g., the house sparrow, *Passer domesticus*, and the fruit fly, *Drosophila melanogaster*), the origin of different traits from constraints and trade-offs have rarely been explicitly studied jointly (Gaston et al., 2008). Hence, there is still uncertainty in the mechanisms structuring intraspecific and interspecific variation, hindering our capacity to forecast species responses and understand adaptive strategies.

In this thesis, I focus on intraspecific (Chapter 2) and interspecific (Chapters 2, 3 and 4) differences with respect to resource abundance (Fig. 1.4). Research at the intraspecific level allows understanding the mechanisms underpinning how traits respond jointly under different environmental conditions. In contrast, investigating interspecific responses in related species exposes the variation in a given trait along with particular environmental predictors. Moreover, exploring interspecific adaptations reflect the alternative evolutionary strategies to cope with certain environmental scenarios.

Conclusions regarding ecophysiological responses and adaptations depend on the choice of the trait(s) and environmental covariate(s) (Brommer, 2013). In this sense, plasticity assessments are typically focused on how traits with a priori established significance can respond to changes along an environmental gradient (Forsman, 2015). However, understanding the effect of environmental predictors on plasticity is complicated by several confounding factors. For example, the use of phenotypic data may lead to the inability to discriminate between genetic (adaptive, in particular) and non-genetic (plastic) sources of variation (Stillwell, 2010). A proposed solution to avoid these issues is to perform analyses under a wide range of environmental conditions or in contrasting environments while simultaneously reducing confounding factors (e.g., as in the classical experiments from Clausen, Keck, Hiesey, et al., 1948; Turesson, 1922), such as common-garden or reciprocal transplant experiments (Yom-Tov & Geffen, 2011). Nevertheless, these experiments are typically not feasible because they involve large samples and individuals' long-term monitoring (Teplitsky & Millien, 2014). For this reason, modelling approaches are major tools to investigate phenotypic responses and adaptations by assessing their physiological origin without such confounding effects. Thus, in this thesis, I rely on a mechanistic description of the individual metabolism to quantify the environment's impact on species traits and strategies.

1.6 DYNAMIC ENERGY BUDGET THEORY AS AN APPROACH TO DISENTANGLE RESPONSES AND ADAPTATIONS TO SEASONALITY

The restrictions on organisms' rate of energy input are the core of life history trade-offs because the amount of energy that any given organism can acquire and process is limited throughout their lifetime (Weiner, 1992). In this context, models that consider individual energy budgets are powerful tools to understand how energetic constraints, mainly imposed by the environment, can affect species (Kearney & White, 2012). Energy budget models describe the rates at which an individual assimilates and uses energy and nutrients for maintenance, growth, and reproduction, depending on the state of the organism (characterized by variables like its age and size) and its environment (e.g., food availability, temperature Nisbet, Jusup, Klanjscek, & Pecquerie, 2012; van der Meer, 2006). Within this framework, the Dynamic Energy Budget (DEB) theory is relevant because it integrates quantitative aspects of individual metabolism associated with life history processes (Kooijman, 2010).

DEB theory provides a characterization of the life cycle of an organism through a model that describes the links between the metabolic processes throughout the lifespan of the individual (Nisbet et al., 2012). Among its many applications, DEB theory has been proposed as a natural approach to describe systems that involve internal symbionts (Muller, Kooijman, Edmunds, Doyle, & Nisbet, 2009), or those constrained by environmental fluctuations (Kearney & White, 2012). However, it has not been previously applied in the research of chemosymbiotic interactions or in understanding the general drivers of phenotypic flexibility. Throughout this dissertation, I rely on the mechanistic description of the individual metabolism and energy allocation provided by the DEB model. I use this framework to link the environmental dynamics to the individual's physiological performance and processes that occur at higher biological levels. Given that physiological processes can be considered the basis of individuals' ecological dynamics (Nisbet et al., 2012), they ultimately help understand the system's emergent properties.

In the DEB model, differences between species metabolic processes are specified by the differences in their parameter values. This provides a "definition" of species based on their parameter values, with the implicit assumption that intraspecific variation can be practically ignored because it is much smaller than interspecific variation. In this dissertation, I take advantage of this species "definition" in two ways. First, in Chapter 2, I reproduce the natural patterns of interspecific variation by simulating different parameter combinations that correspond to different species. Then, I quantify the environment's effect on the traits across individuals and “species”. This approach allows evaluating intra- and interspecific flexibility without confounding factors, particularly non-genetic sources of variation (i.e., developmental noise or plasticity). Second, in Chapter 3, I estimate the model parameters for two related species of thyasirid bivalves. The resulting dissimilarities in the species’ parameters serve to make inferences on their feeding strategies: symbiotic and asymbiotic nutrition. Moreover, in Chapter 4, I use these parameters to predict the population dynamics of both species and investigate how they differ according to their nutrient acquisition strategy. Thus, in this thesis, individual energetics, as specified by the DEB model, are the key to unravel the multiple consequences of a seasonal environment across levels of biological organization.

2

RESOURCE AND SEASONALITY DRIVE INTERSPECIFIC VARIABILITY IN A DYNAMIC ENERGY BUDGET MODEL

Joany Mariño, Suzanne C. Dufour, Amy Hurford, Charlotte Récapet

Animals show a vast array of phenotypic traits in time and space. These variation patterns have traditionally been described as ecogeographical rules; for example, the tendency of body size and clutch size to increase with latitude (Bergman's and Lack's rules, respectively). Despite considerable research into these patterns, the processes behind trait variation remain controversial. Here, we show how food variability, which determines individual energy input and allocation trade-offs, can drive interspecific trait variation. Using a dynamic energy budget (DEB) model, we simulated different food environments as well as interspecific variability in the parameters for energy assimilation, mobilization, and allocation to soma. We found that interspecific variability in biomass and reproduction is greater when the resource is non-limiting, in both constant and seasonal environments. Our findings further show that individuals can reach larger biomass and greater reproductive output in a seasonal environment than in a constant environment of equal average resource because of food surplus peaks. Our results corroborate the classical patterns of interspecific trait variation and provide a mechanistic understanding that supports recent explanatory hypotheses: the resource and the eNPP (net primary production during the growing season) rules. Due to the current alterations to ecosystems and communities, disentangling trait variation is increasingly important to understand and predict biodiversity dynamics under environmental change.

2.1 INTRODUCTION

The variation in life-history traits in animal species across temporal and spatial scales is vast (Healy et al., 2019). Despite considerable research describing these traits' patterns of occurrence, a systematic understanding of the underlying mechanisms and processes remains elusive (Gaston et al., 2008). Disentangling and quantifying variation in biological traits is necessary to explain and predict biodiversity dynamics under environmental change (Cabral et al., 2017; Cardilini et al., 2016), and it may aid in answering broad questions that range from the invasive potential of species (Capellini, Baker, Allen, Street, & Venditti, 2015) and the evolution of senescence (Jones et al., 2014), to predicting the influence of stressors on species assemblages (Darling, Alvarez-Filip, Oliver, McClanahan, & Côté, 2012). Hence, it is fundamental to understand the underlying mechanisms giving rise to animal trait variation.

Among animal traits, body size exhibits substantial diversity within orders and narrower clades of animals, presumably playing a pivotal role in all individual's ecological and physiological processes (Kozłowski, Konarzewski, & Czarnoleski, 2020; Yom-Tov & Geffen, 2011). Variation of body size in time and space is assumed to be a product of evolution modulated by the biotic and abiotic environment (Mayr, 1956; Millien et al., 2006; Yom-Tov & Geffen, 2011). Additionally, body size tends to covary with several life history and morphological traits (Olalla Tárraga et al., 2019). For example, birds' body size is thought to be positively correlated with clutch size (Jetz et al., 2008; Olalla Tárraga et al., 2019). Although there is extensive evidence describing and supporting spatial patterns in body size and reproductive output at different biological scales, the processes that underpin their variation are not fully comprehended (Gaston et al., 2008).

The consistent variation in animal traits across time and space, both within and among species or clades, forms the basis of 'ecogeographical rules' (Boyer & Jetz, 2010; McNab, 2010). Two of the most frequently explored interspecific patterns are the increase of body size in closely related endotherms (and some ectotherms) with latitude ("Bergman's rule"), and the tendency of clutch size to increase with latitude ("Lack's rule"). In general, empirical evidence in endotherms supports both patterns (e.g., for Bergman's rule see Ashton 2002; Ashton, Tracy, and de Queiroz 2000; Blackburn and Hawkins 2004; Cardillo 2002; Clauss, Dittmann, Müller, Meloro, and Codron 2013; Freckleton, Harvey, and Pagel 2003; Morales-Castilla, Olalla-Tárraga, Purvis, Hawkins, and Rodríguez 2012a; Morales-Castilla, Rodríguez, and Hawkins 2012b; Olalla-Tárraga and Rodríguez 2007; Olson et al. 2009; Ramirez, Diniz-Filho, and Hawkins 2008; Rodríguez, López-Sañudo, and Hawkins 2006; Rodríguez, Olalla-Tárraga, and Hawkins 2008; Romano, Séchaud, and Roulin 2020; Torres Romero, Morales Castilla, and Olalla Tárraga 2016 and reviews in Huston and Wolverton 2011; Meiri and Dayan 2003; Watt, Mitchell, and Salewski 2010. For Lack's rule see Ashmole 1963; Cody 1966; Evans, Duncan, Blackburn, and Crick 2005; Griebeler and Böhning-Gaese 2004; Iverson, Balgooyen, Byrd, and Lyddan 1993; Jetz et al. 2008; Kulesza 1990; Lack 1947; Meiri et al. 2020; Mesquita et al. 2016; Moreau 1944; Ricklefs 1980, and review in Boyer, Cartron, and Brown 2010. See Gohli and Voje 2016; Medina, Martí, and Bidau 2007; Meiri, Dayan, and Simberloff 2004; Olalla-Tárraga and Rodríguez 2007 for contradictory or ambiguous results). Bergman suggested that a larger body is an adaptation to colder environments because larger organisms have a lower surface-area ratio than smaller organisms, which allows them to conserve heat more effectively (Salewski & Watt, 2017). Lack attributed the larger clutch size in northern species than those in the tropics to a greater food abundance and longer daylight periods during the breeding period (Lack, 1947). These hypotheses, however, remain highly controversial, and several alternative mechanisms have been proposed (Blackburn, Gaston, & Loder, 1999; Jetz et al., 2008; Meiri, 2011; Olalla-Tárraga, 2011; Pincheira-Donoso, 2010; Searcy, 1980; Stearns, 1976).

Recent hypotheses have explained the variation in body size, reproductive output, and life-history traits based on food availability (Huston & Wolverton, 2011; McNab, 2010). In the "resource rule", Bergman's and Lack's patterns are determined by the size, abundance, and availability of food (McNab, 2010). The "eNPP rule" (or "Geist's rule") further explains that the mechanism driving food availability is the global distribution of net primary productivity during the growing season (eNPP) (Geist, 1987; Huston & Wolverton, 2011). Thus, both hypotheses agree that, in species or groups of closely related species, the largest and with greater reproductive output will occur where food availability (or eNPP) is highest (Huston & Wolverton, 2011; McNab, 2010).

According to the resource and eNPP rules, food availability variation should be the main determinant of energy input (Huston & Wolverton, 2011; McNab, 2010). Thus, we hypothesize that resource availability drives individual energy allocation trade-offs among different life-history traits, particularly body size or mass and reproductive output. Consequently, if food availability is the critical factor determining individual energy allocation, then trait variability would be minimal when the resource becomes limiting, both in a constant or seasonal environment. Hence, for species with limited phenotypic plasticity, we expect that individuals in a low food environment will exhibit more similar body mass and reproductive output than in a higher food environment. Further, when the resource is seasonal, the periods of food surplus should allow individuals to reach a large body size and have greater fecundity, in agreement with the eNPP rule (Huston & Wolverton, 2011). Therefore, we predict that individuals in a seasonal environment should reach a larger body mass and have a greater reproductive output relative to the same organism in an environment with the same average but constant resource.

Research into patterns of trait variation (particularly over large spatial scales) typically expose the variation using some measure of central tendency in the trait of interest concerning particular environmental predictors (Gaston et al., 2008). These patterns are generally approached at three main levels: intraspecific, interspecific, and assemblage-based (Gaston et al., 2008; Yom-Tov & Geffen, 2011). Intraspecific studies focus on explaining patterns in individual species' traits (e.g., fecundity according to the food supply in *Daphnia pulex*; McCauley et al., 1990). Interspecific (or cross-species) research addresses the differences in the pattern of variation in the trait of interest among species, usually within the same clade or taxon (e.g., global variation in avian clutch size; Jetz et al., 2008). Finally, the assemblage or community approach describes traits patterns in communities across different regions (e.g., the latitudinal variation of body size in *Plethodon* salamanders' assemblages in North America; Olalla-Tárraga et al., 2010). Gaps and biases in the knowledge of trait data among species make studies considering the interspecific approach scarcer than those regarding intraspecific or assemblage variation (Gaston et al., 2008). Additionally, the methodological distinction between interspecific and assemblage patterns is often overlooked or confused (Gaston et al., 2008; Olalla-Tárraga et al., 2010). Hence, there is still uncertainty in the mechanisms structuring interspecific variation, hindering our capacity to forecast cross-species responses.

Understanding the effect of environmental predictors on the interspecific variation of body size is complicated by several confounding factors. For example, the use of phenotypic data may lead to the inability to discriminate between genetic (adaptive) and non-genetic (plasticity) sources of variation (Stillwell, 2010). Additionally, the growth conditions can have a strong effect on body size, for which it would be necessary to control for the birth year (Hersteinsson, Yom-Tov, & Geffen, 2009; Yom-Tov & Geffen, 2006; Yom-Tov et al., 2010). A proposed solution to avoid these issues is to conduct common-garden or reciprocal transplant experiments (Yom-Tov & Geffen, 2011). However, these experiments are typically not feasible because they involve large samples and long-term monitoring of individuals (Teplitsky & Millien, 2014). Accordingly, we adopted a modelling approach that allowed us to investigate interspecific variation in traits by assessing their physiological basis without such confounding effects. To test our predictions, we used the ecophysiological description of the individuals proposed by Dynamic Energy Budget (DEB) theory (Kooijman, 2010). In the DEB model, the parameters represent the physiological processes that, together with the environmental conditions, result in different individual traits. The combination of parameter values in the DEB model defines species, and because it has been parameterized for over 2000 animal species (see AmP, 2020, for the complete list), it allowed us to reproduce the natural variation observed in experimental data across species. In this way, we rely on a mechanistic description of the individual metabolism and energy allocation to quantify the environment's effect on cross-species traits.

We evaluated interspecific variability in genetically-determined physiological characters (represented by the model parameters for assimilation, mobilization and allocation of energy) by carrying out numerical simulations of the DEB model and quantifying the differences in individual traits (i.e., biomass, maturity, and reproduction). We considered both constant and seasonal resource conditions in order to provide a complete description of the effect of food availability. We found that resource determines the expression of interspecific differences in the DEB model in both constant and seasonal environments. Further, individuals in a seasonal environment reach a larger body mass and have greater fecundity compared to the same individuals in an environment with an equal average but constant food. Thus, our simulations with the DEB model agree with the expectations according to the resource and eNPP rules and provide a mechanism supporting these hypotheses.

2.2 MATERIALS AND METHODS

To test our prediction regarding the role of resource, we represented interspecific differences with different sets of parameter values and conducted simulations of the DEB model assuming different constant environments. To test our prediction about resource seasonality, we simulated the same interspecific variation in the DEB model but assuming a periodically fluctuating resource. Thus, we evaluated the same set of parameters, each representing a species, both with constant and seasonal resource availability. We then compared the dynamics of two species to highlight the differences due to the resource regime.

2.2.1 The standard DEB model

We focus our analysis on the standard DEB model, which is the simplest non-degenerated model implied by DEB theory and the most commonly analyzed DEB model (Lika et al., 2011a). The standard DEB model applies to heterotrophic animals, and it supposes that the biomass of an individual is partitioned into reserve energy and structural volume (Kooijman, 2010). Hence, four state variables describe individuals: energy in reserve (E, J), structural volume (V, cm^3), cumulative maturity energy (E_H, J), and cumulative reproduction energy (E_R, J). We assume that individuals release the reproduction energy continually as gametes, regardless of the environmental conditions, to neglect its potential contribution to the individuals' biomass. To compensate for the different possible reproduction strategies, we measure reproductive output as lifetime cumulative reproductive energy.

The DEB model assumes that energy from food is assimilated into the reserve (Fig. 2.1) through the assimilation flux ($\dot{p}_A$, J/d). The reserve energy is mobilized according to the mobilization flux ($\dot{p}_C$, J/d). A fixed fraction (κ) of the mobilized reserve is allocated to somatic maintenance and volume growth ($\dot{p}_C - \dot{p}_S$, J/d). The remaining fraction of the mobilized energy ($1 - \kappa$) is allocated to maturity maintenance and maturation in juvenile individuals or maturity maintenance and reproduction in adults ($\dot{p}_C - \dot{p}_J$, J/d). Thus, the temporal dynamic of the individual state variables is:

$$\begin{aligned} \frac{dE}{dt} &= \dot{p}_A - \dot{p}_C, \\ \frac{dV}{dt} &= \kappa(\dot{p}_C - \dot{p}_S)/[E_G], \end{aligned} \tag{2.1}$$

$$
\begin{cases}
\dfrac{dE_H}{dt} = (1-\kappa)\dot{p}_C - \dot{p}_J \text{ and } \dfrac{dE_R}{dt} = 0, & \text{if } (E_H < E_H^p), \\[2em]
\dfrac{dE_H}{dt} = 0 \text{ and } \dfrac{dE_R}{dt} = (1-\kappa)\dot{p}_C - \dot{p}_J, & \text{otherwise,}
\end{cases}
$$

where $[E_G]$ is the volume-specific cost for structure, and the energy fluxes $\dot{p}_i$ for each process i are given in Table 1. The standard DEB model considers organisms with three life stages, as determined by the cumulative maturity level relative to the maturity thresholds parameters, E_H^b for birth and E_H^p for puberty: embryo ($E_H \leq E_H^b$ and $E_H < E_H^p$), juvenile ($E_H > E_H^b$ and $E_H < E_H^p$), and adult ($E_H > E_H^b$ and $E_H \geq E_H^p$).

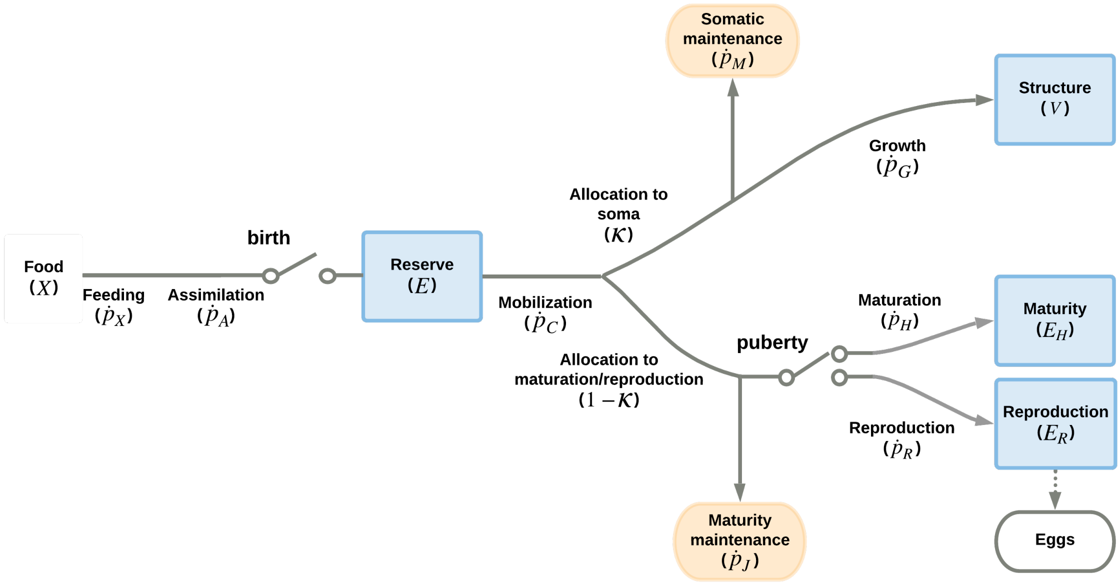

Figure 2.1. Representation of the standard DEB model (eq. 4.7). Square boxes denote the state variables, while round boxes represent energy sinks. Lines and arrows correspond to the energy fluxes ($\dot{p}_i$ J/d, Table 4.1). The switches represent metabolic thresholds: birth indicates the start of feeding, while puberty signals the start of energy allocation to reproduction once maturation is complete.

The mobilization flux ($\dot{p}_C$) includes the specific growth rate in structural volume:

$$\dot{r} = \frac{\kappa \frac{E}{V^{4/3}} \dot{v} \mathcal{M} - [\dot{p}_M]}{\kappa \frac{E}{V} + [E_G]}, \tag{2.2}$$

where $\dot{v}$ is the energy reserve mobilization rate (cm^3/d), and $[\dot{p}_M]$ are the volume-specific somatic maintenance costs ($J/d \cdot cm^3$).

Table 2.1. Energy fluxes ($\dot{p}$, J/d) at each developmental stage. The scaled functional response is f ($0 \leq f \leq 1$, where 1 is the highest amount of food), $\{\dot{p}_{\mathrm{Xm}}\}$ is the maximum surface-area specific ingestion rate ($\{\dot{p}_{\mathrm{Xm}}\} = \{\dot{p}_{\mathrm{Am}}\}/\kappa_X$, J/d · cm^2), $\{\dot{p}_{\mathrm{Am}}\}$ is the maximum surface-area specific assimilation rate (J/cm^3 · d), κ_X is the assimilation efficiency from food to reserve (dimensionless), $\dot{v}$ is the energy conductance rate from the energy reserve (cm^3/d), $[\dot{p}_M]$ is the volume-specific somatic maintenance cost (J/d · cm^3), $\dot{k}_J$ is the maturity maintenance rate coefficient (1/d). Notation: square braces ([ ]) indicate quantities related to structural volume, curly braces ({ }) denote quantities related to structural surface-area, dots (˙) indicate rates.

Flux	Embryo	Juvenile	Adult
	$(E_H \leq E_H^b)$	$(E_H^b > E_H < E_H^p)$	$(E_H \geq E_H^p)$
Feeding, $\dot{p}_X$	0	$f\{\dot{p}_{\mathrm{Xm}}\}$	$f\{\dot{p}_{\mathrm{Xm}}\}$
Assimilation, $\dot{p}_A$	$\kappa_X \dot{p}_X$	$\kappa_X \dot{p}_X$	$\kappa_X \dot{p}_X$
Mobilization, $\dot{p}_C$	$E\dot{v}(V^{-1/3} - \dot{r})$	$E\dot{v}(V^{-1/3} - \dot{r})$	$E\dot{v}(V^{-1/3} - \dot{r})$
Somatic maintenance, $\dot{p}_S$	$[\dot{p}_M]V$	$[\dot{p}_M]V$	$[\dot{p}_M]V$
Maturity maintenance, $\dot{p}_J$	$\dot{k}_J E_H$	$\dot{k}_J E_H$	$\dot{k}_J E_H^p$

In the DEB model, both somatic and maturity maintenance have priority over investment in either growth, maturation, or reproduction. Hence, starvation occurs when mobilized energy does not suffice to cover somatic maintenance ($\kappa \dot{p}_C < \dot{p}_S$) or maturity maintenance ($(1-\kappa)\dot{p}_C < \dot{p}_J$). The standard DEB model makes no assumptions about these situations, meaning that organisms follow the same dynamics previously outlined when subjected to starvation. Consequently, when there is prolonged starvation, individuals will degrade the structural mass to cover maintenance costs and shrink in size (because the specific growth rate $\dot{r}$ becomes negative).

DEB theory assumes that the metabolic rates are affected by the environmental temperature (Kooijman, 2010). Consequently, the model parameters are usually standardized to the reference temperature of 20 °C through the Arrhenius relationship. For simplicity, however, we suppose that the environmental temperature is equal to the reference temperature ($T = 293.15$ K). Moreover, endothermy can be included as an additional somatic maintenance cost. Given that we consider fixed somatic maintenance costs, the predictions should not vary between endotherms and ecotherms. Further, because food availability often covaries with environmental temperature, we assume that the temperature remains constant and evaluate the effect of seasonality only in the resource.

2.2.2 Resource

We assumed that the food density operates directly on the scaled functional response f, facilitating contrasting the model's behaviour across different fluctuation regimes (Muller & Nisbet, 2000). To investigate the effect of interspecific differences, we first conducted simulations assuming a constant resource, ranging from scarce ($f = 0.2$) to maximum availability ($f = 1$). We did not evaluate prolonged periods of limited food because this would require making further assumptions on the handling of starvation.

To evaluate the effect of resource variability, we assumed a periodically changing functional response, which represents the alternation between two levels of food during the year, similar to a seasonal change. Specifically, the functional response at time t oscillates around the average ($\bar{f}$) with amplitude f_a and period equal to the length of one year:

$$f(t) = \bar{f} + f_a \sin\left(2\pi \frac{t}{365}\right). \tag{2.3}$$

We only consider variations in the value of the mean scaled functional response for simplicity, keeping the amplitude of the oscillations fixed. To assess the initial resource's effect, we simulated functional responses that start at four different points in the seasonal cycle: maximum resource, intermediate but decreasing resource, minimum resource, and intermediate but increasing resource. These different initial conditions of food can be understood as corresponding to individuals born at different times throughout the year.

2.2.3 Interspecific variability and parameter space

Despite the diversity of life-history traits and strategies in the animal kingdom, not all strategies are possible (Healy et al., 2019). In order to select a biologically consistent parameter set, we used the AmP collection (a web repository of species parameterized for DEB models; AmP, 2020) and the routines in the AmPtool (version 03/2020 AmPtool, 2020) MATLAB package (version 9.8, The MathWorks Inc., 2020). We started by taking a subset of the species in the AmP collection (Fig. 2.2, panel 1). Then we narrowed down the parameter space according to the occurrence frequency of the parameter combinations (Fig. 2.2, panel 3).

First, our focus was on the species in the AmP collection (Fig. 2.2, panel 1). We selected the species modelled using the standard DEB model and containing lifespan data. To ensure values were consistent, we restricted the entries to those with a lifespan < 100 years and data completeness ≥ 2.5. The data completeness indicates how much data is available to estimate the DEB parameters, ranging from a minimum of 0 when only maximum body weight or size is known, to a maximum of 10 when all aspects of energetics are known (Lika et al., 2011a). Completeness of 2.5 means that there is data for the species on maximum body weight (or size), age, length and weight at birth and puberty, and growth in time ((Lika et al., 2011a)); allowing the estimation of the parameters $\dot{v}$, $\{\dot{p}_{\mathrm{Am}}\}$, $[\dot{p}_M]$, E_H^b and E_H^p (Kooijman et al. 2008). Then, we removed parameter outliers by excluding values 1.5 interquartile ranges above the upper quartile or below the lower quartile of each parameter distribution, which left 216 species.

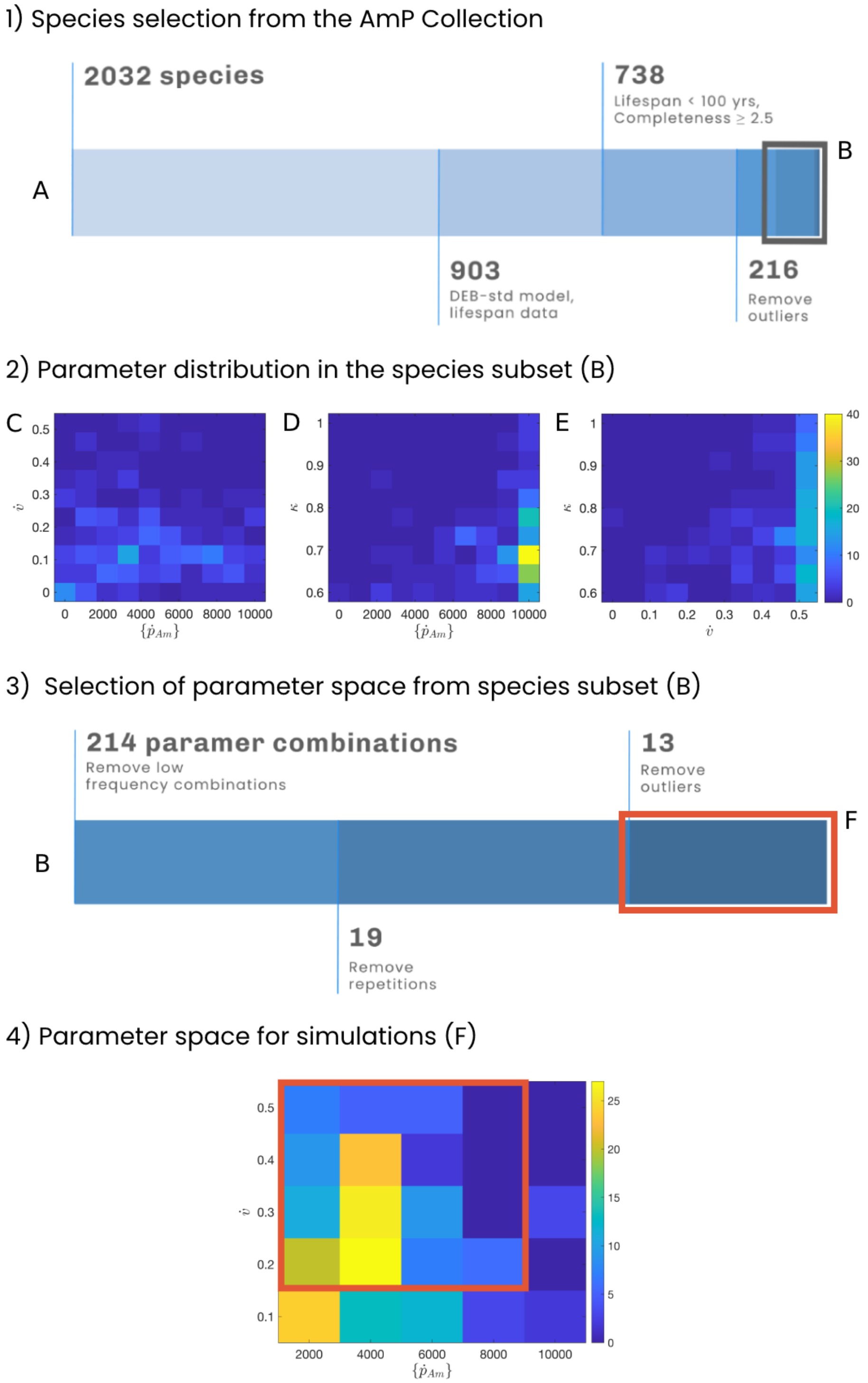

Figure 2.2. Representation of the selection process that assured biological consistency in the parameter space. See the figure caption in the next page.

Figure 2.2. (Previous page) Panel 1 shows the species selection in the AmP collection, starting from all the entries (at 03/2020) to a final subset of 216 species (B). The values indicate the number of species at each step. The steps are: i) subset entries modeled with the DEB-std model and containing lifespan data, ii) subset entries with lifespan below 100 years and data completeness equal or greater than 2.5, and iii) remove entries more than 1.5 interquartile ranges above the upper quartile or below the lower quartile of the parameter distribution. In panel 2, the plots show the bivariate distribution of the parameters $\{\dot{p}_{\mathrm{Am}}\}$, $\dot{v}$, and κ in our 216 species subset (B). For all the plots, the parameters' distribution is not uniform. Hence, all parameter combinations are not equally likely to occur. The colour bar shows the joint frequency of occurrence. Panel 3 shows the selection of the joint parameter space for $\{\dot{p}_{\mathrm{Am}}\}$ and $\dot{v}$ from the species subset B. The values at each step show the number of parameter combinations, starting from 214 to a final subset of 13 parameter combinations (C). The steps are: iv) find the joint distribution of the parameters and remove parameter combinations with a frequency of one, v) remove parameter combinations that are not unique, and vi) remove outlier values. In panel 4, the plot shows the joint distribution of $\{\dot{p}_{\mathrm{Am}}\}$ and $\dot{v}$ for the 214 parameter combinations more likely to occur in our species subset. The box marks the outer boundary of our parameter space in our parameter combination subset (C). Without repetitions, the parameter space C corresponds to the 16 combinations we evaluated for $\{\dot{p}_{\mathrm{Am}}\}$ and $\dot{v}$.

Next, we concentrated on the parameters of the 216 species subset. We focused our analysis on three parameters that directly relate to concepts of life-history theory: maximum assimilation rate ($\{\dot{p}_{\mathrm{Am}}\}$), which reflects the ability to acquire energy; energy conductance ($\dot{v}$), which is related to the "pace-of-life" concept; and energy allocation to maturity and reproduction (κ), which reflects the trade-off between somatic growth and reproduction. All combinations of these three parameters in our subset of species are not equally likely to occur, they may not be biologically realistic, and multiple combinations are repeated (Fig. 2.2, panel 2). For this reason, we calculated the joint distribution of $\{\dot{p}_{\mathrm{Am}}\}$ and $\dot{v}$ by discretizing their joint range into five intervals and assigning the interval's mean as the parameter value. Subsequently, we removed the combinations of $\{\dot{p}_{\mathrm{Am}}\}$ and $\dot{v}$ with a low occurrence frequency, leaving the 214 parameter combinations most likely to occur in our species subset (Fig. 2.2, panel 3). Since these parameter combinations are not unique, we excluded the repetitions, which left 19 unique combinations of $\{\dot{p}_{\mathrm{Am}}\}$ and $\dot{v}$. Then, we removed outlier points at the edges of the discrete distribution, leaving a parameter space consisting of 13 combinations of $\{\dot{p}_{\mathrm{Am}}\}$ and $\dot{v}$. To increase our analysis's resolution, we added combinations that fell within the parameter space range but had a lower occurrence frequency. Hence, we evaluated $\dot{v}$ equal to 0.2, 0.3, 0.4, and 0.5, and $\{\dot{p}_{\mathrm{Am}}\}$ equal to 2000, 4000, 6000, and 8000, which corresponds to 16 different combinations of $\dot{v}$ and $\{\dot{p}_{\mathrm{Am}}\}$ (Fig. 2.2, panel 4).

Reproduction data is required to estimate κ, as well as growth and size at birth and puberty (Lika, Kearney, & Kooijman, 2011b). Given that reproduction is often difficult to quantify, many AmP collection entries assume the predefined value of $\kappa = 0.8$, which results in rapid growth to a large size, long development times, and low reproduction. Even when data is available, due to the simplification of seasonality effects in the data, which do not consider the cycles in up- and down-regulation of metabolism, the parameter estimation is likely to result in a high value for κ (Kooijman & Lika, 2014). Hence, the AmP collection is biased to high values for κ. However, it has been shown that a lower value of κ ($\kappa \leq 0.5$) is likely to fit growth and reproduction data equally well as the larger value, and producing individuals with reduced growth and reproduction ((Lika et al., 2011a), b). Here, we chose to evaluate variations around the lower value of κ to represent more realistic scenarios where limiting food can alter the reproductive output (Lika & Kooijman, 2003). Thus, we assessed κ equal to 0.43, 0.51, and 0.58.

We consider the rest of the model parameters as constants (Table 2.2) because previous interspecific comparisons have shown that maintenance costs and structural costs remain largely similar between species (Freitas et al., 2010; van der Veer, Kooijman, & van der Meer, 2001). To maintain biological consistency among all the parameters, we used the estimated values for *Daphnia magna*. The parameters of *D. magna* have been estimated from multiple experiments, reaching a data completeness of 6, which is the highest in the AmP collection. As such, these values are more likely to represent the individual physiology accurately.

Table 2.2. Parameter values for the simulations of the standard DEB model (equation 4.7) and the resource (equation 2.3). Notation: square braces ([ ]) indicate quantities related to structural volume, curly braces ({ }) denote quantities related to structural surface-area, dots (˙) indicate rates.

Description	Symbol	Value	Unit
Individual dynamics			
Maximum assimilation rate	$\{\dot{p}_{\text{Am}}\}$	[2000, 4000, 6000, 8000]	J/day $\cdot$ cm^2
Assimilation efficiency	κ_X	0.9	-
Energy conductance rate	$\dot{v}$	[0.2, 0.3, 0.4, 0.5]	cm/day
Allocation fraction to soma	κ	[0.43, 0.51, 0.58]	-
Somatic maintenance cost	$[\dot{p}_M]$	1800	J/day $\cdot$ cm^3
Maturity maintenance coefficient	$\dot{k}_J$	0. 52	1/day
Specific cost for structure	$[E_G]$	4400	J/cm^3
Maturity at birth	E_H^b	0.55	J
Maturity at puberty	E_H^p	1.09	J
Initial energy in the embryo	E_0	0.167	J
Shape coefficient	δ_M	1	-
Environmental dynamics			
Environmental temperature	T	293.15	K
Functional response (constant environment)	f	[0.2, 0.4, 0.6, 0.8, 1]	-
Average functional response (seasonal environment)	$\bar{f}$	[0.4, 0.6, 0.8]	-
Functional response (peak) amplitude	f_a	0.2	-

2.2.4 Parameter space validation

To verify our parameter subset's biological relevance, we examined the AmP collection for species within the parameter space. Accordingly, we used the routines in the AmPtool MATLAB package (AmPtool, 2020) to find all the species parameterized with the standard DEB model within the limits of our parameter space for $\dot{v}$ (in the interval [0.15, 0.55]),

$\{\dot{p}_{\mathrm{Am}}\}$ (in [1500, 9500]), and $[\dot{p}_M]$ (in [1600, 2000]). We did not restrict the value of κ to our parameter subset because the collection is biased towards larger values. We quantified the parameter variation in these species through the coefficient of variation ($c_v = \sigma/\mu$).

2.2.5 Relationship between variables and observable quantities

The state variables in the DEB model are not directly measurable; hence, we transform them into quantities that can be observed across individuals. Specifically, the reserve energy (E) plus the structural volume (V) constitute the energy fixed in the individual's biomass. Nonetheless, to calculate the biomass as (dry) weight in grams, we need to account for the density and compositions of both variables, as given by:

$$B = d_V\, L^3 + \frac{w_E}{\overline{\mu}_E}\, E, \tag{2.4}$$

where d_V (g/cm^3) is the density of the structural volume, w_E (g/Cmol) is the molar weight of the energy reserve, and $\overline{\mu}_E$ (J/Cmol) is the chemical potential of the energy reserve (equation 3.3 in Kooijman, 2010). These constants are species-specific; for generality, however, we used the standard values: $d_V = 0.28$, $w_E = 23.9$, and $\overline{\mu}_E = 550000$ (Kooijman, 2010).

We illustrated the model behaviour using the related fan-tailed gerygone, *Gerygone flavolateralis,* and the grey warbler, *G. igata*, as a case study to compare the differences between the constant and seasonal resource environments. For these two species, we transformed the above dry biomass (B) into wet biomass (B_w) assuming the relation $B_w = 5B$, which is based on observations of water content in fledglings of the grey warbler (Gill, 1982).

2.2.6 Model analysis

When there are seasonal fluctuations, the model's nonlinearities make it impossible to determine the dynamics analytically (Muller & Nisbet, 2000). For this reason, we addressed our questions through numerical studies. We implemented the DEB model in the R language (version 3.6.2, R Core Team, 2019), and performed the time integrations using the "lsoda" initial value problem solver from the package **deSolve** (Soetaert, Petzoldt, & Setzer, 2010). We integrated the model for three years, until reaching a steady state or stable limit cycle. When comparing the tropical and temperate species, we used an integration time of six years to better reflect the differences that may accumulate over time. For the simulations considering resource variability, we assumed one seasonal cycle per year, i.e. one period of low and high food availability.

2.2.7 Data analysis and model validation

To show the combined effect of the parameters and the resource, we summarized the model simulations at different food levels through scatterplots. We express the energy reserve and the structural volume variables together as the individual's biomass for conciseness. For comparative purposes, in the constant resource environment, we plot the steady-state value of the biomass. In contrast, in the seasonal environment, we show the average values attained after transient dynamics have been discarded. For the cumulative reproduction energy variable, in both environmental scenarios, we show the average reproductive energy attained in the last two years of the individual's lifespan. Similarly, for the maturity energy variable, we emphasize the time to reach the puberty threshold in both food environments.

To take into account the relative differences between individuals in our analysis, we computed the relative value of each state variable x:

$$d_r(x) = \frac{x}{\bar{x}},$$

where $\bar{x}$ is the mean of all the simulations at the same resource level f, but considering a different parameter set for $\{\dot{p}_{\text{Am}}\}$, $\dot{v}$, and κ.

At constant resource availability, the reserve equation in 4.7 leads to the constant:

$$E = f \cdot V \cdot [E_m], \tag{2.5}$$

where $[E_m] = \{\dot{p}_{\text{Am}}\} / \dot{v}$, which is the maximum value of the reserve density (also called the reserve capacity). Thus, to verify our simulations' accuracy, we compared our model predictions for energy reserves at constant resource with the expected values from equation 2.5.

2.3 RESULTS

2.3.1 Parameter space validation

We found 14 species in the AmP collection modelled with the DEB-std model having parameter values that lie within our parameter space for $\dot{v}$, $\{\dot{p}_{\text{Am}}\}$, and $[\dot{p}_M]$ (Fig. 2.3, Table A.2.1). These species' parameters have values across all our parameter space for $\dot{v}$; however, for $\{\dot{p}_{\text{Am}}\}$ the values are below 8000 (Fig. 2.2, panel 4). All of the species are in the Aves class (superorder Neognathae) likely due to the restriction of selecting entries parameterized with the DEB-std model (which constitute ~45% of the collection) and the high representation of this class in the collection (~21%).

Birds that fall within our parameter space are characterized by being small to medium size (from 15.5 g in the European pied flycatcher to 100 g in the Artic tern, except for the New Zealand pigeon at 590 g), terrestrial, flighted and mostly carnivores (mainly

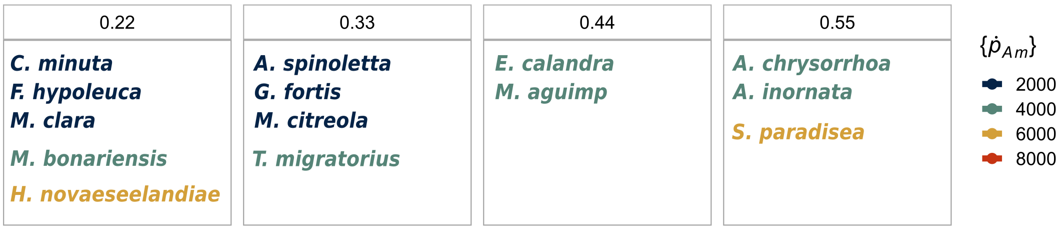

Figure 2.3. Position of the species within our parameter space for $\dot{v}$ and $\{\dot{p}_{\text{Am}}\}$. See Table A.2.1 for parameter values and common names.

insectivores, except for the New Zealand pigeon and the Medium ground finch, which are frugivores or granivores). Relative to the AmP collection, the species' parameters are biased to high values of energy conductance and somatic maintenance costs and intermediate to high assimilation values (AmP, 2020). The parameters for $[E_G]$, E_H^b, and E_H^p, are all above the limits of our parameter space because they correspond to species of a larger size and longer lifespan than *D. magna*.

2.3.2 Model validation

Our model's predictions in the constant food environment match the analytical solutions for the reserve density (Fig. A.2.1), which indicates that the simulations are consistent with the expected results.

2.3.3 Effect of interspecific differences

To test for the consequences of interspecific variability only, we conducted simulations in a constant resource environment. We expected that simulations where the resource is limiting produce similar size and reproductive output individuals because low food should reduce interspecific variability. We found that decreasing resource does minimize the consequences of interspecific differences in biomass and reproduction (Figs. 2.4 and 2.5.

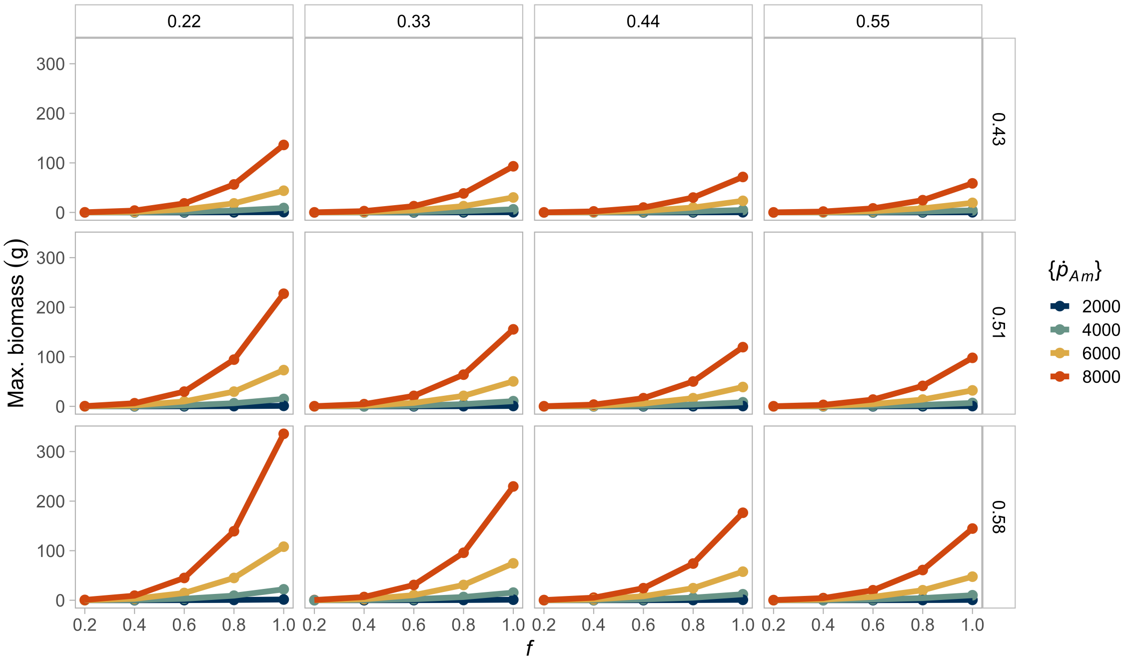

Figure 2.4. A decreasing, constant resource (f) reduces interspecific differences in maximum biomass. The largest biomass is attained when individuals combine high assimilation with low energy conductance. The columns show the different values of energy conductance evaluated ($\dot{v}$). The rows represent the fraction of energy allocated to soma (κ). The colours of the lines indicate the value of the maximum specific assimilation rate ($\{\dot{p}_{\text{Am}}\}$). Lines of the same color in each box (equivalent to a parameter combination) represent the same species at different food levels.

See Figs. A.2.2 and A.2.3 for the differences in reserve energy and structural volume). We found the opposite effect for maturation time, where lower food levels lead to variable development rates (Fig. A.2.4).

When the resource is non-limiting, a combination of high assimilation but low energy mobilization ($\{\dot{p}_{\text{Am}}\} = 8000$, $\dot{v} = 0.2$) produces individuals with the highest biomass (Fig. 2.4). Here, a lower energy conductance magnifies the interspecific differences since the organisms mobilize less energy from the reserves. However, the fraction of energy allocated to soma does not affect the biomass because the increase in energy and volume is proportional.

Interspecific differences are greater in the reproductive output for organisms that combine a large assimilation rate with a high fraction of energy allocation to soma in an environment with high resource availability (Fig. 2.5). This counterintuitive result, where

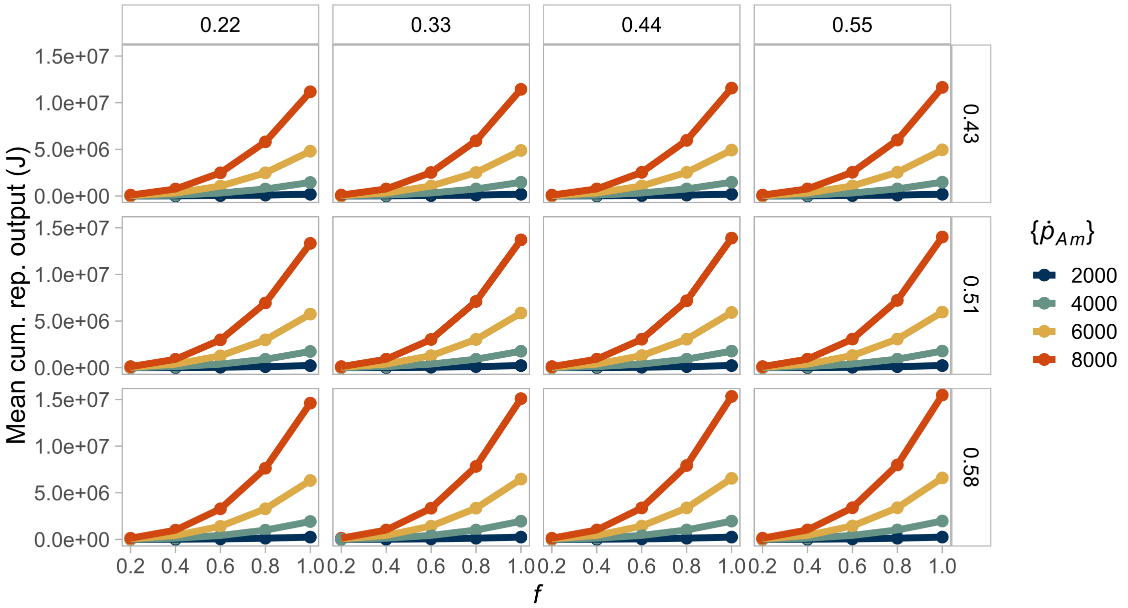

Figure 2.5. A declining, constant resource (f) reduces interspecific variability in mean cumulative reproductive output. Higher reproductive output is reached when the fraction of energy allocated to soma is high. The columns show the different values of energy conductance evaluated ($\dot{v}$). The rows represent the fraction of energy allocated to soma (κ). The colours of the lines indicate the value of the maximum specific assimilation rate ($\{\dot{p}_{\mathrm{Am}}\}$). Lines of the same color in each box (equivalent to a parameter combination) represent the same species at different food levels.

allocating more energy to soma produces higher reproduction (instead of lower reproduction), is caused by the moderate κ values in our parameter space: $\kappa = 0.58$ likely to be close to one of the two optimum points of maximum reproductive output as a function of κ. The energy conductance rate seems not to affect the reproductive output, which may be a consequence of the smaller range evaluated for conductance compared to that of energy assimilation.

The maturation time shows increased variability when the resource is scarce (Fig. A.2.4). The differences in development time are small (between a minimum of 1 day to a maximum of 4 days); however, they are greater for individuals with reduced assimilation and conductance rates at an intermediate value of energy allocation to soma. For example, when food is scarce ($f = 0.2$), and the energy allocation to soma increases ($\kappa = 0.58$), a combination of low energy assimilation ($\{\dot{p}_{\mathrm{Am}}\} = 2000$) and mobilization ($\dot{v} = 0.2$) produces individuals with the slowest maturation (4 days).

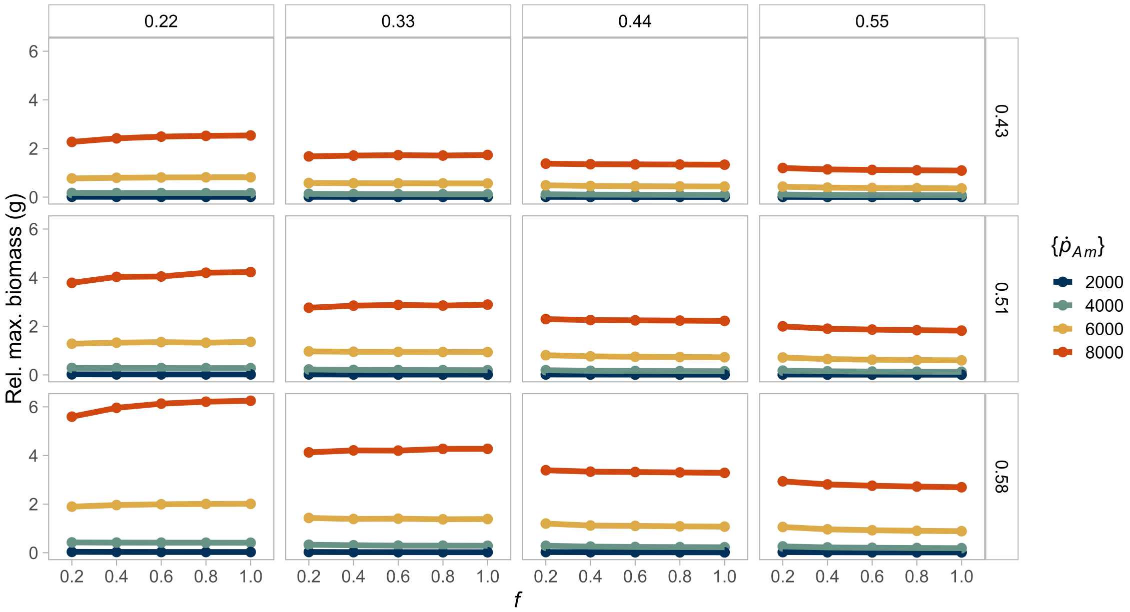

Figure 2.6. A constant resource (f) scales the interspecific differences in biomass. Hence, there are only small relative differences between different food levels for the same species. The columns show the different values of energy conductance evaluated ($\dot{v}$). The rows represent the fraction of energy allocated to soma (κ). The colours of the lines indicate the value of the maximum specific assimilation rate ($\{\dot{p}_{\mathrm{Am}}\}$). Lines of the same color in each box (equivalent to a parameter combination) represent the same species at different food levels.

Organisms grow larger at higher food, thus resulting in larger absolute differences. However, the relative differences in biomass (Fig. 2.6) are not strictly constant, with higher resource leading to relatively higher biomass when energy conductance is low ($\dot{v} = 0.2$) but to relatively lower biomass when mobilization is high ($\dot{v} = 0.5$). These differences in biomass reflect the effect of the energy conductance parameter on the energy reserves (Fig. A.2.5), while the relative differences in structural volume remain constant (Fig. A.2.6). Similarly, the relative differences in reproduction energy show that species' differences are nearly constant across resource levels (Figs. 2.7) or, in the case of maturation time, the differences are small (Fig. A.2.7). These findings indicate that the resource level has mostly a scaling effect on the individual dynamics.

For maturation energy, the relative differences are not identical for each resource level and appear to be larger for a combination of lower resource and energy conductance (Fig.

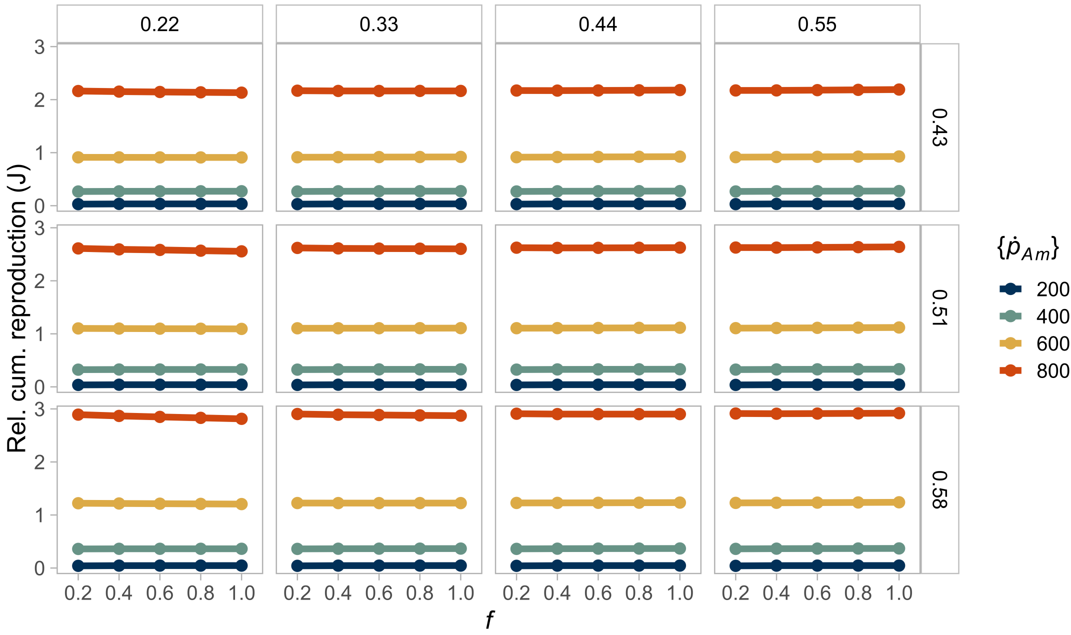

Figure 2.7. A constant resource (f) scales the interspecific differences in reproductive output. Hence, there are no relative differences between different food levels for the same species. The columns show the different values of energy conductance evaluated ($\dot{v}$). The rows represent the fraction of energy allocated to soma (κ). The colours of the lines indicate the value of the maximum specific assimilation rate ($\{\dot{p}_{\mathrm{Am}}\}$). Lines of the same color in each box (equivalent to a parameter combination) represent the same species at different food levels.

A.2.7). However, the range of these differences is small and may not reflect significant differences.

2.3.4 Effect of resource variability

We evaluated the consequences of environmental variability by simulating a seasonally-varying resource. As in the environment with a constant resource, absolute interspecific variability in biomass and reproductive output is greater when average food is more abundant (Figs. A.2.8 to). Further, biomass and cumulative reproductive output are independent of the initial resource density (Figs. to A.2.24), indicating that the individuals can compensate for variations in resource abundance during their lifespan. As expected, the average values for biomass and cumulative reproductive output are larger compared to the same individual in a constant environment with equal mean food availability. We address these results in the next section.

As in the constant environment, the maturation time shows increased variability when the resource is scarce (Fig. A.2.12). Furthermore, interspecific differences are amplified when the initial resource density is low, compared to simulations where the initial resource is high. Individuals born in an environment that slowly becomes hospitable grow slower and remain small during the first season, particularly if they have a low assimilation rate. In contrast, individuals that start at the onset of a good period grow quickly to a large size, especially when the allocation fraction to soma is large. Yet, these differences in maturation may not be significant, given that the development times are equally short (Figs. A.2.25 to A.2.27).

2.3.5 Comparing temperate and tropical species: an example

To better understand the resource's effect, we compared the temporal dynamics of one species (given by the parameter set $\dot{v} = 0.3$, $\{\dot{p}_{\text{Am}}\} =$ 2000, $\kappa = 0.3$, and $[\dot{p}_M] = 1800$) in both a constant and a seasonal resource environment with equal mean resource availability. The dynamics show that, despite having the same parameter values, the individual in the seasonal environment reaches a greater average biomass (Fig. 2.8A) and cumulative reproductive output (Fig. 2.8B) than an individual of the same species in a constant environment with an equal average resource. The resource does not appear to affect the maturation dynamics, given that the maturation threshold parameters are low and can be reached shortly after birth in both environments (Fig. 2.8C).

We further illustrate the model behaviour for the fan-tailed gerygone, *Gerygone flavolateralis,* and the grey warbler, *G. igata*, two related species with parameter values close to each other (Tab. A.2.2). Members of the *Gerygone* genus (Passeriformes, Acanthizidae) are small insectivorous species distributed in the Australasian region (Keast & Recher, 1997), which do not migrate. The grey warbler inhabits temperate forests in the South Island of New Zealand, while the fan-tailed gerygone dwells in the tropical rainforests and savannahs of New Caledonia and Vanatu (Attisano et al., 2019; Gill, 1982). The species differ slightly in their biomass: 6.45 g for the grey warbler (Gill, 1982) and 6.1 g for the Fan-tailed Gerygone (Attisano et al., 2019). The differences in the reproductive output are more pronounced: the grey warbler has two broods per year with an average clutch size of four eggs (Gill, 1982); in contrast, the fan-tailed gerygone has only one brood per year with a mean of two eggs (Attisano et al., 2019).

As expected, our simulations show that, with similar average food density, the grey warbler can reach a similar size and have a greater reproductive output relative to the fan-tailed gerygone (Fig. 2.9). These differences in reproduction are more pronounced than in the previous example (Fig. 2.8) because the species differ in their parameter values, mainly on the energy allocated to soma and the cumulative energy at birth and

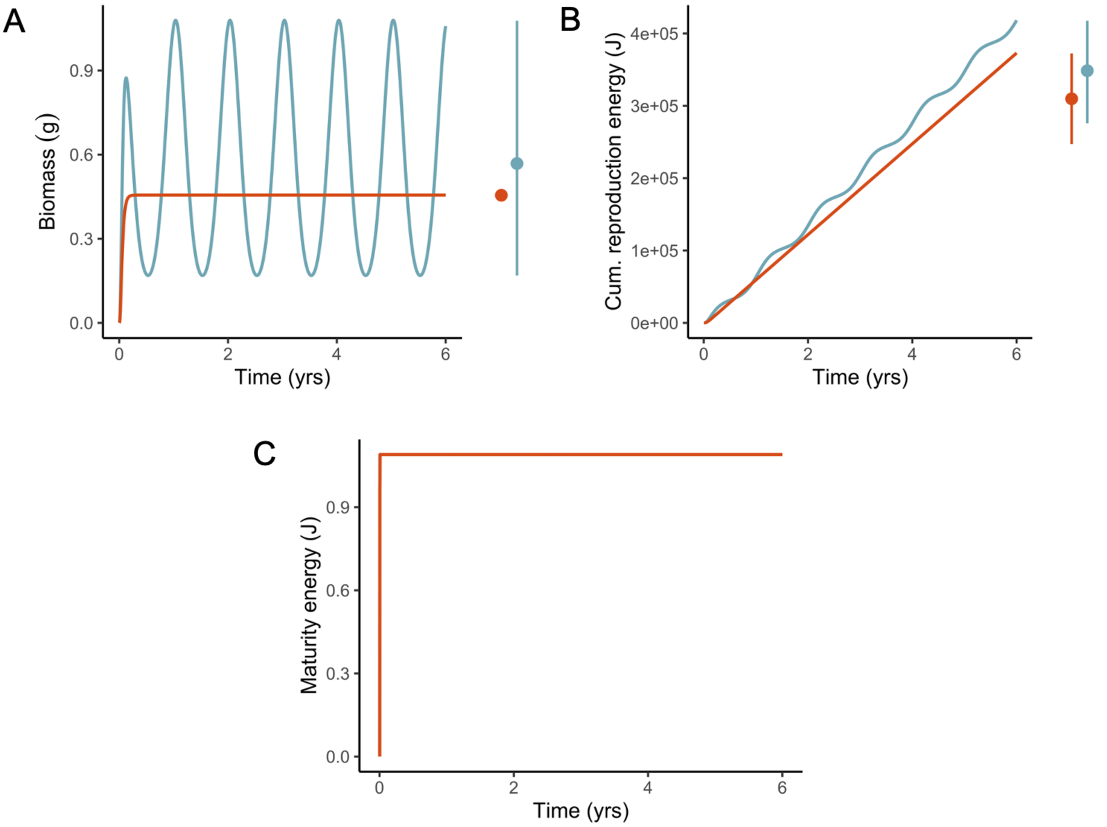

Figure 2.8. Individuals of the same species reach larger average biomass (A) and reproduction (B) in a seasonal resource environment (blue lines) relative to the same individual in an environment with an equal mean resource availability (red lines). In the right panel of (A), for the species in the constant environment, the red point shows the steady-state value of biomass reached at the end of the lifespan. In contrast, for the seasonal environment, the blue point represents the average biomass calculated over the last four years (i.e., years two to six), and lines show the minimum and maximum values. In the right panel of (B), for both species, points represent the average cumulative reproduction energy calculated over the last four years, and lines correspond to the minimum and maximum values. The biomass of the individual in the seasonal environment fluctuates according to the resource because the standard DEB model does not consider limits to individuals' shrinking in size in periods of low food availability. The maturation dynamics (C) are not affected by the resource because the maturation energy threshold parameters are low, and individuals reach puberty shortly after birth. For the simulations, we assume $\bar{f} = 0.8$, and the parameter set of the species is: $\dot{v} = 0.3$, $\{\dot{p}_{\text{Am}}\} = 2000$, $\kappa = 0.3$, and $[\dot{p}_M] = 1800$ (see other parameter values in Table 2.2)

puberty (Tab. A.2.2). Furthermore, the dynamics of the Grey Warbler show pronounced seasonal fluctuations because the standard DEB model does not consider limits to individuals' shrinking in size in periods of low food availability. Consequently, the biomass and reproductive energy of the grey warbler fluctuate according to resource availability. Our predictions underestimate both species' average biomass likely because we do not consider that the reproductive energy contributes to the overall weight of the individuals. This assumption allowed us to measure a continuous reproductive output across our simulations, but it may result in biomass underestimation in species that store reproductive energy between discrete reproductive seasons, such as the grey warbler or the fan-tailed gerygone. Moreover, we assume that the effect of temperature on metabolic rates is negligible. Despite these simplifying assumptions, our forecasts agree with the general pattern between the species and demonstrate the model's behaviour as well as the importance of the resource in contributing to the overall dynamics.

2.4 DISCUSSION

We used the DEB model to describe the individual rates of energy acquisition and partitioning, which lead to different life-history traits. Our approach is novel because we used simulations of the DEB model to perform a comparative analysis of 48 different strategies of energy allocation (equivalent to different species) across different environments to evaluate their consequences in body mass and reproductive output. As expected, we found that absolute interspecific differences in biomass and reproduction are more evident when the resource is non-limiting (Figs. 2.4 and 2.5). The same pattern holds in a seasonal resource environment; moreover, seasonality produces individuals with a greater average biomass and reproductive output relative to the constant environment (Figs. A.2.8 and A.2.9). Our results provide a plausible mechanistic explanation to known interspe-

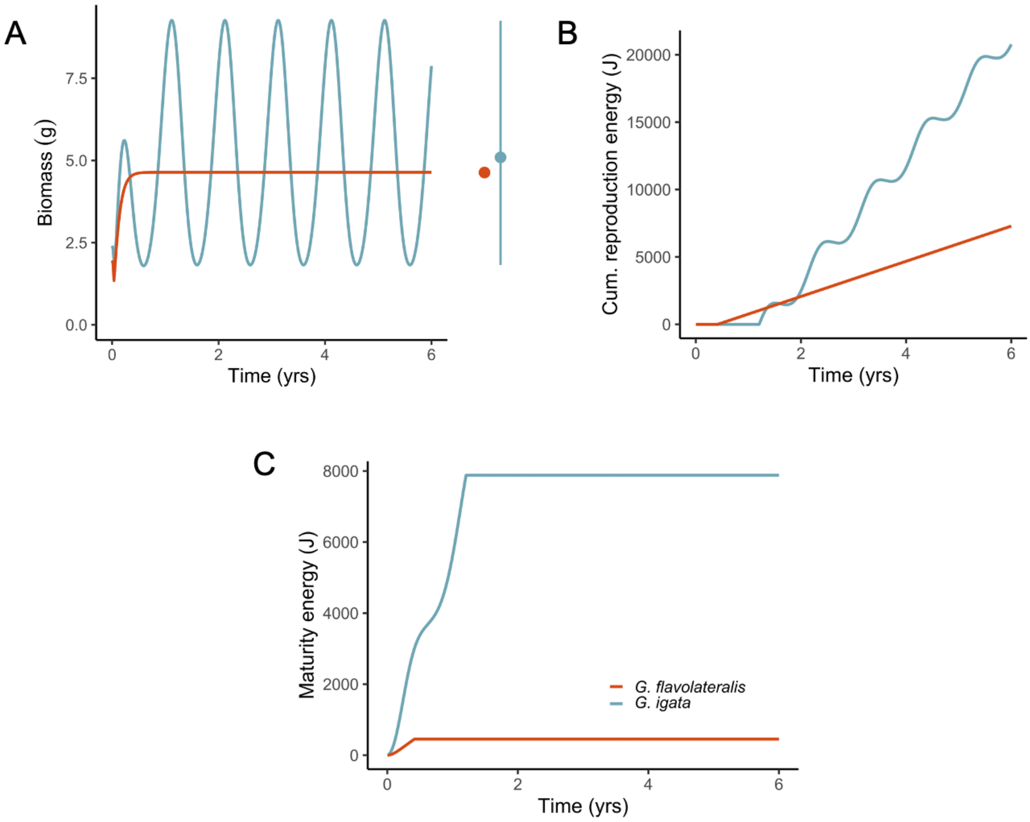

Figure 2.9. Simulations for the grey warbler (*G. igata*) in a seasonal environment with an equal mean resource availability as the fan-tailed gerygone (*G. flavolateralis*) in a constant environment show that the grey warbler dynamics follow the resource oscillations and reach a greater average wet biomass (A) and reproductive output (B) compared to the fan-tailed gerygone. In the right panel of (A), for the species in the constant environment, points show the steady-state value of wet biomass reached at the end of the lifespan. In contrast, for the seasonal environment, points represent the average wet biomass calculated over the last four years (i.e., years two to six), and lines show the minimum and maximum values. In the right panel of (B), for both species, points represent the average cumulative reproduction energy calculated over the last four years, and lines correspond to the minimum and maximum values. The grey warbler biomass fluctuates according to the resource because the standard DEB model does not consider limits to individuals' shrinking in size in periods of low food availability. Differences in the maturation energy between the species (C) are due to different values of the puberty threshold (E_H^p = 453.1 for the fan-tailed gerygone and 7880 for the grey warbler). The simulations assume $\bar{f}$ = 0.8 (see parameter values in Table A.2.2).

cific patterns of body size and reproductive output variation and reaffirm the importance of considering the effects of resource availability changes to predict broad biodiversity dynamics.

2.4.1 Non-limiting resource amplifies interspecific variability in biomass and reproduction

Food availability has been proposed as the primary cause of differences in adult body size and biomass, both among and within species, because it underlines organisms' nutritional requirements, which ultimately drive ontogenetic growth (Huston & Wolverton, 2011). Here, we showed that an abundant resource increases absolute interspecific variability in biomass, regardless of the environment (Fig. 2.4). However, species' differences in biomass are not exactly constant, especially at low values of energy mobilization (Fig. 2.6). Although these differences are small, they indicate that the allometric relationships are not strictly proportional. Such disparities in biomass may suggest a larger sensitivity of the model output to parameter combinations with low mobilization and high assimilation at reduced food availability. Nevertheless, our simulations revealed that, in the DEB model, the resource has a scaling effect on the individual's biomass because a larger food availability directly increases the feeding, assimilation, mobilization, and somatic maintenance fluxes, which result in a greater growth rate.

Our findings are in line with the central role of food availability on biomass (reflected in Bergmann's rule, sizes in deserts, insular dwarfism, Dehnel's phenomenon, and Cope's rule, or more generally the resource rule), by which species become larger or smaller according to the size, abundance, and availability of food (McNab, 2010). Although we did not include the effect of environmental temperature, several case studies using the DEB model have previously illustrated the relevance of food dynamics over temperature in determining growth rate and maximum possible size across different taxa (e.g., Cardoso, Witte, & van der Veer, 2006; Freitas et al., 2009; Marn, Jusup, Catteau, Kooijman, & Klanjšček, 2019).

For example, in two parapatric and genetically distinct populations of loggerhead turtles, a reduction in ultimate size has been shown to be a consequence of constant low food availability (Marn et al., 2019). Thus, within the DEB theory, a reduction in adult size or biomass can be interpreted as a direct consequence of the change in resource and its effect on assimilation (Kearney, 2021), giving further theoretical support to the resource rule.

Animal body size is only one of the traits affected by resource availability; many other characteristics of individuals depend on the extent to which they can be afforded, including maintenance, reproductive output, and activity level (McNab, 2010). Moreover, size alone can be considered a determinant of an organism's ecological and physiological properties, such as reproduction (Klingenberg & Spence, 1997; Litchman, Ohman, & Kiørboe, 2013). Our results indicated that an abundant resource intensifies not only absolute interspecific variability in biomass in the DEB model, but also in reproductive output (Fig. 2.5). Our simulations showed that the resource has a similar effect on the individual's reproductive output, where a greater food availability results in increased cumulative reproduction energy. The limiting effect of food quantity or quality in animal reproduction is well known in the literature (Kozłowski et al., 2020). Nevertheless, this conclusion is not always evident when making interspecific comparisons through the DEB model because of the covariation among parameters. For example, in the aforementioned loggerhead turtles, there is no significant disparity in the reproductive output of populations inhabiting areas with dissimilar food availabilities due to differences in the maturity maintenance and maturity energy thresholds parameters between individuals of the two populations (Marn et al., 2019). However, by fixing these parameters, we have isolated the scaling effect of resource availability on cumulative reproductive output.

In our formulation, we attribute interspecific variation to parameter values. Among the parameters that we evaluated, we found that both maximum assimilation ($\{\dot{p}_{\mathrm{Am}}\}$) and allocation to soma (κ) have the most important role in promoting interspecific differences in individuals' size and reproduction (Figs. 2.4 and 2.5). Such effect has previously been recognized among several marine invertebrates and vertebrates, where species differ mostly in their assimilation rate and the energy partitioning to growth and reproduction (Freitas et al., 2010; Marn et al., 2019; van der Veer et al., 2001). Both are parameters that can be considered highly adaptative, and their values are expected to reflect the conditions of the environment where the species evolved (Muller & Nisbet, 2000).

2.4.2 Environmental variability increases average biomass and reproduction

Food availability is influenced by biotic and abiotic factors, which can in turn covary, causing resource oscillations in time and space that determine the geographical and temporal changes in body size (Yom-Tov & Geffen, 2006, 2011). By fixing the environmental temperature and evaluating different fluctuating resource scenarios, we showed that the surplus in food availability during one season of the year produces organisms that can reach a greater average biomass relative to the same individual in an environment with an equal average but constant resource (Figs. 2.8A and 2.9A). Our results are in agreement with the expectation according to the eNPP rule, in which animals subjected to fluctuations in food availability can do more than compensate for the periods of food deficit during their lifespan, as they gain more body mass during the periods of food surplus (Geist, 1987; Huston & Wolverton, 2011). In the DEB framework, it has been reported that the maximum size rises with the period and amplitude of the resource cycles, rather than to the mean (Muller & Nisbet, 2000). Thus, our findings are in line with the DEB literature and give further support that indicates that the DEB model offers a mechanistic explanation at the interspecific level for the eNPP rule.

As proposed in the eNPP rule, food fluctuations in quantity and quality have further implications in traits associated with evolutionary fitness, most notably reproduction (Huston & Wolverton, 2011). In our simulations in a seasonal environment, we found that the peaks in food availability also produce animals with a larger cumulative reproductive output compared to the same individual in an environment that has an equal average constant resource (Figs. 2.8B and 2.9B). Our results are consistent with previous studies that mention an increase in brood size in birds with latitude (Lack's rule) or, more broadly, eNPP (Boyer & Jetz, 2010). Nonetheless, because of the non-linearities that arise in the DEB model when there are food fluctuations, it has been shown that the total reproductive energy is highly dependent on the organism's energy partitioning as given by the parameter values (Muller & Nisbet, 2000). For example, a decrease in the value of κ (the energy allocation to soma) implies an increased investment of energy to reproduction, and would be expected to simultaneously decrease size, shorten development and maturation times and increase reproduction allocation (Kearney, 2021). However, as our results illustrate, individuals can also have a higher reproductive output when they allocate a greater fraction of energy to soma. Such behaviour occurs because maximum reproductive output as a function of κ has two optimum values: at intermediate ($\kappa \approx 0.5$) and also at high values ($\kappa \approx 0.9$) (Lika et al., 2011b). Hence, for the parameter combinations that we assessed, $\kappa = 0.58$ is likely to correspond to that intermediate optimum value that yields a greater reproductive output. Given that we simulated a restricted range of κ, we would expect that higher values ($0.58 < \kappa \lesssim 0.8$) produce individuals for which reproduction is reduced because an increase in the energy allocation to soma will also increase the maintenance requirements (Muller & Nisbet, 2000). The pattern of greater reproductive output for increasing values of κ also occurs in the seasonal environments that we evaluated. It has been shown that organisms with low to intermediate values of κ, such as the ones we simulated, reproduce more as the amplitude in food fluctuations increase (Muller & Nisbet, 2000). Thus, depending on the underlying life history of the individual, resource seasonality in the DEB model may increase the reproductive output.

2.4.3 Resource availability may influence development rates

According to the eNPP rule, the highest ontogenetic growth rates will occur where food availability is highest (Huston & Wolverton, 2011). Consequently, when the resource is limiting, a delay in the maturation and reproduction rates is expected. For example, in two sympatric and sibling insectivorous bat species (genus *Myotis*) with marked differences in resource supply, there is a delay in the reproduction onset for the species with a lower food availability; however, this difference disappears in years where there is a pulsed input of a secondary resource (Arlettaz, Christe, & Schaub, 2017). In general, our results suggest that there is a delay in maturation time at lower, constant resource levels (Fig. A.2.4). In a seasonal environment, our findings indicate that individuals that start their life at different points of the seasonal cycle do not have the same maturation times (Figs. A.2.25 to A.2.27). More specifically, individuals born during the low food season show a slower development and more variable times to reach puberty, compared to the same organisms born during the high food season (Fig. A.2.12). Similar results have been described for mussels parameterized with the DEB model (Muller & Nisbet, 2000), highlighting the relevance of birth timing in developmental times when resource oscillates. Nevertheless, in both environmental scenarios, our results may not represent a significant difference as the range of the developmental time variation is small because the parameters that define the maturation thresholds are close to each other and remain constant. Thus, even though we find indications of a possible effect of food level on maturation time, further analyses are needed to reveal the potential variation on development according to the resource in the DEB framework.

2.4.4 Life-history traits and parameter space

By matching our parameter subset to real species, we can explain various patterns within the parameter space. We found that the species in our parameter subset combine an intermediate assimilation rate ($\{\dot{p}_{\mathrm{Am}}\} < 8000$) with energy conductance ranging from intermediate to high values ($\dot{v}$ in the interval [0.15, 0.55]), which results in small body weight. In birds, such combination of values for energy conductance and assimilation have been associated with flying adaptations since it usually implies a low reserve density (i.e., a smaller contribution of the energy reserve to biomass; Augustine, Lika, & Kooijman, 2019; Lika, Augustine, & Kooijman, 2019; Lika, Augustine, Pecquerie, & Kooijman, 2014; Teixeira, 2016). Additionally, most of the species within our parameter space have a carnivore diet, which has been linked to larger assimilation and somatic maintenance rates given that it requires greater enzymatic attack and thick stomach muscles (Battley & Piersma, 2005; Ricklefs, 1996; Teixeira, 2016). Only one species, the New Zealand pigeon, constitutes an exception to the previous pattern, as it is larger and primarily frugivorous. This species has an intermediate assimilation rate combined with a lower mobilization rate, which results in a greater biomass due to a larger energy reserve. In general, our subset of species reflects previous findings that indicate that the mobilization rate is one of the most variable DEB parameters for birds (Teixeira, 2016), and seem to suggest a broad link between assimilation rate and diet.

In birds, the average fraction of energy allocated to soma is very high (with a mean of 0.988) and does not exhibit significant variation among species ($c_v = 0.03$, Teixeira, 2016). This evidence suggests that the energy allocated to soma is phylogenetically conserved and that selective pressures have mostly driven birds towards larger investments in growth and maintenance, as well as delayed maturation and relatively low production efficiency (Teixeira, 2016; van der Meer, van Donk, Sotillo, & Lens, 2020). In our species subset, κ ranges from 0.822 to 0.999, and the combination with intermediate assimilation and high somatic maintenance in some species could indicate that they have evolved greater maintenance costs that allow a fast growth to a small size, in accordance with the waste-to-hurry hypothesis (Kooijman, 2013). Nonetheless, in birds, this combination of parameter values seems to be related to flight adaptations (Augustine et al., 2019) rather than to strategies that promote faster growth.

Traits associated with differing life histories are usually classified along a “fast to slow” or “pace-of-life” continuum. For example, compared to temperate birds, tropical birds are typically considered as having a “slow” life history, involving small clutch sizes or low annual reproductive output (Kulesza, 1990; Moreau, 1944), as well as slow growth and maturation of nestlings (Cox & Martin, 2009; Jimenez, Cooper-Mullin, Calhoon, & Williams, 2014; T. E. Martin et al., 2011; Ricklefs, 1968, 1976, 2000). The results of our simulations comparing species in two resource environments agree with the literature, with the species in the seasonal habitat showing a faster growth to a larger body mass and greater reproductive output than the species in the constant habitat (Figs. 2.8 and 2.9). These differences between tropical and temperate birds have been attributed to trade-offs between investment in either reproduction or maintenance, as mediated by the biotic and abiotic environment (Roff, 1992), which correspond to the species’ different parameter values. Nevertheless, our simulations also highlight the effect of the resource in modulating the species traits, which, together with predation risk, has been reported as the main environmental factor affecting growth rate and body size in birds (Bryant & Hails, 1983; Jimenez et al., 2014; T. E. Martin et al., 2011; Pacheco, Beissinger, & Bosque, 2010).

2.4.5 Model limitations

The DEB theory supposes that the parameters do not change over the individuals’ lifespan. Consequently, organisms show a passive phenotypic flexibility in response to resource availability, but there is no plasticity in the physiological mechanisms responsible for development and growth as a response to environmental cues (i.e., active adaptive plasticity).

To modify this assumption would require discerning all possible changes in the conditions experienced by an organism during ontogeny (Pecquerie & Lika, 2017). However, the current lack of understanding of how parameters may vary during an organism's lifespan limits incorporating such responses into the DEB model (Freitas et al., 2009). Thus, to include an adaptive response in the individual energy allocation would require detailed knowledge of the species' long-term seasonal patterns of growth and reproduction.

Quantitative and qualitative changes in food conditions would also be expected to affect individual survivorship and offspring production rate (Huston & Wolverton, 2011). Simulations of the DEB model in a constant environment have suggested an increased lifespan as the resource becomes more abundant (Lika & Kooijman, 2003). When food fluctuates, simulations have shown that individual lifespan is reduced as the oscillations amplitude increase (Muller & Nisbet, 2000). However, we did not consider how resource availability affects individual lifespan or aging because such variations in lifespan are thought to be most significant for large values of κ (Lika & Kooijman, 2003; Muller & Nisbet, 2000), which we did not include in our simulations. Nevertheless, it is possible that including survival could impact the resulting interspecific differences. Regarding the reproduction rate, we have not specified how reproductive energy is transformed into quantity and quality of offspring, given that the optimal strategy will depend on the particular environment experienced by each individual and its effect on growth, survival, and reproduction (Brown, Marquet, & Taper, 1993). Further elaborations of our study could incorporate such details, specifying how energy is allocated to survival and production of offspring over the individual's lifetime.

The standard DEB model does not make any assumptions regarding starvation (Kooijman, 2010). For this reason, the individuals in our model can decrease in size to cover maintenance costs when the resource is limiting, and energy reserves are exhausted. This assumption holds for many species, including platyhelminths, molluscs, and mammals (Downing & Downing, 1993; Genoud, 1988; Saló, 2006; Wikelski & Thom, 2000). Yet, other species may respond to food limitation in different ways. Nevertheless, we do not simulate periods of prolonged resource depletion or scarcity that could lead to starvation. Hence, the results of our simulation are still applicable to broad scenarios of seasonal food variation. Understanding other organisms' strategies to survive seasonality without a reduction in structural mass remains an important topic for future research.

We illustrated the consequences of a constant and a seasonal resource by simulating the dynamics of two bird species parameterized for the DEB model. The fluctuations in biomass and reproductive output observed in the simulations with seasonality result from the lack of assumptions regarding starvation. Given that such a decrease in biomass is larger than the shrinking that birds are actually able to tolerate without dying, our simulations for the grey warbler serve mainly to exemplify a possible consequence of a seasonal environment in an organism's physiology. Our results broadly agreed with the general pattern: temperate species can reach a larger reproductive output and slightly greater biomass than the tropical species. However, our inference is hindered because we did not use real estimates of food availability from the species' habitats, and we simplified the abiotic environment only to resource availability, not considering temperature or biotic interactions, for example. Nevertheless, our purpose was to broadly show the different trends between a constant and a seasonal environment in closely related species.

We have shown how a mechanistic approach based on individual energetics can support empirical evidence on cross-specific trait variation. However, the geographical context of such ecological and evolutionary processes is an important component needed to gain a complete understanding of species' trait gradients (Blackburn & Hawkins, 2004; Olalla-Tárraga et al., 2010). Furthermore, any interspecific analysis must consider the phylogenetic non-independence of the data, i.e., closely related species are more similar than distant species (Olalla-Tárraga et al., 2010). For these reasons, more complex models that integrate a more accurate multidimensional environment with comparative phylogenetic methods are necessary to make stronger inferences of these eco-evolutionary patterns and processes.

2.5 CONCLUSIONS

Using the DEB model, we separated the effects of genetically-determined physiological traits (represented by DEB model parameters) and resource availability. By fixing the resource, we showed that relative trait differences between species in biomass and reproduction are greater when food is non-limiting. We found similar results for simulations in a seasonal environment; moreover, resource fluctuations increase the individuals' average biomass and reproductive output. Our results have potential implications for species of economic interest in which there is a desire to increase the yield in either biomass or reproductive output relative to the food consumption. Furthermore, our findings are a relevant step in forecasting organisms' responses to environmental change. For example, global climate change has been linked to differences in the timing of resource availability and the arrival of migratory species to their feeding grounds. Finally, our simulations offer mechanistic support for patterns of body-size variation between related species arising from epigenetic effects (i.e., Bergman's and Lack's rules, or more generally, the resource and eNPP rules).

2.6 ACKNOWLEDGMENTS

Starrlight Augustine and Bas Kooijman assited in the model parameterization for the *Gerygone* case study. We also thank the members of the Theoretical Biology Laboratory at MUN for their constructive comments on the manuscript. JM was supported by a School of Graduate Studies Baseline Fellowship from Memorial University and by a Mitacs Globalink Research Award. SCD and AH received funding from the Natural Science and Engineering Research Council of Canada (NSERC Discovery Grants 2015-06548 and 2014-05413).

2.7 APPENDIX

2.7.1 Parameter space validation

There are 14 species in the AmP collection (on March 2020) modelled with the DEB-std model with parameter values that lie within our parameter space for $\dot{v}$, $\{\dot{p}_{Am}\}$, and $[\dot{p}_M]$ (Table A.2.1).

Table A.2.1. Species in the AmP collection with parameter values within our parameter space for $\dot{v}$, $\{\dot{p}_{Am}\}$, and $[\dot{p}_M]$. The coefficient of variation (c_v) summarizes the parameter variation across species. See Table 2 in the main file for parameter notation and units.

Species	Common name	κ	$\{\dot{p}_{Am}\}$	$\dot{v}$	$[\dot{p}_M]$	$[E_G]$	E_H^b	E_H^p
Acanthiza chrysorrhoa	Yellow-rumped thornbill	0.996	4724.4	0.50	1992.8	7328.6	54.9	10830
Acanthiza inornata	Western thornbill	0.995	4005.6	0.47	1881.1	7310.6	76.9	7243
Anthus spinoletta	Water pipit	0.997	3286.2	0.27	1670.3	7316.1	36.6	1974
Calidris minuta	Little stint	0.932	3898.4	0.19	1973.6	7338.4	1354.0	387000
Emberiza calandra	Corn bunting	0.915	4797.9	0.41	1949.0	7307.3	1758.0	999500
Ficedula hypoleuca	European pied flycatcher	0.822	3350.8	0.22	1642.7	7310.7	1389.0	823600
Geospiza fortis	Medium ground finch	0.968	3146.2	0.32	1644.7	7316.3	325.9	165000
Hemiphaga novaeseelandiae	New Zealand pigeon	0.990	6900.6	0.17	1605.2	7316.0	570.1	616800
Molothrus bonariensis	Shiny cowbird	0.961	4122.9	0.21	1740.8	7332.9	766.0	277700
Motacilla aguimp	African wagtail	0.999	3804.9	0.45	1670.3	7290.4	13.4	1957
Motacilla citreola	Citrine wagtail	0.999	3204.1	0.31	1670.3	7312.9	6.4	860
Motacilla clara	Mountain wagtail	0.998	3109.4	0.22	1670.3	7330.5	15.1	1355
Sterna paradisaea	Arctic tern	0.991	5604.5	0.45	1681.2	7359.8	691.8	230000
Turdus migratorius	American robin	0.981	4940.2	0.32	1734.4	7306.1	440.3	312100
	Mean	0.967	4206.9	0.32	1751.9	7319.8	535.6	273994
	c_v	0.05	0.26	0.36	0.08	0.00	1.10	1.20

2.7.2 Model validation

At constant food levels, the relative differences between our simulations for reserve density and the analytical solutions (equation 2.5) are close to zero (Figure A.2.1). These small differences at each of the five constant resource levels we evaluated show the consistency of our simulations.

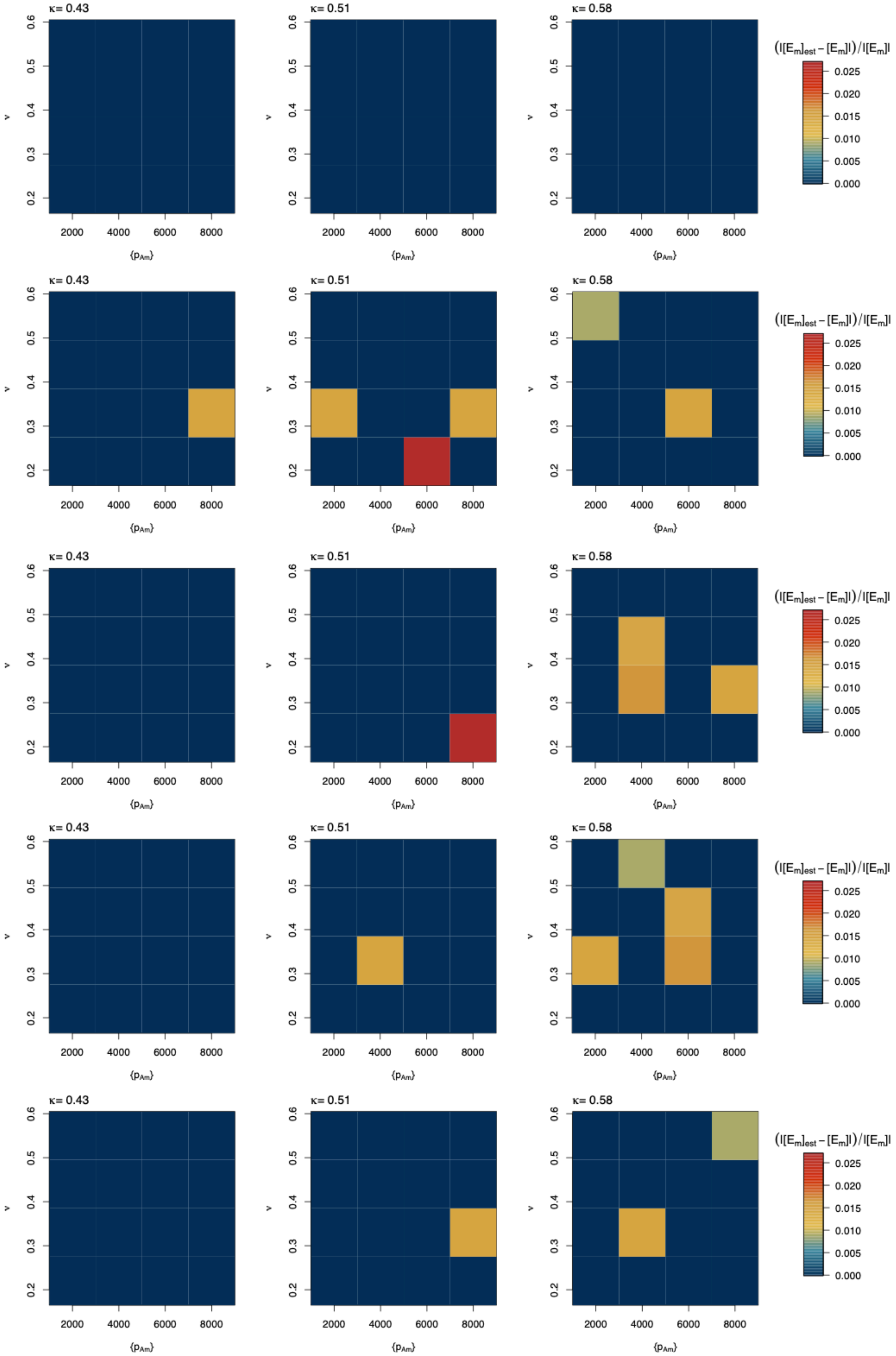

Figure A.2.1. Relative differences between our simulations and the analytical solutions. See the figure caption in the next page.

Figure A.2.1. (Previous page) The relative difference between the model simulations for reserve density ($[E_m]_{est}$) and the analytical solutions ($[E_m]$, equation 2.5) at a constant resource availability are close to zero. The rows correspond to the functional response at the five levels considered in descending order, i.e., from $f = 1$ to $f = 0.2$. The heatmap colour indicates the relative error between the numerical and the analytical solutions.

2.7.3 Effect of interspecific differences

When the resource is constant, a decreasing level minimizes the consequences of interspecific differences in reserve energy and structural volume (Figs. A.2.2 and A.2.3), which are directly reflected in the individual's biomass (Fig. 2.4). The effect is the opposite for the development time (Fig. A.2.4), where the interspecific differences become greater as the resource decreases. However, the differences in time to reach puberty are small, ranging from 2 to 4 days; and are likely not significant.

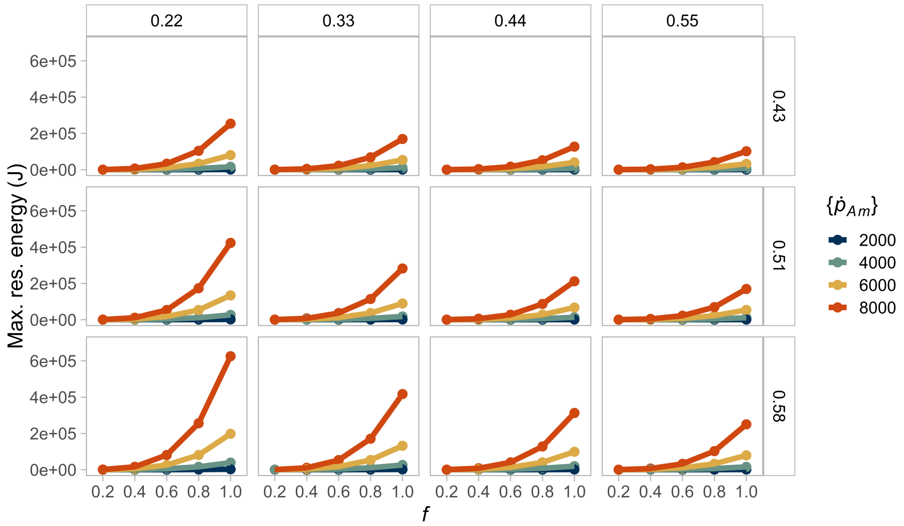

Figure A.2.2. A constant, decreasing resource reduces interspecific differences in reserve energy. The largest reserve is attained when individuals combine high assimilation with low energy conductance. The columns indicate the value of energy conductance, while the rows represent the fraction of energy allocated to soma. Point and line colours indicate the maximum specific assimilation rate value. Points and lines of the same colour in each box (equivalent to a parameter combination) represent the same species at different food conditions.

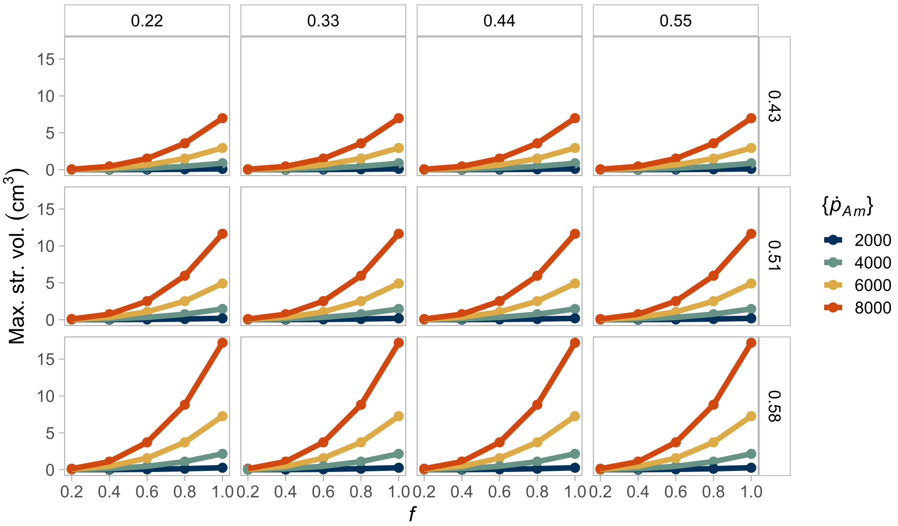

Figure A.2.3. A constant, decreasing resource reduces interspecific differences in structural volume. The largest volume is attained when individuals combine high assimilation with low energy conductance. The columns indicate the value of energy conductance, while the rows represent the fraction of energy allocated to soma. Point and line colours indicate the maximum specific assimilation rate value. Points and lines of the same colour in each box (equivalent to a parameter combination) represent the same species at different food conditions.

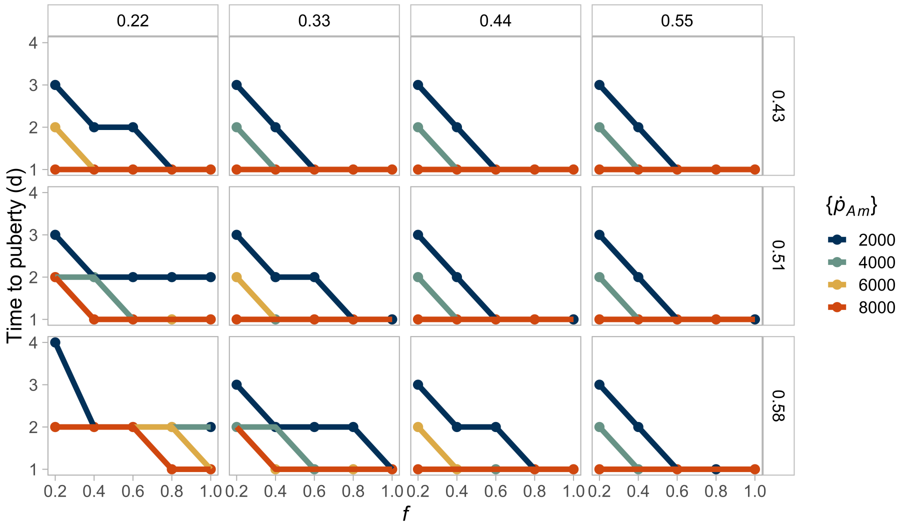

Figure A.2.4. Interspecific differences in the time to reach puberty are amplified when a constant resource decreases. Individuals have faster developing times when the resource is non-limiting, and they combine high assimilation with high energy conductance. The columns indicate the value of energy conductance, while the rows represent the fraction of energy allocated to soma. Point and line colours indicate the maximum specific assimilation rate value. Points and lines of the same colour in each box (equivalent to a parameter combination) represent the same species at different food conditions.

The relative differences across species are nearly constant at any constant resource level for reserve energy (Fig. A.2.5) and are uniform for structural volume (Fig. A.2.6). The small relative differences show that the resource has mainly a scaling effect on both variables. The relative differences in developmental time are not constant but remain small and likely not significant (Fig. A.2.7).

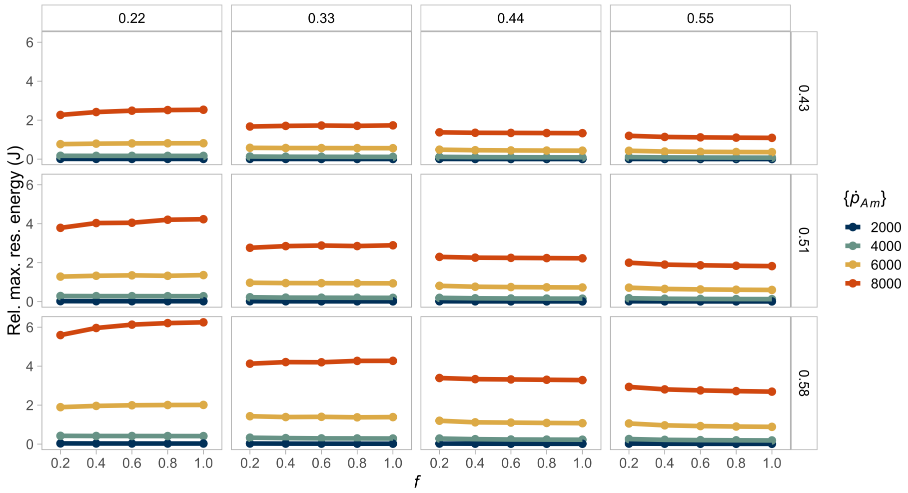

Figure A.2.5. The resource scales the interspecific differences in reserve energy. Hence, differences between different constant food levels for the same species are small. The columns indicate the value of energy conductance, while the rows represent the fraction of energy allocated to soma. Point and line colours indicate the maximum specific assimilation rate value. Points and lines of the same colour in each box (equivalent to a parameter combination) represent the same species at different food conditions.

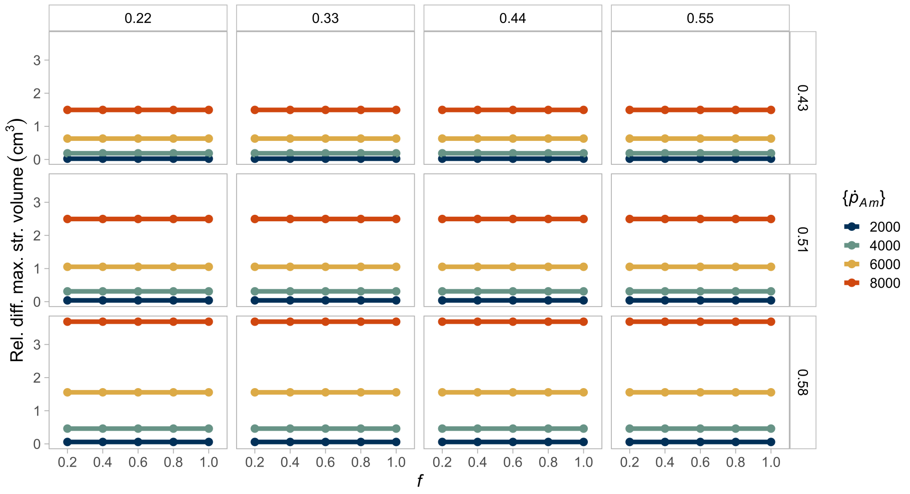

Figure A.2.6. The resource scales the interspecific differences in structural volume. Hence, there are no relative differences between different constant food levels for the same species. The columns indicate the value of energy conductance, while the rows represent the fraction of energy allocated to soma. Point and line colours indicate the maximum specific assimilation rate value. Points and lines of the same colour in each box (equivalent to a parameter combination) represent the same species at different food conditions.

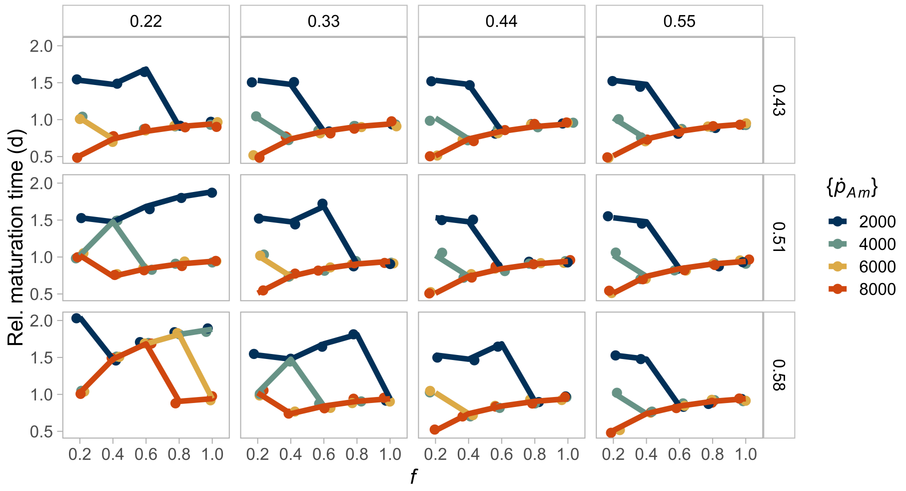

Figure A.2.7. The relative differences between constant food levels in maturation time are small and likely not significant. The columns indicate the value of energy conductance, while the rows represent the fraction of energy allocated to soma. Point and line colours indicate the maximum specific assimilation rate value. Points and lines of the same colour in each box (equivalent to a parameter combination) represent the same species at different food conditions.

2.7.4 Effect of resource variability

A seasonal resource with a greater average amplifies the consequences of interspecific differences in biomass, reproductive output, reserve energy, and structural volume (Figs. A.2.8 to A.2.11, respectively). On the contrary, the interspecific differences in development time become greater as the mean resource decreases (Fig. A.2.12). These differences in time to reach puberty are small and likely not significant. However, they depend on the initial food level or, equivalently, the birth time relative to the resource cycle.

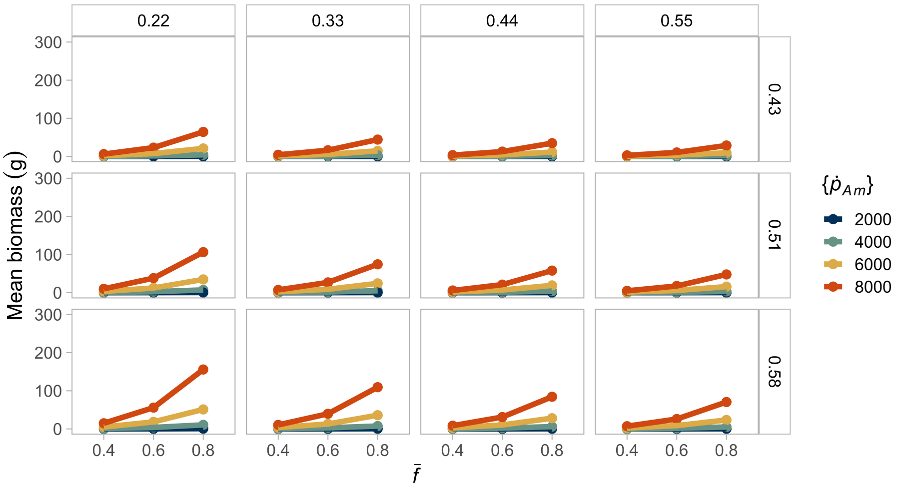

Figure A.2.8. A seasonally varying resource with a lower average reduces interspecific differences in mean biomass, regardless of the initial food level. The largest biomass is attained when individuals combine high assimilation with low energy conductance. The columns indicate the value of energy conductance, while the rows represent the fraction of energy allocated to soma. Point and line colours indicate the maximum specific assimilation rate value. Points and lines of the same colour in each box (equivalent to a parameter combination) represent the same species at different food conditions. The value of $\bar{f}$ indicates the average resource level for each simulation. The initial resource level was set to the highest availability in each case.

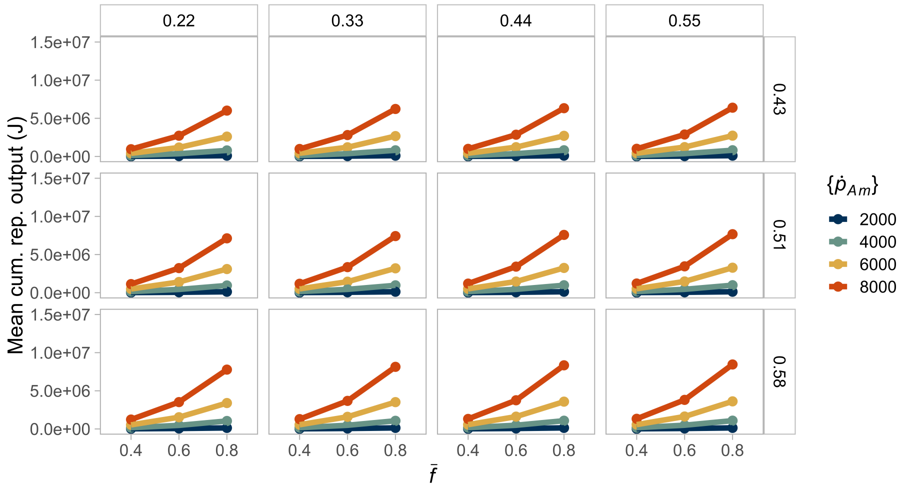

Figure A.2.9. A seasonal and, on average scarcer resource reduces interspecific variability in mean cumulative reproductive output, regardless of the initial resource level. Higher reproductive output is reached when the fraction of energy allocated to soma is high. The columns indicate the value of energy conductance, while the rows represent the fraction of energy allocated to soma. Point and line colours indicate the maximum specific assimilation rate value. Points and lines of the same colour in each box (equivalent to a parameter combination) represent the same species at different food conditions. The value of $\bar{f}$ indicates the average resource level for each simulation. The initial resource level was set to the highest availability in each case (results are similar for all the initial food conditions, see figures A.2.22 to A.2.24).

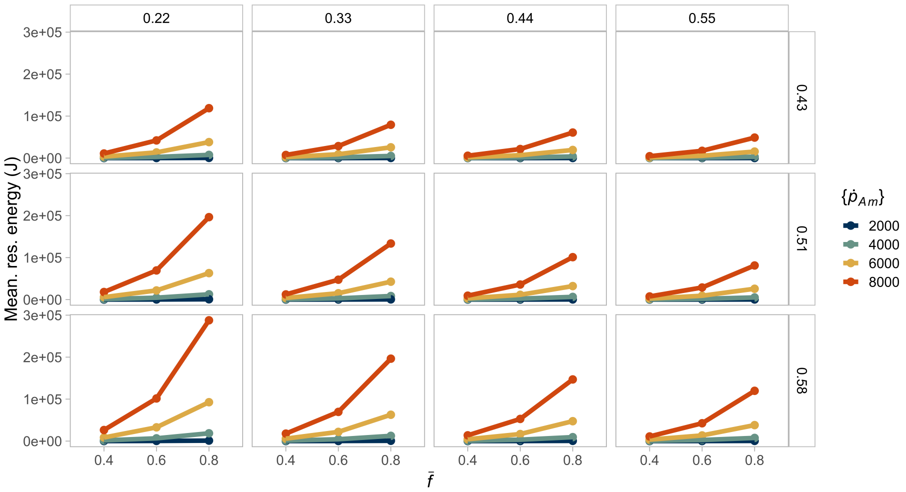

Figure A.2.10. A seasonally varying resource with lower average reduces interspecific differences in mean reserve energy, regardless of the initial food level. The largest energy reserve is attained when individuals combine high assimilation with low energy conductance. The columns indicate the value of energy conductance, while the rows represent the fraction of energy allocated to soma. Point and line colours indicate the maximum specific assimilation rate value. Points and lines of the same colour in each box (equivalent to a parameter combination) represent the same species at different food conditions. The value of $\bar{f}$ indicates the average resource level for each simulation. The initial resource level was set to the highest availability in each case (results are similar for all the initial food conditions, see figures A.2.16 to A.2.18).

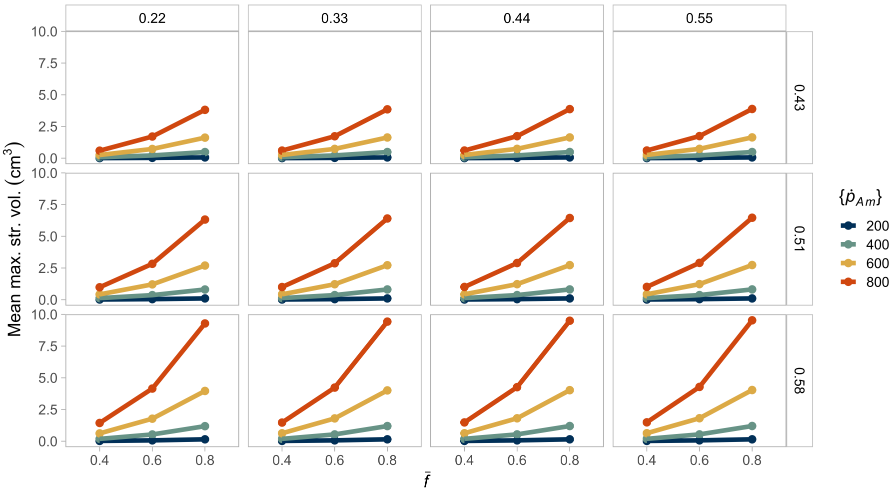

Figure A.2.11. A seasonally varying resource with lower average reduces interspecific differences in mean structural volume, regardless of the initial food level. The largest volume is attained when individuals combine high assimilation with low energy conductance. The columns indicate the value of energy conductance, while the rows represent the fraction of energy allocated to soma. Point and line colours indicate the maximum specific assimilation rate value. Points and lines of the same colour in each box (equivalent to a parameter combination) represent the same species at different food conditions. The value of $\bar{f}$ indicates the average resource level for each simulation. The initial resource level was set to the highest availability in each case (results are similar for all the initial food conditions, see figures A.2.19 to A.2.21).

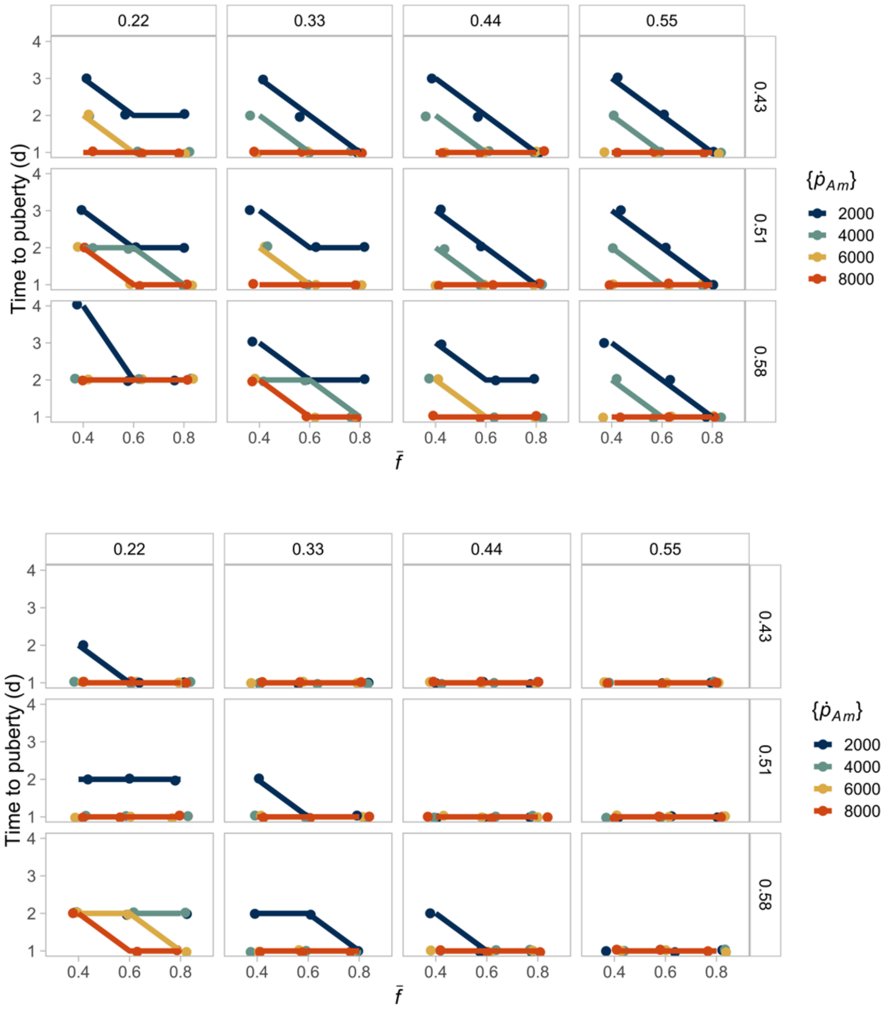

Figure A.2.12. Interspecific differences in the time to reach puberty are amplified when the level of the resource is, on average, lower. A low initial resource produces individuals with slower development times (top) than the same individuals with maximum initial resource availability (bottom). In both scenarios, individuals develop faster when the resource is non-limiting, and they combine high assimilation with high energy conductance. The columns indicate the value of energy conductance, while the rows represent the fraction of energy allocated to soma. Point and line colours indicate the maximum specific assimilation rate value. Points and lines of the same colour in each box (equivalent to a parameter combination) represent the same species at different food conditions. The value of $\bar{f}$ indicates the average resource level for each simulation (see figures A.2.25 to A.2.27 for comparison among different initial resource conditions).

2.7.5 Comparison across initial resource conditions

Regardless of the initial resource level, seasonality amplifies the consequences of interspecific differences in biomass (Figs. A.2.13 to A.2.15), reserve energy (Figs. A.2.16 to

A.2.18), structural volume (Figs. A.2.19 to A.2.21), and reproductive output (Figs. A.2.22 to A.2.24). The mean resource level seems to have a greater effect than the initial resource conditions on the development time (Figs. A.2.25 to A.2.27). However, the differences in time to reach puberty are likely not significant because their variation ranges from 2 to 4 days.

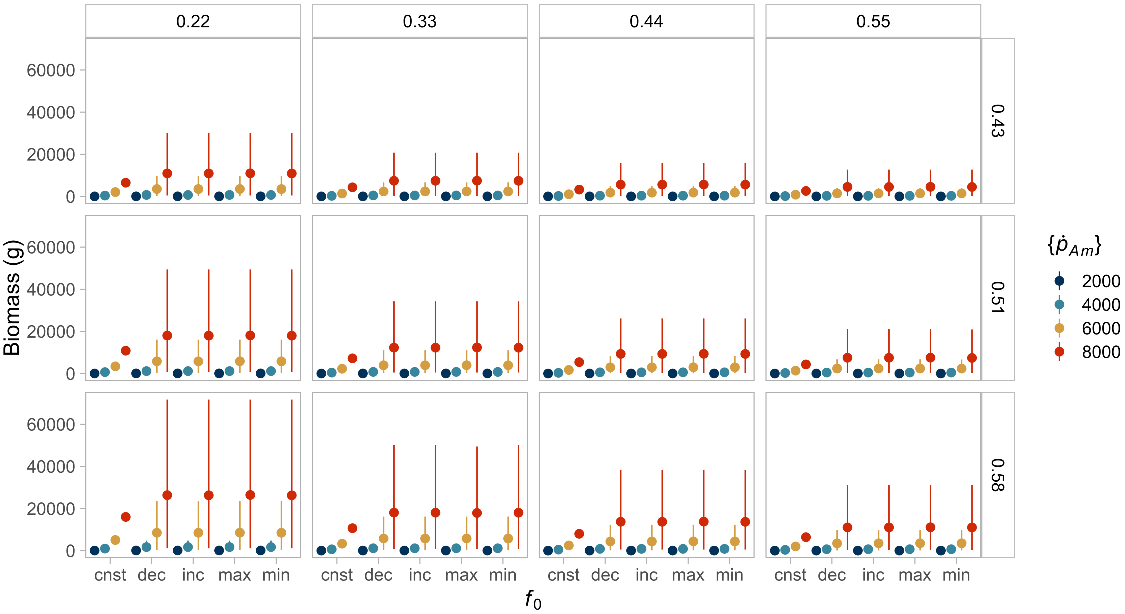

Figure A.2.13. Individuals in a seasonal environment reach larger average biomass than the same individual in a constant environment with an equal mean resource availability, regardless of the initial resource condition f_0. Here, we compare individuals in a constant resource environment (cnst, $f = 0.4$) to those experiencing seasonality ($\bar{f} = 0.4$). We contrasted four different initial conditions for the seasonal environment, which means that individuals can be born when the resource is decreasing (dec, $f_0 = 0.3$), at the minimum level (min, $f_0 = 0.2$), increasing (inc, $f_0 = 0.3$) or at the maximum level (max, $f_0 = 0.4$). In the constant environment, points show the steady-state value reached at the end of the simulations (i.e., year three). In contrast, for the seasonal environment, points represent the average reserve energy calculated over the last two years (i.e., years one to three), and lines correspond to the minimum and maximum values. The columns indicate the value of energy conductance, while the rows represent the fraction of energy allocated to soma. Point and line colours indicate the maximum specific assimilation rate value. Points and lines of the same colour in each box (equivalent to a parameter combination) represent the same species at different food conditions.

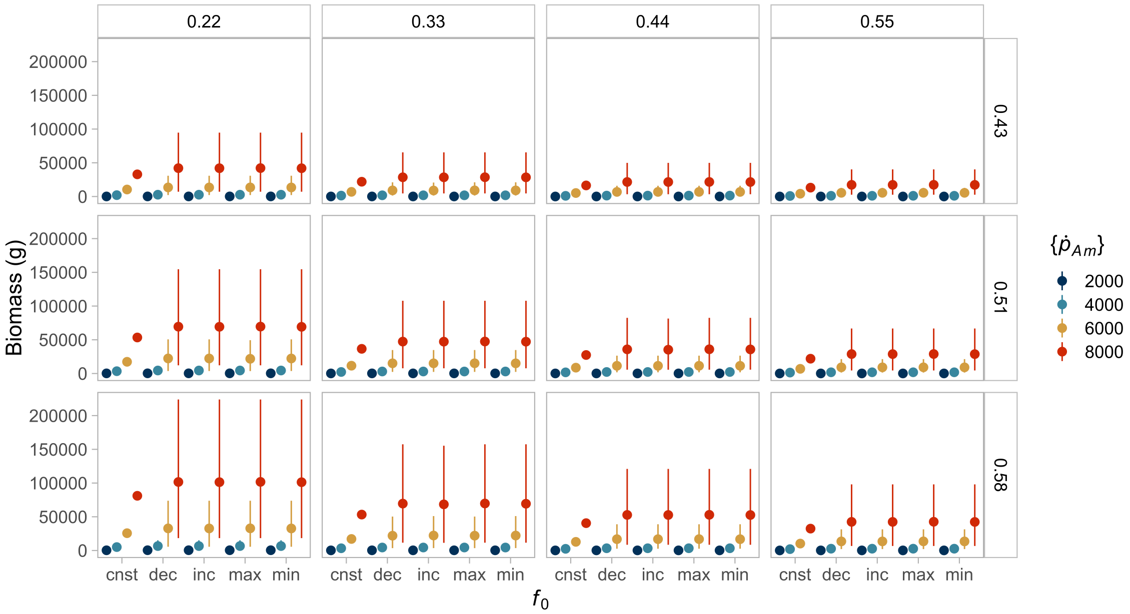

Figure A.2.14. Individuals in a seasonal environment reach larger average biomass than the same individual in a constant environment with an equal mean resource availability, regardless of the initial resource condition f_0. Here, we compare individuals in a constant resource environment (cnst, $f = 0.6$) to those experiencing seasonality ($\bar{f} = 0.6$). We contrasted four different initial conditions for the seasonal environment, which means that individuals can be born when the resource is decreasing (dec, $f_0 = 0.5$), at the minimum level (min, $f_0 = 0.4$), increasing (*inc*,$f_0 = 0.5$) or at the maximum level (max, $f_0 = 0.8$). In the constant environment, points show the steady-state value reached at the end of the simulations (i.e., year three). In contrast, for the seasonal environment, points represent the average reserve energy calculated over the last two years (i.e., years one to three), and lines correspond to the minimum and maximum values. The columns indicate the value of energy conductance, while the rows represent the fraction of energy allocated to soma. Point and line colours indicate the maximum specific assimilation rate value. Points and lines of the same colour in each box (equivalent to a parameter combination) represent the same species at different food conditions.

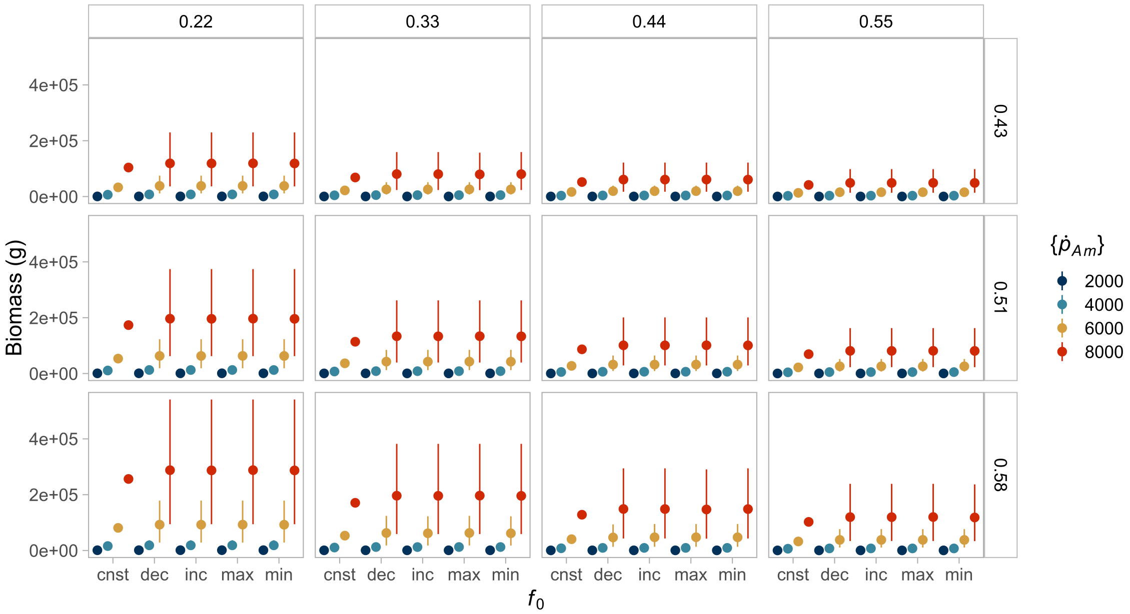

Figure A.2.15. Individuals in a seasonal environment reach larger average biomass than the same individual in a constant environment with an equal mean resource availability, regardless of the initial resource condition f_0. Here, we compare individuals in a constant resource environment (cnst, $f = 0.8$) to those experiencing seasonality ($\bar{f} = 0.8$). We contrasted four different initial conditions for the seasonal environment, which means that individuals can be born when the resource is decreasing (dec, $f_0 = 0.7$), at the minimum level (min, $f_0 = 0.6$), increasing (inc, $f_0 = 0.7$) or at the maximum level (max, $f_0 = 1$). In the constant environment, points show the steady-state value reached at the end of the simulations (i.e., year three). In contrast, for the seasonal environment, points represent the average reserve energy calculated over the last two years (i.e., years one to three), and lines correspond to the minimum and maximum values. The columns indicate the value of energy conductance, while the rows represent the fraction of energy allocated to soma. Point and line colours indicate the maximum specific assimilation rate value. Points and lines of the same colour in each box (equivalent to a parameter combination) represent the same species at different food conditions.

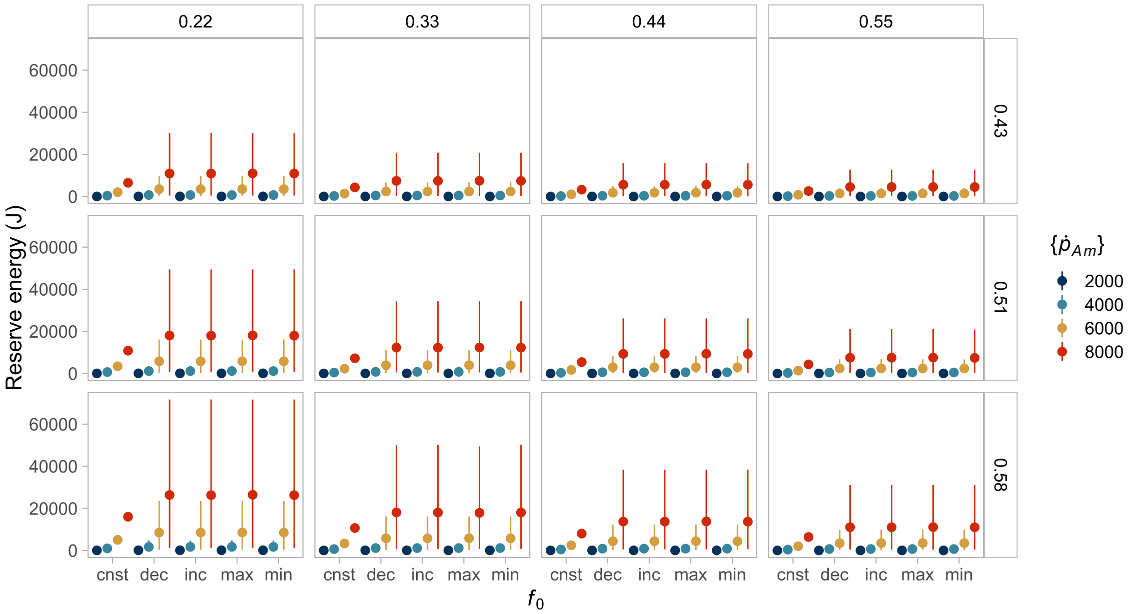

Figure A.2.16. Individuals in a seasonal environment reach larger average reserve energy than the same individual in a constant environment with an equal mean resource availability, regardless of the initial resource condition f_0. Here, we compare individuals in a constant resource environment (cnst, $f = 0.4$) to those experiencing seasonality ($\bar{f} = 0.4$). We contrasted four different initial conditions for the seasonal environment, which means that individuals can be born when the resource is decreasing (dec, $f_0 = 0.3$), at the minimum level (min, $f_0 = 0.2$), increasing (inc, $f_0 = 0.3$) or at the maximum level (max, $f_0 = 0.4$). In the constant environment, points show the steady-state value reached at the end of the simulations (i.e., year three). In contrast, for the seasonal environment, points represent the average reserve energy calculated over the last two years (i.e., years one to three), and lines correspond to the minimum and maximum values. The columns indicate the value of energy conductance, while the rows represent the fraction of energy allocated to soma. Point and line colours indicate the maximum specific assimilation rate value. Points and lines of the same colour in each box (equivalent to a parameter combination) represent the same species at different food conditions.

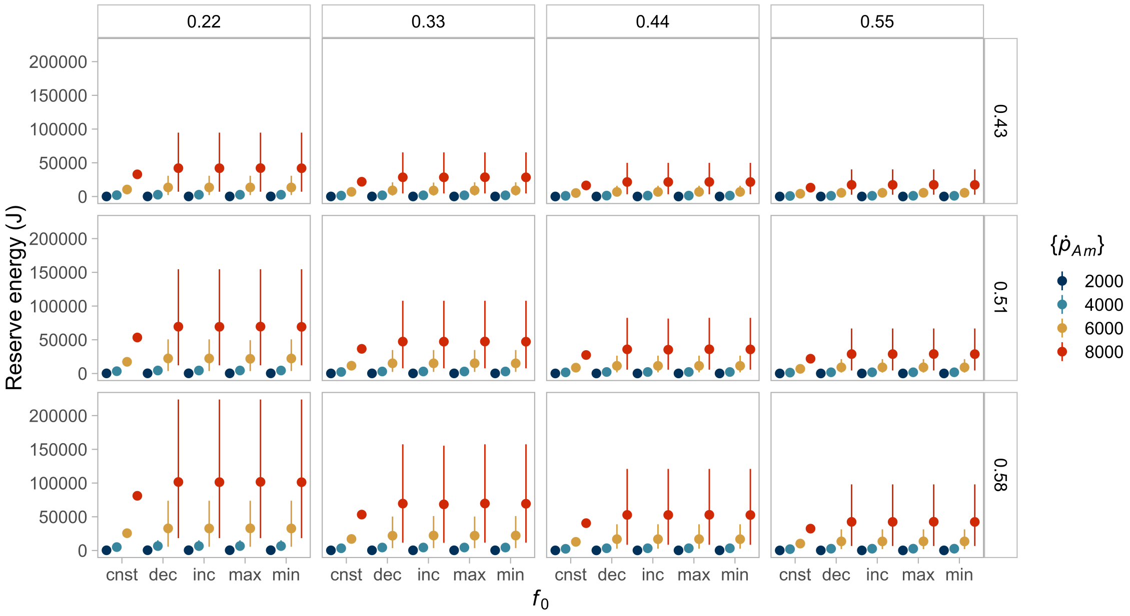

Figure A.2.17. Individuals in a seasonal environment reach larger average reserve energy than the same individual in a constant environment with an equal mean resource availability, regardless of the initial resource condition f_0. Here, we compare individuals in a constant resource environment (cnst, $f = 0.6$) to those experiencing seasonality ($\bar{f} = 0.6$). We contrasted four different initial conditions for the seasonal environment, which means that individuals can be born when the resource is decreasing (dec, $f_0 = 0.5$), at the minimum level (min, $f_0 = 0.4$), increasing (inc, $f_0 = 0.5$) or at the maximum level (max, $f_0 = 0.8$). In the constant environment, points show the steady-state value reached at the end of the simulations (i.e., year three). In contrast, for the seasonal environment, points represent the average reserve energy calculated over the last two years (i.e., years one to three), and lines correspond to the minimum and maximum values. The columns indicate the value of energy conductance, while the rows represent the fraction of energy allocated to soma. Point and line colours indicate the maximum specific assimilation rate value. Points and lines of the same colour in each box (equivalent to a parameter combination) represent the same species at different food conditions.

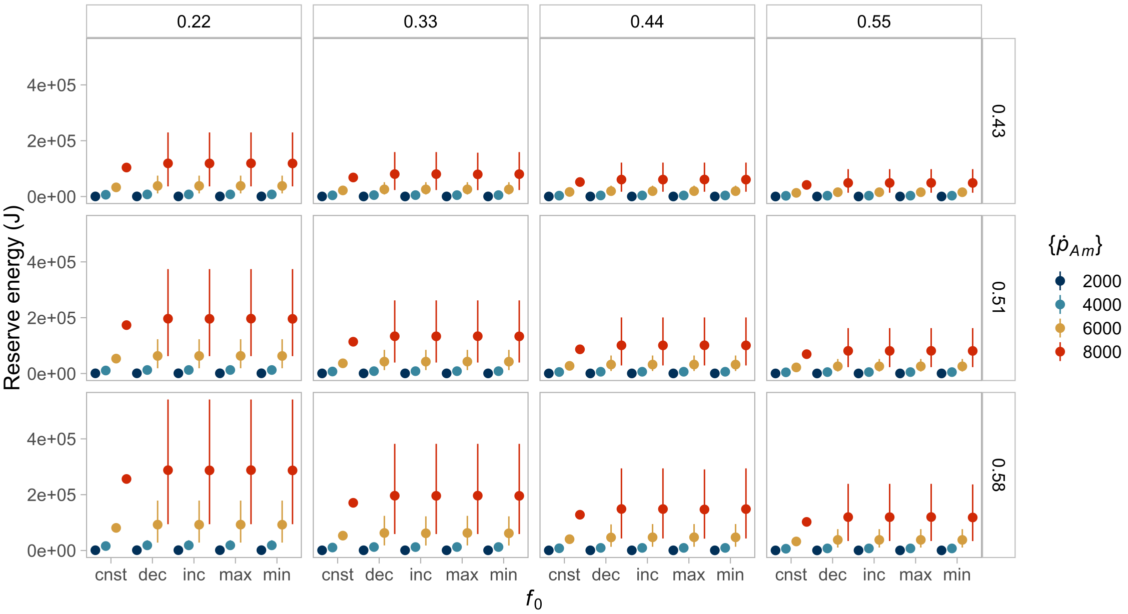

Figure A.2.18. Individuals in a seasonal environment reach larger average reserve energy than the same individual in a constant environment with an equal mean resource availability, regardless of the initial resource condition f_0. Here, we compare individuals in a constant resource environment (cnst, $f = 0.8$) to those experiencing seasonality ($\bar{f} = 0.8$). We contrasted four different initial conditions for the seasonal environment, which means that individuals can be born when the resource is decreasing (dec, $f_0 = 0.7$), at the minimum level (min, $f_0 = 0.6$), increasing (inc, $f_0 = 0.7$) or at the maximum level (max, $f_0 = 1$). In the constant environment, points show the steady-state value reached at the end of the simulations (i.e., year three). In contrast, for the seasonal environment, points represent the average reserve energy calculated over the last two years (i.e., years one to three), and lines correspond to the minimum and maximum values. The columns indicate the value of energy conductance, while the rows represent the fraction of energy allocated to soma. Point and line colours indicate the maximum specific assimilation rate value. Points and lines of the same colour in each box (equivalent to a parameter combination) represent the same species at different food conditions.

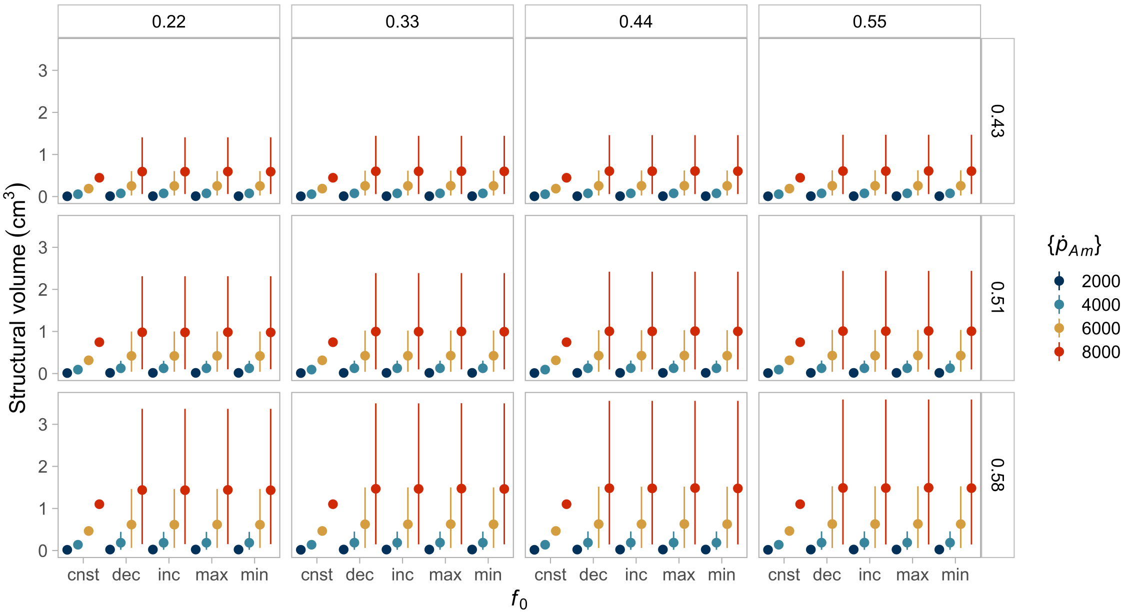

Figure A.2.19. Individuals in a seasonal environment reach greater average structural volume than the same individual in a constant environment with an equal mean resource availability, regardless of the initial resource condition f_0. Here, we compare individuals in a constant resource environment (cnst, $f = 0.4$) to those experiencing seasonality ($\bar{f} = 0.4$). We contrasted four different initial conditions for the seasonal environment, which means that individuals can be born when the resource is decreasing (dec, $f_0 = 0.3$), at the minimum level (min, $f_0 = 0.2$), increasing (inc, $f_0 = 0.3$) or at the maximum level (max, $f_0 = 0.4$). In the constant environment, points show the steady-state value reached at the end of the simulations (i.e., year three). In contrast, for the seasonal environment, points represent the average structural volume calculated over the last two years (i.e., years one to three), and lines correspond to the minimum and maximum values. The columns indicate the value of energy conductance, while the rows represent the fraction of energy allocated to soma. Point and line colours indicate the maximum specific assimilation rate value. Points and lines of the same colour in each box (equivalent to a parameter combination) represent the same species at different food conditions.

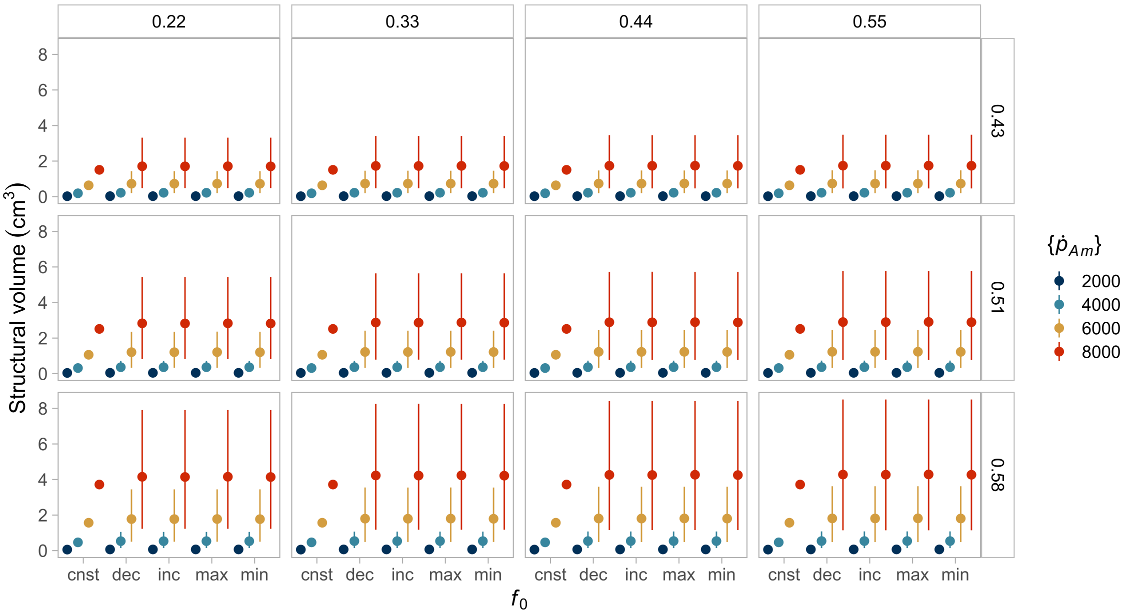

Figure A.2.20. Individuals in a seasonal environment reach greater average structural volume than the same individual in a constant environment with an equal mean resource availability, regardless of the initial resource condition f_0. Here, we compare individuals in a constant resource environment (cnst, $f = 0.6$) to those experiencing seasonality ($\bar{f} = 0.6$). We contrasted four different initial conditions for the seasonal environment, which means that individuals can be born when the resource is decreasing (dec, $f_0 = 0.5$), at the minimum level (min, $f_0 = 0.4$), increasing (inc, $f_0 = 0.5$) or at the maximum level (max, $f_0 = 0.8$). In the constant environment, points show the steady-state value reached at the end of the simulations (i.e., year three). In contrast, for the seasonal environment, points represent the average structural volume calculated over the last two years (i.e., years one to three), and lines correspond to the minimum and maximum values. The columns indicate the value of energy conductance, while the rows represent the fraction of energy allocated to soma. Point and line colours indicate the maximum specific assimilation rate value. Points and lines of the same colour in each box (equivalent to a parameter combination) represent the same species at different food conditions.

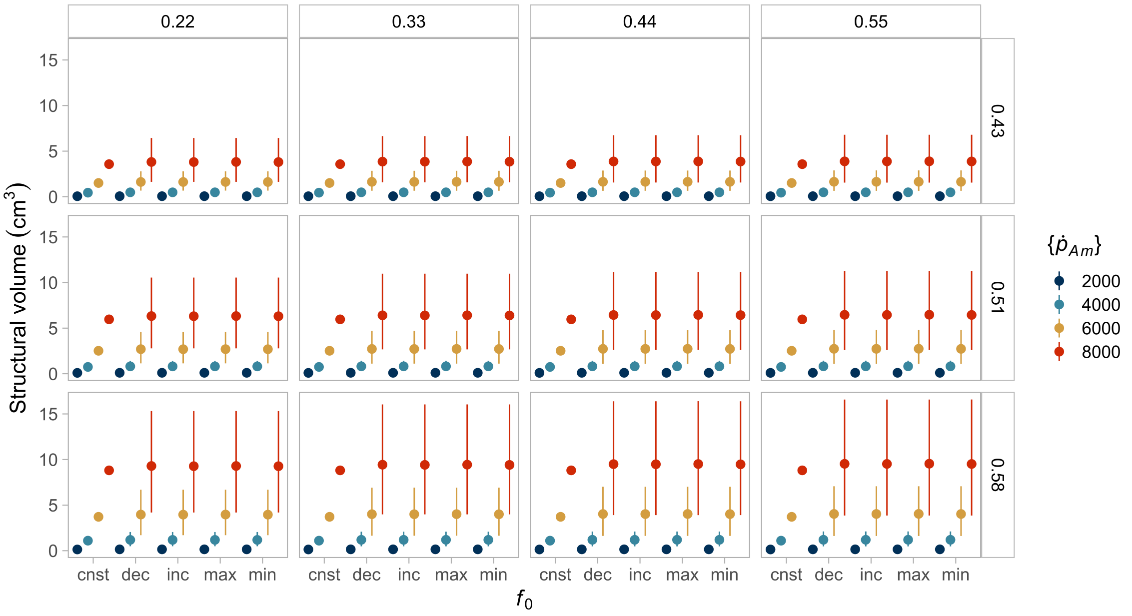

Figure A.2.21. Individuals in a seasonal environment reach greater average structural volume than the same individual in a constant environment with an equal mean resource availability, regardless of the initial resource condition f_0. Here, we compare individuals in a constant resource environment (cnst, $f = 0.8$) to those experiencing seasonality ($\bar{f} = 0.8$). We contrasted four different initial conditions for the seasonal environment, which means that individuals can be born when the resource is decreasing (dec, $f_0 = 0.7$), at the minimum level (min, $f_0 = 0.6$), increasing (inc, $f_0 = 0.7$) or at the maximum level (max, $f_0 = 1$). In the constant environment, points show the steady-state value reached at the end of the simulations (i.e., year three). In contrast, for the seasonal environment, points represent the average structural volume calculated over the last two years (i.e., years one to three), and lines correspond to the minimum and maximum values. The columns indicate the value of energy conductance, while the rows represent the fraction of energy allocated to soma. Point and line colours indicate the maximum specific assimilation rate value. Points and lines of the same colour in each box (equivalent to a parameter combination) represent the same species at different food conditions.

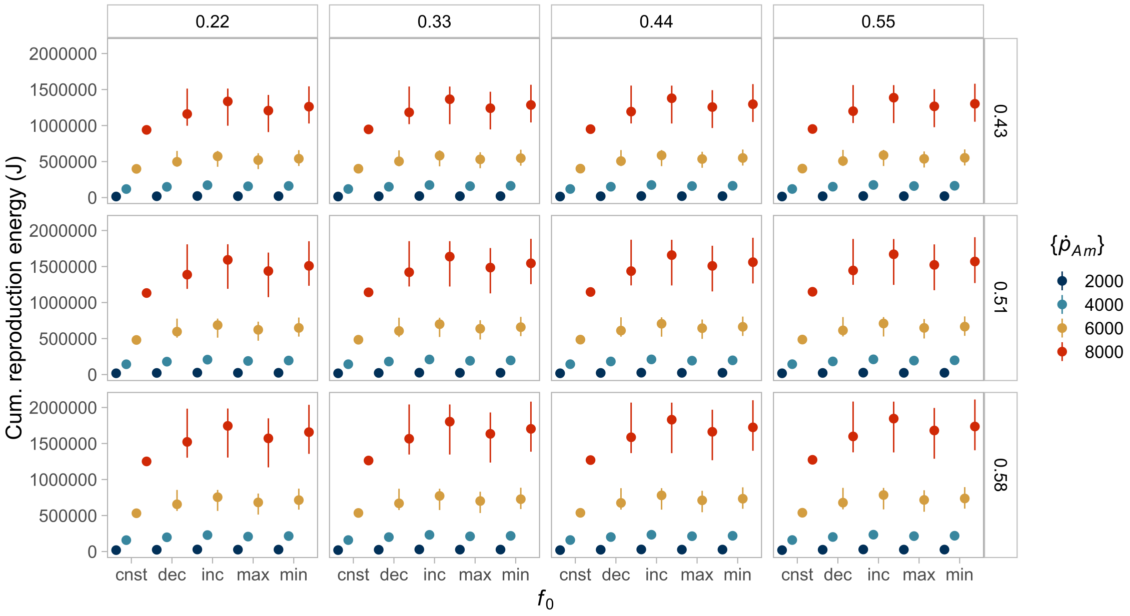

Figure A.2.22. Individuals in a seasonal environment reach greater average cumulative reproduction energy than the same individual in a constant environment with an equal mean resource availability, regardless of the initial resource condition f_0. Here, we compare individuals in a constant resource environment (cnst, $f = 0.4$) to those experiencing seasonality ($\bar{f} = 0.4$). We contrasted four different initial conditions for the seasonal environment, which means that individuals can be born when the resource is decreasing (dec, $f_0 = 0.3$), at the minimum level (min, $f_0 = 0.2$), increasing (inc, $f_0 = 0.3$) or at the maximum level (max, $f_0 = 0.4$). In the constant environment, points show the steady-state value reached at the end of the simulations (i.e., year three). In contrast, for the seasonal environment, points represent the average structural volume calculated over the last two years (i.e., years one to three), and lines correspond to the minimum and maximum values. The columns indicate the value of energy conductance, while the rows represent the fraction of energy allocated to soma. Point and line colours indicate the maximum specific assimilation rate value. Points and lines of the same colour in each box (equivalent to a parameter combination) represent the same species at different food conditions.

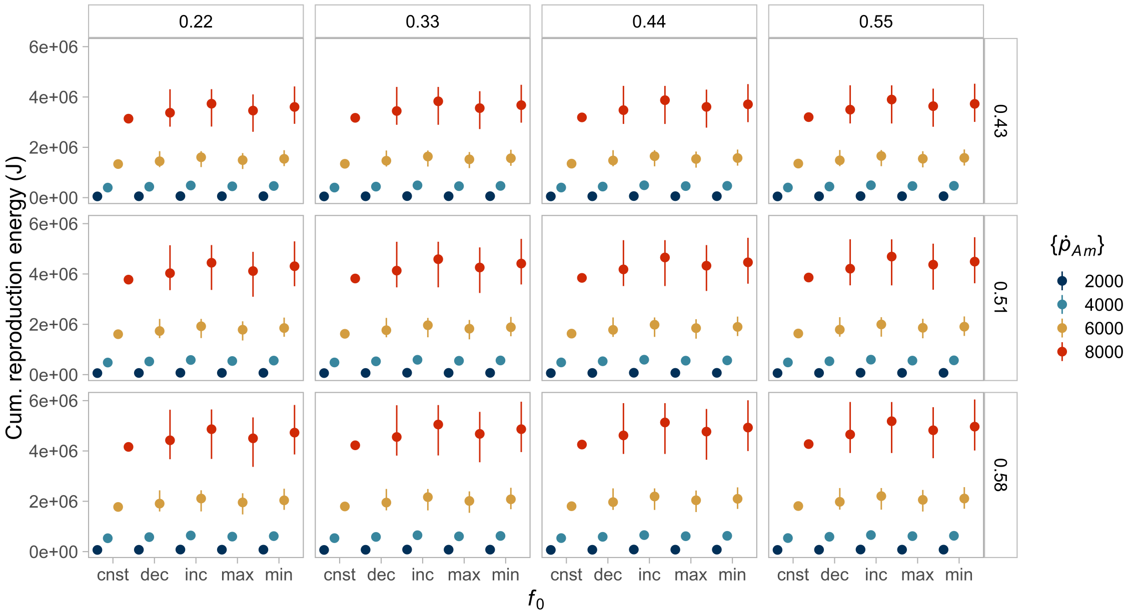

Figure A.2.23. Individuals in a seasonal environment reach greater average cumulative reproduction energy than the same individual in a constant environment with an equal mean resource availability, regardless of the initial resource condition f_0. Here, we compare individuals in a constant resource environment (cnst, $f = 0.6$) to those experiencing seasonality ($\bar{f} = 0.6$). We contrasted four different initial conditions for the seasonal environment, which means that individuals can be born when the resource is decreasing (dec, $f_0 = 0.5$), at the minimum level (min, $f_0 = 0.4$), increasing (inc, $f_0 = 0.5$) or at the maximum level (max, $f_0 = 0.8$). In the constant environment, points show the steady-state value reached at the end of the simulations (i.e., year three). In contrast, for the seasonal environment, points represent the average structural volume calculated over the last two years (i.e., years one to three), and lines correspond to the minimum and maximum values. The columns indicate the value of energy conductance, while the rows represent the fraction of energy allocated to soma. Point and line colours indicate the maximum specific assimilation rate value. Points and lines of the same colour in each box (equivalent to a parameter combination) represent the same species at different food conditions.

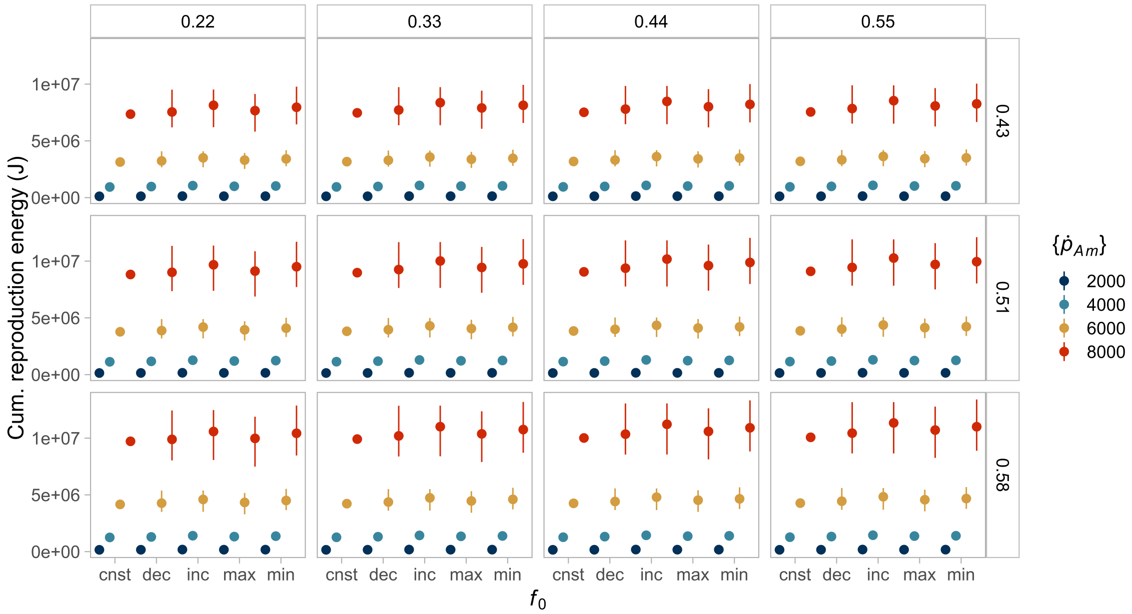

Figure A.2.24. Individuals in a seasonal environment reach greater average cumulative reproduction energy than the same individual in a constant environment with an equal mean resource availability, regardless of the initial resource condition f_0. Here, we compare individuals in a constant resource environment (cnst, $f = 0.8$) to those experiencing seasonality ($\bar{f} = 0.8$). We contrasted four different initial conditions for the seasonal environment, which means that individuals can be born when the resource is decreasing (dec, $f_0 = 0.7$), at the minimum level (min, $f_0 = 0.6$), increasing (inc, $f_0 = 0.7$) or at the maximum level (max, $f_0 = 1$). In the constant environment, points show the steady-state value reached at the end of the simulations (i.e., year three). In contrast, for the seasonal environment, points represent the average structural volume calculated over the last two years (i.e., years one to three), and lines correspond to the minimum and maximum values. The columns indicate the value of energy conductance, while the rows represent the fraction of energy allocated to soma. Point and line colours indicate the maximum specific assimilation rate value. Points and lines of the same colour in each box (equivalent to a parameter combination) represent the same species at different food conditions.

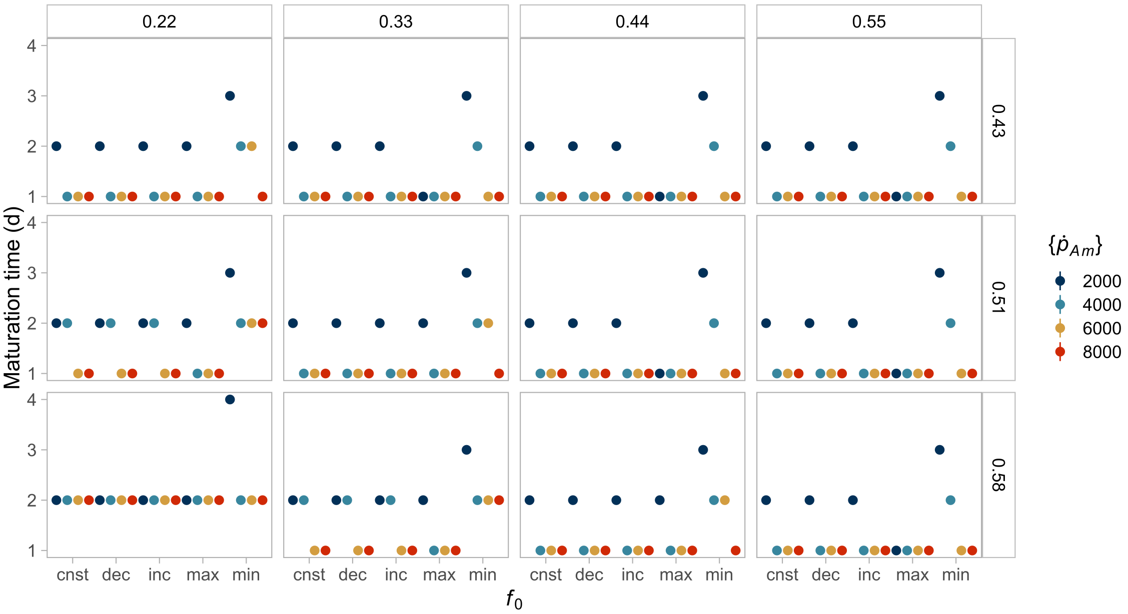

Figure A.2.25. Interspecific differences in the time to reach puberty between individuals in a seasonal environment and the same individual in a constant environment with an equal mean resource availability do not seem to be dependent on the initial resource condition, f_0. Here, we compare individuals in a constant resource environment (cnst, $f = 0.4$) to those experiencing seasonality ($\bar{f} = 0.4$). We contrasted four different initial conditions for the seasonal environment, which means that individuals can be born when the resource is decreasing (dec, $f_0 = 0.3$), at the minimum level (min, $f_0 = 0.2$), increasing (inc, $f_0 = 0.3$) or at the maximum level (max, $f_0 = 0.6$). In all environments, points show the numbers of days required to reach the puberty threshold (E_H^p). The columns indicate the value of energy conductance, while the rows represent the fraction of energy allocated to soma. Point colours indicate the maximum specific assimilation rate value. Points of the same colour in each box (equivalent to a parameter combination) represent the same species at different food conditions.

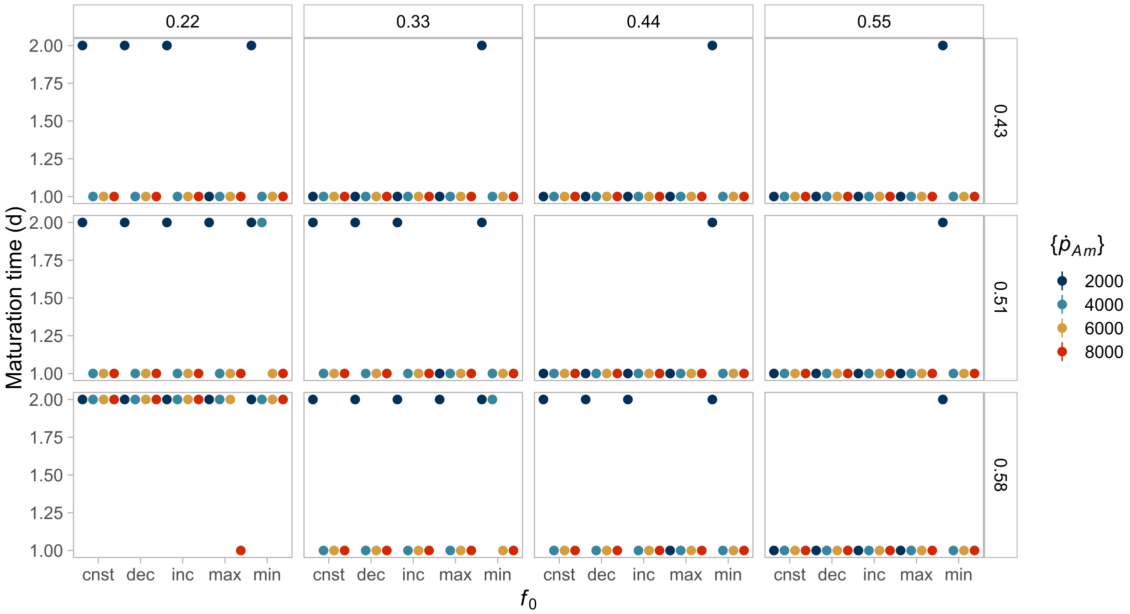

Figure A.2.26. Interspecific differences in the time to reach puberty between individuals in a seasonal environment and the same individual in a constant environment with an equal mean resource availability do not seem to be dependent on the initial resource condition, f_0. Here, we compare individuals in a constant resource environment (cnst, $f = 0.6$) to those experiencing seasonality ($\bar{f} = 0.6$). We contrasted four different initial conditions for the seasonal environment, which means that individuals can be born when the resource is decreasing (dec, $f_0 = 0.5$), at the minimum level (min, $f_0 = 0.4$), increasing (inc, $f_0 = 0.5$) or at the maximum level (max, $f_0 = 0.8$). In all environments, points show the numbers of days required to reach the puberty threshold (E_H^p). The columns indicate the value of energy conductance, while the rows represent the fraction of energy allocated to soma. Point colours indicate the maximum specific assimilation rate value. Points of the same colour in each box (equivalent to a parameter combination) represent the same species at different food conditions.

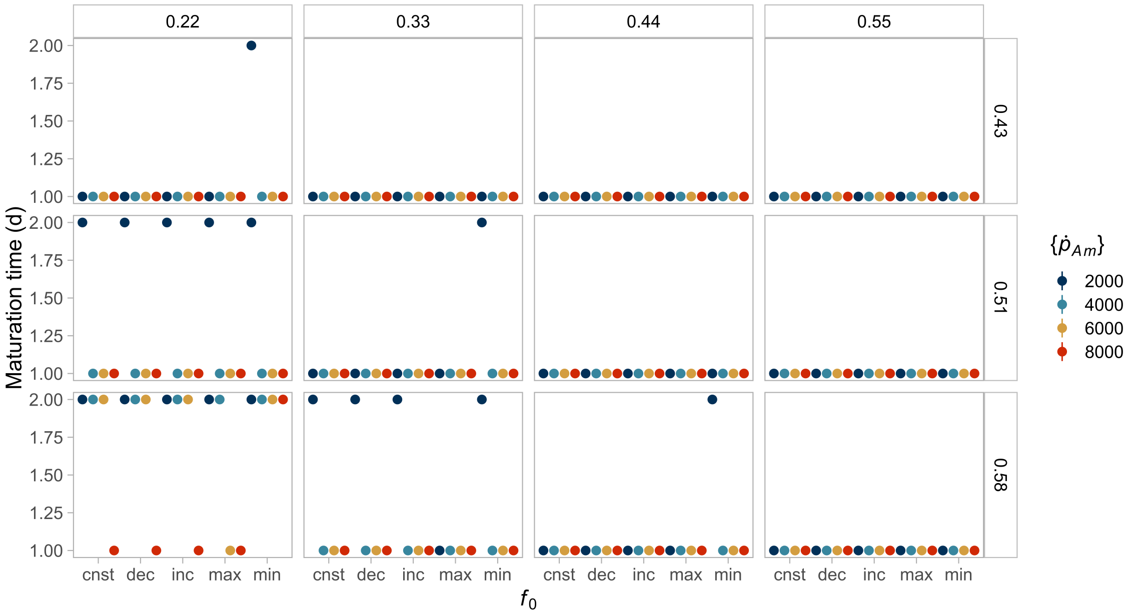

Figure A.2.27. Interspecific differences in the time to reach puberty between individuals in a seasonal environment and the same individual in a constant environment with an equal mean resource availability do not seem to be dependent on the initial resource condition, f_0. Here, we compare individuals in a constant resource environment (cnst, $f = 0.8$) to those experiencing seasonality ($\bar{f} = 0.8$). We contrasted four different initial conditions for the seasonal environment, which means that individuals can be born when the resource is decreasing (dec, $f_0 = 0.7$), at the minimum level (min, $f_0 = 0.6$), increasing (inc, $f_0 = 0.7$) or at the maximum level (max, $f_0 = 1$). In all environments, points show the numbers of days required to reach the puberty threshold (E_H^p). The columns indicate the value of energy conductance, while the rows represent the fraction of energy allocated to soma. Point colours indicate the maximum specific assimilation rate value. Points of the same colour in each box (equivalent to a parameter combination) represent the same species at different food conditions.

2.7.6 Comparing temperate and tropical species: an example

We used the fan-tailed gerygone, *Gerygone flavolateralis*, and the grey warbler, *G. igata*, to compare the traits exhibited by related species in contrasting environments. We chose these species because they were originally within our parameter space. However, we included more data and reestimated their parameters to improve the accuracy of the predictions (Tab. A.2.2).

Table A.2.2. Parameter values for the two species used to compare tropical versus temperate species.

Species	Common name	κ	$\{\dot{p}_{Am}\}$	$\dot{v}$	$[\dot{p}_M]$	$[E_G]$	E_H^b	E_H^p
Gerygone flavolateralis	Fan-tailed gerygone	0.998	4692.6	0.08	5084.7	7338	7.647	453.1
Gerygone igata	Grey warbler	0.983	4878.1	0.05	6045.1	7351	71.74	7880

3

DYNAMIC ENERGY BUDGET THEORY PREDICTS SMALLER ENERGY RESERVES IN THYASIRID BIVALVES THAT HARBOUR SYMBIONTS

Joany Mariño, Starrlight Augustine, Suzanne C. Dufour, Amy Hurford

Dynamic energy budget (DEB) theory describes the ecophysiology of individuals and distinguishes between the biomass of an organism that functions as an energy reserve and as a structure. DEB theory offers a robust framework to infer and contrast energy allocation patterns, even in data-poor species. We used this approach to compare two thyasirid bivalves that have scarce data: *Thyasira* cf. *gouldi* and *Parathyasira* sp., which co-occur in a seasonal environment, show similar life history features, and are both particulate feeders. However, *T.* cf. *gouldi* hosts chemosymbiotic bacteria that are digested as an additional resource, and how this mixotrophy affects the energy budget of these chemosymbiotic thyasirids is unknown. We used allometric and life history data to parameterize a DEB model for each species and found that symbiotic *T.* cf. *gouldi* has a smaller fraction of its biomass as an energy reserve relative to *Parathyasira*. A smaller energy reserve, in turn, implies reduced energy assimilation and mobilization fluxes, lower somatic maintenance costs and growth rate, and larger energy allocation to maturity and reproduction in symbiotic *T.* cf. *gouldi*. For a thyasirid inhabiting an environment with seasonal forcing, these life history traits may represent an evolutionary strategy where the symbionts function as a partial energy reserve. Our results elucidate a potential role of the chemosymbiotic bacteria in the ecophysiology of a bivalve host, and highlight how the symbiotic association is likely to alter the energy budget of a mixotrophic thyasirid.

Published in Journal of Sea Research (2019) 143: 119-127

3.1 INTRODUCTION

Among symbiotic relationships, the association between chemosynthetic bacteria and invertebrate animals is a prominent example because of its prevalence in diverse marine habitats and within multiple phyla of hosts (Dubilier et al., 2008), especially within the Bivalvia (Roeselers & Newton, 2012). One particular family of bivalves, the Thyasiridae, is notable for containing symbiotic as well as asymbiotic species (Southward, 1986; Taylor et al., 2007). Thyasirids gain nutrients by particulate feeding, with symbiotic and some asymbiotic species likely ingesting free-living, sediment-dwelling chemosynthetic bacteria collected using their elongated foot (Zanzerl & Dufour, 2017). Symbiotic thyasirids, such as *Thyasira* cf. *gouldi*, periodically endocytose and digest symbionts (Dufour et al., 2014), which are harboured extracellularly on gill epithelial cells (Southward, 1986). For the thyasirid host, symbiosis is a trophic interaction where bacterial endosymbionts constitute an additional food source (Dando & Spiro, 1993). However, the thyasirids are still one of the least studied bivalve groups: their taxonomic classification remains uncertain (with many unnamed species), and their symbiotic interaction is poorly understood (Taylor & Glover, 2010). Specifically, the relative importance of chemosymbiosis and particulate feeding (i.e. a mixotrophic diet) in the energy budget of symbiotic thyasirids has yet to be determined.

Representatives of the Thyasiridae are sympatric within the fjord of Bonne Bay (Newfoundland, Canada), an environment that experiences strong seasonal cycles (Laurich et al., 2015). One species, *Parathyasira* sp., is asymbiotic (Batstone et al., 2014). The other taxon resembles *Thyasira gouldi* (in shell characteristics and internal anatomy, hence referred to as *T.* cf. *gouldi*), and forms a complex of cryptic species, which has been provisionally described as three Operational Taxonomic Units (OTUs; Batstone et al., 2014). *T.* cf. *gouldi* displays a unique condition among bivalves that appear to belong to the same species: two of the OTUs are symbiotic and closely related with each other while the third

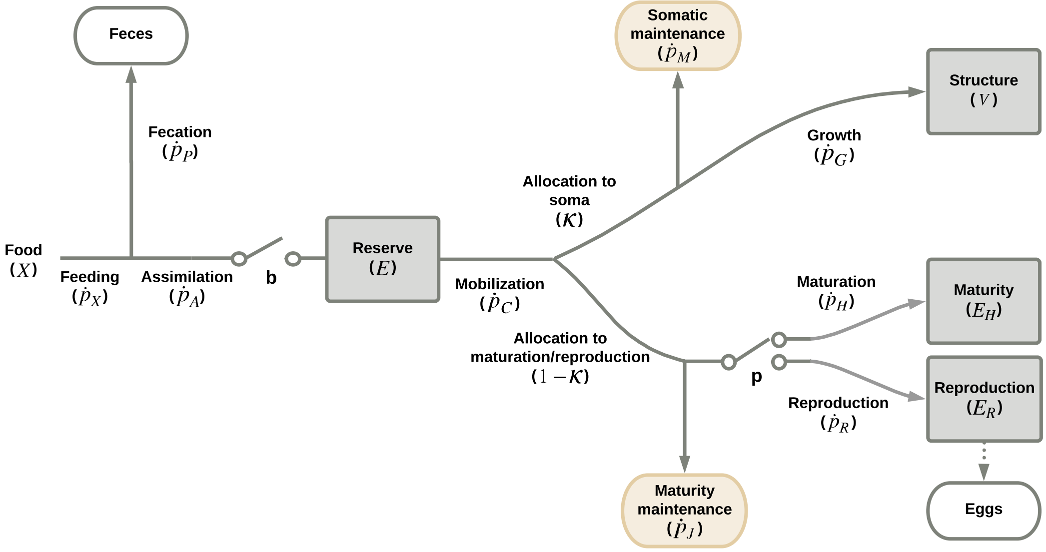

Figure 3.1. Schematic representation of the DEB model. Square boxes denote state variables (see Eq. 3.1), round boxes indicate energy sinks, lines and arrows correspond to the energy fluxes (J/d, see Tab. 3.1), dots ($\dot{}$) indicate rates. The switches b and p represent metabolic thresholds at birth and puberty, respectively. Food is taken as a forcing variable. See Table 3.3 for symbol definitions.

one is asymbiotic (Batstone et al., 2014); here, we focus solely on the symbiotic OTUs 1 and 2. Despite their nutritional differences, *Parathyasira* sp. and symbiotic *T.* cf. *gouldi* (OTUs 1 and 2) share key life history traits, particularly puberty and adult sizes (Dufour, 2017), and the role that the symbionts play in the ecophysiology of the host is not clear.

Thyasirids exemplify species in which detailed data are scarce, and in such cases, Dynamic Energy Budget (DEB) theory offers a mechanistic framework to make life history inferences. From general energy partitioning postulates, DEB theory can identify broad metabolic patterns at different stages of an organisms' life cycle. In particular, DEB theory assumes that the energy from food is assimilated into a reserve. A fixed fraction (κ) of the energy reserve is then allocated and used for somatic maintenance and growth, while the rest is invested into maturity maintenance and maturity or reproduction (Fig. 3.1; Kooijman, 2010). The biomass of the organism is the sum of the masses of reserve and structure; energy invested in maturity and reproduction is assumed to be released into the environment (for complete list of postulates see Tab. 2.4 in Kooijman, 2010).

The assumptions of DEB theory enable relating simple, measurable quantities (e.g. length at birth, maximum length, length vs. age, weight vs. length) to physiological investment and energy allocation (Kooijman, 2010). For example, an organism that has a large ultimate size also has a high energy assimilation flux and a large energy reserve capacity, relative to a smaller organism of the same species. In this way, we use DEB theory to understand how the thyasirids of Bonne Bay partition their energy. To clarify the underlying effects of mixotrophy in the energy budget of the chemosymbiotic thyasirids, we make quantitative comparisons between the ecophysiological parameters of symbiotic *T.* cf. *gouldi* (OTUs 1 and 2) and *Parathyasira* sp. In this study we focus on elucidating the impact of harbouring symbionts in the life history strategies of *T.* cf. *gouldi*, which may be interpreted as a response to a fluctuating environment.

3.2 METHODS

3.2.1 DEB-abj model

The individual is represented by four state variables, namely: energy reserve (E, J), volume of structure (V, cm^3), cumulative energy invested into maturation (E_H, J), and cumulative energy invested into reproduction (E_R, J). The dynamic of the individual in time is given by:

$$
\begin{aligned}
\frac{dE}{dt} &= \dot{p}_A - \dot{p}_C, \\
\frac{dV}{dt} &= \dot{p}_G/[E_G], \\
\frac{dE_H}{dt} &= \dot{p}_H(E_H < E_H^p), \\
\frac{dE_R}{dt} &= \dot{p}_R(E_H = E_H^p),
\end{aligned}
\tag{3.1}
$$

where $[E_G]$ is the specific cost for structure, E_H^p is the puberty threshold, and $\dot{p}_i$ gives the energy flux of each process i (Tab. 3.1).

The cumulative energy invested into maturity (E_H) represents the developmental stage of the organism relative to energy thresholds at developmental milestones (Fig. 3.2; Augustine, 2017). The first maturity threshold is birth ($E_H = E_H^b$), defined by the beginning of the ingestion of food that is then assimilated into the energy reserve. The next maturity threshold is metamorphosis ($E_H = E_H^j$), because it is assumed that after birth and before puberty there is a different metabolic rate, which results in a temporarily faster growth rate (a pattern termed metabolic or $\mathcal{M}$ acceleration; Kooijman, 2014). The last threshold is puberty ($E_H = E_H^p$), defined as the start of allocation towards reproduction. The puberty threshold is denoted in Equation 3.1 by the boolean ($E_H < E_H^p$), defined to have value 1 if true and 0 if false. Once puberty is reached, the cumulative energy invested into reproduction (E_R, or reproduction buffer) is constantly being used in the production of gametes. The DEB-abj model (see details in the Appendix) is a one parameter extension of the standard DEB model, modified to account for the metabolic acceleration, a pattern recognized in bivalves and many other taxa (Kooijman, 2014; Marques et al., 2018a).

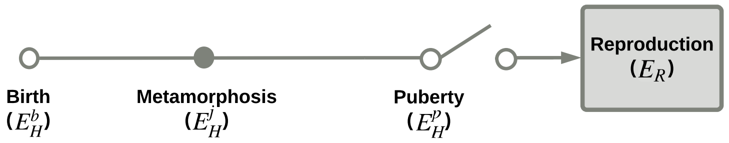

Figure 3.2. Life stages in the DEB-abj model are represented by energy thresholds given by the cumulative energy invested in maturity (E_H, Eq. 3.1). The first threshold is birth ($E_H = E_H^b$), defined as the beginning of assimilation from food and the start of metabolic acceleration. The closed circle denotes the metamorphosis threshold, when metabolic acceleration ceases ($E_H = E_H^j$). Puberty is the last threshold ($E_H = E_H^p$), after which allocation to reproduction starts ($E_H = E_R$).

Table 3.1. Energy fluxes (J/d) considered in the DEB-abj model (Kooijman, 2010, 2014). The digestion efficiency from food to reserve is κ_X, κ_P is the fecation efficiency from food to feces, f is the scaled functional response ($0 \leqslant f \leqslant 1$, where 1 is the highest amount of food), $\{\dot{p}_{Am}\}$ is the maximum surface-area specific assimilation rate ($J/d \cdot cm^2$), $\mathcal{M}$ is the metabolic acceleration, $\dot{v}$ is the energy conductance rate from the energy reserve (cm/d), L is the structural length ($L = V^{1/3}$), $\dot{r}$ is the specific growth rate ($1/d$), κ is the fraction of mobilized reserve allocated to soma, $[\dot{p}_M]$ is the volume-specific somatic maintenance cost ($J/d \cdot cm^3$), $\dot{k}_J$ is the maturity maintenance rate coefficient ($1/d$). Notation: square brackets ([ ]) indicate quantities related to structural volume, curly brackets ({ }) denote quantities related to structural surface-area, dots ($\dot{}$) indicate rates. See DEB-abj model section in the Appendix for definitions.

Flux	Equation
Ingestion/feeding	$\dot{p}_X = \dot{p}_A/\kappa_X$
Fecation	$\dot{p}_P = \kappa_P \dot{p}_X$
Assimilation	$\dot{p}_A = f\{\dot{p}_{Am}\}\mathcal{M}(E_H \geq E_H^b)$
Mobilization	$\dot{p}_C = E(\dot{v}\mathcal{M}/L - \dot{r})$
Allocation to soma	$\kappa \dot{p}_C$
Somatic maintenance	$\dot{p}_M = [\dot{p}_M]L^3$
Growth	$\dot{p}_G = \kappa \dot{p}_C - \dot{p}_M$
Allocation to maturity/reproduction	$(1-\kappa)\dot{p}_C$
Maturity maintenance	$\dot{p}_J = \dot{k}_J E_H$
Maturation	$\dot{p}_H = (1-\kappa)\dot{p}_C \dot{p}_J$
Reproduction	$\dot{p}_R = (1-\kappa)\dot{p}_C \dot{k}_J E_H^p$

3.2.2 Data

Data are classified as either zero- or uni-variate (Lika et al., 2011a). Zero-variate data are the values of a dependent response variable of the organism at a given time (they constitute single data points, e.g.: length at birth, weight at maximum size). In contrast, uni-variate data consist of values of an independent variable and a dependent response variable (e.g.: length as a function of age, weight as a function of length). In addition to the empirical data from the species, the covariation method used for parameter estimation employs pseudo-data, which act similarly to a prior in Bayesian parameter estimation (Lika et al., 2011a). Pseudo-data are typical, but not species-specific, parameter values from different data sets of a variety of taxa (Tab. 8.1 Kooijman, 2010; Lika et al., 2011a). These values are not expected to deviate greatly across species, because the magnitude of their variation is restricted by the same physical and chemical constraints that determine the shared metabolic properties of the organisms.

DEB theory treats food and temperature as forcing variables, and assumes that temperature affects all metabolic rates equally (see Section 1.3 in Kooijman, 2010). The model parameters, as well as the empirical and the pseudo-data, are standardized to a reference temperature of 20°C ($T_{ref} = 293.15$K; Lika et al., 2011a). The correction between the reference temperature and the empirical temperature T is done through the Arrhenius relationship (Eq. 1.2 in Kooijman, 2010):

$$c(T) = \exp\Big(\frac{T_A}{T_{ref}} - \frac{T_A}{T}\Big),$$

where $c(T)$ is the correction factor for a certain temperature T, T_A is the Arrhenius temperature ($T_A = 8000$K; Lika et al., 2011a), and T_{ref} is the reference temperature. For example, the reproduction flux (Tab. 3.1) at temperature T becomes: $\dot{p}_R(T) = \dot{p}_R(T_{ref}) \cdot c(T)$.

Food level is quantified by the scaled functional response f, which can range from no assimilation ($f = 0$) to the highest amount of assimilation ($f = 1$). However, our study focuses on organisms sampled in the field (where individuals were likely to experience a variety of food levels); we do not have precise information on food availability or quality, and how it may change over time. In such cases, the covariation method assumes that food is abundantly available ($f = 1$ for all data sets; Lika et al., 2014). This should be taken as a reference value from which we can compare growth between species (assuming they are subject to the same food availability) as well as between sites in the future (e.g. Ballesta-Artero et al., 2019, this special issue). Further, we assumed that the organism was in equilibrium with the environment, meaning that the reserve density is constant: $d[E]/dt = 0$. These assumptions are included in the covariation method, as they simplify the estimation procedure and allow estimating parameters for species with limited available data (Lika et al., 2014).

The data sets used for both species, including empirical and pseudo-data, are summarized in Table 3.2. We took the maximum reproductive rate as being equal to that of *Thyasira gouldi*, a closely related species similar in size and habitat (Blacknell, 1973). For the thyasirids collected in Bonne Bay we assumed a body temperature equal to that of the sediment, $T = 6°\text{C}$ (which represents the yearly average; Laurich et al., 2015). For the validation data of *Thyasira gouldi* we set $T = 10°\text{C}$, after Blacknell, 1973. Details regarding data measurements are presented in the Data collection section of the Appendix.

Table 3.2. Data sets considered in the parameterization and validation of the DEB-abj model. The first row section corresponds to empirical zero- and uni-variate data from the symbiotic *Thyasira* cf. *gouldi* and the asymbiotic *Parathyasira* sp. The second row section indicates uni-variate validation data from *Thyasira gouldi*. The last row section shows the pseudo-data, as specified by the covariation method (Lika et al., 2011a; Lika, Kearney, & Kooijman, 2011b). Notation: square brackets ([ ]) indicate quantities related to structural volume, dots ($\dot{}$) denote rates. See Data collection section of the Appendix for details on measurements.

Symbol	Unit	Description
a_m	d	Life span[a]
L_b	cm	Length at birth[b]
L_p	cm	Length at puberty[c]
L_i	cm	Ultimate total length[d]
Wd_i	g	Ultimate ash-free dry weight
$\dot{R}_m$	$\#/d$	Maximum reproduction rate
tL	d	Length as a function of time
LW_d	-	Ash-free dry weight as a function of length
LN	# eggs	Fecundity as a function of size
TJO	ml/h	Respiration as a function of temperature
WTO	ml/h	Respiration as a function of weight
$\dot{v}$	cm/d	Energy conductance
κ	-	Allocation fraction to soma
$[\dot{p}_M]$	$(J/d \cdot cm^3)$	Volume-specific somatic maintenance cost
κ_G	-	Growth efficiency
$\dot{k}_J$	$1/d$	Maturity maintenance coefficient
κ_R	-	Reproduction efficiency

[a] Average number of annuli in the adult shell.

[b] Length (maximal dimension) of the larval shell.

[c] Size of the smallest individuals seen to bear eggs.

[d] Size of the largest individuals recorded.

3.2.3 Parameter estimation and measure of fit

To fit the model and estimate the primary parameters, we used an improved version of the covariation method, described in Marques et al. (2018a) and provided in the free and open-source software DEBtool v2017 (Lika et al., 2011a; Lika et al., 2011b), implemented in Matlab (TheMathWorksInc, 2017). This approach takes advantage of the known covariation patterns in the parameters of the DEB model across species and, together with auxiliary theory that links the data to the variables, specifies the mapping functions between the data and the parameter space (Lika et al., 2014; Lika et al., 2011a; Lika et al., 2011b). In this way, all the parameters of the model are estimated simultaneously by fitting the model to the empirical and pseudo-data sets. The estimation consists of simultaneously minimizing the deviation of the model from the data through the Nelder-Mead simplex method (Marques, Lika, Augustine, Pecquerie, & Kooijman, 2018b). Formally, the objective function to be minimized is:

$$\sum_{i=1}^{n}\sum_{j=1}^{n_i} w_{i,j}\frac{(\hat{Y}_{i,j}-Y_{i,j})^2}{\bar{Y}_i^2+\hat{\bar{Y}}_i^2},$$

where $Y_{i,j}$ is the data indexed by data set, i, and by points within that data set, j. The respective estimate (prediction) of the model is $\hat{Y}_{i,j}$, and $w_{i,j}$ is the weight coefficient. The mean of all data points ($Y_{i,j}$) across the data set i is $\bar{Y}_i$, and the mean of all predictions ($\hat{Y}_{i,j}$) is $\hat{\bar{Y}}_i$. The number of points within the data set i is n_i, and n is the total number of data sets.

The goodness of fit of the model for each data set i is assessed by the relative error (RE). The overall goodness of fit of the model to the data of each species is measured by the mean relative error ($MRE \in [0,\infty)$) and by the symmetric mean squared error ($SMSE \in [0,1]$). For all cases, error values of 0 indicate an exact match between the predictions of the model and the data. Details on the approach are given in the Parameter estimation section in the Appendix.

Using the estimated primary parameters of the model we calculated compound parameters (i.e. simple functions of primary parameters) and implied properties (quantities which also depend on food). All quantities were computed for *ad libitum* food at the typical temperature of 6°C (Tab. 3.3).

3.2.4 Model validation

Once the parameters of the model were estimated, we validated its predictions with data from *Thyasira gouldi* (Blacknell & Ansell, 1974). These data were chosen as validation because they constitute the only quantitative record of the physiology of thyasirids, obtained under controlled laboratory conditions and at different temperatures. However, these complementary data were excluded from the parameterization (setting a weight coefficient equal to zero) because, although closely related, the measurements correspond to a different species. We digitized these data sets through WebPlotDigitizer (Rohatgi, 2017), and they are presented in Table 3.2.

Table 3.3. Definitions of the compound parameters and implied properties calculated from the primary parameters of the DEB-abj model (Eq. 3.1) for the symbiotic *Thyasira* cf. *gouldi* and the asymbiotic *Parathyasira* sp. The maximum surface-area specific assimilation rate is $\{\dot{p}_{Am}\}$ ($J/d \cdot cm^2$), $\dot{v}$ is the energy conductance rate from the energy reserve (cm/d), $[E_G]$ is the volume-specific cost for structure ($J/d \cdot cm^3$), κ is the fraction of mobilized reserve allocated to soma, $[\dot{p}_M]$ is the volume-specific somatic maintenance cost ($J/d \cdot cm^3$), $\dot{k}_J$ is the maturity maintenance rate coefficient ($1/d$). At equilibrium ($d[E]/dt = 0$) $e = f$. Implied properties are evaluated at $f = 1$. Notation: square brackets ([ ]) indicate quantities related to structural volume, curly brackets ({ }) denote quantities related to structural surface-area, dots ($\dot{}$) indicate rates.

Symbol	Unit	Description	Definition	Reference
$[E_m]$	J/cm^3	Maximum reserve density	$\{\dot{p}_{Am}\}/\dot{v}$	Tab. 3.3, Kooijman 2010
e	-	Scaled energy density	$[E]/[E_m]$	p. 473, Kooijman 2010
$\dot{k}_M$	$1/d$	Somatic maintenance coefficient	$[\dot{p}_M]/[E_G]$	Tab. 3.3, Kooijman 2010
k	-	Maintenance ratio	$\dot{k}_J/\dot{k}_M$	p. 47, Kooijman 2010
g	-	Energy investment ratio	$[E_G]\dot{v}/(\kappa\{\dot{p}_{Am}\})$	Tab. 3.3, Kooijman 2010
$\dot{r}_B$	$1/d$	von Bertalanffy growth rate	$\frac{\dot{k}_M g}{3(e+g)}$	p. 59, Kooijman 2010
E_0	J	Energy reserve in embryo	Eq. 2.42	Kooijman 2010
N_i	#	Lifetime reproductive output	$\max(0, \frac{\kappa_R \dot{p}_R}{E_0})$	Eq. 2.56, Kooijman 2010
Wd_0	g	Ash-free dry weight of an embryo	Eq. 3.3	Kooijman 2010
Wd_{N0}	g	Weight of lifetime reproductive output	$N_i \cdot Wd_0$	
a_i	d	Age at each developmental threshold i		

3.2.5 Interspecific comparison of the parameters

In order to quantify the differences between *T.* cf. *gouldi* and *Parathyasira* (considered as the reference species), for each estimated parameter or implied property $\hat{\theta}$ we defined the following relative difference:

$$\rho = \frac{\hat{\theta}_{Thyasira} - \hat{\theta}_{Parathyasira}}{\hat{\theta}_{Parathyasira}}, \tag{3.2}$$

where $\hat{\theta}_{Thyasira}$ is the value of the parameter or implied property for *T.* cf. *gouldi*, and $\hat{\theta}_{Parathyasira}$ is the value of the corresponding parameter or implied property for *Parathyasira*. According to our formulation, $\rho > 0$ indicates a greater value of the parameter or implied property for *T.* cf. *gouldi* with respect to *Parathyasira* sp., while, $\rho < 0$ indicates a lower quantify for *T.* cf. *gouldi*.

3.3 RESULTS

3.3.1 Data, model fit, and validation

The completeness of the data that we compiled is 1.5 (according to the criteria defined by Lika et al., 2011a, which range from a minimum of 0 to a maximum of 10), both for *T.* cf. *gouldi* as well as for *Parathyasira* sp. This level corresponds to data on lengths and weights at specific developmental stages, mean life span, weight as a function of length, and growth in time; which together comprise 7 empirical data sets for each species (Tab. 3.4). The fit of the model is consistent with the available data for both thyasirids, as indicated by values of the MRE and the SMSE close to zero (Tab. 3.4, Fig. 3.3). Overall, the fit of the model is more accurate for *T.* cf. *gouldi*.

Table 3.4. Data and model fit for the symbiotic *Thyasira* cf. *gouldi* and the asymbiotic *Parathyasira* sp. Estimation was performed assuming the reference condition of $f = 1$. The first row section corresponds to empirical zero- and uni-variate data, and the second row section indicates the pseudo-data, which are given for the reference temperature of 20°C. The fit of the model to each data set is measured by the Relative Error (RE). The last row section indicates the overall fit, quantified by the Mean Relative Error ($MRE \in [0, \infty)$) and the Symmetric Mean Squared Error ($SMSE \in [0, 1]$). In all cases, values of error close to zero indicate a good fit of the model to the data. The reference column indicates the source of the data. Notation: square brackets ([ ]) indicate quantities related to structural volume, dots (˙) denote rates. See Table 3.2 for symbol definitions.

	Thyasira cf. *gouldi*			*Parathyasira* sp.			
Symbol	Data	Prediction	RE	Data	Prediction	RE	Reference
a_m	2190	2190	4.633×10^{-8}	2190	2186	0.002	This study
L_b	0.018	0.019	0.004	0.014	0.014	0.002	Giolland and Dufour 2015
L_p	0.28	0.28	2.942×10^{-4}	0.28	0.28	0.001	Dufour 2017
L_i	0.514	0.534	0.039	0.514	0.488	0.05	Dufour 2017
Wd_i	0.002	0.002	0.02	0.003	0.003	0.045	This study
$\dot{R}_m$	6.137	6.145	0.001	6.137	6.105	0.005	Blacknell and Ansell 1974
tL	Fig. 3.3		0.028	Fig. 3.3		0.087	This study
LW_d	Fig. 3.3		0.33	Fig. 3.3		0.338	This study
$\dot{v}$	0.02	0.02	0.004	0.02	0.02	0.013	Lika et al. 2011a
κ	0.8	0.882	0.103	0.8	0.958	0.197	Lika et al. 2011a
$[\dot{p}_M]$	18	15.78	0.124	18	23.61	0.312	Lika et al. 2011a
κ_G	0.8	0.8	6.495×10^{-4}	0.8	0.802	0.002	Lika et al. 2011a
$\dot{k}_J$	0.002	0.002	0	0.002	0.002	0	Lika et al. 2011a
κ_R	0.95	0.95	0	0.95	0.95	0	Lika et al. 2011a
MRE			0.053			0.066	
$SMSE$			0.111			0.116	

The predictions of the fitted model for respiration and fecundity agree with the validation data of *Thyasira gouldi* (Tab. 3.5, Fig. 3.4). Model predictions concerning the fecundity and the respiration per gram of dry weight fit better for *T.* cf. *gouldi* than for *Parathyasira*

(Fig. 3.4A,B). However, the predictions regarding respiration as a function of dry weight at different temperatures fit better for *Parathyasira* (Fig. 3.4C,D).

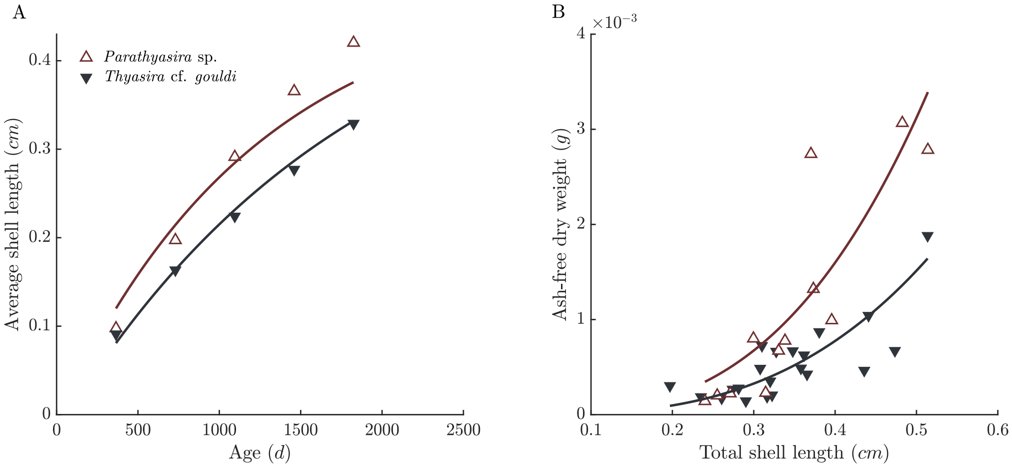

Figure 3.3. Uni-variate data (triangles) and model fit (lines) for the symbiotic *Thyasira* cf. *gouldi* and the asymbiotic *Parathyasira* sp. Estimation was performed assuming reference conditions of $f = 1$ and $T = 20$°C. (A) Average shell length growth (*cm*) in time (*d*) for *T.* cf. *gouldi* ($RE = 0.028$), and *Parathyasira* ($RE = 0.087$). (B) Ash-free dry mass (*g*) as a function of length (*cm*) for *T.* cf. *gouldi* ($RE = 0.33$), and *Parathyasira* ($RE = 0.338$). Both figures show a good fit of the model to the data, particularly for *T.* cf. *gouldi*, as indicated by values of the Relative Error (*RE*) close to zero.

Table 3.5. Validation data and model predictions for the symbiotic *Thyasira* cf. *gouldi*, the asymbiotic *Parathyasira* sp., and *Thyasira gouldi*. Estimation was performed assuming the reference condition of $f = 1$. The fit of the model to each data set is measured by the Relative Error (RE). The last row section indicates the overall fit, quantified by the Mean Relative Error ($MRE \in [0, \infty)$) and the Symmetric Mean Squared Error ($SMSE \in [0, 1]$). In all cases, values of error close to zero indicate a good fit of the model to the data. The reference column indicates the source of the data. See Table 3.2 for symbol definitions.

	Thyasira cf. *gouldi*		*Parathyasira* sp.		
Symbol	Data and prediction	RE	Data and prediction	RE	Reference
LN	Fig. 3.4A	0.534	Fig. 3.4A	1.051	Blacknell 1973
TJO	Fig. 3.4B	0.192	Fig. 3.4B	0.596	Blacknell 1973
$WJO5$	Fig. 3.4C	0.426	Fig. 3.4D	1.072	Blacknell 1973
$WJO10$	Fig. 3.4C	0.522	Fig. 3.4D	0.323	Blacknell 1973
$WJO15$	Fig. 3.4C	0.241	Fig. 3.4D	0.221	Blacknell 1973
MRE		0.182		0.299	
$SMSE$		0.263		0.279	

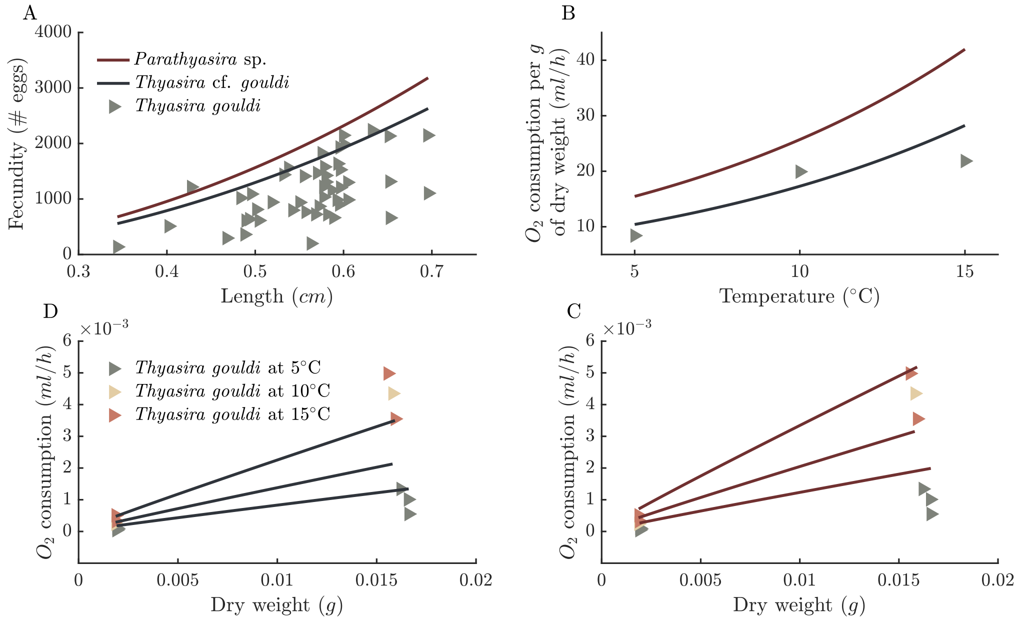

Figure 3.4. Uni-variate *Thyasira gouldi* validation data (triangles) and model predictions (lines) for the symbiotic *Thyasira* cf. *gouldi* and the asymbiotic *Parathyasira* sp. The estimation was performed assuming reference conditions of $f = 1$ and $T = 20$°C. (A) Fecundity (# eggs) as a function of shell length (cm) for *T.* cf. *gouldi* ($RE = 0.534$), and *Parathyasira* ($RE = 1.051$). (B) Oxygen consumption (ml/h) for 1 g of dry weight as a function of temperature for *T.* cf. *gouldi* ($RE = 0.192$), and *Parathyasira* ($RE = 0.596$). (C, D) Oxygen consumption (ml/h) as a function of dry weight (g) at different temperatures (°C): (C) for *T.* cf. *gouldi* at 5 ($RE = 0.426$), 10 ($RE = 0.522$) and 15 ($RE = 0.241$), and (D) for *Parathyasira* at 5 ($RE = 1.072$), 10 ($RE = 0.323$) and 15 ($RE = 0.221$). Despite of the limited available data for validation, the figures and the values of the Relative Error (RE) close to zero show that the model predictions and the validation data agree.

3.3.2 Model parameters

Despite of the limited amount of available data, we were able to estimate the values of ten primary parameters of the model for each of the species. The estimated primary parameters are presented in Table 3.6, and the resulting compound parameters and implied properties in Table 3.7. The relative difference for each parameter or implied property between *T.* cf. *gouldi* and *Parathyasira* (ρ, Eq. 3.2) is shown in Figure 3.5.

The symbiotic *T.* cf. *gouldi* has a greater fraction of structural biomass (δ_V), which corresponds to a lower fraction of energy reserve (E) and a lower maximum reserve capacity ($[E_m]$) when compared to *Parathyasira* (Tab. 3.7, Fig. 3.5B). The rates of assimilation $\{\dot{p}_{Am}\}$

and somatic maintenance $[\dot{p}_M]$ are also lower for *T.* cf. *gouldi* (Tab. 3.6, Fig. 3.5A). The energy conductance rate ($\dot{v}$) and the specific costs for structure ($[E_G]$) do not differ greatly between the two thyasirids (Tab. 3.6, Fig. 3.5A).

Table 3.6. Primary parameter estimates of the DEB-abj model (Eq. 3.1) for the symbiotic *Thyasira* cf. *gouldi* and the asymbiotic *Parathyasira* sp. Rates were calculated at $T = 20°C$. Notation: square brackets ([ ]) indicate quantities related to structural volume, curly brackets ({ }) denote quantities related to structural surface-area, dots ($\dot{}$) indicate rates.

Symbol	*Thyasira* cf. *gouldi*	*Parathyasira* sp.	Unit	Description
$\{\dot{p}_{Am}\}$	1.427	2.547	$J/d \cdot cm^2$	Maximum surface-area assimilation rate
$\dot{v}$	0.02	0.02	cm/d	Energy conductance rate
κ	0.883	0.958	-	Allocation fraction to soma
$[\dot{p}_M]$	15.78	23.61	$J/d \cdot cm^3$	Volume-specific somatic maintenance cost
$[E_G]$	2355	2348	J/cm^3	Specific cost for structure
E_H^b	2.639×10^{-4}	7.193×10^{-5}	J	Maturity at birth
E_H^j	0.011	0.002	J	Maturity at metamorphosis
E_H^p	1.283	0.96	J	Maturity at puberty
$\dot{h}_a$	9.844×10^{-8}	1.262×10^{-7}	$1/d^2$	Weibull aging acceleration
δ_M	0.507	0.64	-	Shape coefficient

Table 3.7. Compound parameters and implied properties of the DEB-abj model (Eq. 3.1) for the symbiotic *Thyasira* cf. *gouldi* and the asymbiotic *Parathyasira* sp. All of the quantities were calculated at $f = 1$ and $T = 6°C$. Notation: square brackets ([ ]) indicate quantities related to structural volume, dots ($\dot{}$) denote rates. See Table 3.3 for symbol definitions.

Symbol	*Thyasira* cf. *gouldi*	*Parathyasira* sp.	Unit	Description
δ_V	0.967	0.943	-	Fraction of weight that is structure
$[E_m]$	71.585	125.662	J/cm^3	Maximum reserve capacity
$\dot{k}_M$	0.007	0.01	$1/d$	Somatic maintenance rate coefficient
$\dot{r}_B$	5.535×10^{-4}	8.113×10^{-4}	$1/d$	von Bertalanffy growth rate
g	37.287	19.514	-	Energy investment ratio
k	0.3	0.2	-	Maintenance ratio
a_b	11.625	9.662	d	Age at birth
a_j	306.811	136.823	d	Age at metamorphosis
a_p	1423.35	1075.13	d	Age at puberty
N_i	1.065×10^3	2.214×10^3	#	Lifetime reproductive output
Wd_0	1.003×10^{-7}	7.742×10^{-8}	g	Dry weight of embryo
Wd_{N0}	1.068×10^{-4}	1.715×10^{-4}	g	Dry weight of total lifetime reproductive output
E_0	2.308×10^{-3}	1.782×10^{-3}	J	Energy reserve in embryo
z	0.08	0.103	-	Zoom factor

The allocation of reserve energy towards somatic maintenance and growth (κ), is lower for *T.* cf. *gouldi* in comparison to the asymbiotic *Parathyasira* (Tab. 3.6, Fig. 3.5A). Consequently, the fraction allocated towards maturity maintenance and maturation/reproduction $(1 - \kappa)$ is greater in *T.* cf. *gouldi*, and the initial reserve present in the embryo is also higher (E_0, Tab. 3.3). This suggests larger embryos in the symbiotic thyasirid, as indicated by their estimated weight (Wd_0). Yet, the weight of all the eggs produced in the life time is comparatively less relative to *Parathyasira*, due to fewer embryos being produced (Wd_{N0} and N_i; Tab. 3.7, Fig. 3.5B).

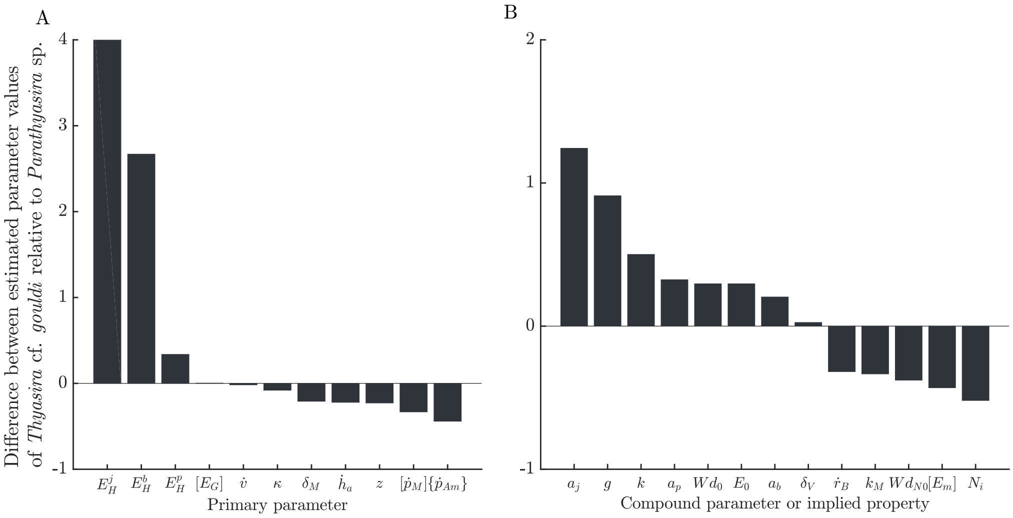

Figure 3.5. Relative difference (ρ, Eq. 3.2) between the estimated values of primary parameters (A, Tab. 3.6), compound parameters and implied properties (B, Tab. 3.3) of the DEB-abj model (Eq. 3.1) for the symbiotic *Thyasira* cf. *gouldi* relative to the asymbiotic *Parathyasira* sp. Values above 0 are greater for *T.* cf. *gouldi* relative to *Parathyasira*, while values below 0 are lower for *T.* cf. *gouldi*. The cumulative maturity energy thresholds of life history transitions (E_H^b, E_H^j, and E_H^p), the ages at each stage transition (a_b, a_j, and a_p), the fraction of adult weight that is structure (δ_V), and the embryo weight (Wd_0) are greater for *T.* cf. *gouldi*. The somatic maintenance cost ($[\dot{p}_M]$), reserve capacity ($[E_m]$), maximum assimilation rate ($\{\dot{p}_{Am}\}$), von Bertalanffy growth rate ($\dot{r}_B$), and the lifetime weight of the reproductive output (Wd_{N0}) are all lower for *T.* cf. *gouldi* with respect to *Parathyasira*. See Tables 3.3, 3.6, and 3.7 for notation and definitions.

A greater initial energy reserve is reflected in the energy invested into maturity at each developmental stage (E_H^b, E_H^j, E_H^p, Tab. 3.6), and in the ages at which they are reached (a_b, a_j, a_p, Tab. 3.7), all of which are greater for *T.* cf. *gouldi* relative to *Parathyasira* (Fig. 3.5A). This means that the symbiotic *T.* cf. *gouldi* requires greater amounts of energy and more time to reach the same developmental thresholds (Fig. 3.6). The growth rate, measured by the von Bertalanffy growth rate ($\dot{r}_B$), is also lower for *T.* cf. *gouldi* with respect to *Parathyasira* (Tab. 3.3, Figs. 3.3A, 3.5B).

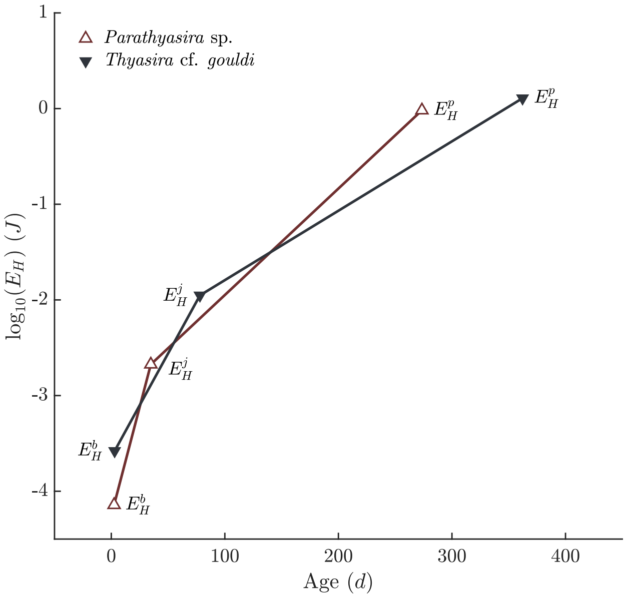

Figure 3.6. Log-transformed cumulative energy at birth (E_H^b, J), metamorphosis (E_H^j, J), and puberty (E_H^p, J) for the symbiotic *Thyasira* cf. *gouldi* and the asymbiotic *Parathyasira* sp. as a function of age (d). All maturity thresholds and ages are higher for *T.* cf. *gouldi*, indicating a slower development relative to *Parathyasira*. The cumulative energy at puberty is similar for both species, although *T.* cf. *gouldi* needs more time to reach this threshold (Tabs. 3.3, 3.6).

The main ecophysiological traits linked to the presence of chemoautotrophic symbionts in thyasirid hosts are summarized in Table 3.8.

Table 3.8. Summary of the life history traits of the symbiotic *Thyasira* cf. *gouldi* relative to the asymbiotic *Parathyasira* sp., as evidenced by the estimated parameters of the DEB-abj model for each species.

Feature	Reference
Biomass composed of a greater proportion of structure and less of energy reserve.	Tab. 3.7
Lower assimilation flux and somatic maintenance cost.	Tab. 3.6, Fig. 3.5A
Lower proportion of energy allocated to somatic maintenance and growth; greater proportion allocated towards maturity maintenance and maturation or maturity.	Tab. 3.6
Greater cumulative energy thresholds and ages, at birth, metamorphosis, and puberty.	Tabs. 3.6, 3.7, Fig. 3.6
Lower growth rate.	Tab. 3.7, Fig. 3.6
Greater weight of eggs but lower weight of total embryos, due to production of lower number of embryos.	Tab. 3.7, Fig. 3.5B

3.4 DISCUSSION

The parameterization of the DEB model for both species predicts that symbiotic *T.* cf. *gouldi* has a smaller fraction of energy reserves relative to *Parathyasira*. A smaller energy reserve in turn implies differences in energy allocation throughout the life history of *T.* cf. *gouldi* (see Tab. 3.8). Taking into account the habitat of the thyasirids, these features may suggest an adaptative strategy in response to a fluctuating resource availability, where the symbionts are likely to function as a partial energy reserve for the host.

3.4.1 Structure and energy reserve biomass

We found that symbiotic *T.* cf. *gouldi* has a greater proportion of structural biomass relative to *Parathyasira* (Tab. 3.7, Fig. 3.5): this finding has two potential explanations. First, an increased structural volume likely corresponds to the enlarged gills of *T.* cf. *gouldi*, which constitute an adaptation to harbour bacterial symbionts (Dufour, 2005), and so less of *T.* cf. *gouldi* biomass is storage due to the relatively larger structural volume. Second, a greater proportion of structure also implies lower energy reserves for *T.* cf. *gouldi*. Considering that the abundance, uptake, and digestion of the bacterial symbionts show a cyclical trend (Laurich et al., 2015), a low energy reserve suggests that the symbionts may buffer resource fluctuations. For the thyasirids, reserves would be of particular importance given that they combine foraging on particulate organic matter and on sulfur-oxidizing bacteria from the sediment, both of which are subject to seasonal variations (Dufour & Felbeck, 2003; Dufour et al., 2014). Evidence of this is the larger energy reserve present in the asymbiotic *Parathyasira*, which may represent an adaptation in response to variable food availability. The evolution of an energy reserve has been shown to be an evolutionary stable strategy in fluctuating environments, and at ecological time scales both strategies, with and without energy reserve, can coexist (Kooi & Troost, 2006).

Relating the state variables of the DEB model to measurable components of individuals would provide a test of our hypothesis describing the potential function of symbionts in thyasirids. Specifically, the biochemical estimation of the amount of energy reserves could be achieved by quantifying glycogen or lipid levels. However, due to the small size of the thyasirids, most analyses have to be done combining samples in bulk, which make it difficult to discriminate between the reserve compounds present in different tissues.

3.4.2 Assimilation, mobilization, allocation to soma and somatic maintenance

Our results indicate that the fraction of energy allocated to somatic maintenance and growth is lower in *T.* cf. *gouldi*, relative to *Parathyasira* (Tab. 3.6, Fig. 3.5A). A lower investment in somatic maintenance and growth is consistent with our explanation of the likely role of the symbionts in averaging resource availability when other sources of food are rare: in species that rely on constant resources, such an allocation pattern has been proposed as an adaptation to reduce the minimum resources required by reducing ultimate size (Kooijman, 2010). However, for *T.* cf. *gouldi* there does not appear to be a reduction in ultimate size, but rather a reduction in growth rate.

The amount of energy reserve in the organism is directly linked to the fluxes of assimilation and mobilization, as well as to the density of the energy reserve itself (Eq. 3.1, Tab. 3.1). A lower amount of energy reserve in symbiotic *T.* cf. *gouldi* indicates that the assimilation flux is also low, as it is shown by the maximum assimilation rate (Tab. 3.6, Fig. 3.5A). Hence, although *T.* cf. *gouldi* may have a constant resource availability, since the symbionts decrease the energy reserve density, the host would be able to sustain a low assimilation rate. The mobilization flux depends on the energy reserve density and on the structural volume (Tab. 3.1); consequently —and even with similar conductance rates—, the symbiotic *T.* cf. *gouldi* would have a lower mobilization flux relative to *Parathyasira* (Tab. 3.6, Fig. 3.5A). Both findings signify that *T.* cf. *gouldi* has a lower ratio of assimilation to mobilization flux compared to *Parathyasira*.

The estimated value of the somatic maintenance cost for *T.* cf. *gouldi* is lower relative to *Parathyasira* (Tab. 3.6, Fig. 3.5A), which agrees with the likely role of the bacterial symbionts in buffering resource seasonality. Constant resource availability may allow the host to minimize a possible 'waste' of energy reserve in somatic maintenance (Kooijman, 2013), while being able to attain a similar size and reproductive output than the asymbiotic *Parathyasira*. The significance of the values of somatic maintenance are better understood by contrasting them with those of other taxa. In order to make comparisons, the somatic maintenance must be corrected by their specific density: $[\dot{p}_M]/d_V$ (for $d_V = 0.09$ in bivalves). This correction yields costs of 175.3 $J/g \cdot d$ for the symbiotic *T.* cf. *gouldi*, and 262.3 $J/g \cdot d$ for *Parathyasira*, while the mean value across the bivalves is 255.1 $J/g \cdot d$, and the typical value across all taxa is 200 $J/g \cdot d$. This way, the somatic maintenance for *T.* cf. *gouldi* is also lower relative to the average cost across bivalves and to the typical animal. This finding coincides with the pattern exhibited by the photosymbiotic, tropical bivalve *Tridacna gigas*, which shows the lowest somatic maintenance cost among the bivalves modeled using the DEB framework ($[\dot{p}_M]/d_V = 5.4\ J/d \cdot cm^3$), despite being orders of magnitude higher in size (137 cm in length, and 2000 g in weight; AmP, 2017). Differences in the physiology and habitat of this unrelated species constrain such a direct comparison; however, the broad similarity in the somatic maintenance may give a general insight into a plausible consequence of harbouring symbionts in the overall energy partitioning of a bivalve host.

The most informative experiments, in terms of data that can be used to parameterize the DEB model, would be those in which growth, reproduction, and respiration are determined simultaneously under different resource conditions (Lika et al., 2014). In thyasirids such assays are challenging due to the difficulty in replicating their habitat in the laboratory for prolonged periods of time, especially because it is unfeasible to regulate the densities of free-living and symbiotic bacteria. Respiration measurements of starved individuals would yield information related to somatic maintenance, but these measurements would also reflect other processes such as maturity maintenance, and for symbiotic individuals they would also include symbiont consumption. To overcome these limitations, we suggest respiration studies conducted at different temperatures (like those performed in *Thyasira gouldi* by Blacknell, 1973), which would enable the estimation of the Arrhenius temperature, and would provide insight on the variation of the metabolic rate with temperature.

3.4.3 Growth and life history strategies

The assimilation rate and the somatic maintenance, together with the resource density, determine the growth rate of the individual (Tab. 3.1). For *ad libitum* food, a low assimilation rate and a low somatic maintenance in *T.* cf. *gouldi* are consistent with a lower growth rate relative to *Parathyasira*. This is evident in the slower development of *T.* cf. *gouldi*, and likely corresponds to a divergent reproductive strategy: all the maturity thresholds are reached later with respect to *Parathyasira*, and symbiotic *T.* cf. *gouldi* produces fewer, larger embryos, each with a greater amount of reserve energy (Tab. 3.7, Fig. 3.6). The cumulative energy invested in maturity is generally linked to gonad tissue, but in thyasirids the gonads are intermixed with the digestive gland, which precludes the use of traditional measurements (i.e. the gonadosomatic index). Future investigations should instead focus on determining egg and embryo sizes, fecundity as a function of length, and whether there is a correlation with seasonal changes.

Regardless of their differences in timing or energy requirements, *T.* cf. *gouldi* and *Parathyasira* show an extended stage before metamorphosis. A prolonged development agrees with the described ontogeny of the closest extant relatives of both species: *P. equalis* is characterized by an extended lecithotrophic development (i.e. a non-feeding larva that depends on the egg's reserves; Ockelmann, 1958); whereas *T. gouldi* has a lecithotrophic development, albeit benthic and direct (i.e. juveniles hatch from the egg; Blacknell & Ansell, 1974). It is noteworthy that this ontogenetic pattern may indicate that hatching from the egg occurs before birth as defined in DEB theory, because juveniles are not likely to feed immediately after hatching. Therefore, it would be relevant to further characterize the ontogenetic development of both species.

3.5 CONCLUSIONS

Our results suggest the mechanisms underlying two alternative evolutionary strategies for a thyasirid bivalve in an environment with seasonal forcing: for *T.* cf. *gouldi*, the bacterial symbionts may constitute an adaptation to buffer fluctuating resources by providing sustained nutrition to the host, which leads to an increase in the allocation flux towards maturation or reproduction. Conversely, the asymbiotic *Parathyasira* feeds on a seasonal resource, builds a comparatively larger energy reserve and has a faster life cycle with greater maintenance costs. These findings are likely to reflect a plausible role of the chemosymbiotic bacteria in the ecophysiology of the bivalve host, and highlight how the symbiotic association may alter the energy budget of a mixotrophic thyasirid.

Our findings are conditioned by the data that we used in the parameter estimation, which bound the species to the same puberty and ultimate sizes, in addition to an equal life span and reproductive output. These measurements are limited by low sample sizes and by anatomical characteristics of the thyasirids, which hinder the precision of our inference. However, our results indicate priority areas for future experiments to test the predictions of the model, and to further resolve the differences between symbiotic and asymbiotic thyasirids, particularly with respect to their reproductive biology. It would also be valuable to assess thyasirids from other regions to verify that the patterns in the data and in our estimation hold for populations outside of Bonne Bay. Our parameter estimates could be used to gain insight into the dynamics of resource availability and their relationship with the energy reserves, or to explore the consequences of the thyasirids' energy budget at the population and community levels.

3.6 ACKNOWLEDGEMENTS

We thank the staff of the Bonne Bay Marine Station for assistance during sampling. Alison Pye and Rachelle Dove helped with the weighing of the samples at the Stable Isotope Laboratory (CREAIT – TERRA Facility, MUN). We further thank the reviewers, Michael Kearney (guest editor of this special issue), and the Hurford lab for their constructive comments on the manuscript. SA was supported by the Norwegian Science Council (NFR 255295). SCD was supported by a Natural Science and Engineering Research Council of Canada (NSERC) Discovery Grant (2015-06548). AH acknowledges financial support from a Natural Sciences and Engineering Research Council of Canada (NSERC) Discovery Grant (RGPIN 2014-05413) and the President's Doctoral Student Investment Fund (Memorial University).

3.7 APPENDIX

3.7.1 DEB-abj model

The change in shape during larval growth implies a change in assimilation and reserve mobilization, as a consequence, the intrinsic growth rate ($\dot{r}$) depends on the shape correction function $\mathcal{M}$:

$$\mathcal{M} = \max(L_b, \min(L, L_j))/L_b,$$

where L is the structural length ($L = V^{(1/3)}$) that is related to the physical length by $\mathcal{L} = L/\delta_M$, for a shape coefficient δ_M. The structural lengths at the beginning and at the end of the acceleration are L_b and L_j, which correspond to the structural lengths at birth and at metamorphosis.

The nutritional condition of the organism is indicated by the ratio $e = [E]/[E_m]$, which represents the scaled reserve density for a maximum reserve density $[E_m]$, given by $[E_m] = \{\dot{p}_{Am}\}/\dot{v}$. This way, the specific growth rate is:

$$\dot{r} = \frac{\kappa[E]\dot{v}\mathcal{M}/L - [\dot{p}_M]}{\kappa[E] + [E_G]}.$$

3.7.2 Parameter estimation

The mapping functions from data to parameter space are given by the improved covariation method (Marques et al., 2018a), which are included in the DEBtool package (Lika et al., 2014). The particular routines used to fit the zero-variate data are given in Table 3.9.

Table 3.9. Computation of zero-variate data sets considered in the parameterization of the DEB-abj model.

Symbol	Unit	Description	Equation/DEBtool routine
a_m	d	Life span	`get_tm_s`
L_b	cm	Structural length at birth	`get_lj`
L_p	cm	Structural length at puberty	`get_lj`
L_i	cm	Ultimate total length	`get_tj`
Wd_i	g	Ultimate ash-free dry weight	Eq. 3.3, Kooijman 2010
$\dot{R}_m$	$\#/d$	Maximum reproduction rate	`reprod_rate_j`

3.7.2.1 Weight coefficients

To ensure that each data set contributes equally to the minimization of the loss function, we used automatized weight setting (specified in Marques et al., 2018b), in which every element of the zero- and uni-variate data sets is assigned a weight coefficient:

$$w_{i,j} = \frac{1}{n_i},$$

for a data point j in a data set i, where n_i denotes the number of points within the data set i. For the pseudo-data, the covariation method assigns each data point a weight coefficient equal to 0.1, except for κ_G, whose weight coefficient is set equal to 20 (see Table 2 in Marques et al., 2018a).

3.7.2.2 Evaluation of model fit

The goodness of fit of the model for each data set i with weight coefficient $w_i = \sum_{j=1}^{n_i} w_{i,j} > 0$, is measured by the relative error (RE):

$$RE_i = \sum_{j=1}^{n_i} \frac{w_{ij}}{w_i} \frac{|\hat{Y}_{ij} - Y_{ij}|}{|\bar{Y}_i|},$$

and by the symmetric squared error (SSE):

$$SSE_i = \sum_{j=1}^{n_i} \frac{w_{ij}}{w_i} \frac{(\hat{Y}_{ij} - Y_{ij})^2}{\bar{Y}_i^2 + \hat{\bar{Y}}_i^2},$$

where $Y_{i,j}$ is the data, and $\hat{Y}_{i,j}$ is the estimate (predictions) of the model. The mean of all data points in data set i ($Y_{i,j}$) is $\bar{Y}_i = \frac{1}{n_i} \sum_{j=1}^{n_i} Y_{i,j}$, and the mean of all predictions ($\hat{Y}_{i,j}$) is $\hat{\bar{Y}}_i = \frac{1}{n_i} \sum_{j=1}^{n_i} \hat{Y}_{i,j}$.

The fit of the model to all data sets is measured by the mean of all the relative errors ($MRE \in [0, \infty)$):

$$MRE = \frac{1}{n'} \sum_{i=1}^{n_i} RE_i,$$

and by the symmetric mean squared error ($SMSE \in [0, 1]$):

$$SMSE = \sqrt{\frac{1}{n'} \sum_{i=1}^{n_i} SSE_i},$$

where n' denotes the number of data sets with $w_i > 0$. The MRE assesses the differences between the data and the estimates additively (i.e. an overestimation and an underestimation of the same relative size have the same contribution), while the $SMSE$ evaluates the difference multiplicatively (i.e. an overestimation and an underestimation of equivalent ratio have the same contribution). In both cases, a value of 0 means that model predictions match the data exactly (Marques et al., 2018a).

3.7.2.3 Code

The species *Thyasira* cf. *gouldi* (OTUs 1 and 2 of Batstone et al., 2014) and *Parathyasira* sp. are included in the AmP database (AmP, 2018). The scripts for the parameter estimation are available at http://www.bio.vu.nl/thb/deb/deblab/add_my_pet/entries_web/Thyasira_cf_gouldi/Thyasira_cf_gouldi_res.html and http://www.bio.vu.nl/thb/deb/deblab/add_my_pet/entries_web/Parathyasira_sp/Parathyasira_sp_res.html.

3.7.3 Data collection

3.7.3.1 Growth and life span

Growth rates of *T.* cf. *gouldi* (OTUs 1 and 2) and *Parathyasira* were determined by measuring external shell disturbance lines along the dorso-ventral axis, which are considered to represent annual growth bands (Seed, 1980). In bivalves, annuli appear as thin bands and form during periods of decreased growth, such as winter months in the Northern hemisphere (Gosling, 2015).

Thyasirids were collected from Bonne Bay, Newfoundland in April, June and October 2011 from the sites and following methods described in Batstone et al. (2014). We photographed the external surface of empty valves of 16 *T.* cf. *gouldi* and 17 *Parathyasira*, using an Olympus SZ stereomicroscope. Through the software ImageJ (Abramoff, Magalhaes, & Ram, 2004), we measured distances from the umbo to each annulus, along the normal axis, to the nearest 0.1 mm (Seed, 1980). We considered the total number of annuli to correspond to the life span of each individual.

3.7.3.2 Weight as a function of length

We collected thyasirids from two sites within the East Arm of the Bonne Bay fjord (Southeast Arm 49°27.687′N 57°43.107′W, 38 m depth; and Deer Arm 49°33.161′N 57°50.311′W, 30 m depth), in June and September 2017, according to the sampling methods described in Batstone et al., 2014. We photographed 21 *T.* cf. *gouldi* (OTUs 1 and 2) and 12 *Parathyasira* through an Olympus SZ stereomicroscope. We measured the shell length (anterior-posterior) of each individual to the nearest 0.1 mm using the software ImageJ (Abramoff et al., 2004). Later, we dried the samples in an embedding oven at 60 °C for 2 days. In order to obtain the ash-free dry weight, we combusted each sample in a furnace at 350 °C for 24 h; we then weighted each specimen to the nearest 1 μg.

4

SYMBIOSIS INCREASES POPULATION SIZE AND BUFFERS ENVIRONMENTAL FLUCTUATIONS IN A PHYSIOLOGICALLY-STRUCTURED MODEL PARAMETERIZED FOR THYASIRID BIVALVES

Joany Mariño, Suzanne C. Dufour, Amy Hurford

Symbioses whereby one partner provisions a nutritional resource to the other may alter energy allocation towards reproduction and survival in the recipient partner, potentially impacting population dynamics. Asymbiotic thyasirid bivalves feed predominantly on free-living bacteria, which fluctuate in abundance due to seasonality-driven temperature variations. Symbiotic thyasirids are mixotrophs, gaining nutrients from free-living bacteria and symbiotic bacteria that they host on their enlarged gills. Symbiotic bacteria may function as an additional energy reserve for thyasirids, allowing the hosts to allocate more energy to reproduction. We hypothesize that, for symbiotic thyasirids, the symbionts are a nutritional source that mitigates resource limitation. Using Dynamic Energy Budget theory, we built a physiologically-structured population model assuming equal mortality rates in both species. We find that without seasonal fluctuations, symbiotic thyasirids have higher abundances than asymbiotic thyasirids since the symbionts increase reproduction. Both species have similar population sizes in fluctuating environments, suggesting different adaptations to seasonality: asymbiotic thyasirids have adapted their physiology, while symbiotic thyasirids have adapted through mixotrophy. Our results highlight the significance of linking individual energetics and life-history traits to population dynamics and are the first step towards understanding the role of symbioses in population and community dynamics.

4.1 INTRODUCTION

Nutritional symbiosis is a prevalent interaction that can increase the metabolic capabilities of the host (Dubilier et al., 2008; Moran, 2006). Hence, symbiosis has the potential to affect host life-history traits, such as fecundity and survival, which, in turn, determine population dynamics. However, how symbiosis can influence host ecology and how this would be translated into population and community dynamics is not known (Yule et al., 2013). Disentangling the bottom-up effect of trophic symbiosis on ecological timescales, in both constant and heterogeneous environments, is crucial to understanding the conditions that lead to the persistence of populations and communities (Miller & Rudgers, 2014).

Environmental heterogeneity and the pattern of environmental variation are thought to be determinant factors in the evolution of the niche breadth, particularly for traits such as foraging strategies (Kassen, 2002; Lynch & Gabriel, 1987). Theory suggests that selection favours generalist strategies in populations experiencing environmental heterogeneity (Futuyma & Moreno, 1988; Levins, 1968; Lynch & Gabriel, 1987). Experimental results have confirmed such findings (Bell & Reboud, 1997; Kassen & Bell, 1998; Reboud & Bell, 1997). For example, selection experiments in *Chlamydomonas* in constant environments have led to the evolution of specialists, either autotrophic or heterotrophic. Conversely, in temporally varying environments, selection favours generalists capable of both autotrophic and heterotrophic nutrition. However, in spatially varying environments, both specialists can be retained in the population (Bell & Reboud, 1997; Kassen & Bell, 1998; Reboud & Bell, 1997). Broadly, these results suggest that ecological specialists tend to be selected in environments that are homogeneous in space or time, whereas generalists tend to favoured in temporally varying environments (Ackermann & Doebeli, 2004; Futuyma & Moreno, 1988; Kassen, 2002; Levins, 1968; Lynch & Gabriel, 1987).

Nutritional symbioses in which the host has a mixotrophic nutrition (i.e. the host can combine the nutritional input from the symbionts with heterotrophic or autotrophic feeding; Rossi et al., 2017) can be considered to be generalist feeding strategies. For instance, mixotrophic symbioses are frequent in marine suspension feeders, which live in environments where light and plankton concentration are variable and often limiting (Grottoli et al., 2006; Muller et al., 2001). In octocorals, such trophic flexibility has been proposed to maximize nutrient uptake, allowing for increased energy acquisition, relative to asymbiotic species (Gori et al., 2012; Grottoli et al., 2006). Moreover, the loss of symbionts may not significantly affect the host's energetic input, making the host less affected by environmental variability (Fabricius et al., 1995; Ferrier-Pagès et al., 2015; Rossi et al., 2017; Sorokin, 1991; Viladrich et al., 2017). Thus, in seasonal environments, symbionts can provide energy to a mixotrophic host and stabilize the discontinuous energy inputs in resource availability (Gori et al., 2012; Rossi et al., 2017; Viladrich et al., 2017).

Another notable example of mixotrophy occurs in symbiotic thyasirid bivalves, a family that stands out for including symbiotic as well as asymbiotic members (Southward, 1986; Taylor et al., 2007). Symbiotic thyasirids are flexible mixotrophs that can digest their symbionts depending on environmental conditions, particularly the presence of sulfide and external particulate food (Dando & Spiro, 1993; Dufour & Felbeck, 2006). Evidence in other bivalves suggests that changes in the relative importance of different food sources are likely correlated to particulate food abundance (Pile & Young, 1999). A mixotrophic nutrition is considered a strategy that allows symbiotic thyasirids to thrive in fluctuating environments (Dufour & Felbeck, 2006; Duperron et al., 2013).

In the fjord of Bonne Bay (Newfoundland, Canada), two species of thyasirids are sympatric and have a patchy distribution. The first species resembles *Thyasira gouldi* (in shell characteristics and internal anatomy) and therefore is referred to as *T.* cf. *gouldi*; the second species, *Parathyasira* sp., is asymbiotic. Both symbiotic *T.* cf. *gouldi* and asymbiotic *Parathyasira* are particulate feeders that rely on chemoautotrophic bacteria as their primary resource (60% and 70%, respectively), with lesser contributions of suspended and particulate organic matter (Zanzerl et al., 2019). However, rather than collecting chemoautotrophic bacteria from sediments through pedal feeding, *T.* cf. *gouldi* harbours these bacteria extracellularly as symbionts on enlarged gills and digests them as an additional resource (Laurich et al., 2015; Zanzerl et al., 2019); hence, it is considered a mixotrophic species. For *T. sarsi*, another mixotrophic thyasirid, between 26 and 76% of their nutrition has been estimated to be obtained from the bacterial symbionts (Dando & Spiro, 1993). Given that the carbon isotope composition in *T.* cf. *gouldi* overlaps the lower range of the isotopic signature of *T. sarsi* (Dando & Spiro, 1993; Zanzerl et al., 2019), it is likely that the reliance of *T.* cf. *gouldi* on symbionts may be similar to the lower limit of *T. sarsi*'s, comprising approximately 25% of their diet. For thyasirids inhabiting an environment with strong seasonality, temperature and resource fluctuations will affect the individual metabolic rates and the costs associated with maintaining the symbionts. Previous theoretical research showed that symbiotic *T.* cf. *gouldi* has a smaller energy reserve, which implies reduced energy assimilation and mobilization fluxes, lower somatic maintenance costs and growth rate, and more significant energy allocation to maturity and reproduction (Mariño, Augustine, Dufour, & Hurford, 2019). However, how the nutritional differences between symbiotic *T.* cf. *gouldi* and asymbiotic *Parathyasira* are reflected at the population and community levels is not known.

Our previous results support the hypothesis that a mixotrophic (generalist) strategy results in higher energy allocation to reproduction (George, 1994; McKillup & Butler, 1979; Thompson, 1983; Viladrich et al., 2017). Thus, in a constant environment, a mixotrophic population should have larger abundances than the asymbiotic (specialist) population. Here, we hypothesize that when there is seasonality, relying on symbionts will buffer the fluctuations in resource availability for the host population. We predict that if symbionts effectively mitigate resource variability, then the mixotrophic population will be less prone to extinction during winter when the abundance of free-living bacteria becomes limiting. Our prediction should hold while the abundance of symbionts is not zero and is at least equal to the lowest free-living bacterial abundance. However, the buffering effect of the symbionts should decrease as the host becomes more specialized and increases reliance on the symbionts. Hence, in highly seasonal environments, a low or intermediate level of dependence on symbionts (i.e. a generalist strategy) should be favoured over the specialist strategy.

Since the physiological responses of individuals can be considered the underlying basis of their ecological dynamics, models that consider the organismal bioenergetics are powerful tools to understand how energetic constraints determine changes in the niche of a species as a consequence of environment fluctuations (Nisbet et al., 2012). Energy budget models describe the rates at which an individual assimilates and uses energy for maintenance, growth, and reproduction (Kooijman, 2010; van der Meer, 2006). To understand how the differences due to feeding and symbiosis translate to the population level and shape host population dynamics, we combine the individual-level energy budget dynamics with a physiologically-structured population model (de Roos, Galic, & Heesterbeek, 2009; Kooijman, 2010). We built a population model that accounts for the species' physiology according to the individual DEB model and takes into account the seasonal pattern of temperature and resource abundance. Using this model, we simulated the dynamics of the symbiotic *T.* cf. *gouldi* and the asymbiotic *Parathyasira*.

Previously, we suggested that the energy allocation patterns in symbiotic thyasirids may represent an evolutionary strategy where the symbionts function as a partial energy reserve, allowing the individuals to invest more energy in reproduction (Mariño et al., 2019). Here, we focus on the differences in populations inhabiting a constant versus seasonal environment, and evaluate different scenarios of symbiont dependence and abundance. We show how the symbiotic strategy is likely to mitigate the effects of environmental variability in a population of symbiotic thyasirids. We discuss the buffering effect of the symbionts in terms of the evolution and ecological adaptation of thyasirids and mixotrophic bivalves.

4.2 METHODS

4.2.1 The model

We formulated a continuous population model that focuses on the representation of individual physiology and life history. To describe individuals, we used the DEB-abj model (Kooijman, 2014), which is structured by energy, volume, maturity and reproduction (Fig. 4.1). We used published data from *T.* cf. *gouldi* and *Parathyasira* sp. to parameterize the model (Mariño et al., 2019). We assumed that individuals in the population could exploit one or two resources, depending on whether they are asymbiotic or symbiotic. To explicitly include the dependency of the resource on the environmental temperature, we modelled the resource according to relationships derived from the Metabolic Theory of Ecology (Savage, Gillooly, Brown, West, & Charnov, 2004). To test our predictions of how symbiosis affects populations of thyasirid bivalves, we conducted numerical simulations for *T.* cf. *gouldi* and *Parathyasira* in different environmental conditions that consider various temperature and resource availability scenarios. To further analyze the possible effects of symbiosis on populations of *T.* cf. *gouldi*, we carried out simulations representing different relative symbiont abundances and different contribution of symbionts to the host's diet.

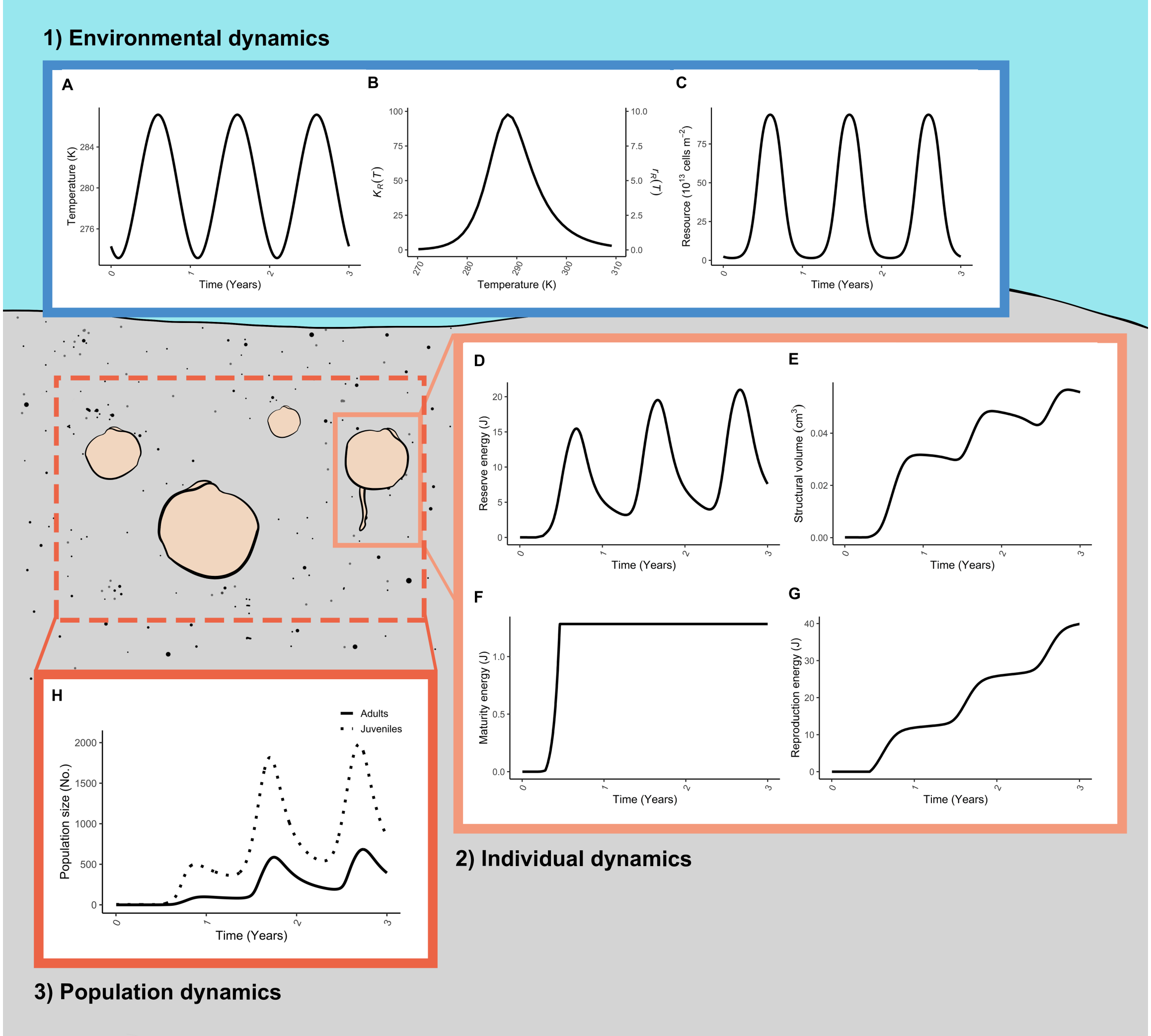

Figure 4.1. Representation of the three main components of the model for *Thyasira* cf. *gouldi* in time: 1) the environment (A, B, C), 2) the individual (D, E, F, G) and 3) the population (H). The environmental variables of temperature (A, equation 4.1) and free-living bacterial resource (C, equation 4.2) determine each individual's dynamics. The carrying capacity of the free-living bacterial resource ($K_R(T)$) and its growth rate ($r_R(T)$) are functions of the environmental temperature (B, equations 4.3 and 4.4). For both parameters, we follow relationships derived from the Metabolic Theory of Ecology (Savage, Gillooly, Brown, West, & Charnov, 2004). We characterize the individuals by four variables: energy in reserve (D), structural volume (E), maturity (F) and reproduction energy (G), according to the DEB model (equation 4.7). We obtain the population dynamics (H) by numerically integrating over all the individuals (equation 4.10). The simulations' parameters are given in Tables 4.2 and 4.3. We assumed an initial condition of 5 embryos for the simulation of the population.

4.2.2 Environment

4.2.2.1 Temperature

We modelled an annual cycle that corresponds to the seafloor temperatures at Bonne Bay, which range from 0.7 to 14 °C, approximately (Laurich et al., 2015, see Fig. 4.1A). More specifically, the temperature at time t oscillates around the average temperature ($\bar{T}$) with amplitude T_a and period equal to the length of the year:

$$T\left(t\right) = \bar{T} + T_a \sin\left(2\pi \frac{t}{365}\right). \tag{4.1}$$

For comparative purposes, we also modelled a constant environment assuming that the temperature is equal to the mean annual temperature, $\bar{T}$.

4.2.2.2 Resource

The primary resource for *T.* cf. *gouldi* and *Parathyasira* is free-living, chemoautotrophic bacteria (Zanzerl et al., 2019). In cold, marine sediments, such as Bonne Bay, bacterial production is typically seasonal, with specific growth rates increasing with temperature; further, bacterial production is directly proportional to bacterial biomass (Sander & Kalff, 1993). Thus, we assumed that the free-living bacterial resource R is a function of the environmental temperature T, and follows logistic growth:

$$R(T) = r_R(T)R\left(\frac{K_R(T) - R}{K_R(T)}\right), \tag{4.2}$$

where r_R is the resource growth rate and K_R is the maximum resource density. For notational simplicity, we let $T = T(t)$; however, it should be understood that temperature may be a function of time as described in equation 4.1.

To include the dependence of the resource on the environmental temperature, we described both resource parameters using relationships derived from the Metabolic Theory of Ecology (Savage et al., 2004). We assumed that the growth rate and carrying capacity increase exponentially with temperature. Further, around the limits of the bacteria's thermal niche, both parameters drop steeply to zero, according to a Sharpe-Schoolfield term (Schoolfield, Sharpe, & Magnuson, 1981, see Fig. 4.1B). Hence, the resource growth rate is given by:

$$\begin{aligned} r_R(T) = \; & r_0 e^{(-\mathcal{E}/k_B)(1/T-1/T_0)} \Big(1 + e^{(-\mathcal{E}_L/k_B)(1/T-1/T_L)} \\ & + e^{(-\mathcal{E}_H/k_B)(-1/T+1/T_H)} \Big)^{-1}, \end{aligned} \tag{4.3}$$

where r_0 is the resource growth rate at a reference temperature T_0, k_B is the Boltzmann constant, $\mathcal{E}$ is the average activation energy driving resource growth at intermediate temperatures, $\mathcal{E}_L$ and $\mathcal{E}_H$ are the inactivation energies that determine the slope of the resource growth rate as it drops to zero at the lower and upper thermal tolerance limits, T_L and T_H, respectively.

The maximum resource density follows a similar formulation:

$$\begin{aligned} K_R(T) = \; & K_0 e^{(-\mathcal{E}/k_B)(1/T-1/T_0)} \Big(1 + e^{(-\mathcal{E}_L/k_B)(1/T-1/T_L)} \\ & + e^{(-\mathcal{E}_H/k_B)(-1/T+1/T_H)} \Big)^{-1}, \end{aligned} \tag{4.4}$$

where K_0 is the maximum resource density at a reference temperature T_0. As with the resource growth rate, the parameters $\mathcal{E}$, $\mathcal{E}_L$ and $\mathcal{E}_H$ represent the temperature sensitivity of the maximum resource density within and outside of the lower and upper temperature thresholds, T_L and T_H.

4.2.3 Individual dynamics

We described the individual life history and physiology (i.e. feeding, growth, and reproduction) as a function of the individual state variables and the state of the environment.

4.2.3.1 Feeding

All individuals forage on the resource (free-living bacteria) following a functional response $f(t, T, R)$, which is a function of the time of the year, the temperature and the resource abundance. Asymbiotic individuals feed only on one resource according to the scaled functional response:

$$f_A(R) = \frac{R(T)}{R_{\text{max}}}, \tag{4.5}$$

where R_{max} is the maximum resource density.

Symbiotic individuals can forage on the symbionts as an additional resource, which we modelled as a constant, scaled abundance S. Thus, the functional response for symbiotic individuals $f_S(t, T, R)$ includes their reliance on symbionts α, and is given by:

$$f_S(R) = (1 - \alpha)\left(\frac{R(T)}{R_{\text{max}}}\right) + \alpha\left(\frac{S}{R_{\text{max}}}\right). \tag{4.6}$$

4.2.3.2 Growth and reproduction: DEB-abj model

The individual dynamics are according to the Dynamic Energy Budget theory (Kooijman, 2010). This approach distinguishes between the biomass of the organism that functions as an energy reserve and as structure. Specifically, we use the DEB-abj model, which is a one parameter extension of the standard DEB model that accounts for a growth pattern recognized in bivalves termed metabolic acceleration (Kooijman, 2014).

Each individual is characterized by four state variables: energy in reserve (E), structural volume (L^3), cumulative energy invested into maturation (E_H), and cumulative energy invested into reproduction (E_R). The dynamic of the individual in time is given by:

$$
\begin{aligned}
\frac{dE}{dt} &= \dot{p}_A - \dot{p}_C, \\[2ex]
\frac{dL^3}{dt} &= \kappa(\dot{p}_C - \dot{p}_S)/[E_G],
\end{aligned}
\tag{4.7}
$$

$$
\begin{cases}
\dfrac{dE_H}{dt} = (1-\kappa)\dot{p}_C - \dot{p}_J \text{ and } \dfrac{dE_R}{dt} = 0, & \text{if } (E_H < E_H^p), \\[4ex]
\dfrac{dE_H}{dt} = 0 \text{ and } \dfrac{dE_R}{dt} = (1-\kappa)\dot{p}_C - \dot{p}_J, & \text{otherwise,}
\end{cases}
$$

where the energy fluxes are denoted by $\dot{p}$ (see Table 4.1), κ is the fraction of mobilized reserve allocated to somatic metabolism, $[E_G]$ is the specific cost to grow one unit of structure, and E_H^p is the puberty threshold.

Table 4.1. Energy fluxes ($\dot{p}$, J/d) and shape correction function ($\mathcal{M}$) at each developmental stage. Each stage is defined according to the cumulative maturity thresholds E_H^b, E_H^j and E_H^p, which represent birth, metamorphosis, and puberty, respectively. The scaled functional response is f ($0 \leq f \leq 1$, where 1 is the highest amount of food), $\{\dot{p}_{\mathrm{Xm}}\}$ is the maximum surface-area specific ingestion rate ($\{\dot{p}_{\mathrm{Xm}}\} = \{\dot{p}_{\mathrm{Am}}\} \;/\; \kappa_X$, J/day · cm^2, for a maximum surface-area specific assimilation rate $\{\dot{p}_{\mathrm{Am}}\}$), κ_X is the assimilation efficiency from food to reserve, $\dot{v}$ is the energy conductance rate from the energy reserve (cm/day), $\dot{r}$ is the individual growth rate (1/day, equation 4.8), $[\dot{p}_M]$ is the volume-specific somatic maintenance cost (J/day · cm^3), $\dot{k}_J$ is the maturity maintenance rate coefficient. The structural lengths at the beginning and at the end of the acceleration are L_b and L_j, which correspond to the structural lengths at birth and at metamorphosis. Notation: square brackets ([ ]) indicate quantities related to structural volume, curly brackets ({ }) denote quantities related to structural surface-area, dots (˙) indicate rates.

Flux	Embryo ($E_H \leq E_H^b$)	Early juvenile ($E_H^b < E_H \leq E_H^j$)	Late juvenile ($E_H^j < E_H < E_H^p$)	Adult ($E_H \geq E_H^p$)
Feeding, $\dot{p}_X$	0	$f\{\dot{p}_{\mathrm{Xm}}\}\mathcal{M}$	$f\{\dot{p}_{\mathrm{Xm}}\}\mathcal{M}$	$f\{\dot{p}_{\mathrm{Xm}}\}\mathcal{M}$
Assimilation, $\dot{p}_A$	$\kappa_X\dot{p}_X$	$\kappa_X\dot{p}_X$	$\kappa_X\dot{p}_X$	$\kappa_X\dot{p}_X$
Mobilization, $\dot{p}_C$	$E\dot{v}(\mathcal{M}/L - \dot{r})$	$E\dot{v}(\mathcal{M}/L - \dot{r})$	$E\dot{v}(\mathcal{M}/L - \dot{r})$	$E\dot{v}(\mathcal{M}/L - \dot{r})$
Soma maint., $\dot{p}_S$	$[\dot{p}_M]L^3$	$[\dot{p}_M]L^3$	$[\dot{p}_M]L^3$	$[\dot{p}_M]L^3$
Maturity maint., $\dot{p}_J$	$\dot{k}_J E_H$	$\dot{k}_J E_H$	$\dot{k}_J E_H$	$\dot{k}_J E_H^p$
Shape function, $\mathcal{M}$	$L_b/L_b = 1$	L/L_b	L_j/L_b	L_j/L_b

The growth rate for each individual is given by:

$$\dot{r} = \frac{\kappa \frac{E}{L^4}\dot{v}\mathcal{M} - [\dot{p}_M]}{\kappa \frac{E}{L^3} + [E_G]}, \tag{4.8}$$

where $\mathcal{M}$ is a shape correction function that varies according to the stage of the individual (see Table 4.1), $\dot{v}$ is the energy conductance rate, and $[\dot{p}_M]$ is the somatic maintenance cost.

The energy fluxes for all the metabolic rates are temperature-dependent (see Section 1.3 in Kooijman, 2010), therefore the parameters of the model are standardized to a reference temperature of 20°C. The correction between the reference temperature and the empirical temperature T is done through the Arrhenius relationship:

$$c_T = \exp\left(\frac{T_A}{T_{\text{ref}}} - \frac{T_A}{T}\right), \tag{4.9}$$

where $c(T)$ is the correction factor for a certain temperature T, T_A is the Arrhenius temperature and T_{ref} is the reference temperature. For example, the mobilization flux (Table 4.1) at temperature T becomes: $\dot{p}_C(T) = \dot{p}_C(T_{ref}) \cdot c(T)$.

Table 4.2. Parameter values for the individual-level dynamics (equation 4.7) for the symbiotic *Thyasira* cf. *gouldi* and the asymbiotic *Parathyasira* sp. (Mariño, Augustine, Dufour, & Hurford, 2019). Notation: square brackets ([ ]) indicate quantities related to structural volume, curly brackets ({ }) denote quantities related to structural surface-area, dots (˙) indicate rates.

Description	Symbol	*Thyasira* cf. *gouldi*	*Parathyasira*	Unit
Maximum assimilation rate	$\{\dot{p}_{\text{Am}}\}$	1.427	2.547	J/day · cm^2
Assimilation efficiency	κ_X	0.8	0.8	-
Energy conductance rate	$\dot{v}$	0.02	0.02	cm/day
Allocation fraction to soma	κ	0.883	0.958	-
Somatic maintenance cost	$[\dot{p}_M]$	15.78	23.61	J/day · cm^3
Maturity maintenance coefficient	$\dot{k}_J$	0.002	0.002	1/day
Specific cost for structure	$[E_G]$	2355	2348	J/cm^3
Maturity at birth	E_H^b	2.639e-4	7.193e-5	J
Maturity at metamorphosis	E_H^j	0.011	0.002	J
Maturity at puberty	E_H^p	1.283	0.96	J
Weibull aging acceleration	$\dot{h}_a$	9.844e-8	1.262e-7	1/day^2
Shape coefficient	δ_M	0.507	0.64	-
Arrhenius temperature	T_A	8000	8000	K
Reference temperature	T_{ref}	293.15	293.15	K

4.2.4 Population dynamics

We represent the population by a density n, which is a function of the four individual DEB model (or i-states) variables ($n(t, E(t), V(t), E_H(t), E_R(t))$) and its dynamic in time is given by:

$$\frac{\partial n}{\partial t} + \frac{\partial n}{\partial E}\frac{dE}{dt} + \frac{\partial n}{\partial V}\frac{dV}{dt} + \frac{\partial n}{\partial E_H}\frac{dE_H}{dt} + \frac{\partial n}{\partial E_R}\frac{dE_R}{dt} \quad = -\mu(n + n^2), \tag{4.10}$$

where μ is the per capita mortality rate. The set of all the possible i-states defines the population state space $\Omega \subset \mathbb{R}^n$. To prevent individuals from leaving the domain, we included no-flux boundary conditions for each i-state variable: $E_{|\partial\Omega} \equiv 0, V_{|\partial\Omega} \equiv 0, E_{H_{|\partial\Omega}} \equiv 0, E_{R_{|\partial\Omega}} \equiv 0$.

The population state space is divided into subsets that represent the different life stages of the individuals. For simplicity, we group the two juvenile stages together, and consider the domains Ω_J, and Ω_A, corresponding to the juvenile and adult stages. The boundary between these subsets is given by the cumulative maturity energy threshold parameter E_H^p. Here, we assume that once individuals are adults they cannot rejuvenate and decrease their maturity level. Hence, we further suppose the no-flux boundary:

$$E_H(x) = \begin{cases} E_H(x) & \text{if } E_H(x) \geq 0, \\ 0 & \text{otherwise,} \end{cases} \qquad \forall x \in \partial\Omega_J. \tag{4.11}$$

The reproduction of the adult population gives the boundary condition at age zero:

$$n(t, E_0, V_0, E_{H_0}, E_{R_0}) = \int_{\Omega_A} \beta\, n\, dE\, dV\, dE_H\, dE_R, \tag{4.12}$$

where we consider that the per capita fecundity rate β is a constant. Additionally, we assume that individuals are born in the population at the origin of the domain.

4.2.5 Model analysis

We implemented our population model in the R language (R Core Team, 2019) and solved it as an initial value problem through the methods of lines. For this, we discretized the evolution equations with finite differences and performed the time integration using the lsoda initial value problem solver from the package deSolve (Soetaert et al., 2010). Our simulations represented experimental populations that start with 5 embryos, for either species (as in B. T. Martin, Jager, Nisbet, Preuss, & Grimm, 2013; B. T. Martin, Zimmer, Grimm, & Jager, 2012). Thus, the initial conditions for our numerical simulations were:

$$n(t=0,x) = \begin{cases} 5, & \text{if } x = \left(E_0, V_0, E_{H_0}, E_{R_0}\right), \\ 0, & \text{otherwise.} \end{cases} \tag{4.13}$$

To investigate how symbiosis affects population dynamics, we conducted simulations at constant and fluctuating environments for both species. The environment and population parameters are given in Table 4.3, the parameters for the individual dynamics are given in Table 4.2. For these simulations, we assumed that the abundance of the symbionts was equal to the mean abundance of the free-living bacterial resource ($S = \bar{R}$). Further, we assumed that symbionts provide 25% of the diet of symbiotic individuals ($\alpha = 0.25$).

Table 4.3. Parameter values for the environment and population-level dynamics for the symbiotic *Thyasira* cf. *gouldi* and asymbiotic *Parathyasira* sp. We assume that the parameter values are equal for both populations.

Description	Symbol	Value	Unit	Reference
Environment				
Temperature	T	variable	K	Laurich, Batstone, and Dufour, 2015
Mean temperature	$\bar{T}$	279.15	K	Laurich, Batstone, and Dufour, 2015
Temperature amplitude	T_a	7	-	Laurich, Batstone, and Dufour, 2015
Lower temperature limit for survival	T_L	273.15	K	-
Upper temperature limit for survival	T_H	303.15	K	-
Reference temperature	T_0	288.15	K	$(T_H + T_L)/2$
Mean activation energy	$\mathcal{E}$	0.43	J	Savage, Gillooly, Brown, West, and Charnov, 2004
Lower tolerance limit inactivation energy	$\mathcal{E}_L$	1.9	-	-
Upper tolerance limit inactivation energy	$\mathcal{E}_H$	1.9	-	-
Boltzman constant	k_B	$8.617e^{-5}$	eV/K	-
Free-living bacterial resource	R	variable	-	-
Free-living bacterial resource growth rate at T_0	r_0	$5e^6$	day^{-1}	-
Free-living bacterial resource density at T_0	K_0	$5e^7$	day^{-1}	-
Maximum free-living bacterial resource density	R_{max}	variable	-	-
Symbiont scaled abundance	S	variable	-	-
Population				
Birth rate	β	0.005	day^{-1}	-
Death rate	μ	0.001	day^{-1}	de Roos and Persson, 2001

To analyse the effect of the abundance of symbionts in a host population inhabiting a fluctuating environment, we investigated three possible cases: i) the abundance of the symbionts is equal to the average abundance of the resource ($S = \bar{R}$); ii) the symbionts are more abundant than the resource ($S = R_{\text{max}}$); and iii) the symbionts are less abundant than the resource ($S = R_{\text{min}}$). Here, we also assumed that the contribution of symbionts to a host individuals' diet is 25% ($\alpha = 0.25$). Further, to assess how the reliance on symbionts alters the abundance of the host population, we evaluated the impact of the dependence on symbionts (α) for the case $S = \bar{R}$. This way, we consider several values of α, ranging from individuals that do not rely on symbionts ($\alpha = 0$), to those that rely solely on symbionts as their resource ($\alpha = 1$). The results presented for these sections correspond to the values of the population after transient dynamics have disappeared.

4.3 RESULTS

4.3.1 The symbiotic population has a greater proportion of adults

In the constant environment, both the asymbiotic and the symbiotic ($\alpha = 25\%$) species reach carrying capacity and stabilize after two years (Fig. 4.2A). Both populations are dominated by individuals in the juvenile classes, with all the stages following the same growth pattern (Fig. 4.2B, C). However, the symbiotic *T.* cf. *gouldi* population shows a faster growth rate and reaches a higher carrying capacity, relative to the asymbiotic *Parathyasira* (Fig. 4.2A-C) since individuals of *T.* cf. *gouldi* allocate more energy to reproduction (Mariño et al., 2019). Further, in the symbiotic population, a larger proportion of individuals are in the adult stage (Fig. 4.2C).

In the seasonal environment, the populations of both species experience yearly cycles of low temperatures and low abundances of free-living bacteria (Fig. 4.1A, B), which cause a decrease in the individual growth and maturity rates as well as in the production of offspring (Fig. 4.1D, F). Consequently, both populations exhibit similar amplitude fluctuations with a one-year periodicity (Fig. 4.2D). During the periods of low free-living bacteria abundance, the symbiotic and asymbiotic thyasirid populations have similar sizes (Fig. 4.2D). Individuals in all the stages follow the same regular oscillations, with juveniles being the most abundant class in both populations (Fig. 4.2E). However, the proportion of adults is higher in the symbiotic population, reaching a greater abundance and a larger minimum size than the asymbiotic population (Fig. 4.2F).

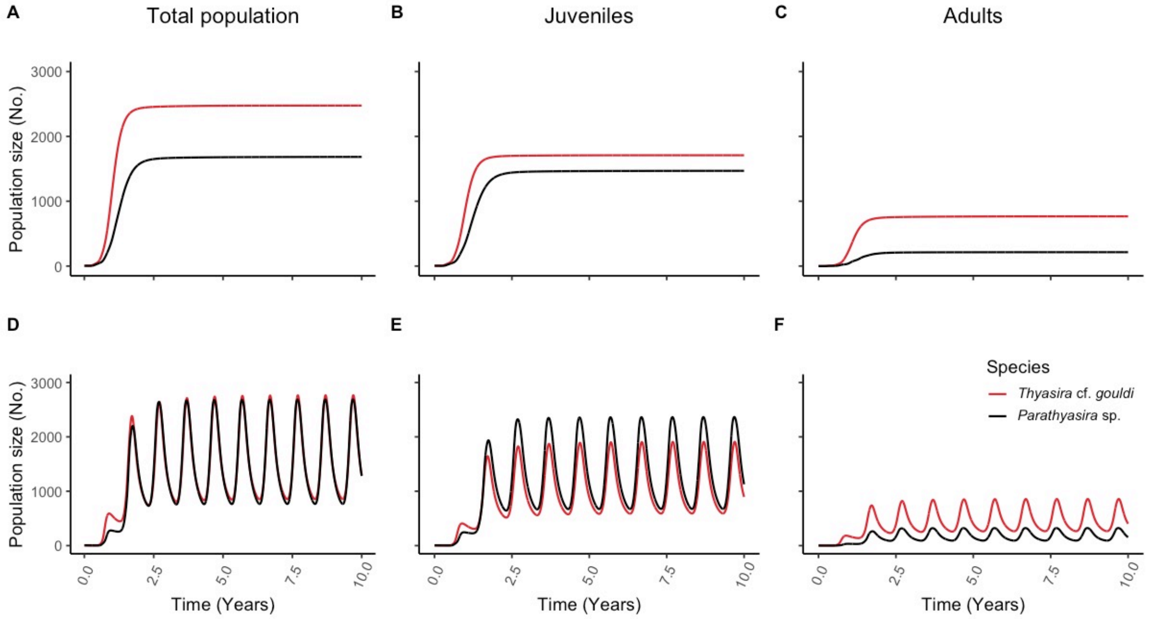

Figure 4.2. Modelled long term population dynamics for the symbiotic T. cf. gouldi and asymbiotic Parathyasira sp. in a constant (A-C) or fluctuating environment (D-F). For all cases, the initial population consists of five embryos. The reliance of T. cf. gouldi on symbionts is assumed to correspond to 25% of their diet. The symbiotic strategy allows individuals to invest more energy in reproduction, resulting in larger population sizes than the asymbiotic population in the constant environment (A). In the seasonal environment (D), both populations exhibit yearly cycles due to the combined effect of temperature and resource fluctuations. The stage dynamics for juvenile individuals (B, E) and adult individuals (C, F) exhibit the same pattern as the total population, with juveniles dominating both species' populations. In both environment scenarios, the proportion of adults is greater in the symbiotic population.

4.3.2 Increasing symbiont abundance increases the population size of the host

In the seasonal environment, the dynamics of the population of symbiotic *T.* cf. *gouldi* vary according to the abundance of symbiotic bacteria (Fig. 4.3A). The population attains the largest size when the abundance of symbionts is greater than the abundance of the free-living bacteria (i.e. $S > R$, Fig. 4.3A). In this case, the mean population size and the amplitude of the yearly cycles are larger than in the other scenarios. As the abundance of the symbionts decreases (i.e. $S < R$), the host population exhibits cycles of smaller amplitudes and reaches a smaller mean size (Fig. 4.3A).

In the three scenarios of symbiont abundance that we considered, the dynamics of the different age classes of symbiotic *T.* cf. *gouldi* follow the same pattern as the population (Fig. 4.3B). Individuals in the juvenile stage dominate the populations and exhibit the largest amplitude in abundance when the conditions for the symbionts are favourable. In contrast, fluctuations in amplitude are smaller for the adult stage. Nevertheless, an increase in the abundance of symbionts favours a higher mean number of adults.

4.3.3 Increasing reliance on symbionts reduces the amplitude of the population cycles of the host

For populations of symbiotic *T.* cf. *gouldi* in a seasonal environment, the amplitude of the yearly cycles depends on the reliance of each individual host on the symbiotic bacteria (Fig. 4.4A). The largest mean population size and annual cycles with the highest amplitude occur in the population where individuals do not obtain nutrients from symbionts (i.e. $\alpha = 0$, equivalent to asymbiotic individuals, Fig. 4.4A). An increasing reliance on symbionts reduces the effect of seasonal fluctuations in the free-living bacterial resource. Consequently, both the amplitude of the population cycles and the mean population size decrease. The smallest amplitudes and mean population sizes occur in the population

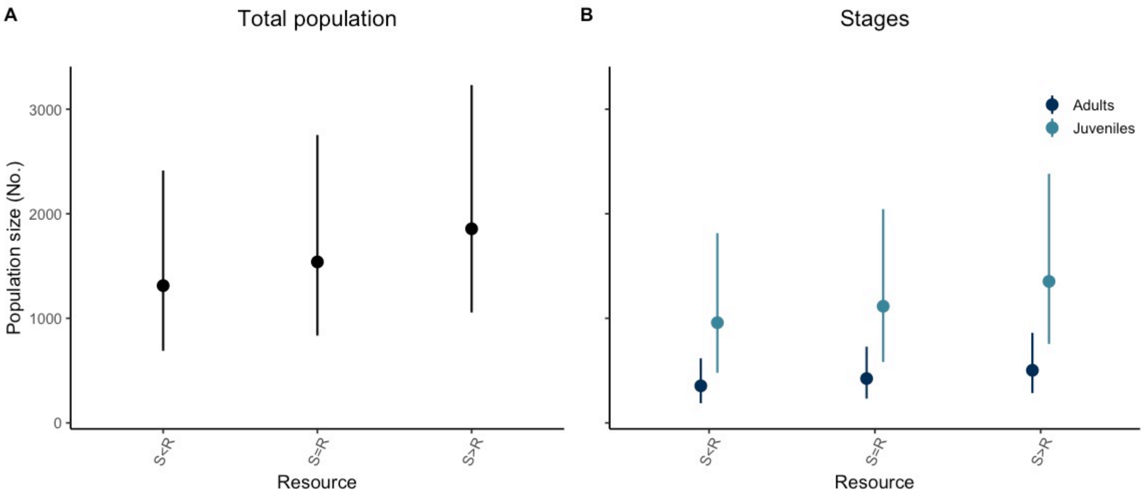

Figure 4.3. Effect of different symbiont abundances (S) relative to the free-living bacteria (R) on the host population of T. cf. gouldi in a seasonal environment. For all cases, the initial population consists of five embryos, and the reliance of T. cf. gouldi on symbionts corresponds to 25% of their diet. Points represent the average population size after discarding transient dynamics, and lines correspond to the yearly cycle's amplitude. An increasing relative symbiont abundance is predicted to increase the average, minimum and maximum population sizes in T. cf. gouldi (A). The stage dynamics exhibit the same pattern as the total population, with juveniles dominating both species' populations (B).

where hosts rely entirely on symbionts (i.e. $\alpha = 1$, equivalent to obligate symbiosis), given that they are not affected by fluctuations in resource availability. However, populations that rely entirely on symbionts still experience fluctuations in abundance since temperature affects the metabolic rates. Furthermore, the minimum population size rises with increasing reliance on symbionts, the highest minimum occurring in the population where individuals are obligate symbionts. Therefore, in a seasonal environment, populations with a greater dependence on symbionts are less likely to experience extinction.

As in our previous results, the dynamics of the two stages of symbiotic *T.* cf. *gouldi* follow the same fluctuating pattern as the combined population (Fig. 4.4B). In all the scenarios considered, juvenile individuals predominate and show the greatest variation in abundance, whereas individuals in the adult class exhibit cycles of smaller amplitude. Both the adult and juvenile stages reach a greater average population size when they have a low reliance on symbionts. Similarly, the mean population size of both stages decreases

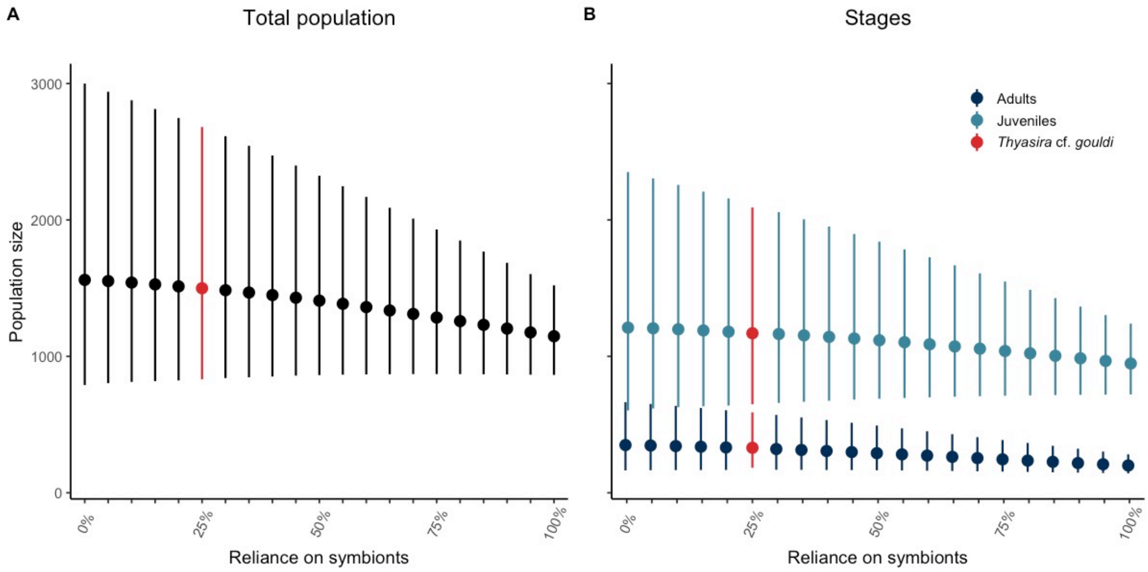

Figure 4.4. Effect of varying symbiont reliance (α) on the host populations in a seasonal environment. For all simulations, the initial population consists of five embryos. T. cf. gouldi, which has a dependence on symbionts assumed to be 25%, is highlighted for reference. Points represent the average population size after discarding transient dynamics, and lines correspond to the amplitude of the yearly cycle. An increasing symbiont dependence decreases the magnitude of the annual population cycles (A). As dependence on symbionts increases, the average and maximum population sizes decrease; however, the minimum population size increases. The stage dynamics exhibit the same pattern as the total population, with juveniles dominating both species' populations (B).

with an increase in the individual specialization on the symbionts. For the two stages, the minimum population size shows an increase as the dependence on symbionts increases.

4.4 DISCUSSION

We show how the host's individual physiology and the abundance of and dependence on symbionts affect thyasirid population dynamics in constant and seasonal environments. Our simulations for a constant environment reveal that the mixotrophic species reaches a higher population size than the asymbiotic species. In a seasonal environment, the population of symbiotic adults has a higher growth rate during periods of the year with higher temperatures and a greater abundance of free-living resources. Similarly, in periods where the temperatures are low, and resource is limiting, the mixotrophic adult population is less prone to extinction due to the assimilation of symbiotic bacteria. Moreover, the symbiont abundance and the degree of specialization in the host's diet modulate the effect of symbiosis. Thus, our results support our initial hypothesis that symbiosis with an intermediate level of reliance on the symbionts mitigates the impact of resource seasonality.

4.4.1 Population dynamics

We found that symbiotic thyasirids reach larger population sizes and have faster population growth than the asymbiotic species in a constant environment (Fig. 4.2A). A similar pattern has been found in *T. sarsi*, which has an intermediate reliance on bacterial symbionts (between 26 to 76%) and exhibits a faster population growth rate, reaching larger population sizes when compared to the sympatric and less symbiont dependent *T. equalis* (which has a reliance below 26%) (Dando & Spiro, 1993). However, unlike *T. equalis*, the asymbiotic *Parathyasira* have higher somatic growth rates and reach larger sizes at maturity, relative to the symbiotic *T.* cf. *gouldi* (Mariño et al., 2019). Further, our results show that both populations are composed mostly of juvenile individuals (Fig. 4.2B, E). A comparable population structure has been observed in *Thyasira gouldi*, which exhibits a bimodal distribution year-round (Blacknell, 1973). Our findings for a seasonal environment show that both populations experience yearly cycles. Similarly, for *Thyasira gouldi*, *T. sarsi*, and *T. equalis* empirical data has suggested that they have variable population sizes (Blacknell, 1973; Dando & Southward, 1986). Thus, despite the limited empirical evidence from other thyasirid bivalves or symbiotic animals, our results broadly agree with the literature.

4.4.2 Effect of symbiosis on the host population

In our simulations, the symbiotic population of *T.* cf. *gouldi* experiences oscillations of a similar amplitude relative to the asymbiotic population (Fig. 4.2D). When we consider a symbiotic population in which the symbionts are more abundant, the amplitude of the population cycles increases (Fig. 4.3). Conversely, when the individuals have a higher dependency on the symbionts, the yearly cycles have smaller amplitudes (Fig. 4.4). Broadly, our results indicate that the magnitude of these population cycles is likely an effect of the mixotrophic diet and reduced energy reserves of the individual hosts (Mariño et al., 2019). In general, when the free-living bacteria become a limiting resource, the symbionts provide a stable alternative nutritional source for the host (Gori et al., 2012; Rossi et al., 2017; Viladrich et al., 2017), which does not need to rely on an energy reserve. As a consequence, when the resource is abundant, hosts do not need to build up a large energy reserve. Instead, the individual hosts can allocate more energy to reproduction. This effect is evident in the constant environment when the resource is not limiting, where symbiotic thyasirids reach higher abundances than the asymbiotic population (Fig. 4.2A).

Benefits of symbiosis at low resource concentrations have been documented before, theoretically and experimentally, in photomixotrophic and aposymbiotic organisms (e.g. in ciliates and in hydra; Goetsch, 1924; Karakashian, 1963; Muscatine & Lenhoff, 1965; Stabell, Andersen, & Klaveness, 2002). The literature agrees that, at low resource concentrations, mixotrophic populations have significantly higher growth rates than aposymbiotic populations, which is sufficient to prevent extinction. At high resource availability, theory suggests that the benefits of symbiosis are in reducing loss rates (Stabell et al., 2002), which agrees with our previous finding of lower somatic maintenance costs for the symbiotic *T.* cf. *gouldi* when compared to the asymbiotic *Parathyasira* (Mariño et al., 2019). The role of symbionts in building-up and performing the primary energy and carbon storage for a host has only recently been described (in the chemosymbiotic flatworm *Paracatenula*; Jäckle et al., 2019). Therefore, evidence agrees with our analysis and suggests a potential role of symbiosis in mitigating environmental fluctuations in populations of mixotrophic individuals.

4.4.3 Model assumptions and limitations

Our results are related to our assumptions regarding the fecundity, mortality, and competition of the individuals in the populations. For the thyasirids of Bonne Bay, we do not have enough evidence to suggest that reproduction occurs in discrete events or that there is competition for resources between the species. Therefore, in our model, reproduction occurs continuously, and each species can graze independently of the other on the free-living bacterial resource. Likewise, for simplicity and lack of detailed information, we assumed that mortality was equal for both species in all the stages. The consequences of our assumptions could influence the population structure in our results. For example, in a population of *T. gouldi*, it has been proposed that juveniles do not uniformly predominate because early juveniles are likely to suffer a greater mortality rate, compared to late juveniles and adults (Blacknell, 1973). Nonetheless, these simplifying assumptions are unlikely to affect the overarching pattern regarding the effect of the symbiotic strategy.

The yearly cycles experienced by both populations are a direct result of the fluctuations in temperature and its effect on the resource. We modelled the temperature oscillations according to the natural variation pattern observed in Bonne Bay. The free-living bacteria are also known to be subject to seasonal variations (Laurich et al., 2015); therefore, we used a framework derived from the Metabolic Theory of Ecology to couple the environmental temperatures to the resource abundance. Even though the abundance and digestion of the bacterial symbionts in *T.* cf. *gouldi* also show a cyclical trend (Laurich et al., 2015), in our formulation, we treat the symbiont abundance as constant, considering that they provide a more stable source of nutrition. Despite our assumptions, the strength of our physiologically structured model is illustrated by the differences that we revealed between the two species' populations.

4.4.4 Reliance on symbionts

Differences in individual energy allocation have suggested that for *T.* cf. *gouldi* the symbionts may buffer resource fluctuations (Mariño et al., 2019). Our simulations suggest that symbiotic and asymbiotic thyasirids have different adaptations to persist during winter conditions when the temperatures are low, and free-living bacteria are rare. Asymbiotic thyasirids have physiological adaptations that allow them to build a larger energy reserve, which can be mobilized more when the resource is scarce. Symbiotic thyasirids have adapted via their symbionts: the reliance on a constant supply of symbiotic bacteria buffers against the effects of seasonal lows in the abundance of free-living bacteria. Thus, for the thyasirids from Bonne Bay, both the generalist mixotrophic and the specialist diet are equally successful strategies.

Our results motivate the question of why symbiotic thyasirids do not rely more on their symbionts, or equivalently, why asymbiotic thyasirids do not have a broader diet. Both alternatives could lead to individuals less sensitive to environmental fluctuations and more stable populations sizes (Fig. 4.4A, B). Such questions are associated with the phenotypic traits that determine resource acquisition, which are thought to be defined by an intraspecific correlation between the individual morphology, physiology and behavior. In general, it is understood that there are costs that prevent the evolution of niche generalism, for example, phylogenetic constrains (Ackermann & Doebeli, 2004; Futuyma & Moreno, 1988). For symbiotic thyasirids, the gill size of the host imposes a limit to the space available for colonization by symbionts (Dufour, 2005). If the surface area of thyasirid gills shows a positive allometric relationship to body size, as observed in other chemosymbiotic bivalves with similarly filibranchiate gills (Duperron, Quiles, Szafranski, Léger, & Shillito, 2016), the small body size of thyasirids may prevent them from harbouring the number of symbionts that would be necessary for a greater reliance (i.e., equivalent to the symbiont dependencies observed in larger bivalves). Another likely explanation is that the costs of maintaining symbionts may rise during the winter, due to an increment in the bioirrigation necessary to control the symbiont population size or to an increase in the digestion of symbionts (Zanzerl et al., 2019). For asymbiotic thyasirids, there may be similar phylogenetic limitations that have prevented a change in diet and have instead promoted faster somatic growth and maturation rates. Moreover, an environment with spatial variation, such as the infaunal habitat of the thyasirids, could equally favour diet specialization (Reboud & Bell, 1997). The limited evidence available for the thyasirids hinders a more robust inference; however, it is clear that both strategies are successfully maintained in the community.

The ubiquity of symbiosis makes it a crucial factor that can determine the outcome of ecological and evolutionary processes (Moran, 2006). Nevertheless, how symbiosis affects ecology and evolution remains mostly unknown. In this study, we show how trophic symbiosis can mitigate the effect of a seasonal environment in a population of bivalve hosts. Although we parameterized our model for the particular system of thyasirid bivalves from the fjord of Bonne Bay, Canada, our approach has a general nature, and our results are relevant in a variety of trophic symbiosis. Our results highlight the relevance of linking individual energetics and life history to population dynamics and are the first step towards a general understanding of the role of symbiosis in populations' resilience.

4.5 ACKNOWLEDGEMENTS

We thank the members of the Theoretical Biology Laboratory at MUN for their constructive comments on the manuscript. JM was supported by the School of Graduate Studies Baseline Fellowship from Memorial University. SCD and AH received funding from the

Natural Science and Engineering Research Council of Canada (NSERC Discovery Grants 2015-06548 and 2014-05413).

4.6 APPENDIX

4.6.1 Individual model

4.6.1.1 Metabolic acceleration: DEB-abj model

In the DEB theory framework, species with larval development typically exhibit a slow embryonic development combined with a faster development during the late juvenile and adult stages (Kooijman, 2014). This permanent increase in the metabolic rate is called metabolic acceleration. The most common type of acceleration, called $\mathcal{M}$ acceleration, involves a simultaneous increase in the assimilation and reserve mobilization rates between birth and metamorphosis, as well as an increase in growth, maturation, reproduction and respiration. We quantified the metabolic increase in type $\mathcal{M}$ acceleration according to the shape correction function:

$$\mathcal{M} = \max(L_b, \min(L, L_j))/L_b,$$

where L is the length in structure, and L_b and L_j represent the structural lengths at the beginning and at the end of the acceleration, which correspond to the structural lengths at birth and at metamorphosis.

4.6.1.2 Observables: fecundity

The state variables of the DEB model are quantities that are not directly measurable. Hence, to calculate how the cumulative energy invested into reproduction (E_R) translates to number of embryos per time, we used the following relation (Eq. 2.56 in Kooijman, 2010):

$$\dot{R} = \frac{\kappa_R E_R}{E_0},$$

where κ_R is the reproduction efficiency (set to the standard value of 0.95) and E_0 (J) is the amount of initial energy reserve invested into each embryo (i.e. the cost of an egg). To calculate E_0 (Eq. 2.42 in Kooijman, 2010) we used the routine `initial_scaled_reserve` in the DEBtool MATLAB package (Lika et al., 2014).

4.6.2 Grid resolution and computational time

We ran the models for Section 3.1 using a grid resolution of 30^3 cells for ten years, measuring each day's population density. In Section 3.2, we used a grid resolution of 20^3 cells for six years, with output also given every day. Similarly, for Section 3.3, we integrated the model for six years with output each day, but using a grid of 15^3 cells.

We used an Intel Xeon E5-1650 v2 @ 3.50GHz processor to run the models. We measured the integration time in core-years (calculated as hours · (nodes · cores) / (365 · 24)). The integration time for the models for *Thyasira* cf. *gouldi* and *Parathyasira* sp. in a constant environment at a resolution of 30^3 cells was 0.002 and 0.012 core-years respectively. For the same grid size in the seasonal scenarios, the running time was 0.218 core-years for *T.* cf. *gouldi* and 0.232 core-years for *Parathyasira*. The simulations for *T.* cf. *gouldi* at a 20^3 resolution took 0.018 core-years to complete, and 0.004 core-years using a grid size of 15^3 cells.

2

5 CODA: DISCUSSION AND AFTERTHOUGHTS

> *Abstracting is only one part of the process of seeking understanding.*
> *The inverse process is the return to the world in which the abstractions were made.*
> *—Lewontin and Levins, 2007b.*

The structure and dynamics of ecological systems arise from individual organisms as they interact and respond to the biotic and abiotic environment (Clark et al., 2011; Grimm, Ayllón, & Railsback, 2017; Huston, DeAngelis, & Post, 1988). Throughout this thesis, I have shown how environmental factors have a central role in determining individual dynamics. In particular, I have emphasized how the nutritional resources can drive individual behaviour by determining energy input. In many species, however, resource acquisition is performed by or mediated by organisms of another species through a symbiotic interaction. Consequently, improving our understanding and forecasting of ecological systems requires integrating the multiple nutritional resources used by individuals. In this dissertation, I have shown that an individual-based approach can increase mechanistic understanding and the ability to test predictions about the dynamics of populations and broader biodiversity patterns. Through the explicit consideration of resource availability on individual life history, I have revealed some of the ecological consequences of a seasonal resource (Chapter 2) and nutritional symbiosis (Chapters 3 and 4). Here, I discuss the main contributions from the previous chapters and look ahead at how these individual responses could be affected if other factors are taken into account.

5.1 PHENOTYPIC FLEXIBILITY AS A RESPONSE TO RESOURCE SEASONALITY

> *The phenotype of an animal*
> *is the result of a compromise between many conflicting selection pressures.*
> *Every exception to the ecogeographical rules is an indication of such a conflict.*
> *—Mayr, 1956.*

All organisms are plastic, at least in some traits, and because several processes can produce plasticity, the precise mechanisms behind trait variation remain controversial (Windig et al., 2004). Chapter 2 contributes to filling this gap by isolating one of these processes and analyzing its impact on individual flexibility. The main finding of Chapter 2 is that variations in resource alone are sufficient to promote intra- and interspecific plasticity through its effect in the energy allocation process. This occurs because the plasticity displayed by the individuals is passive, meaning that the variation stems from the direct environmental influence on the expression of the trait (e.g., such as in a stunted growth owing to low food levels) (Doughty & Reznick, 2004; Forsman, 2015). Hence, passive phenotypic flexibility is sufficient to explain basic intra- and interspecific differences via energy constraints arising from differential resource abundance.

When the phenotypic flexibility is a direct consequence of the environment, the phenotypic changes are often proportional to the environmental differences (Scheiner, 2006). In Chapter 2, this was evidenced when contrasting the responses within different constant resource environments or within different seasonal environments. However, when comparing the consequences of a constant environment with a seasonal environment with an equal average resource level, the phenotypic changes are no longer directly proportional to the environment differential. In this case, it is not the average value of the resource but rather the amplitude of resource abundance that determines the mean trait value. More specifically, the peaks in resource availability create a surplus of energy input that promotes growth and reproduction. Therefore, this mechanism explains well-known ecogeographical patterns of body size and clutch-size variation, known as Bergman's rule and Lack's rule, by taking into account the energy available to fuel individual-level processes.

5.2 TROPHIC SYMBIOSIS AS AN ADAPTATION TO RESOURCE SEASONALITY

> *Multiple solutions for biological needs are the general rule in evolution.*
>
> *—Mayr, 1956.*

Symbiotic interactions are widespread and contribute to biodiversity as they often link different guilds across trophic levels (Hay et al., 2004). However, despite increasing awareness of the prevalence of symbiosis across taxa and ecosystems, our understanding of the possible far-reaching consequences of these interactions remains limited. Our lack of knowledge is critical under the current context of climate change, as it has been shown that symbioses can give rise to stabilizing feedbacks that eventually maintain diversity and ecosystem functioning (Bastolla et al., 2009; Thrall, Hochberg, Burdon, & Bever, 2007). As a result of our limited understanding, our ability to accurately measure, predict, and manage the consequences of biodiversity loss due to climate change is hindered.

Nutritional symbioses can increase the host's metabolic capacities by giving access to additional resources. In Chapter 3, I demonstrated that trophic symbiosis could alter the energy allocation patterns of the individual. In Chapter 4, I showed how the effects of symbiosis could also be reflected in the population dynamics. Nutritional symbiosis directly affects the individual's energy budget because it constitutes an additional resource for the host. Consequently, the functional response and the available energy is enhanced in symbiotic hosts. This means that the host can have the same energy intake with lower assimilation rates and somatic maintenance costs than an asymbiotic individual (Chapter

3). Such additional energy sources can be adaptive because they may provide the host with a stable resource, particularly in environments where the non-symbiotic resource is limiting (Gori et al., 2012; Rossi et al., 2017; Viladrich et al., 2017). Thus, hosts do not depend on building a large energy reserve and can allocate more energy to other processes, such as reproduction. This mechanism emphasizes the key role that trophic symbiosis can play in determining an individual's energy budget.

In Chapter 2, I argued that the resource abundance is sufficient to promote individual phenotypic flexibility by modifying the energy budget of the organisms. At the same time, in Chapters 3 and 4, I showed how nutritional symbiosis could determine the energy allocation pattern in hosts. Nonetheless, both mechanisms are not mutually exclusive, and we can evaluate their joint effect by considering the main hypotheses and predictions that arise in each case. According to the results of Chapter 2, organisms that feed on a constant resource should reach a smaller biomass and have a lower reproductive output than in a seasonal resource environment. In Chapter 3, I hypothesized that the symbionts make the host experience a more constant resource environment, while the asymbiotic species depends on a seasonal resource. By combining both, we can formulate the meta-prediction that if symbiotic organisms experience a constant resource, they should achieve smaller biomass and have a reduced reproductive output than asymbiotic individuals feeding on a seasonal resource.

As discussed in Chapters 3 and 4 thyasirid bivalves are an ideal group to evaluate predictions regarding symbiosis. Here, I consider the simplest case in which an asymbiotic thyasirid experiences an environment with seasonality in resource and temperature. In contrast, the symbiotic thyasirid grows in a constant environment for both factors. In this scenario, the symbiotic species reaches a smaller biomass than the asymbiotic species (Figure 5.1A), agreeing with the available field measurements (Chapter 3). However, the symbiotic species sustains a greater reproductive output compared to the asymbiotic species (Figure 5.1B). Hence, these preliminary analyses agree with the predictions for biomass as determined by the resource but not for the predictions regarding reproductive output, indicating that other factors may have a more relevant impact on this trait.

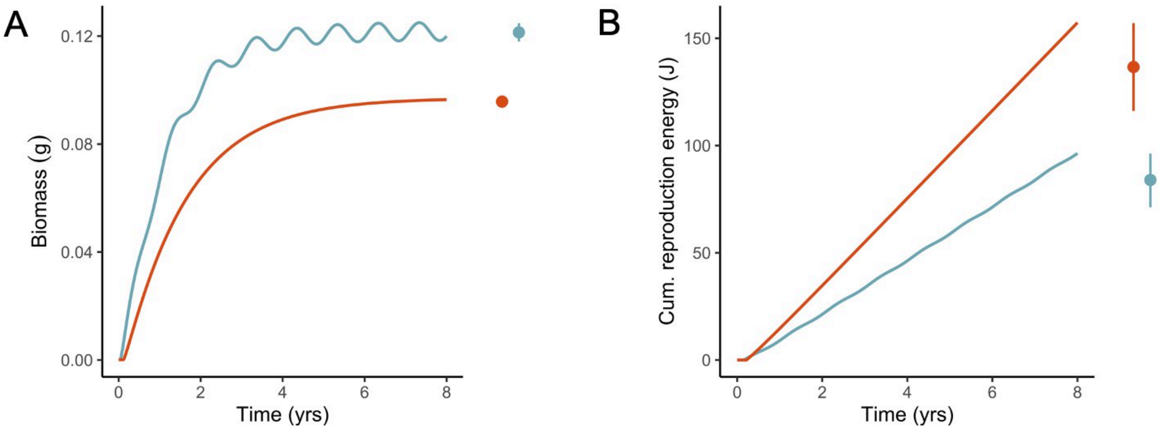

Figure 5.1. Simulations for the asymbiotic *Parathyasira* sp. in a seasonal resource environment (blue) with an equal mean resource availability as the symbiotic *Thyasira* cf. *gouldi* in a constant environment (red) show that *Parathyasira* dynamics follow the resource oscillations and reach greater average biomass (A) but a smaller reproductive output (B) than *T.* cf. *gouldi*. In the right panel of (A), for *T.* cf. *gouldi*, the point shows the steady-state value of biomass reached at the end of the lifespan. In contrast, for *Parathyasira*, the point represents the average biomass calculated over the last two years (i.e., years six to eight), and lines show the minimum and maximum values. In the right panel of (B), for both species, points represent the average cumulative reproduction energy calculated over the last two years, and lines correspond to the minimum and maximum values. The biomass of *Parathyasira* sp. fluctuates according to the resource because the model does not consider limits to individuals' shrinking in size in periods of low food availability. The simulations assume $\bar{f} = 0.8$ and $\bar{T} = \sim 6°\text{C}$ (see parameter values in Table 3.6, Chapter 3).

The differences between the species in the previous example can result from assuming that the symbiotic species experiences an environment that is constant not only in the resource but also in temperature. Moreover, these factors may be correlated. For instance, resource availability often covaries with temperature, increasing primary production due to temperature seasonality. For this reason, it is pertinent to evaluate the same case study with the thyasirids considering a more complex environmental forcing. One possible approximation is given by the Metabolic Theory of Ecology (Savage et al., 2004), whereby the growth rate and the carrying capacity of the resource can be functions of the environmental temperature (as in Chapter 4). In this case, both species experience an environment with seasonality in resource correlated with temperature, but the symbiotic species has an additional resource that remains constant. Here, the previous pattern where the asymbiotic species reaches a larger size (Figure 5.2A) while the symbiotic species has a greater reproductive output (Figure 5.2B) remains unchanged. Including a seasonal temperature produces oscillations in the dynamics of biomass and reproductive energy for both species. However, the amplitude of the fluctuations is larger for the asymbiotic species than the symbiotic individual (Figures 5.2A and B). Hence, including more complexity in the environment does not eliminate the differences between the species that result from a symbiotic lifestyle coupled with a seasonal resource.

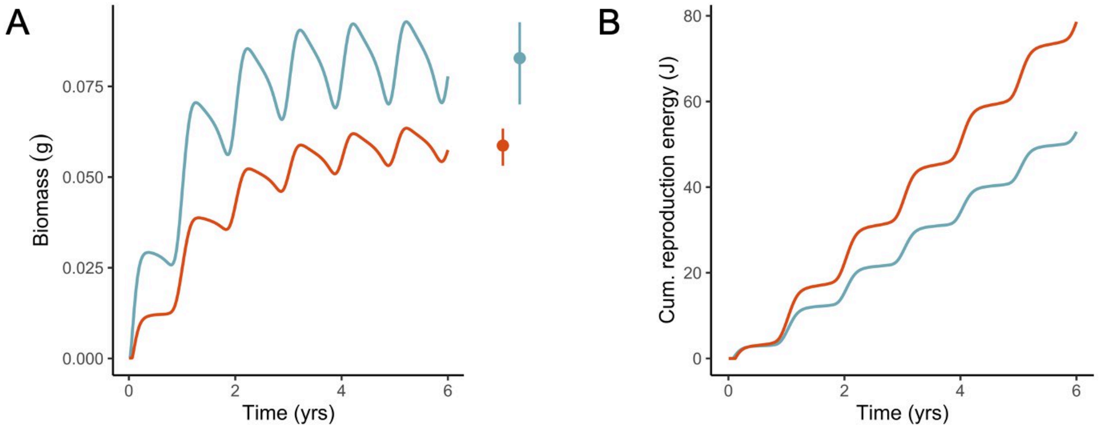

Figure 5.2. Simulations for the symbiotic *Thyasira* cf. *gouldi* (red) and the asymbiotic *Parathyasira* sp. (blue) in a seasonal environment for resource and temperature show that the dynamics of both species follow the resource oscillations, with *Parathyasira* reaching greater average biomass (A) but smaller reproductive output (B) compared to *T.* cf. *gouldi*. In the right panels of (A) and (B), points represent the average value calculated over the last two years (i.e., years four to six), and lines show the minimum and maximum values. For both species, the biomass fluctuates according to the resource because the model does not consider limits to individuals' shrinking in size in periods of low food availability. The simulations assume $\bar{f} = 0.8$ and $\bar{T} = \sim 6°C$ (see parameter values in Table 3.6, Chapter 4).

The simulations of the thyasirids' dynamics illustrate how nutritional symbiosis may be an adaptation to an environment with a seasonal resource. Empirical evidence indicates that body size and biomass have the potential to affect vital rates (e.g., feeding, growth, survival, reproduction; Arendt, 2011; Glazier, 2005; King, Milicich, & Burns, 2011; Kiørboe, 2011; Kiørboe & Hirst, 2014) and ecological processes (e.g., from individual performance to ecosystem function; Brown, Gillooly, Allen, Savage, & West, 2004). Moreover, reproductive output is usually thought to be proportional to size or biomass (Blueweiss et al., 1978; Tessier & Consolatti, 1989), which is in accordance with the expectation according to the results in Chapter 2. Thus, because individual size or biomass are directly linked to evolutionary fitness (Lynch, 1977), a decrease in size or biomass may lead to a decline in fitness (Tessier & Consolatti, 1989). However, that the symbiotic species reaches a small size while allocating more energy to reproduction may be exposing a fitness advantage through the decoupling of resource acquisition from the reproductive output. Experimental findings have indeed suggested that populations of symbiotic hosts have significantly higher fecundity rates than aposymbiotic populations at low resource concentrations (e.g. in ciliates and in hydra Goetsch, 1924; Karakashian, 1963; Muscatine & Lenhoff, 1965; Stabell et al., 2002). Therefore, evidence agrees that nutritional symbiosis is likely to be an adaptive strategy in a seasonal resource environment that enhances reproduction.

5.3 INTERACTION BETWEEN RESOURCE AND OTHER ENVIRONMENTAL FACTORS

> *When we abstract from the reality of interest to create mathematical objects,*
> *we do this because some questions that would seem intractable*
> *can now be grasped immediately.*
> *—Lewontin and Levins, 2007b.*

In Chapter 2, I showed how resource abundance is sufficient to determine individual flexibility through responses in the energy allocation process. In the previous section, I claimed that resource availability could drive the evolution of strategies that promote nutrient acquisition and, consequently, decouple biomass production from investment in reproduction. However, it can be argued that other environmental factors can affect the energy budget of an organism (e.g., temperature, oxygen availability, predation pressure) and have a similar outcome. In this section, I propose that the resource can determine individual energetics even when considering other environmental factors.

Among abiotic factors, temperature could be considered the most relevant in modulating phenotypic flexibility since metabolic rates depend on body temperature. The effects of environmental temperature have long been proposed to explain not only individual variability but also growth rate (Dawidowicz & Loose, 1992; Lampert & Trubetskova, 1996), egg size (Fischer, Brakefield, & Zwaan, 2003) and sex (Shine, 1999). Nevertheless, the effect of temperature may differ according to the trait. For instance, the variation in adult size of the daphnids *Ceriodaphnia reticulata* and *Daphnia magna* reared at different constant temperatures are negligible when food is abundant (Kooijman, 1988). In contrast, the production of offspring in *D. pulex* and *D. magna* exhibits a hump-shaped relationship with temperature, increasing until the optimal temperature is reached and declining at higher temperatures (Goss & Bunting, 1983). Yet, in *D. magna*, this thermal reaction norm only occurs when the resource is abundant (Giebelhausen & Lampert, 2001). More than variations of a single environmental factor, the interaction between them has a greater potential to influence individual flexibility. For example, experiments with *D. magna*, have shown a significant temperature-resource interaction that can increase variability in developmental rates, size at maturity and number of offspring (Giebelhausen & Lampert, 2001). However, these effects seem again to depend on food abundance (Giebelhausen & Lampert, 2001; Orcutt & Porter, 1984), highlighting the role of resource as shown in Chapter 2.

The experimental results that suggest that food availability is the main driver of individual flexibility, even when there is an interaction with temperature, can also be explained through the framework used in Chapter 2. In terms of this approach, when the resource is constant, adult size L_m is equal to:

$$L_m = \kappa \cdot \{\dot{p}_{Am}\} \ / \ [\dot{p}_m], \tag{5.1}$$

where κ is the fraction of energy allocated to somatic growth, $\{\dot{p}_{Am}\}$ is the assimilation flux, and $[\dot{p}_m]$ is the somatic maintenance flux. Both fluxes are temperature-dependent, and temperature can be assumed to affect them in the same way (Jusup et al., 2017; Kooijman, 2010; Sousa, Domingos, & Kooijman, 2008). However, since the adult size is given by the ratio of the two fluxes, size does not depend on temperature, even though it modulates the growth rate. Moreover, since biomass scales approximately with length cubed, adult biomass is also independent of temperature. Thus, contrary to resource, variations in temperature alone should not contribute to individual flexibility in final size or biomass.

As shown in Chapter 2, when the resource is not constant, adult size and biomass will vary according to the resource availability. These variations occur as individuals store more energy reserves when food is abundant but deplete them as food becomes scarce to fuel their metabolism. If the temperature is also seasonal, individuals will grow faster during the warmer season but slower during the colder season. More specifically, when organisms are already experiencing a cycle of growth and shrinking (or degrowth) due to oscillations in the resource, the temperature should affect the growth rate during the season with abundant food and the shrinking rate during the season with scarce food. Together, these variations imply that the interaction between food and temperature would only potentiate the individual flexibility in size or biomass already exposed by a differential resource availability. To better illustrate this, I consider a simple example —after the case study in Chapter 2— in which both resource and temperature follow seasonal dynamics (Figure 5.3). In this simple case, it is evident that when the oscillations of both resource and temperature are in phase, the effect of temperature only enhances the flexibility already exposed by variations in the resource.

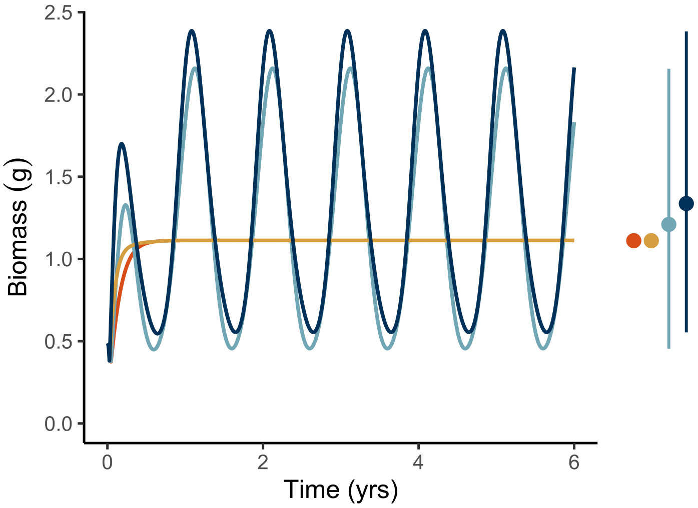

Figure 5.3. Simulations for the Grey warbler (*Gerygone igata*) across environments show that seasonality in resource alone (light blue line) can promote plasticity, resulting in a greater average biomass. In contrast, seasonality in temperature alone (yellow line) increases the growth rate but does not change the adult biomass when compared to a constant environment in both resource and temperature (red line). The combined effect of seasonality in resource and temperature (dark blue line) enhances the mean value of biomass through an additive effect. For the constant and seasonal temperature environments, points in the right panel show the steady-state value of biomass reached at the end of the lifespan. For the environments with seasonality in resource and temperature as well as in resource alone, points in the right panel represent the average biomass calculated over the last two years (i.e., years four to six), and lines show the minimum and maximum values. The biomass fluctuates according to the resource because the model does not consider limits to individuals' shrinking in size in periods of low food availability. The simulations assume $\bar{f} = 0.8$ and $\bar{T} = \sim 20°\text{C}$ (see parameter values in Table A2.2, Chapter 2).

In the formulation used in Chapter 2, an organism experiencing a seasonal resource will exhibit fluctuations in its reproductive output as more or less energy becomes available for assimilation and production of offspring. Additionally, warmer temperatures within the temperature tolerance range should increase the reproductive output by increasing the assimilation, mobilization and maturity maintenance fluxes because the energy investment in reproduction is not given by a simple ratio (in contrast to size, see equation 5.1). For seasonal temperatures, this means that the cumulative reproductive output oscillates at the same frequency as the temperature cycles. However, this fluctuation would follow the same general trend as the average temperature because the seasonal variation should mostly cancel out (e.g., the increase in reproduction from the season with higher temperature will roughly cancel out the decrease from the season with lower temperature). Consequently, we can expect that variations in temperature alone have a similar effect to that of the resource on the reproductive output flexibility. The situation is more complex if we consider the interaction between seasonal food and temperature, as the assimilation, mobilization and maturity maintenance fluxes would fluctuate according to the environment, but assimilation and mobilization are also a function of the changing food availability. For example, if we suppose that the cycles of abundant food and high temperature are in phase, then the joint variation in resource and temperature are likely to have an additive effect on the reproductive output (Figure 5.4). Hence, the effect of an interaction between resource and temperature will depend on the correlation between these factors and whether they are in or out of phase.

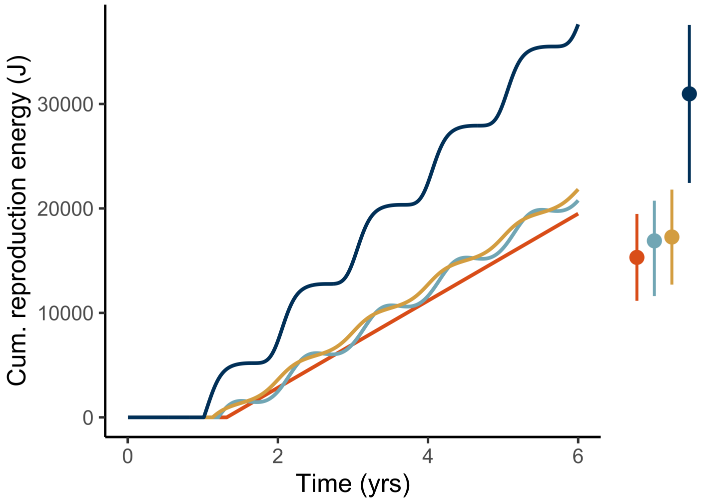

Figure 5.4. Simulations for the Grey warbler (*Gerygone igata*) across environments show that seasonality in resource (light blue line) or temperature alone (yellow line) can promote plasticity that results in a greater average reproductive output compared to a constant environment in both resource and temperature (red line). However, the combined effect of seasonality in resource and temperature (dark blue line) enhances the mean value of reproduction. In the right panel, points represent the average cumulative reproduction energy calculated over the last two years, and lines correspond to the minimum and maximum values. The simulations assume $\bar{f} = 0.8$ and $\bar{T} = \sim 20°\mathrm{C}$ (see parameter values in Table A2.2, Chapter 2).

These preliminary analyses further support the fundamental role of resource abundance in driving individual dynamics as maintained in Chapter 2. Moreover, because joint seasonality in resource and temperature has an additive effect on reproductive output, they show that this interaction is not sufficient to decouple the investment in biomass and reproduction, which was proposed to be a consequence of the symbiotic interaction in Chapters 3 and 4. Given that both biomass and reproductive output are important predictors of fitness, and that increased temperatures and habitat degradation are prominent features of climate change, it is increasingly relevant to better understand these mechanisms and predict their consequences. Changes in biomass and fecundity will not only affect fitness, but can also have an impact on community persistence by altering the connectivity of food webs and the structure of populations. Furthermore, changes in food availability can reduce interspecific variability and consequently the potential of organisms to adapt.

5.4 FUTURE RESEARCH

Thus far, I have focused on disentangling the role of a seasonal resource in individual dynamics. I have shown how this can be achieved by combining individual life history with ecological interactions and environmental factors. Nevertheless, any modelling approach has trade-offs and limitations inherent to simplifying a complex and heterogeneous nature. In this section, I explore further aspects that would provide fruitful research avenues.

5.4.1 Complex food webs

Throughout this thesis, I have considered the interplay between individuals and their environment. In Chapter 2, I investigated the responses to a seasonal resource environment, and in Chapters 3 and 4, I also considered seasonal temperatures and nutritional symbiotic interactions. Biological systems are, however, more complex: individuals have a plethora of interactions, both inter and intraspecific, which vary in sign (beneficial, neutral, detrimental) and magnitude (strong to weak) (Chamberlain, Bronstein, & Rudgers, 2014; Parmentier & Michel, 2013). Given that many supra-individual features are emerging properties arising from individuals' characteristics and behaviours (Grimm & Railsback, 2005), their interactions and variation can profoundly impact population stability, species abundance, community composition and ecosystem functions.

In this thesis, I considered a minimalistic food web consisting of a physiologically-structured consumer feeding on an unstructured resource. In Chapters 3 and 4, these two trophic levels are exemplified by the thyasirid bivalves that feed on free-living and symbiotic chemosynthetic bacteria. In this case, both thyasirids share one common resource: the free-living bacteria. Nevertheless, no evidence indicates limits in the abundance of free-living bacteria that could lead to competition between the species for the shared resource. However, this may not be true for many species belonging to the same trophic level, and competition for the limited resource can arise either through exploitation or interference. When this happens, regardless of the mechanisms involved, the competition between the consumers can potentially shape the structure and persistence of the populations involved through density-dependence. For example, intraspecific competition for the resource between individuals in different stages has been shown to produce population cycles (de Roos & Persson, 2003), while the environmental factors have been proposed to modulate their phase and synchronization over large scales (Ryabov, de Roos, Meyer, Kawaguchi, & Blasius, 2017). Hence, investigating the ecophysiological consequences of consumer competition and the bi-directional interaction in which individuals depend on the resource and the resource is affected by the organisms that consume it still requires investigation in different environmental scenarios.

In many ecosystems, there are also levels above the consumers that represent the primary and secondary predators. This sequence of consumer-resource interactions are thought to play a pivotal role in community organization (Carpenter, Kitchell, & Hodgson, 1985; Hairston, Smith, & Slobodkin, 1960; Williams & Martinez, 2000). For instance, theoretical results have shown positive feedbacks in predator-consumer-resource systems that can determine the size structure of the populations and can even promote the collapse of top predators (de Roos & Persson, 2002). Thus, predators can affect the prey populations' life-history traits and, consequently, their own food availability. Moreover, when there is more than one predator, they can interact (through resource competition) and produce non-intuitive dynamics. For example, selective predation over the same resource may produce emergent Allee effects and facilitation for the predators, resulting in species coexistence (de Roos, Schellekens, Van Kooten, & Persson, 2008). Hence, further work is needed to fully understand the ecological and evolutionary implications of predation and interaction between predators.

5.4.2 Symbiosis with variable outcomes

In Chapters 3 and 4, I evaluated the consequences of the symbiotic interaction between the thyasirid bivalves and their symbiotic bacterial partners. From the host's perspective, this interaction is positive in sign since the bivalves gain additional nutrition from the bacteria. As a result, the hosts have a large investment in reproduction (Chapter 3), which is translated into a population that fluctuates less in a seasonal environment (Chapter 4). Recent evidence shows that the sign or magnitude of symbiotic interactions can change, on ecological time scales, as a function of the biotic or abiotic context along a Mutualism-Parasitism Continuum (Chamberlain et al., 2014; Parmentier & Michel, 2013). Such changes in the sign of a symbiotic interaction can determine the persistence of populations and community structure because these features are emergent properties of individuals (Grimm & Railsback, 2005). In particular, the outcome of variable symbioses can pave the way for an ecosystem to switch to an alternative stable state. When these regime shifts are sudden, they usually involve dramatic ecological and economic consequences, including changes in biodiversity, habitats and ecosystem services (Folke et al., 2004; Folke, Edwards, Conversi, & Mo, 2015). The role of context-dependent symbiotic interactions in regime shifts remains unknown and it is critical under the current climate change, as it has been shown that symbioses can give rise to stabilizing feedbacks that eventually maintain diversity and ecosystem functioning (Bastolla et al., 2009; Thrall et al., 2007). Thus, future research should be undertaken to establish how the outcome of variable symbiotic interactions can contribute to environmental shifts in response to environmental pressures. Disentangling these processes would increase our ability to accurately measure, predict, and manage the consequences of biodiversity loss due to climate change.

5.4.3 Adaptive and developmental phenotypic plasticity

In response to variable environmental conditions, many life-history traits are plastic (Caswell, 1983), and, in consequence, the demographic rates and ecological interactions can become altered (Miner, Sultan, Morgan, Padilla, & Relyea, 2005). It has been suggested that, when faced with a changing environment, phenotypic plasticity contributes more to adaptation than genetic evolution (Hendry, 2016). In line with this evidence, a main assumption of this thesis is the absence of active plasticity in individuals, which allows building the necessary foundation for understanding the most basal ecophysiological responses to a changing environment. Nevertheless, a natural progression of this work is the inclusion of variability within the individuals to analyze the consequences of adaptive phenotypic change in a variable environment, either through phenotypic plasticity or genetic evolution. The potential outcomes of these studies would shed light on the conditions that increase population viability and stability, as well as the composition and structure of the populations and communities. Moreover, they would contribute to understanding the role of evolutionary processes on ecosystem properties, such as resilience in response to a changing environment.

5.4.4 Alternative hypotheses and mechanisms

The first overarching hypothesis of this thesis (Chapter 2) is that resource seasonality can be responsible for generating broad ecogeographical patterns of trait variation, particularly in body size and reproductive output. When these patterns are considered at the interspecific level, they are traditionally termed Bergman's rule and Lack's rule, respectively. Empirical evidence for both rules is broad in endotherms, but they have also been contended, especially in other groups. Nevertheless, the study of such patterns is well established in the field of biogeography, and the questions that remain open are mostly concerned with the interaction among the mechanisms underlying them. As such, further studies could assess the combined effects of seasonality in the resource with other environmental factors, as well as evaluate alternative explanatory hypotheses. In birds, for example, the egg viability hypothesis and the nest microclimate have been proposed as an alternative mechanism to the resource or eNPP rule (Lundblad & Conway, 2021). Moreover, a model that imposes limits to the individuals shrinking in size could provide more realistic results. In this way, further elucidating the origin of trait variation can enhance our predictive capabilities, which is particularly relevant under the current climate change.

5.4.5 Broader evidence

The second hypothesis of this dissertation (Chapters 3 and 4) is that, in trophic symbiosis, the symbionts can act similarly to an external energy reserve for the host. Consequently, nutritional symbiosis reduces the possible seasonal resource fluctuations experienced by the host. This is a novel hypothesis that stems from differences in the parameterization of the DEB model for the thyasirid species (Chapter 3), and that has implications for the populations inhabiting a highly seasonal environment (Chapter 4). The novelty of these findings means that there is limited supporting evidence in other biological systems. For instance, that the symbionts can serve as the main energy reserve was only recently described in the marine flatworm *Paracatenula* (Jäckle et al., 2019). Individuals of *Paracatenula* are obligate hosts of the chemoautotrophic bacteria *Candidatus* Riegeria, as they lack both mouth and gut. In this species, the bacterial symbiont occupies half of the hosts' biomass and stocks up and maintains carbon and energy in the form of sugars. The symbiont then provisions its host through outer-membrane vesicle secretion, and the host rarely digests the symbionts. This nutrient translocation strategy is also unique among most chemoautotrophic symbioses, where symbiont cell digestion drives nutrient transfer (as in the thyasirids). Hence, further research should focus on determining whether this strategy occurs in other trophic symbioses. As symbiosis is a ubiquitous strategy in nature, additional evidence supporting this finding could potentially change our understanding of community and ecosystem functioning.

5.5 CONCLUSIONS

Ecological dynamics can be very complex and highly dependent on multiple forcing variables and initial conditions. In this context, the individual can be considered the fundamental level of biological function because, through their abiotic and biotic interactions, individuals contribute to the higher hierarchical levels and determine population, community and ecosystem dynamics. As such, individual dynamics are necessary to predict the emergent processes of higher levels of organization. In this thesis, I have shown that a bottom-up approach focused on the individual can be used to predict the major features of population dynamics and broader trait patterns. The results presented in this dissertation contribute to understanding the consequences of a seasonal environment on individuals.

Beyond the ecogeographical rules and symbiosis in thyasirid bivalves, in this thesis, I have revealed how resource availability can contribute to individual dynamics, being sufficient to promote individual flexibility and possibly driving the evolution of strategies that confer an advantage for resource acquisition. Moreover, these results suggest that ecosystem function may depend on nutrient dynamics that constrain energy acquisition, fostering the evolution of interactions between organisms to acquire nutrients more efficiently. These findings are based on the explicit consideration of individual energetics and how the individual's ability to acquire energy can connect life-history strategies to higher levels of organization. In this sense, focusing on individual energetics and its interaction with the resource, we can summarize relevant ecological features, simplify the complexity, and improve our forecasting ability. Thus, the methods and results presented in this thesis are a first step towards answering issues that can include more complex interspecific interactions and environmental change.

REFERENCES

Abramoff, M., Magalhaes, P., & Ram, S. (2004). Image processing with ImageJ. *Biophotonics International*, *11*, 36–42.

Ackermann, M., & Doebeli, M. (2004). Evolution of niche width and adaptive diversification. *Evolution*, *58*(12), 2599–2612.

Agrawal, A. A. (2001). Phenotypic plasticity in the interactions and evolution of species. *Science*, *294*(5541), 321–326.

Allen, J. A. (1958). On the basic form and adaptations to habitat in the Lucinacea (Eulamellibranchia). *Philosophical Transactions of the Royal Society of London. Series B, Biological Sciences*, *241*(684), 421–484.

AmP. (2017). Tridacna gigas*, version 2017/08/07*. Retrieved from http://www.bio.vu.nl/thb/deb/deblab/add_my_pet/entries_web/Tridacna_gigas/Tridacna_gigas_res.html

AmP. (2018). *Online database of DEB parameters, implied properties and referenced underlying data*. Retrieved January 15, 2018, from bio.vu.nl/thb/deb/deblab/add_my_pet

AmP. (2020). Online database of DEB parameters, implied properties and referenced underlying data. Retrieved March 30, 2020, from bio.vu.nl/thb/deb/deblab/add_my_pet/

AmPtool. (2020). AmPtool: Functions for the visualisation and analysis of patterns in (functions of) parameter values of the Add-my-Pet (AmP) collection. Retrieved March 30, 2020, from https://add-my-pet.github.io/AmPtool/docs/index.html

Arendt, J. D. (2011). Size-fecundity relationships, growth trajectories, and the temperature-size rule for ectotherms. *Evolution*, *65*(1), 43–51.

Arlettaz, R., Christe, P., & Schaub, M. (2017). Food availability as a major driver in the evolution of life-history strategies of sibling species. *Ecology and Evolution*, *7*(12), 4163–4172. doi:10.1002/ece3.2909

Ashmole, N. P. (1963). The regulation of numbers of tropical oceanic birds. *Ibis*, *103*(3), 458–473. doi:10.1111/j.1474-919X.1963.tb06766.x

Ashton, K. G. (2002). Patterns of within-species body size variation of birds: Strong evidence for Bergmann's rule. *Global Ecology and Biogeography*, *11*(6), 505–523. doi:10.1046/j.1466-822X.2002.00313.x

Ashton, K. G., Tracy, M. C., & de Queiroz, A. (2000). Is Bergmann's rule valid for mammals? *The American Naturalist*, *156*(4), 390–415.

Attisano, A., Thiel, F., Sato, N., Okahisa, Y., Bolopo, D., Tanaka, K. D., ... Theuerkauf, J. (2019). Breeding biology of the Fan-tailed Gerygone *Gerygone flavolateralis* in relation to parasitism by the Shining Bronze-cuckoo *Chalcites lucidus*. *Journal of Ornithology*, *160*(1), 91–103. doi:10.1007/s10336-018-1592-6

Augustine, S. (2017). Maturity as quantifier for physiological time. *Physics of Life Reviews*, *20*, 40–42. doi:10.1016/j.plrev.2017.01.009

Augustine, S., Lika, K., & Kooijman, S. A. L. M. (2019). Altricial-precocial spectra in animal kingdom. *Journal of Sea Research*, *143*, 27–34.

Ballesta-Artero, I., Augustine, S., Witbaard, R., Carroll, M. L., Mette, M. J., Alan, D. W., & van der Meer, J. (2019). Energetics of the extremely long-living bivalve *Arctica islandica* based on a Dynamic Energy Budget model. *Journal of sea research*, *143*, 173–182.

Bastolla, U., Fortuna, M. A., Pascual-Garcıa, A., Ferrera, A., Luque, B., & Bascompte, J. (2009). The architecture of mutualistic networks minimizes competition and increases biodiversity. *Nature*, *458*(7241), 1018–1020.

Batstone, R. T., & Dufour, S. C. (2016). Closely related thyasirid bivalves associate with multiple symbiont phylotypes. *Marine Ecology*, *37*(5), 988–997.

Batstone, R. T., Laurich, J. R., Salvo, F., & Dufour, S. C. (2014). Divergent chemosymbiosis-related characters in *Thyasira* cf. *gouldi* (Bivalvia: Thyasiridae). *PLoS ONE*, *9*(3), 1–9. doi:10.1371/journal.pone.0092856

Battley, P. F., & Piersma, T. (2005). Adaptive interplay between feeding ecology and features of the digestive tract in birds. In J. M. Starck & T. Wang (Eds.), *Physiological and Ecological Adaptations to Feeding in Vertebrates* (pp. 202–228). OCLC: 51992588. Enfield, New Hampshire: Science Publishers.

Bell, G., & Reboud, X. (1997). Experimental evolution in *Chlamydomonas* II. Genetic variation in strongly contrasted environments. *Heredity*, *78*(5), 498–506.

Bjorndal, K. A., Schroeder, B. A., Foley, A. M., Witherington, B. E., Bresette, M., Clark, D., … Meylan, A. B., et al. (2013). Temporal, spatial, and body size effects on growth rates of loggerhead sea turtles (*Caretta caretta*) in the northwest atlantic. *Marine Biology*, *160*(10), 2711–2721.

Blackburn, T. M., Gaston, K. J., & Loder, N. (1999). Geographic gradients in body size: A clarification of Bergmann's rule. *Diversity and Distributions*, *5*(4), 165–174. doi:https://doi.org/10.1046/j.1472-4642.1999.00046.x

Blackburn, T. M., & Hawkins, B. A. (2004). Bergmann's rule and the mammal fauna of northern North America. *Ecography*, *27*(6), 715–724. doi:10.1111/j.0906-7590.2004.03999.x

Blacknell, W. M. (1973). *Aspects of the biology of* Thyasira gouldi *(Philippi) and its copepod parasite* Axinophilus thyasirae *(Bresciani and Ockelmann)* (PhD, University of Stirling).

Blacknell, W. M., & Ansell, A. D. (1974). The direct development of Bivalve Thyasira gouldi (Phillipi). *Thallasia Jugoslavica*, *10*(1/2), 23–43.

Blueweiss, L., Fox, H., Kudzma, V., Nakashima, D., Peters, R., & Sams, S. (1978). Relationships between body size and some life history parameters. *Oecologia*, *37*(2), 257–272.

Bosch, T. C., & McFall-Ngai, M. J. (2011). Metaorganisms as the new frontier. *Zoology*, *114*(4), 185–190.

Boyer, A. G., Cartron, J.-L. E., & Brown, J. H. (2010). Interspecific pairwise relationships among body size, clutch size and latitude: Deconstructing a macroecological triangle in birds. *Journal of Biogeography*, *37*(1), 47–56. doi:10.1111/j.1365-2699.2009.02175.x

Boyer, A. G., & Jetz, W. (2010). Biogeography of body size in Pacific island birds. *Ecography*, *33*(2), 369–379. doi:10.1111/j.1600-0587.2010.06315.x

Brommer, J. E. (2013). Phenotypic plasticity of labile traits in the wild. *Current Zoology*, *59*(4), 485–505.

Brown, J. H., Gillooly, J. F., Allen, A. P., Savage, V. M., & West, G. B. (2004). Toward a Metabolic Theory of Ecology. *Ecology*, *85*(7), 1771–1789.

Brown, J. H., Marquet, P. A., & Taper, M. L. (1993). Evolution of body size: Consequences of an energetic definition of fitness. *The American Naturalist*, *142*(4), 573–584. doi:10.1086/285558

Bryant, D. M., & Hails, C. J. (1983). Energetics and growth patterns of three tropical bird species. *The Auk*, *100*(2), 425–439. doi:10.1093/auk/100.2.425

Cabral, J. S., Valente, L., & Hartig, F. (2017). Mechanistic simulation models in macroecology and biogeography: State-of-art and prospects. *Ecography*, *40*(2), 267–280. doi:10.1111/ecog.02480

Capellini, I., Baker, J., Allen, W. L., Street, S. E., & Venditti, C. (2015). The role of life history traits in mammalian invasion success. *Ecology Letters*, *18*(10), 1099–1107. doi:https://doi.org/10.1111/ele.12493

Cardilini, A. P. A., Buchanan, K. L., Sherman, C. D. H., Cassey, P., & Symonds, M. R. E. (2016). Tests of ecogeographical relationships in a non-native species: What rules avian morphology? *Oecologia*, *181*(3), 783–793. doi:10.1007/s00442-016-3590-9

Cardillo, M. (2002). The life-history basis of latitudinal diversity gradients: How do species traits vary from the poles to the equator? *Journal of Animal Ecology*, *71*(1), 79–87. doi:10.1046/j.0021-8790.2001.00577.x

Cardoso, J. F. M. F., Witte, J. I. J., & van der Veer, H. W. (2006). Intra- and interspecies comparison of energy flow in bivalve species in Dutch coastal waters by means of the Dynamic Energy Budget (DEB) theory. *Journal of Sea Research*, *56*(2), 182–197. doi:10.1016/j.seares.2006.03.011

Carpenter, S. R., Kitchell, J. F., & Hodgson, J. R. (1985). Cascading trophic interactions and lake productivity. *BioScience*, *35*(10), 634–639.

Caswell, H. (1983). Phenotypic plasticity in life-history traits: Demographic effects and evolutionary consequences. *American Zoologist*, *23*(1), 35–46.

Cavanaugh, C. M., Mckiness, Z. P., Newton, I. L., & Stewart, F. J. (2006). Marine chemosynthetic symbioses. *Prokaryotes*, *1*, 545–577. doi:10.1007/978-3-642-30194-0

Chamberlain, S. A., Bronstein, J. L., & Rudgers, J. A. (2014). How context dependent are species interactions? *Ecology Letters*, *17*(7), 881–890. doi:https://doi.org/10.1111/ele.12279

Chase, J. M. (2011). Ecological niche theory. In S. M. Scheiner & M. R. Willig (Eds.), *The theory of ecology* (pp. 93–107). University of Chicago Press Chicago.

Chesson, P. (2000). Mechanisms of maintenance of species diversity. *Annual review of Ecology and Systematics*, *31*(1), 343–366.

Clark, J. S., Bell, D. M., Hersh, M. H., Kwit, M. C., Moran, E., Salk, C., … Zhu, K. (2011). Individual-scale variation, species-scale differences: Inference needed to understand diversity. *Ecology Letters*, *14*(12), 1273–1287.

Clausen, J., Keck, D. D., Hiesey, W. M., et al. (1948). Experimental studies on the nature of species. iii. environresponses of climatic races of *Achillea*. *Experimental studies on the nature of species. III. Environresponses of climatic races of* Achillea. (Publ. No. 581).

Clauss, M., Dittmann, M. T., Müller, D. W. H., Meloro, C., & Codron, D. (2013). Bergmann′s rule in mammals: A cross-species interspecific pattern. *Oikos*, *122*(10), 1465–1472. doi:https://doi.org/10.1111/j.1600-0706.2013.00463.x

Cody, M. L. (1966). A general theory of clutch size. *Evolution*, *20*, 174–184.

Cox, W. A., & Martin, T. E. (2009). Breeding Biology of the Three-Striped Warbler in Venezuela: A Contrast between Tropical and Temperate Parulids. *The Wilson Journal of Ornithology*, *121*(4), 667–678. doi:10.1676/08-133.1

Dalby, L., McGill, B. J., Fox, A. D., & Svenning, J.-C. (2014). Seasonality drives global-scale diversity patterns in waterfowl (Anseriformes) via temporal niche exploitation. *Global Ecology and Biogeography*, *23*(5), 550–562.

Dando, P. R., & Southward, A. J. (1986). Chemoautotrophy in bivalve molluscs of the genus *Thyasira*. *Journal of the Marine Biological Association of the UK*, *66*, 915–929.

Dando, P. R., Southward, A. J., & Southward, E. C. (2004). Rates of sediment sulphide oxidation by the bivalve mollusc *Thyasira sarsi*. *Marine Ecology Progress Series*, *280*, 181–187. ISBN: 0171-8630. doi:10.3354/meps280181

Dando, P. R., & Spiro, B. (1993). Varying nutritional dependence of the thyasirid bivalves *Thyasira sarsi* and *T. equalis* on chemoautotrophic symbiotic bacteria, demonstrated by isotope ratios of tissue carbon and shell carbonate. *Marine Ecology Progress Series*, *92*(1-2), 151–158. doi:10.3354/meps092151

Darling, E. S., Alvarez-Filip, L., Oliver, T. A., McClanahan, T. R., & Côté, I. M. (2012). Evaluating life-history strategies of reef corals from species traits. *Ecology Letters*, *15*(12), 1378–1386. doi:10.1111/j.1461-0248.2012.01861.x

Dawidowicz, P., & Loose, C. J. (1992). Cost of swimming by *Daphnia* during diel vertical migration. *Limnology and Oceanography*, *37*(3), 665–669.

de Bary, A. (1879). *Die Erscheinung der Symbiose: Vortrag gehalten auf der Versammlung Deutscher Naturforscher und Aerzte zu Cassel*. Trübner.

de Roos, A. M., Galic, N., & Heesterbeek, H. (2009). How resource competition shapes individual life history for nonplastic growth: Ungulates in seasonal food environments. *Ecology*, *90*(4), 945–960.

de Roos, A. M., & Persson, L. (2001). Physiologically structured models–from versatile technique to ecological theory. *Oikos*, *94*(1), 51–71.

de Roos, A. M., & Persson, L. (2002). Size-dependent life-history traits promote catastrophic collapses of top predators. *Proceedings of the National Academy of Sciences*, *99*(20), 12907–12912.

de Roos, A. M., & Persson, L. (2003). Competition in size-structured populations: Mechanisms inducing cohort formation and population cycles. *Theoretical population biology*, *63*(1), 1–16.

de Roos, A. M., Schellekens, T., Van Kooten, T., & Persson, L. (2008). Stage-specific predator species help each other to persist while competing for a single prey. *Proceedings of the National Academy of Sciences*, *105*(37), 13930–13935.

Distel, D. L. (1998). Evolution of chemoautotrophic endosymbioses in bivalves: Bivalve-bacteria chemosymbioses are phylogenetically diverse but morphologically similar. *BioScience*, *48*(4), 277–286.

Doughty, P., & Reznick, D. N. (2004). Patterns and analysis of adaptive phenotypic plasticity in animals. In T. J. DeWitt & S. M. Scheiner (Eds.), *Phenotypic plasticity: Functional and conceptual approaches* (pp. 126–150). Oxford University Press New York.

Downing, W. L., & Downing, J. A. (1993). Molluscan shell growth and loss. *Nature*, *362*(6420), 506–506. doi:10.1038/362506a0

Dubilier, N., Bergin, C., & Lott, C. (2008). Symbiotic diversity in marine animals: The art of harnessing chemosynthesis. *Nature reviews. Microbiology*, *6*(10), 725–740. doi:10.1038/nrmicro1992

Dufour, S. C. (2005). Gill anatomy and the evolution of symbiosis in the bivalve family Thyasiridae. *Biological Bulletin*, *208*(3), 200–212. ISBN: 0006-3185.

Dufour, S. C. (2017). No Title. *Personal Communication*.

Dufour, S. C., & Felbeck, H. (2003). Sulphide mining by the superextensile foot of symbiotic thyasirid bivalves. *Nature*, *426*, 65–67. doi:10.1029/2000JB000090

Dufour, S. C., & Felbeck, H. (2006). Symbiont abundance in thyasirids (Bivalvia) is related to particulate food and sulphide availability. *Marine Ecology Progress Series*, *320*, 185–194. doi:10.3354/meps320185

Dufour, S. C., Laurich, J. R., Batstone, R. T., McCuaig, B., Elliott, A., & Poduska, K. M. (2014). Magnetosome-containing bacteria living as symbionts of bivalves. *The ISME journal*, *8*(12), 2453–62. doi:10.1038/ismej.2014.93

Duperron, S., Gaudron, S. M., Rodrigues, C. F., Cunha, M. R., Decker, C., & Olu, K. (2013). An overview of chemosynthetic symbioses in bivalves from the North Atlantic and Mediterranean Sea. *Biogeosciences*, *10*(5), 3241–3267. ISBN: 1726-4170. doi:10.5194/bg-10-3241-2013

Duperron, S., Quiles, A., Szafranski, K. M., Léger, N., & Shillito, B. (2016). Estimating symbiont abundances and gill surface areas in specimens of the hydrothermal vent mussel *Bathymodiolus puteoserpentis* maintained in pressure vessels. *Frontiers in Marine Science*, *3*, 16. doi:10.3389/fmars.2016.00016

Evans, K. L., Duncan, R. P., Blackburn, T. M., & Crick, H. Q. P. (2005). Investigating geographic variation in clutch size using a natural experiment. *Functional Ecology*, *19*(4), 616–624. doi:10.1111/j.1365-2435.2005.01016.x

Fabricius, K. E., Genin, A., & Benayahu, Y. (1995). Flow-dependent herbivory and growth in zooxanthellae-free soft corals. *Limnology and Oceanography*, *40*(7), 1290–1301.

Ferrier-Pagès, C., Reynaud, S., Béraud, E., Rottier, C., Menu, D., Duong, G., & Gévaert, F. (2015). Photophysiology and daily primary production of a temperate symbiotic gorgonian. *Photosynthesis Research*, *123*(1), 95–104.

Fischer, K., Brakefield, P. M., & Zwaan, B. J. (2003). Plasticity in butterfly egg size: Why larger offspring at lower temperatures? *Ecology*, *84*(12), 3138–3147.

Folke, C., Carpenter, S., Walker, B., Scheffer, M., Elmqvist, T., Gunderson, L., & Holling, C. (2004). Regime Shifts, Resilience, and Biodiversity in Ecosystem Management. *Annual Review of Ecology, Evolution, and Systematics*, *35*(1), 557–581. doi:10.1146/annurev.ecolsys.35.021103.105711

Folke, C., Edwards, M., Conversi, A., & Mo, C. (2015). Marine regime shifts around the globe: Theory, drivers and impacts. *Philosophical Transactions of the Royal Society B: Biological Sciences*, *370*.

Forsman, A. (2015). Rethinking phenotypic plasticity and its consequences for individuals, populations and species. *Heredity*, *115*(4), 276–284.

Freckleton, R. P., Harvey, P. H., & Pagel, M. (2003). Bergmann's rule and body size in mammals. *The American Naturalist*, *161*(5), 821–825. doi:10.1086/374346

Freitas, V., Cardoso, J. F. M. F., Lika, K., Peck, M. A., Campos, J., Kooijman, S. A. L. M., & Van der Veer, H. W. (2010). Temperature tolerance and energetics: A dynamic energy budget-based comparison of North Atlantic marine species. *Philosophical Transactions of the Royal Society B: Biological Sciences*, *365*(1557), 3553–3565. doi:10.1098/rstb.2010.0049

Freitas, V., Cardoso, J. F. M. F., Santos, S., Campos, J., Drent, J., Saraiva, S., … Van der Veer, H. W. (2009). Reconstruction of food conditions for Northeast Atlantic bivalve species based on Dynamic Energy Budgets. *Journal of Sea Research*, *62*(2-3), 75–82. doi:10.1016/j.seares.2009.07.004

Futuyma, D. J., & Kirkpatrick, M. (2005). Evolution. Sinauer Associates, Sunderland, MA.

Futuyma, D. J., & Moreno, G. (1988). The evolution of ecological specialization. *Annual Review of Ecology and Systematics*, *19*(1), 207–233.

Gaston, K. J., Chown, S. L., & Evans, K. L. (2008). Ecogeographical rules: Elements of a synthesis. *Journal of Biogeography*, *35*(3), 483–500. doi:10.1111/j.1365-2699.2007.01772.x

Gebhardt, M. D., & Stearns, S. C. (1988). Reaction norms for developmental time and weight at eclosion in *Drosophila mercatorum*. *Journal of Evolutionary Biology*, *1*(4), 335–354.

Geist, V. (1987). Bergmann's rule is invalid. *Canadian Journal of Zoology*, *65*(4), 1035–1038. doi:10.1139/z87-164

Genoud, M. (1988). Energetic strategies of shrews: Ecological constraints and evolutionary implications. *Mammal Review*, *18*(4), 173–193. doi:10.1111/j.1365-2907.1988.tb00083.x

George, S. B. (1994). Population differences in maternal size and offspring quality for *Leptasterias epichlora* (Brandt) (Echinodermata: Asteroidea). *Journal of Experimental Marine Biology and Ecology*, *175*(1), 121–131.

Giebelhausen, B., & Lampert, W. (2001). Temperature reaction norms of *Daphnia magna*: The effect of food concentration. *Freshwater Biology*, *46*(3), 281–289.

Gilbert, S. F., Bosch, T. C., & Ledón-Rettig, C. (2015). Eco-evo-devo: Developmental symbiosis and developmental plasticity as evolutionary agents. *Nature Reviews Genetics*, *16*(10), 611–622.

Gill, B. J. (1982). Breeding of the grey warbler *Gerygone igata* at Kaikoura, New Zealand. *Ibis*, *124*(2), 123–147. doi:10.1111/j.1474-919X.1982.tb03752.x

Giolland, M., & Dufour, S. C. (2015). Identification de bivalves de la famille des Thyasiridés formant un complexe d'espèces cryptiques dans un fjord de Terre-Neuve (Canada). *Unpublished*.

Glazier, D. S. (2005). Beyond the '3/4-power law': Variation in the intra-and interspecific scaling of metabolic rate in animals. *Biological reviews*, *80*(4), 611–662.

Goetsch, W. (1924). Die symbiose der süsswasser-hydroiden und ihre künstliche beeinflussung. *Zeitschrift für Morphologie und Ökologie der Tiere*, *1*(4), 660–751.

Gohli, J., & Voje, K. L. (2016). An interspecific assessment of Bergmann's rule in 22 mammalian families. *BMC Evolutionary Biology*, *16*(1), 222. doi:10.1186/s12862-016-0778-x

Gori, A., Viladrich, N., Gili, J. M., Kotta, M., Cucio, C., Magni, L., … Rossi, S. (2012). Reproductive cycle and trophic ecology in deep versus shallow populations of the Mediterranean gorgonian *Eunicella singularis* (Cap de Creus, northwestern Mediterranean Sea). *Coral Reefs*, *31*(3), 823–837.

Gosling, E. (2015). *Marine Bivalve Molluscs* (2nd). doi:10.1002/9781119045212

Goss, L. B., & Bunting, D. L. (1983). *Daphnia* development and reproduction: Responses to temperature. *Journal of Thermal Biology*, *8*(4), 375–380.

Griebeler, E. M., & Böhning-Gaese, K. (2004). Evolution of clutch size along latitudinal gradients: Revisiting Ashmole's hypothesis. *Evolutionary Ecology Research*, *6*, 679–694.

Grimm, V., Ayllón, D., & Railsback, S. F. (2017). Next-Generation Individual-Based Models integrate biodiversity and ecosystems: yes we can, and yes we must. *Ecosystems*, *20*(2), 229–236. doi:10.1007/s10021-016-0071-2

Grimm, V., & Railsback, S. F. (2005). *Individual-based Modeling and Ecology*. Princeton University Press.

Grottoli, A. G., Rodrigues, L. J., & Palardy, J. E. (2006). Heterotrophic plasticity and resilience in bleached corals. *Nature*, *440*(7088), 1186–1189.

Hairston, N. G., Smith, F. E., & Slobodkin, L. B. (1960). Community Structure, Population Control, and Competition. *The American Naturalist*, *94*(879), 421. doi:10.1086/282146

Halliday, F. W., Umbanhowar, J., & Mitchell, C. E. (2017). Interactions among symbionts operate across scales to influence parasite epidemics. *Ecology Letters*, *20*(10), 1285–1294. doi:10.1111/ele.12825

Hay, M. E., Parker, J. D., Burkepile, D. E., Caudill, C. C., Wilson, A. E., Hallinan, Z. P., & Chequer, A. D. (2004). Mutualisms and aquatic community structure: the enemy of my enemy is my friend. *Annual Review of Ecology, Evolution, and Systematics*, *35*(1), 175–197. doi:10.1146/annurev.ecolsys.34.011802.132357

Healy, K., Ezard, T. H. G., Jones, O. R., Salguero-Gómez, R., & Buckley, Y. M. (2019). Animal life history is shaped by the pace of life and the distribution of age-specific mortality and reproduction. *Nature Ecology & Evolution*, *3*(8), 1217–1224. doi:10.1038/s41559-019-0938-7

Hendry, A. P. (2016). Key questions on the role of phenotypic plasticity in eco-evolutionary dynamics. *Journal of Heredity*, *107*(1), 25–41.

Hersteinsson, P., Yom-Tov, Y., & Geffen, E. (2009). Effect of Sub-Polar Gyre, North Atlantic Oscillation and ambient temperature on size and abundance in the Icelandic Arctic fox. *Global Change Biology*, *15*(6), 1423–1433. doi:10.1111/j.1365-2486.2008.01765.x

Hurlbert, A. H., & Haskell, J. P. (2003). The effect of energy and seasonality on avian species richness and community composition. *The American Naturalist*, *161*(1), 83–97.

Huston, M. A., DeAngelis, D., & Post, W. (1988). New computer models unify ecological theory: Computer simulations show that many ecological patterns can be explained by interactions among individual organisms. *BioScience*, *38*(10), 682–691.

Huston, M. A., & Wolverton, S. (2011). Regulation of animal size by eNPP, Bergmann's rule, and related phenomena. *Ecological Monographs*, *81*(3), 349–405. doi:10.1890/10-1523.1

Iverson, J. B., Balgooyen, C. P., Byrd, K. K., & Lyddan, K. K. (1993). Latitudinal variation in egg and clutch size in turtles. *Canadian Journal of Zoology*, *71*(12), 2448–2461. doi:10.1139/z93-341

Jäckle, O., Seah, B. K., Tietjen, M., Leisch, N., Liebeke, M., Kleiner, M., … Gruber-Vodicka, H. R. (2019). Chemosynthetic symbiont with a drastically reduced genome serves as primary energy storage in the marine flatworm *Paracatenula*. *Proceedings of the National Academy of Sciences*, *116*(17), 8505–8514.

James, C. D., & Whitford, W. G. (1994). An experimental study of phenotypic plasticity in the clutch size of a lizard. *Oikos*, 49–56.

Jetz, W., Sekercioglu, C. H., & Böhning-Gaese, K. (2008). The worldwide variation in avian clutch size across species and space. *PLoS Biology*, *6*(12), e303. doi:10.1371/journal.pbio.0060303

Jimenez, A. G., Cooper-Mullin, C., Calhoon, E. A., & Williams, J. B. (2014). Physiological underpinnings associated with differences in pace of life and metabolic rate in north temperate and neotropical birds. *Journal of Comparative Physiology B*, *184*(5), 545–561. doi:10.1007/s00360-014-0825-0

Jones, O. R., Scheuerlein, A., Salguero-Gómez, R., Camarda, C. G., Schaible, R., Casper, B. B., … Vaupel, J. W. (2014). Diversity of ageing across the tree of life. *Nature*, *505*(7482), 169–173. doi:10.1038/nature12789

Jusup, M., Sousa, T., Domingos, T., Labinac, V., Marn, N., Wang, Z., & Klanjšček, T. (2017). Physics of metabolic organization. *Physics of Life Reviews*, *20*, 1–39. doi:10.1016/j.plrev.2016.09.001

Karakashian, S. J. (1963). Growth of *Paramecium bursaria* as influenced by the presence of algal symbionts. *Physiological Zoology*, *36*(1), 52–68.

Kassen, R. (2002). The experimental evolution of specialists, generalists, and the maintenance of diversity. *Journal of Evolutionary Biology*, *15*(2), 173–190.

Kassen, R., & Bell, G. (1998). Experimental evolution in *Chlamydomonas*. IV. Selection in environments that vary through time at different scales. *Heredity*, *80*(6), 732–741.

Kearney, M. R. (2021). What is the status of metabolic theory one century after pütter invented the von Bertalanffy growth curve? *Biological Reviews*, *96*(2), 557–575. doi:10.1111/brv.12668

Kearney, M. R., & White, C. R. (2012). Testing metabolic theories. *The American Naturalist*, *180*(5), 546–565.

Keast, A., & Recher, H. F. (1997). The Adaptive Zone of the Genus *Gerygone* (Acanthizidae) as Shown by Morphology and Feeding Habits. *Emu - Austral Ornithology*, *97*(1), 1–17. doi:10.1071/MU97001

King, P., Milicich, L., & Burns, K. C. (2011). Body size determines rates of seed dispersal by giant king crickets. *Population Ecology*, *53*(1), 73–80.

Kiørboe, T. (2011). How zooplankton feed: Mechanisms, traits and trade-offs. *Biological reviews*, *86*(2), 311–339.

Kiørboe, T., & Hirst, A. G. (2014). Shifts in mass scaling of respiration, feeding, and growth rates across life-form transitions in marine pelagic organisms. *The American Naturalist*, *183*(4), E118–E130.

Kivelä, S. M., Välimäki, P., & Gotthard, K. (2013). Seasonality maintains alternative life-history phenotypes. *Evolution*, *67*(11), 3145–3160.

Klingenberg, C. P., & Spence, J. (1997). On the role of body size for life history evolution. *Ecological Entomology*, *22*(1), 55–68. doi:10.1046/j.1365-2311.1997.00031.x

Kooi, B. W., & Troost, T. A. (2006). Advantage of storage in a fluctuating environment. *Theoretical Population Biology*, *70*(4), 527–541. doi:10.1016/j.tpb.2006.07.005

Kooijman, S. A. L. M. (1988). The von Bertalanffy growth rate as a function of physiological parameters; a comparative analysis. In T. G. Hallam, L. J. Gross, & S. A. Levin (Eds.), *Mathematical ecology.* (pp. 3–45). World Scientific, Singapore.

Kooijman, S. A. L. M. (2010). *Dynamic Energy Budget theory for metabolic organisation* (3rd). doi:10.1098/rstb.2010.0167

Kooijman, S. A. L. M. (2013). Waste to hurry: Dynamic energy budgets explain the need of wasting to fully exploit blooming resources. *Oikos*, *122*(3), 348–357. doi:10.1111/j.1600-0706.2012.00098.x

Kooijman, S. A. L. M. (2014). Metabolic acceleration in animal ontogeny: An evolutionary perspective. *Journal of Sea Research*, *94*, 128–137. doi:10.1016/j.seares.2014.06.005

Kooijman, S. A. L. M., & Lika, K. (2014). Comparative energetics of the 5 fish classes on the basis of dynamic energy budgets. *Journal of Sea Research*, *94*, 19–28. doi:10.1016/j.seares.2014.01.015

Kozłowski, J., Konarzewski, M., & Czarnoleski, M. (2020). Coevolution of body size and metabolic rate in vertebrates: A life history perspective. *Biological Reviews*, *95*(5), 1393–1417. doi:10.1111/brv.12615

Kulesza, G. (1990). An analysis of clutch-size in New World passerine birds. *Ibis*, *132*(3), 407–422. doi:10.1111/j.1474-919X.1990.tb01059.x

Lack, D. (1947). The significance of clutch-size. *Ibis*, *89*(2), 302–352. doi:https://doi.org/10.1111/j.1474-919X.1947.tb04155.x

Lafuente, E., & Beldade, P. (2019). Genomics of developmental plasticity in animals. *Frontiers in genetics*, *10*, 720.

Lampert, W., & Trubetskova, I. (1996). Juvenile growth rate as a measure of fitness in *Daphnia*. *Functional Ecology*, 631–635.

Laurich, J. R., Batstone, R. T., & Dufour, S. C. (2015). Temporal variation in chemoautotrophic symbiont abundance in the thyasirid bivalve *Thyasira* cf. *gouldi*. *Marine Biology*, *162*(10), 2017–2028. doi:10.1007/s00227-015-2727-4

Levins, R. (1968). *Evolution in changing environments: Some theoretical explorations*. Princeton University Press.

Lewontin, R., & Levins, R. (2007a). False dichotomies. In *Biology under the influence: Dialectical essays on the coevolution of nature and society* (pp. 23–26). NYU Press.

Lewontin, R., & Levins, R. (2007b). Strategies of abstraction. In *Biology under the influence: Dialectical essays on the coevolution of nature and society* (pp. 149–166). NYU Press.

Lika, K., Augustine, S., & Kooijman, S. A. L. M. (2019). Body size as emergent property of metabolism. *Journal of Sea Research*, *143*, 8–17.

Lika, K., Augustine, S., Pecquerie, L., & Kooijman, S. A. L. M. (2014). The bijection from data to parameter space with the standard DEB model quantifies the supply-demand spectrum. *Journal of Theoretical Biology*, *354*, 35–47. doi:10.1016/j.jtbi.2014.03.025

Lika, K., Kearney, M. R., Freitas, V., van der Veer, H. W., van der Meer, J., Wijsman, J. W. M., … Kooijman, S. A. L. M. (2011a). The "covariation method" for estimating the parameters of the standard Dynamic Energy Budget model I: Philosophy and approach. *Journal of Sea Research*, *66*(4), 270–277. doi:10.1016/j.seares.2011.07.010

Lika, K., Kearney, M. R., & Kooijman, S. A. L. M. (2011b). The "covariation method" for estimating the parameters of the standard Dynamic Energy Budget model II: Properties and preliminary patterns. *Journal of Sea Research*, *66*(4), 278–288. doi:10.1016/j.seares.2011.09.004

Lika, K., & Kooijman, S. A. L. M. (2003). Life history implications of allocation to growth versus reproduction in dynamic energy budgets. *Bulletin of Mathematical Biology*, *65*(5), 809–834.

Litchman, E., Ohman, M. D., & Kiørboe, T. (2013). Trait-based approaches to zooplankton communities. *Journal of Plankton Research*, *35*(3), 473–484. doi:10.1093/plankt/fbt019

Lundblad, C. G., & Conway, C. J. (2021). Ashmole's hypothesis and the latitudinal gradient in clutch size. *Biological Reviews*, 000–000. doi:10.1111/brv.12705

Lynch, M. (1977). Fitness and optimal body size in zooplankton population. *Ecology*, 763–774.

Lynch, M., & Gabriel, W. (1987). Environmental tolerance. *The American Naturalist*, *129*(2), 283–303.

Madsen, T., & Shine, R. (1999). The adjustment of reproductive threshold to prey abundance in a capital breeder. *Journal of Animal Ecology*, *68*(3), 571–580.

Mariño, J., Augustine, S., Dufour, S. C., & Hurford, A. (2019). Dynamic Energy Budget theory predicts smaller energy reserves in thyasirid bivalves that harbour symbionts. *Journal of Sea Research*, *143*, 119–127. doi:10.1016/j.seares.2018.07.015

Marn, N., Jusup, M., Catteau, S., Kooijman, S. A. L. M., & Klanjšček, T. (2019). Comparative physiological energetics of mediterranean and north atlantic loggerhead turtles. *Journal of Sea Research*, *143*, 100–118.

Marques, G. M., Augustine, S., Lika, K., Pecquerie, L., Domingos, T., & Kooijman, S. A. L. M. (2018a). The AmP project: Comparing species on the basis of dynamic energy budget parameters. *PLOS Computational Biology*, *14*(5), e1006100. doi:10.1371/journal.pcbi.1006100

Marques, G. M., Lika, K., Augustine, S., Pecquerie, L. T., & Kooijman, S. A. L. M. (2018b). Fitting multiple models to multiple data. *Journal of Sea Research*. Retrieved from https://doi.org/10.1016/j.seares.2018.07.004

Martin, B. T., Jager, T., Nisbet, R. M., Preuss, T. G., & Grimm, V. (2013). Predicting population dynamics from the properties of individuals: A cross-level test of Dynamic Energy Budget theory. *The American Naturalist*, *181*(4), 506–519. doi:10.1086/669904

Martin, B. T., Zimmer, E. I., Grimm, V., & Jager, T. (2012). Dynamic Energy Budget theory meets individual-based modelling: A generic and accessible implementation. *Methods in Ecology and Evolution*, *3*(2), 445–449. doi:10.1111/j.2041-210X.2011.00168.x

Martin, T. E., Lloyd, P., Bosque, C., Barton, D. C., Biancucci, A. L., Cheng, Y.-R., & Ton, R. (2011). Growth rate variation among passerine species in tropical and temperate sites: An antagonistic interaction between parental food provisioning and nest predation risk. *Evolution*, *65*(6), 1607–1622. doi:10.1111/j.1558-5646.2011.01227.x

Mayr, E. (1956). Geographical character gradients and climatic adaptation. *Evolution*, *10*(1), 105–108.

McCauley, E., Murdoch, W. W., & Nisbet, R. M. (1990). Growth, reproduction, and mortality of *Daphnia pulex* Leydig: Life at fow food. *Functional Ecology*, *4*(4), 505. doi:10.2307/2389318

McCuaig, B., Liboiron, F., & Dufour, S. C. (2017). The bivalve *Thyasira* cf. *gouldi* hosts chemoautotrophic symbiont populations with strain level diversity. *PeerJ*, *5*, e3597.

McKillup, S. C., & Butler, A. J. (1979). Modification of egg production and packaging in response to food availability by *Nassarius pauperatus*. *Oecologia*, *43*(2), 221–231.

McNab, B. K. (2010). Geographic and temporal correlations of mammalian size reconsidered: A resource rule. *Oecologia*, *164*(1), 13–23. doi:10.1007/s00442-010-1621-5

McNamara, J. M., & Houston, A. I. (2008). Optimal annual routines: Behaviour in the context of physiology and ecology. *Philosophical Transactions of the Royal Society B: Biological Sciences*, *363*(1490), 301–319.

Medina, A. I., Martí, D. A., & Bidau, C. J. (2007). Subterranean rodents of the genus *Ctenomys* (Caviomorpha, Ctenomyidae) follow the converse to Bergmann's rule: Converse Bergmann's rule in Ctenomys. *Journal of Biogeography*, *34*(8), 1439–1454. doi:10.1111/j.1365-2699.2007.01708.x

Meiri, S. (2011). Bergmann's Rule – what's in a name? *Global Ecology and Biogeography*, *20*(1), 203–207. doi:https://doi.org/10.1111/j.1466-8238.2010.00577.x

Meiri, S., Avila, L., Bauer, A. M., Chapple, D. G., Das, I., Doan, T. M., … Roll, U. (2020). The global diversity and distribution of lizard clutch sizes. *Global Ecology and Biogeography*, *29*(9), 1515–1530. doi:10.1111/geb.13124

Meiri, S., & Dayan, T. (2003). On the validity of Bergmann's rule. *Journal of Biogeography*, *30*(3), 331–351. doi:https://doi.org/10.1046/j.1365-2699.2003.00837.x

Meiri, S., Dayan, T., & Simberloff, D. (2004). Carnivores, biases and Bergmann's rule. *Biological Journal of the Linnean Society*, *81*(4), 579–588. doi:10.1111/j.1095-8312.2004.00310.x

Mesquita, D. O., Costa, G. C., Colli, G. R., Costa, T. B., Shepard, D. B., Vitt, L. J., & Pianka, E. R. (2016). Life-history patterns of lizards of the world. *The American Naturalist*, *187*(6), 689–705. doi:10.1086/686055

Miller, T. E., & Rudgers, J. A. (2014). Niche differentiation in the dynamics of host-symbiont interactions: Symbiont prevalence as a coexistence problem. *The American Naturalist*, *183*(4), 506–518.

Millien, V., Lyons, S. K., Olson, L., Smith, F. A., Wilson, A. B., & Yom Tov, Y. (2006). Ecotypic variation in the context of global climate change: Revisiting the rules. *Ecology Letters*, *9*(7), 853–869. doi:https://doi.org/10.1111/j.1461-0248.2006.00928.x

Miner, B. G., Sultan, S. E., Morgan, S. G., Padilla, D. K., & Relyea, R. A. (2005). Ecological consequences of phenotypic plasticity. *Trends in ecology & evolution*, *20*(12), 685–692.

Morales-Castilla, I., Olalla-Tárraga, M. Á., Purvis, A., Hawkins, B. A., & Rodríguez, M. Á. (2012a). The imprint of Cenozoic migrations and evolutionary history on the biogeographic gradient of body size in New World mammals. *The American Naturalist*, *180*(2), 246–256. Publisher: The University of Chicago Press. doi:10.1086/666608

Morales-Castilla, I., Rodríguez, M. Á., & Hawkins, B. A. (2012b). Deep phylogeny, net primary productivity, and global body size gradient in birds. *Biological Journal of the Linnean Society*, *106*(4), 880–892. doi:10.1111/j.1095-8312.2012.01917.x

Moran, N. A. (2006). Symbiosis. *Current biology*, *16*(20), 866–871.

Moran, N. A., & Yun, Y. (2015). Experimental replacement of an obligate insect symbiont. *Proceedings of the National Academy of Sciences*, *112*(7), 2093–2096.

Moreau, R. E. (1944). Clutch-size: A comparative study, with special reference to african birds. *Ibis*, *86*(3), 286–347. doi:10.1111/j.1474-919X.1944.tb04093.x

Mueller, E. A., Wisnoski, N. I., Peralta, A. L., & Lennon, J. T. (2020). Microbial rescue effects: How microbiomes can save hosts from extinction. *Functional Ecology*, *34*(10), 2055–2064. doi:10.1111/1365-2435.13493

Muller, E. B., Kooijman, S. A. L. M., Edmunds, P. J., Doyle, F. J., & Nisbet, R. M. (2009). Dynamic energy budgets in syntrophic symbiotic relationships between heterotrophic hosts and photoautotrophic symbionts. *Journal of Theoretical Biology*, *259*(1), 44–57. ISBN: 0022-5193. doi:10.1016/j.jtbi.2009.03.004

Muller, E. B., & Nisbet, R. M. (2000). Survival and production in variable resource environments. *Bulletin of Mathematical Biology*, *62*(6), 1163–1189.

Muller, E. B., Nisbet, R. M., Kooijman, S. A. L. M., Elser, J. J., & McCauley, E. (2001). Stoichiometric food quality and herbivore dynamics. *Ecology Letters*, *4*(6), 519–529. doi:10.1046/j.1461-0248.2001.00240.x

Muscatine, L., & Lenhoff, H. M. (1965). Symbiosis of *Hydra* and algae. II. Effects of limited food and starvation on growth of symbiotic and aposymbiotic hydra. *The Biological Bulletin*, *129*(2), 316–328.

Nisbet, R. M., Jusup, M., Klanjscek, T., & Pecquerie, L. (2012). Integrating Dynamic Energy Budget (DEB) theory with traditional bioenergetic models. *The Journal of experimental biology*, *215*(6), 892–902. doi:10.1242/jeb.059675

Ockelmann, W. K. (1958). The zoology of east Greenland: Marine Lamellibranchiata. *Meddelelser om Grønland*, *18*, 1–256.

Olalla-Tárraga, M. Á. (2011). "Nullius in Bergmann" or the pluralistic approach to ecogeographical rules: A reply to Watt et al. (2010). *Oikos*, *120*(10), 1441–1444. doi:10.1111/j.1600-0706.2011.19319.x

Olalla-Tárraga, M. Á., Bini, L. M., Diniz-Filho, J. A. F., & Rodríguez, M. Á. (2010). Cross-species and assemblage-based approaches to Bergmann's rule and the biogeography of body size in *Plethodon* salamanders of eastern North America. *Ecography*, 33–46. doi:10.1111/j.1600-0587.2010.06244.x

Olalla-Tárraga, M. Á., & Rodríguez, M. Á. (2007). Energy and interspecific body size patterns of amphibian faunas in Europe and North America: Anurans follow Bergmann's rule, urodeles its converse. *Global Ecology and Biogeography*, *16*(5), 606–617. doi:10.1111/j.1466-8238.2007.00309.x

Olalla Tárraga, M. Á., Amado, T. F., Bini, L. M., Martínez, P. A., Morales Castilla, I., Torres Romero, E. J., & Villalobos, F. (2019). Biological traits, phylogeny and human footprint signatures on the geographical range size of passerines (Order *Passeriformes*) worldwide. *Global Ecology and Biogeography*, 1183–1194. doi:10.1111/geb.12924

Oliver, K. M., Degnan, P. H., Hunter, M. S., & Moran, N. A. (2009). Bacteriophages encode factors required for protection in a symbiotic mutualism. *Science*, *325*(5943), 992–994.

Olson, V. A., Davies, R. G., Orme, C. D. L., Thomas, G. H., Meiri, S., Blackburn, T. M., ... Bennett, P. M. (2009). Global biogeography and ecology of body size in birds. *Ecology Letters*, *12*(3), 249–259. doi:10.1111/j.1461-0248.2009.01281.x

Orcutt, J. D., & Porter, K. G. (1984). The synergistic effects of temperature and food concentration of life history parameters of *Daphnia*. *Oecologia*, *63*(3), 300–306.

Pacheco, M. A., Beissinger, S. R., & Bosque, C. (2010). Why grow slowly in a dangerous place? Postnatal growth, thermoregulation, and energetics of nestling Green-Rumped Parrotlets (*Forpus passerinus*). *The Auk*, *127*(3), 558–570. doi:10.1525/auk.2009.09190

Parmentier, E., & Michel, L. (2013). Boundary lines in symbiosis forms. *Symbiosis*, *60*(1), 1–5. doi:10.1007/s13199-013-0236-0

Pecquerie, L., & Lika, K. (2017). Is reproduction limiting growth?: Comment on "physics of metabolic organization" by Marko Jusup et al. *Physics of life reviews*, *20*, 75–77.

Piersma, T., & Van Gils, J. A. (2011). *The flexible phenotype: A body-centred integration of ecology, physiology, and behaviour*. Oxford University Press.

Pijpe, J., Brakefield, P. M., & Zwaan, B. J. (2007). Phenotypic plasticity of starvation resistance in the butterfly *Bicyclus anynana*. *Evolutionary Ecology*, *21*(5), 589–600.

Pile, A. J., & Young, C. M. (1999). Plankton availability and retention efficiencies of cold-seep symbiotic mussels. *Limnology and Oceanography*, *44*(7), 1833–1839.

Pincheira-Donoso, D. (2010). The balance between predictions and evidence and the search for universal macroecological patterns: Taking Bergmann's rule back to its endothermic origin. *Theory in Biosciences*, *129*(4), 247–253. doi:10.1007/s12064-010-0101-0

Piovano, S., Clusa, M., Carreras, C., Giacoma, C., Pascual, M., & Cardona, L. (2011). Different growth rates between loggerhead sea turtles (*Caretta caretta*) of Mediterranean and Atlantic origin in the Mediterranean Sea. *Marine Biology*, *158*(11), 2577–2587.

R Core Team. (2019). *R: A Language and Environment for Statistical Computing* (3.6.2). R Foundation for Statistical Computing. Retrieved from https://www.R-project.org/

Ramirez, L., Diniz-Filho, J. A. F., & Hawkins, B. A. (2008). Partitioning phylogenetic and adaptive components of the geographical body-size pattern of New World birds. *Global Ecology and Biogeography*, *17*, 100–110. doi:10.1111/j.1466-8238.2007.00346.x

Reboud, X., & Bell, G. (1997). Experimental evolution in *Chlamydomonas*. III. Evolution of specialist and generalist types in environments that vary in space and time. *Heredity*, *78*(5), 507–514.

Reid, R. B., McMahon, R., Foighil, D. Ó., & Finnigan, R. (1992). Anterior inhalant currents and pedal feeding in bivalves. *The Veliger*, *35*(2), 93–104.

Ricklefs, R. E. (1968). Patterns of growth in birds. *Ibis*, *110*(4), 419–451. doi:10.1111/j.1474-919X.1968.tb00058.x

Ricklefs, R. E. (1976). Growth rates of birds in the humid New World tropics. *Ibis*, *118*(2), 179–207. doi:10.1111/j.1474-919X.1976.tb03065.x

Ricklefs, R. E. (1980). Geographical variation in clutch size among passerine birds: Ashmole's hypothesis. *The Auk*, *97*(1), 38–49.

Ricklefs, R. E. (1996). Morphometry of the digestive tracts of some passerine birds. *The Condor*, *98*(2), 279–292. doi:10.2307/1369146

Ricklefs, R. E. (2000). Density dependence, evolutionary optimization, and the diversification of avian life histories. *The Condor*, *102*(1), 9–22.

Rodríguez, M. Á., López-Sañudo, I. L., & Hawkins, B. A. (2006). The geographic distribution of mammal body size in Europe: Mammal body size gradient. *Global Ecology and Biogeography*, *15*(2), 173–181. doi:10.1111/j.1466-822X.2006.00206.x

Rodríguez, M. Á., Olalla-Tárraga, M. Á., & Hawkins, B. A. (2008). Bergmann's rule and the geography of mammal body size in the Western Hemisphere. *Global Ecology and Biogeography*, *17*(2), 274–283. doi:10.1111/j.1466-8238.2007.00363.x

Roeselers, G., & Newton, I. L. G. (2012). On the evolutionary ecology of symbioses between chemosynthetic bacteria and bivalves. *Applied Microbiology and Biotechnology*, *94*(1), 1–10. doi:10.1007/s00253-011-3819-9

Roff, D. A. (1992). *The evolution of life histories: Theory and analysis*. New York: Chapman and Hall.

Rohatgi, A. (2017). WebPlotDigitizer 4.0. Retrieved June 10, 2017, from https://automeris.io/WebPlotDigitizer

Romano, A., Séchaud, R., & Roulin, A. (2020). Generalized evidence for Bergmann's rule: Body size variation in a cosmopolitan owl genus. *Journal of Biogeography*, *48*(1), 51–63. doi:https://doi.org/10.1111/jbi.13981

Rosenberg, E., Koren, O., Reshef, L., Efrony, R., & Zilber-Rosenberg, I. (2007). The role of microorganisms in coral health, disease and evolution. *Nature Reviews Microbiology*, *5*(5), 355–362.

Rossi, S., Coppari, M., & Viladrich, N. (2017). Benthic-pelagic coupling: New perspectives in the animal forests. In S. Rossi, L. Bramanti, A. Gori, & C. Orejas (Eds.), *Marine animal forests: The ecology of benthic biodiversity hotspots* (pp. 855–885). Springer International Publishing.

Ryabov, A. B., de Roos, A. M., Meyer, B., Kawaguchi, S., & Blasius, B. (2017). Competition-induced starvation drives large-scale population cycles in antarctic krill. *Nature ecology & evolution*, *1*(7), 1–8.

Salewski, V., & Watt, C. (2017). Bergmann's rule: A biophysiological rule examined in birds. *Oikos*, *126*. doi:10.1111/oik.03698

Saló, E. (2006). The power of regeneration and the stem-cell kingdom: Freshwater planarians (Platyhelminthes). *BioEssays*, *28*(5), 546–559. doi:10.1002/bies.20416

Sander, B. C., & Kalff, J. (1993). Factors controlling bacterial production in marine and freshwater sediments. *Microbial Ecology*, *26*(2), 79–99.

Sarkar, S. (2004). From the reaktionsnorm to the evolution of adaptive plasticity. In T. J. DeWitt & S. M. Scheiner (Eds.), *Phenotypic plasticity: Functional and conceptual approaches* (pp. 10–30). Oxford University Press, New York.

Savage, V. M., Gillooly, J. F., Brown, J. H., West, G. B., & Charnov, E. L. (2004). Effects of body size and temperature on population growth. *The American Naturalist*, *163*(3), 429–441.

Scheiner, S. (2006). Genotype-environment interactions and evolution. In C. W. Fox & J. B. Wolf (Eds.), *Evolutionary genetics: Concepts and case studies* (pp. 326–338). Oxford University Press London, UK.

Schoolfield, R. M., Sharpe, P. J. H., & Magnuson, C. E. (1981). Non-linear regression of biological temperature-dependent rate models based on absolute reaction-rate theory. *Journal of Theoretical Biology*, *88*(4), 719–731.

Searcy, W. A. (1980). Optimum body sizes at different ambient temperatures: An energetics explanation of Bergmann's rule. *Journal of Theoretical Biology*, *83*(4), 579–593. doi:10.1016/0022-5193(80)90190-3

Seed, R. (1980). Shell growth and form in the Bivalvia. In D. Rhoads & R. A. Lutz (Eds.), *Skeletal growth of aquatic organisms: Biological records of environmental change* (pp. 23–67). New York: Plenum Press.

Shapiro, A. M. (1976). Seasonal polyphenism. In *Evolutionary biology* (pp. 259–333). Springer.

Shine, R. (1999). Why is sex determined by nest temperature in many reptiles? *Trends in Ecology & Evolution*, *14*(5), 186–189.

Shine, R., Madsen, T. R., Elphick, M. J., & Harlow, P. S. (1997). The influence of nest temperatures and maternal brooding on hatchling phenotypes in water pythons. *Ecology*, *78*(6), 1713–1721.

Snell-Rood, E. C. (2013). An overview of the evolutionary causes and consequences of behavioural plasticity. *Animal Behaviour*, *85*(5), 1004–1011.

Soetaert, K., Petzoldt, T., & Setzer, R. W. (2010). Solving differential equations in R: Package deSolve. *Journal of Statistical Software*, *33*(9), 1–25. doi:10.18637/jss.v033.i09

Sorokin, Y. (1991). Biomass, metabolic rates and feeding of some common reef zoantharians and octocorals. *Marine and Freshwater Research*, *42*(6), 729–741.

Sousa, T., Domingos, T., & Kooijman, S. A. L. M. (2008). From empirical patterns to theory: A formal metabolic theory of life. *Philosophical transactions of the Royal Society of London. Series B, Biological sciences*, *363*(1502), 2453–2464. doi:10.1098/rstb.2007.2230

Southward, E. C. (1986). Gill symbionts in thyasirids and other bivalve molluscs. *Journal of the Marine Biological Association of the United Kingdom*, *66*, 889–914.

Stabell, T., Andersen, T., & Klaveness, D. (2002). Ecological significance of endosymbionts in a mixotrophic ciliate—an experimental test of a simple model of growth coordination between host and symbiont. *Journal of Plankton Research*, *24*(9), 889–899.

Stachowicz, J. J. (2001). Mutualism, facilitation, and the structure of ecological communities. *BioScience*, *51*(3), 235–246.

Stearns, S. C. (1976). Life-history tactics: A review of the ideas. *The Quarterly Review of Biology*, *51*(1), 3–47. doi:10.1086/409052

Stearns, S. C. (1989a). The evolutionary significance of phenotypic plasticity. *Bioscience*, *39*(7), 436–445.

Stearns, S. C. (1989b). Trade-Offs in life-history evolution. *Functional Ecology*, *3*(3), 259. doi:10.2307/2389364

Stearns, S. C. (1992). *The evolution of life histories*. Oxford University Press.

Stillwell, R. C. (2010). Are latitudinal clines in body size adaptive? *Oikos*, *119*(9), 1387–1390. doi:10.1111/j.1600-0706.2010.18670.x

Taylor, J. D., & Glover, E. A. (2010). Chemosymbiotic bivalves. In S. Kiel (Ed.), *The Vent and Seep Biota* (Vol. 33, pp. 107–135). doi:10.1007/978-90-481-9572-5

Taylor, J. D., Williams, S. T., & Glover, E. A. (2007). Evolutionary relationships of the bivalve family Thyasiridae (Mollusca: Bivalvia), monophyly and superfamily status. *Journal of the Marine Biological Association of the United Kingdom*, *87*(02), 565–574. doi:doi:10.1017/S0025315407054409

Teixeira, C. M. G. L. (2016). *Application of Dynamic Energy Budget theory for conservation relevant modelling of bird life histories* (Ph.D. Universidade Técnica de Lisboa & Vrije Universiteit Amsterdam, Lisboa & Amsterdam). Retrieved from https://research.vu.nl/en/publications/application-of-dynamic-energy-budget-theory-for-conservation-rele

Teplitsky, C., & Millien, V. (2014). Climate warming and Bergmann's rule through time: Is there any evidence? *Evolutionary Applications*, *7*(1), 156–168. doi:10.1111/eva.12129

Tessier, A. J., & Consolatti, N. L. (1989). Variation in offspring size in *Daphnia* and consequences for individual fitness. *Oikos*, 269–276.

The MathWorks Inc. (2020). *MATLAB Release 2020b*. Natick, Massachusetts, United States.

TheMathWorksInc. (2017). *MATLAB Release 2017a*. Natick, Massachusetts, United States.

Thompson, R. J. (1983). The relationship between food ration and reproductive effort in the green sea urchin, *Strongylocentrotus droebachiensis*. *Oecologia*, *56*(1), 50–57.

Thrall, P. H., Hochberg, M. E., Burdon, J. J., & Bever, J. D. (2007). Coevolution of symbiotic mutualists and parasites in a community context. *Trends in Ecology & Evolution*, *22*(3), 120–126. doi:10.1016/j.tree.2006.11.007

Tonkin, J. D., Bogan, M. T., Bonada, N., Rios-Touma, B., & Lytle, D. A. (2017). Seasonality and predictability shape temporal species diversity. *Ecology*, *98*(5), 1201–1216.

Torres Romero, E. J., Morales Castilla, I., & Olalla Tárraga, M. Á. (2016). Bergmann's rule in the oceans? Temperature strongly correlates with global interspecific patterns of body size in marine mammals. *Global Ecology and Biogeography*, *25*(10), 1206–1215. doi:https://doi.org/10.1111/geb.12476

Turesson, G. (1922). The genotypical response of the plant species to the habitat. *Hereditas*, *3*(3), 211–350.

van der Meer, J. (2006). Metabolic theories in ecology. *Trends in Ecology and Evolution*, *21*(3), 136–140. doi:10.1016/j.tree.2005.11.004

van der Meer, J., van Donk, S., Sotillo, A., & Lens, L. (2020). Predicting post-natal energy intake of lesser black-backed gull chicks by Dynamic Energy Budget modeling. *Ecological Modelling*, *423*, 109005. doi:10.1016/j.ecolmodel.2020.109005

van der Veer, H. W., Kooijman, S. A. L. M., & van der Meer, J. (2001). Intra- and interspecies comparison of energy flow in North Atlantic flatfish species by means of dynamic energy budgets. *Journal of Sea Research*, *45*(3-4), 303–320. doi:10.1016/S1385-1101(01)00061-2

Varpe, Ø. (2017). Life history adaptations to seasonality. *Integrative and comparative biology*, *57*(5), 943–960.

Via, S., & Lande, R. (1985). Genotype-environment interaction and the evolution of phenotypic plasticity. *Evolution*, *39*(3), 505–522.

Viladrich, N., Bramanti, L., Tsounis, G., Martínez-Quintana, A., Ferrier-Pagès, C., & Rossi, S. (2017). Variation of lipid and free fatty acid contents during larval release in two temperate octocorals according to their trophic strategy. *Marine Ecology Progress Series*, *573*, 117–128.

Violle, C., Enquist, B. J., McGill, B. J., Jiang, L., Albert, C. H., Hulshof, C., … Messier, J. (2012). The return of the variance: Intraspecific variability in community ecology. *Trends in Ecology and Evolution*, *27*(4), 244–252.

Watt, C., Mitchell, S., & Salewski, V. (2010). Bergmann's rule; a concept cluster? *Oikos*, *119*(1), 89–100. doi:10.1111/j.1600-0706.2009.17959.x

Weiner, J. (1992). Physiological limits to sustainable energy budgets in birds and mammals: Ecological implications. *Trends in Ecology & Evolution*, *7*(11), 384–388.

Wikelski, M., & Thom, C. (2000). Marine iguanas shrink to survive El Niño. *Nature*, *403*(6765), 37–38. doi:10.1038/47396

Williams, R. J., & Martinez, N. D. (2000). Simple rules yield complex food webs. *Nature*, *404*(6774), 180–183.

Windig, J. J., De Kovel, C. G., & De Jong, G. (2004). Genetics and mechanics of plasticity. In T. J. DeWitt & S. M. Scheiner (Eds.), *Phenotypic plasticity: Functional and conceptual approaches* (pp. 31–49). Oxford University Press, Oxford.

Yom-Tov, Y., & Geffen, E. (2006). Geographic variation in body size: The effects of ambient temperature and precipitation. *Oecologia*, *148*(2), 213–218. doi:10.1007/s00442-006-0364-9

Yom-Tov, Y., & Geffen, E. (2011). Recent spatial and temporal changes in body size of terrestrial vertebrates: Probable causes and pitfalls. *Biological Reviews*, *86*(2), 531–541. doi:10.1111/j.1469-185X.2010.00168.x

Yom-Tov, Y., Roos, A., Mortensen, P., Wiig, Ø., Yom-Tov, S., & Heggberget, T. M. (2010). Recent changes in body size of the Eurasian Otter *Lutra lutra* in Sweden. *AMBIO*, *39*(7), 496–503. doi:10.1007/s13280-010-0074-8

Yule, K. M., Miller, T. E., & Rudgers, J. A. (2013). Costs, benefits, and loss of vertically transmitted symbionts affect host population dynamics. *Oikos*, *122*(10), 1512–1520.

Zanzerl, H., & Dufour, S. C. (2017). The burrowing behaviour of symbiotic and asymbiotic thyasirid bivalves. *Journal of Conchology*, *42*(5), 299–308.

Zanzerl, H., Salvo, F., Jones, S. W., & Dufour, S. C. (2019). Feeding strategies in symbiotic and asymbiotic thyasirid bivalves. *Journal of Sea Research*, *145*, 16–23. doi:10.1016/j.seares.2018.12.005

This document was typeseted in LaTeX using the `classicthesis` style developed by André Miede and Ivo Pletikosić.

September 9, 2021